Part I
Manual.
The occurrence, measurement, mechanics, prediction, and control of subsidence

I Introduction, by Working Group 8.4, International Hydrological Programme

1.1 BACKGROUND INFORMATION

The increasing exploitation of ground water, especially in basins filled with unconsolidated alluvial, lacustrine, or shallow marine deposits, has as one of its consequences the sinking or settlement of the land surface--land subsidence (see Glossary, Appendix D).

The occurrence of major land subsidence due to the withdrawal of ground water is relatively common in highly developed areas. Case studies on land subsidence and on remedial measures taken will be useful for developing areas facing similar problems in the future.

The problems of land subsidence were included in the programme of the International Hydrological Decade. During the Decade the major action with respect to land subsidence was the organization of the International Symposium on Land Subsidence held in Tokyo in 1969. The subject has also been retained under the framework of the International Hydrological Programme and included in the work plan for the first phase of the Programme (1975-1980) as IHP subproject 8.4.

In April 1975, the Intergovernmental Council for the International Hydrological Programme, at its first session in Paris, established a Working Group for coordination of IHP subproject 8.4, "Investigation on land subsidence due to ground-water exploitation." The Working Group members are listed below. In addition, A. I. Johnson, Vice President of the International Association of Hydrological Sciences, was the designated liaison from that international organization.

UNESCO Working Group on Land Subsidence

Due to Ground-Water Withdrawal

Mr. Joseph F. Poland, Chairman
U.S. Geological Survey
Rm. W-2528, Federal Building
2800 Cottage Way
Sacramento, California 95825

Mr. Germán Figueroa Vega
Comisión de Aguas de Valle de México
Balderas No. 55-20. Piso.
México 1, D.F.

Ms. Laura Carbognin
National Research Council
1364 San Polo
Venice, Italy 30125

Mr. Ivan Johnson
Representative of IAHS
Woodward-Clyde Consultants
2909 West 7th Avenue
Denver, Colorado,80204

Mr. Soki Yamamoto
Rissho University
4-2-16 Osaki, Shingawa-ku
Tokyo 141, Japan

1.2 PURPOSE AND SCOPE OF GUIDEBOOK

The group was asked to prepare a guidebook on subsidence due to ground-water withdrawal, paying particular attention to measures to control and arrest subsidence, the use of artificial recharge, and the repressuring of aquifers. The goal was to produce a guidebook that will serve as a guide to engineers, geologists, and hydrologists faced with the problem of land subsidence, particularly in developing countries. They may be asked to answer the questions of whether land subsidence is occurring, if so, where and at what rate, the cause or causes, and what can be done to stop it or at least slow it down. The guidebook should be of assistance in planning and undertaking the field studies.

The first session of the Working Group was held in December 1976 in connection with the Second IAHS-UNESCO International Symposium on Land Subsidence in Anaheim, California. At that meeting the group drafted the general outline of the guidebook and decided on the distribution of work.

The guidebook is organized in two parts. Part I is a manual of seven chapters on the occurrence, measurement, mechanics, prediction, and control of land subsidence due to groundwater withdrawal. It has been prepared as a joint effort of the Working Group members.

Part II is a series of invited case histories of land subsidence due to ground-water withdrawal, prepared by individual authors. The first chapter in Part II (Chapter 8) is a brief discussion of other types of land subsidence written by Ms. Alice Allen. Subsidence may occur from many other causes than withdrawal of ground water. Some occurrences are due to natural causes and some are the work of man. Anyone investigating subsidence due to ground-water withdrawal should have at least an elementary knowledge of other types of subsidence and the geologic environments in which they are likely to occur. Although the present discussion by Ms. Allen is brief, it contains 62 references, which should prove very helpful to the reader who wishes to learn more about any particular subsidence process.

The second chapter in Part II (Chapter 9) consists of 15 case histories of subsidence due to ground-water withdrawal, prepared by individual authors. These case histories cover a wide range of conditions and magnitudes of subsidence. Of the occurrences described, 12 are areas of ground-water withdrawal for use and 3 represent conditions where ground water is withdrawn as a step in obtaining a resource. These are Latrobe Valley, Australia (withdrawal to permit mining brown coal), Niigata, Japan (withdrawal to obtain natural gas), and Wairakei, New Zealand (withdrawal of hot water for geothermal power).

1.3 OCCURRENCE OF SUBSIDENCE

The chief source of information on areas of land subsidence due to ground-water withdrawal is the Questionnaire on Land-Subsidence Occurrence, Research, and Remedial Work that was distributed worldwide in 1975-78 by A. I. Johnson, then President of the International Commission of Subsurface Water of IAHS. The results of this survey are being compiled for publication by UNESCO and IAHS. Other sources of data are (1) the 15 case histories in Part II of this casebook, (2) the Proceedings of the lst International Symposium on Land Subsidence held in Tokyo, Japan, in September 1969, and (3) the Proceedings of the 2nd International Symposium on Land Subsidence held in Anaheim, California, in December 1976.

Table 1.1, based on the information listed above, summarizes information on 42 subsidence areas worldwide, of which 18 are in the United States and 10 are in Japan (Figure 1-1). Actually, Japan has the largest number of subsiding areas of any country. According to Yamamoto (1977, p. 9 and Figure 2), the number of subsiding areas in Japan has reached 40 and is still increasing. Most of the subsidence is due to ground-water withdrawal from thickly populated topographically low areas bordering the ocean. Only the 10 chief subsidence areas in Japan due to ground-water withdrawal are reported in Table 1.1 and shown in Figure 1.1. All of these border the ocean.

In terms of vertical magnitude, the subsiding areas listed in Table 1.1 range from reported minor casing protrusion in Bangkok, Thailand, and 0.15 m of subsidence in Venice, Italy, to 15 m in the Cheshire district of Great Britain where rock salt has been mined by solution since Roman times. As a result of man-induced sinkhole development in carbonate terrane in Alabama, we even have a reported maximum of 37 m. The areal extent of subsidence, worldwide, ranges from 10 km^2 in the San Jacinto Valley to 13,500 km^2 in the San Joaquin Valley, both in California (USA).

Figure 1.2 shows the geographic location of the 17 areas in the United States (exclusive of the Alabama sinkhole area) on a map of conterminous United States. Subsidence of the land surface in the 17 areas ranges from 0.3 m at Savannah, Georgia to 9 m. on the west side of the San Joaquin Valley (Los Banos-Kettleman City area) in California (Figure 1.3). Subsidence exceeding 1 metre occurs in four States: Texas, Arizona, Nevada, and California. The areal extent ranges from 10 km^2 in San Jacinto Valley, California, to 13,500 km^2 in the San Joaquin Valley. California is the State ranking number one for the dubious honor of having the largest area of subsidence --about 16,000 km^2. Close behind is Texas with 12,000 km^2; and Arizona is third with 2,700 km^2.

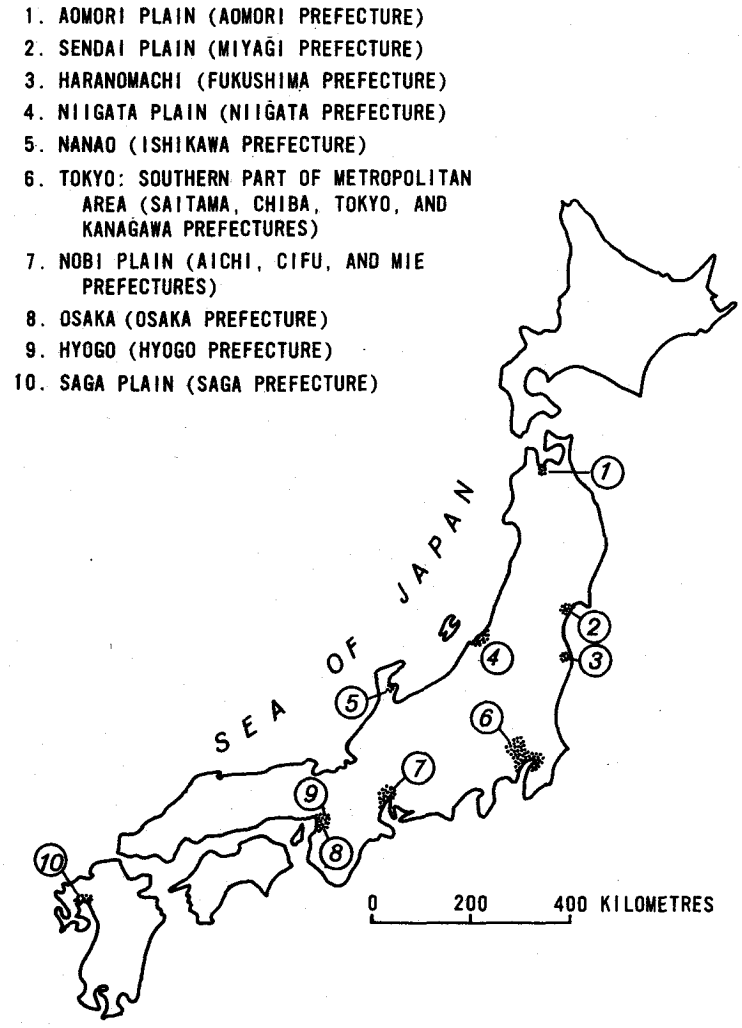

Figure 1.1 Chief subsidence areas in Japan.

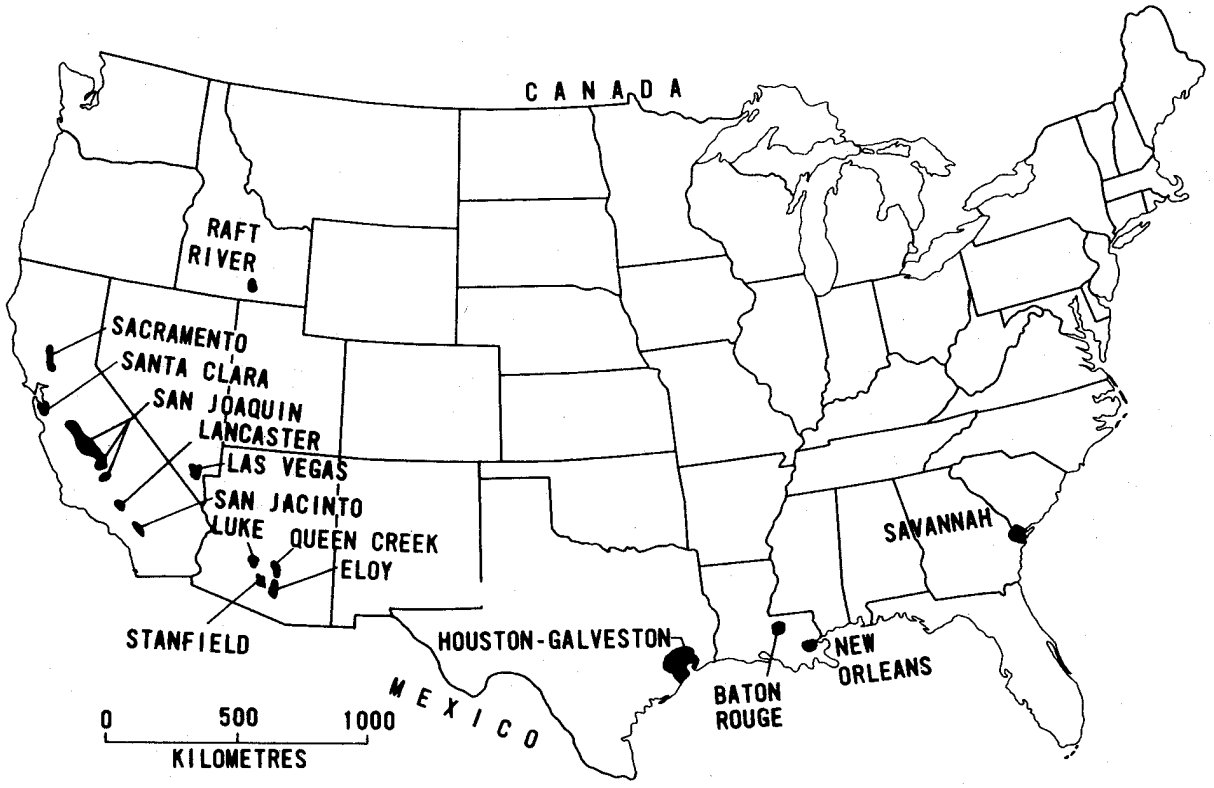

Figure 1.2 Areas of land subsidence from ground-water withdrawal, USA.

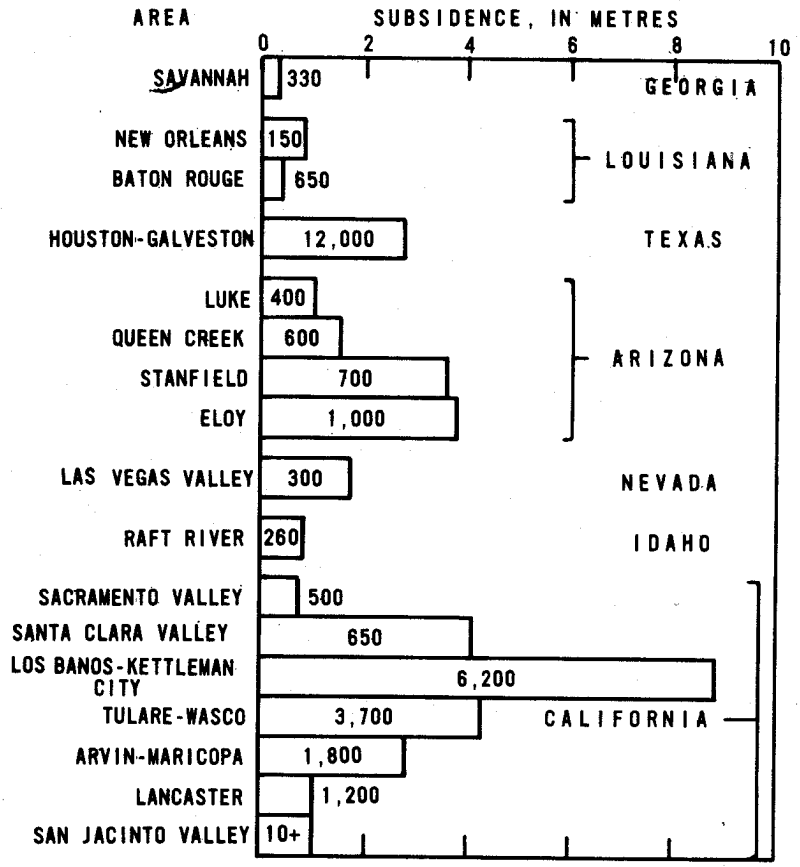

Figure 1.3 Magnitude of land subsidence from ground-water withdrawal, USA (number in column represents area in square kilometres).

Table 1.1. Areas of land subsidence due to ground-water withdrawal

Location	Depositional environment and age	Depth range of compacting beds (m)	Maximum subsidence (m)	Area of subsidence (km^2)	Time of principal occurrence	Remedial or protective measures taken	Principal reference(s)
Australia:							
Latrobe Valley.	Lacustrine and fluviatile; early Tertiary.	10-300	1.6 (1977)	100 (>0.2 m)	1961-78	Reduction in artesian ground-water pressures, necessary for mining coal. Restrictions placed on building in critical area.	Gloe (1977); Gloe, Guidebook, Ch. 9.1.
China:							
Shanghai.	Alternating freshwater and marine; Quaternary.	3-300	2.63 (1965)	121	1921-65	Restricted use of ground water; artificial recharge by injection of treated river water into wells; adjustment of pumping pattern.	Shanghai Hydrogeological Team (1973); Luxiang and Manfang, Guidebook, Ch. 9.2.
Taipei Basin.	do.	10-240	1.9 (1974)	235	1955-74	In 1968, legal action taken to limit ground-water pumpage.	Hwang and Wu (1969); Wu (1977).
Great Britain:							
London.	London Clay of Eocene age overlying chalk aquifer of Cretaceous age.	50-100	0.35 (1976)	450	1865-1932	None.	Longfield (1932); Wilson and Grace (1942); Water Resources Board (1972).
Cheshire district.	Sandstone, marl, and rock salt; Triassic.	100-300	15 (1977)	1,500	1533-1977	Reduced pumping of brine; installed flexible foundations; regraded railways roads, canals.	Howell and Jenkins (1977); Collins (1971).
Hungary:							
Debrecen.	Fluviatile; Quaternary.	50-250	0.42 (1975)	390	1920-75	None.	Orlóczi (1969); Miskolczi (1967); Szekely (1975).
Visonta.	Fluviatile and swampy; late Cenozoic.	20-100	0.5 (1975)	40	1961-75	None.	Kesserü (1970); Kesserü (1972).
Italy:							
Po Delta.	Alluvial, lagoonal, and shallow marine; Quaternary.	100-600	3.2	2,600	1951-66	Pumping of gas-bearing water stopped by legal action.	Schrefler, Lewis, and Norris (1977); Zambon (1967); Caputo, et al (1970).
Ravenna.	Alluvial, lacustrine, and shallow marine; Neozoic.	80-500	1.20 (1977)	about 600	1955-77	None (project plans underway).	Bertoni, et al (1973); Carbognin, et al (1978); Guidebook, Ch. 9.15.
Venezia.	Alluvial, lacustrine, and shallow marine; Neozoic.	70-350	0.15 (1976)	about 400	1952-70	A 70-percent shutdown of active artesian wells including some principal ones, and construction of two river-fed aqueducts supplying mainly the industrial zone.	Gambolati and Freeze (1973); Gambolati, et al (1974); Carbognin, et al (1977) (reprinted in Guidebook as Ch. 9.3).
Japan:							
Aomori.	Alluvial and lacustrine; late Cenozoic.	0-600	0.45 (1977)	65	1958-78	Reduced withdrawal of ground water by regulation	Aomori Pref. (1974).
Sendai.	Alluvial and shallow marine; late Cenozoic.	0-300	0.57 (1977)	90	1966-78	As above and introducing water from river	
Haranomachi. City.	Alluvial and shallow marine; late Cenozoic.	100-200	2	25	1965-78+	Regulation of ground water withdrawal; constructed multipurpose dams and water-supply systems	IAHS questionnaire.
Nanao.	Alluvial and shallow marine; late Cenozoic.	0-200	0.53 (1977)	80	1972-78	Reduced withdrawal of ground water by regulation	Murakami and Takahashi (1969)

Tokyo, including Chiba, Saitama, and Kanagawa Prefectures.	Alluvial and shallow marine; late Cenozoic.	0-400 and *800-2,000	4.59 (1975)	3,420	1918-78+	Built reservoirs and canals to import surface water-from R. Tone and reduce ground-water withdrawal	Miyabe (1962); Aoki and Miyabe (1969); Ishii, et al (1977); Yamamoto, Guide book, Ch. 9.4.
Niigata	Shallow marine and marine; late Cenozoic.	0-1,000	2.65 (1965)	430	1957-78+	Reduced withdrawal of gas-bearing water by regulation; since 1973, all gas water reinjected into reservoirs.	Takeuchi et al (1969); Aoki (1977); Yamamoto, Guidebook, Ch. 9.7.
Nobi (Aichi, Gifu, and Mie Prefectures.	Alluvial and lacustrine; late Cenozoic.	0-300	1.53 (1970)	1,140	1932-78+	Diverted Aichi irrigation water and constructed dam; reduced ground-water withdrawal by regulation.	Kuwahara, et al (1977); Yamamoto, Guidebook, Ch. 9.6.
Osaka.	Alluvial and lacustrine; Quaternary.	0-400	2.88 (1970)	630	1935-70	Imported surface water from R. Yodo and reduced ground-water withdrawal.	Murayama (1969); Ikebe, et al (1970); Nakamachi (1977); Editorial Comm. (1969); Yamamoto, Guidebook, Ch. 9.5.
Hyogo.	do.	0-200	2.84 (1960)	100	1932-70	do.	
Saga.	Alluvial and shallow marine; Quaternary.	0-200	1.20 (1977)	300	1957-78+	Imported surface water; dam under construction.	Kumai, et al (1969).
México:							
México city.	Alluvial, lacustrine; Quaternary and Tertiary.	0-50	9(1978)	about 225	1891-1978	Holding withdrawal constant and undertaking delivery of surface water into the valley of Mexico to diminish and eventually eliminate ground-water overdraft.	Marsal y Mazari (1959); CHCVM (1953-1970); CAVM (1975); Figueroa-Vega, Guidebook, Ch. 9.8.
New Zealand:							
Wairakei.	Volcanic flows and breccias; Pleistocene.	250-800	6-7 (1975)	30	1952-78	None.	Stilwell, Hall, and Tawhai (1975); Bixley, Guidebook, Ch. 9.9.
South Africa:							
Far West Rand.	Dolomite Series, Paleozoic, and weathered overburden.	30-200 for overburden; 30-1,200 for dolomite.	9(overburden)	?	1959-75	Artificial recharge of dolomitic compartments with ground water pumped from mines.	Bezuidenhout and Enslin (1969); Enslin, et al (1977).
Thailand:							
Bangkok.	Alluvial and shallow marine; Quaternary.	0-200	Well casing protrusion reported.	?	1978-	None.	Piancharoen (1977); Brand and Balasubramaniam (1977); Yamamoto, Guidebook, Ch. 9.10.
United States:							
Alabama:	Carbonate terrane; unconsolidated deposits on bedrock.	10-100	37(?)	4,000 man-made sinkholes, 1-1,000 m in diameter.	1900-75	Removal of surface water; bridging of railroads and highways; removal of unconsolidated deposits.	Newton (1977); Newton, Guide book, Ch. 9.11.
Arizona**:							
Luke area.	Alluvial and lacustrine; Cenozoic	50-350	1(1967)	400	1950(?)-1978	Damaged well casings repaired	Laney, Raymond, and Winikka (1978).
Queen Creek area.	do.	50-350	1.5 (1976)	600	1950(?)-1978	Constructing major aqueduct to import Colorado River water and reducing overdraft.	Winikka and Wold (1977); Schumann (1914).

Table 1.1. Areas of land subsidence due to ground-water withdrawal--Continued

Location	Depositional environment and age	Depth range of compacting beds (m)	Maximum subsidence (m)	Area of subsidence (km^2)	Time of principal occurrence	Remedial or protective measures taken	Principal reference(s)
United States--Continued:							
Arizona--Continued:							
Stanfield area.	Alluvial and lacustrine; Cenozoic.	50-350	3.6 (1977)	700	1950(?)-78	Well casings repaired.	
Eloy area.	do.	50-350	3.8 (1977)	1,000	1950(?)-78	Well casings, highway, and railroad repaired.	Schumann and Poland (1969).
California							
Sacramento Valley.	Alluvial and fluviatile; late Cenozoic.	30-300	0.7	500	1955-78+	None.	Lofgren and Ireland (1973).
Santa Clara Valley.	Alluvial and shallow marine; late Cenozoic.	50-330	4.1 (1975)	650	1918-70	Built detention dams; increased local recharge; built levees; imported water; many damaged well casings repaired or wells replaced.	Poland (1977); Poland, Guide book, Ch. 9.14.
San Joaquin Valley							
Los Banos-Kettleman City area.	Alluvial and lacustrine; late Cenozoic.	60-900	9.0 (1977)	6,200	1930-75	Built dams and canals to import surface water and reduce groundwater withdrawal. Repaired many well casings damaged by compressive stresses.	Poland, Lofgren, Ireland, and Pugh (1975); Bull (1975); Poland and Lofgren, Guide book, Ch. 9.13.
Tulare-Wasco area.	Alluvial, lacustrine, and shallow marine; late Cenozoic.	60-700	4.3 (1970)	3,680	1930-70	do.	Lofgren and Klausing (1969); Poland and others (1975).
Arvin-Maricopa area.	Alluvial and lacustrine; late Cenozoic.	60-500	2.8 (1970)	1,800	1940-70	do.	Lofgren (1975); Poland and others (1975).
Lancaster area.	Alluvial and lacustrine; late Cenozoic.	60-300	1+ (1976)	1,200	1955-78	Damaged well casings repaired.	Lewis and Miller (1968); McMillan (1973).
San Jacinto Valley.	Alluvial; late Cenozoic.	60-300	1+ (1974)	10+	1950-75+	None.	Lofgren (1976).
Georgia:							
Savannah area.	Marine; Tertiary.	50-150	0.3	330	1933-75+	None.	Davis, Counts, and Holdahl (1977).
Idaho:							
Raft River.	Alluvial; late Cenozoic.	50-300	10.8 (1975)	260	1960-75+	None.	Lofgren (1975).
Louisiana:							
Baton Rouge.	Fluviatile and shallow marine; late Cenozoic.	120-900	0.38 (1976)	650+	1935-76+	None.	Davis and Rollo (1969); Wintz, Kazmann, and Smith (1970); Smith and Kazmann (1978).
New Orleans.	Fluviatile and shallow marine; Quaternary(?).	150-260	0.8 (1975)	150	1940-75+	None.	Rollo (1966); Kazmann and Heath (1968).
Nevada:							
Las Vegas.	Alluvial; late Cenozoic.	60-300	1-1.7 (1972)	300	1935-75+	Moved well field away from fine-grained deposits; imported Colorado River water.	Malmberg (1964); Kindling (1971).
Texas:							
Houston-Galveston area.	Fluviatile and shallow marine; late Cenozoic.	60-900	2.75 (1973)	12,000 >15 cm	1943-78	Built reservoirs and importing surface water to reduce overdraft; Subsidence Control District created.	Gabrysch and Bonnet (1975); Gabrysch, Guidebook, Ch. 9.12.

*Extraction of natural gas.
**Data chiefly from questionnaires for IAHS completed by Carl Winikka, January 1978.

1.4 GEOLOGICAL ENVIRONMENTS OF OCCURRENCE

Subsidence due to ground-water withdrawal develops principally under two contrasting environments and mechanics. One environment is that of carbonate rocks overlain by unconsolidated deposits, or old sinkholes filled with unconsolidated deposits, that receive buoyant support from the ground-water body. When the water table is lowered, the buoyant support removed, and the hydraulic gradient increased, the unconsolidated material may move downward into openings in the underlying carbonate rocks, sometimes causing catastrophic collapses of the roof. In Alabama, according to J. G. Newton (1977 and Chapter 9.11), an estimated 4,000 man-induced sinkholes have formed since 1900 in contrast to less than 50 natural collapses. In the United States manmade sinkhole occurrence is common in carbonate terranes from Florida to Pennsylvania, numbering many thousands. The individual sinkhole area is small, however, the diameter usually ranging from 1 to 100 m (Stringfield and Rapp, 1977). Carbonate terrane susceptible to sinkhole formation when the water table is lowered occurs in many parts of the world. In populated areas the formation of sinkholes can produce a variety of problems related to the maintenance of manmade structures and the pollution of water supplies. Newton discusses some of these problems in Chapter 9.11. The overall subject is broad and beyond the scope of this guidebook.

The other environment and by far the most extensive occurrence is that of young unconsolidated or semiconsolidated clastic sediments of high porosity laid down in alluvial, lacustrine, or shallow marine environments. Almost all the subsiding areas included in Table 1.1 are underlain by semiconfined or confined aquifer systems containing aquifers of sand and/or gravel of high permeability and low compressibility, interbedded with clayey aquitards of low vertical permeability and high compressibility under virgin stresses. All the compacting deposits were normally loaded, or approximately so, before man applied stresses exceeding preconsolidation stress. These aquifer systems compact in response to increased effective stress caused by artesian-head decline in the coarse-grained aquifers and time-dependent pore-pressure reduction in the fine-grained compressible aquitards, causing land-surface subsidence.

Of the principal clay minerals--montmorillonite, illite, and kaolinite--montmorillonite is the most compressible. Montmorillonite is the predominant clay mineral in the compacting aquifer systems in southwestern United States--California (Meade, 1967), south-central Arizona (Poland, 1968), and Texas (Corliss and Meade, 1964)--also in Mexico City (Marsal and Mazari, 1959). Montmorillonite comprises 60 to 80 per cent of the clay-mineral assemblage in each of these areas. Illite is the chief clay mineral in the Taipei basin (Hwang and Wu, 1969), and in the Quaternary deposits in Tokyo (Tokyo Metropolitan Govt., 1969).

Another occurrence of subsidence due to ground-water withdrawal that is not represented in Table 1.1 has developed at many sites in Sweden and Norway and probably in other glaciated areas of similar geologic and hydrologic environments. According to Broms, Fredriksson, and Carlsson (1977), most of the bedrock in Sweden is crystalline rock, favorable for construction of underground structures, especially tunnels, because of high strength and because loose and weathered parts have been removed by the glaciation. After the latest glaciation, clay and silt were deposited on a thin layer of till or sand and gravel resting on the bedrock surface, especially in bedrock depressions that commonly are indicative of tectonic zones deepened by the ice. The areas covered with clay are small but the urban regions are mostly in these areas. Deep tunnels cutting through tectonic zones act as drains, lowering the pore-water pressure first in the pervious bottom layers (confined aquifers), and then gradually (over a period of years) in the overlying clay layer. Broms and others (1977) describe damages cause by this type of subsidence and steps that can be taken to mitigate or prevent the subsidence. They can be summarized as follows:

1. Before the construction of a tunnel, by avoiding areas which can be affected by subsidence;

2. During the construction, by pregrouting;

3. After the construction, by grouting, in order to reduce the leakage or by artificial infiltration of water to maintain the pore pressure in the compressible layers.

Moreover it is often possible to decrease the subsidence in soft clays by preloading. It is also possible to preload the compressible layers in advance by temporarily lowering the groundwater level by pumping from deep wells.

1.5 PROBLEMS AND REMEDIAL STEPS

Principal problems caused by the subsidences listed in Table 1.1 are (1) differential changes in elevation and gradient of stream channels, drains, and water-transport structures, (2) failure of water-well casings due to compressive stresses generated by compaction of aquifer systems, (3) tidal encroachment in lowland coastal areas, and (4) in areas of intensive subsidence, development of tensional or compressional strain in engineering structures. Additional details on problems are discussed in the case histories of Chapter 9.

Remedial or protective measures of some sort have been taken in 10 of the 15 case-history areas and 30 of the 42 areas listed in Table 1.1. The various steps that have been taken to control or ameliorate subsidence will be discussed in Chapter 7. The methods employed and the results attained should be of interest to anyone facing a subsidence problem due to water-level decline from overpumping. In Part I of this guidebook, frequent reference will be made to pertinent case histories.

1.6 ACKNOWLEDGMENTS

Beyond the joint efforts of the Working Group, several people have assisted in preparation or review of chapters. In preparation of Table 1.1, Marcelo Lippmann assisted by contacting countries in South America concerning possible subsidence. Chapter 2 reviewers included R. K. Gabrysch, R. L. Ireland, R. L. Laney, H. H. Schumann, and especially F. S. Riley, for his many helpful suggestions. Chapter 3 was reviewed in detail by D. C. Helm, who also made a major contribution to Chapter 5. He is the author of section 5.3.6, including discussion of the depth-porosity model and the aquitard-drainage model. J. A. daCosta was very helpful in editorial review of several chapters and case histories. Also, we are indebted to Mrs. Margaret Farmer for her patient and careful typing and retyping of manuscript drafts.

1.7 REFERENCES

AOKI, S. 1977. Land Subsidence in Niigata. IAHS/AISH Pub. No. 121, p. 105-112.

AOKI, S., and MIYABE, N. 1969. Studies on partial compaction of soil layer in reference to land subsidence in Tokyo. IAHS/AISH Pub. No. 89, p. 354-360.

AOMORI PREFECTURE. 1974. Report on water balance study in Aomori region. Environment and Health Dept., p. 1-111 (in Japanese).

BERTONI, W., CARBOGNIN, L., GATTO, P., and MOZZI, G. 1973. Note interpretative preliminari sulle cause della subsidenza in atto a Ravenna. C.N.R., Lab. per lo Studio della Dinamica delle Gradi Masse, Tech. Rept. 65, Venezia.

BEZUIDENHOUT, C. A., and ENSLIN, J. F. 1969. Surface subsidence and sinkholes in the dolomitic areas of the Far West Rand, Transvaal, Republic of South Africa, in Tison, L. J., ed., Land Subsidence, V. 2. IAHS/AISH Pub. No. 89, p. 482-495.

BROMS, B. B., FREDRICKSSON, ANDERS. 1977. Land subsidence in Sweden due to water-leakage into deep-lying tunnels and its effects on pile-supported structures. IAHS/AISH Pub. No. 121, p. 375-387.

BUREAU OF CONSTRUCTION, TOKYO METROPOLITAN GOVERNMENT, 1969. Land Subsidence and flood control measures in Tokyo. p. 1-40.

CARBOGNIN, L., GATTO, P., MOZZI, G., GAMBOLATI, G., and RICCARI, G. 1977. New trend in the subsidence of Venice. IAHS/AISH Pub. No. 121, p. 65-81.

CARBOGNIN, L., GATTO, P., MOZZI, G., and GAMBOLATI, G. 1978. Land subsidence of Ravenna and its similarities with the Venice case. American Soc. Civil Engineers, Proceedings of Eng. Found. Conf. on Evaluation and Prediction of Subsidence, Pensacola Beach, Florida. Jan. 1978.

COLLINS, J. F. N. 1971. Salt: A policy for the control of salt extraction in Cheshire. Chesire County Council.

COMISIÓN HIDRÓLOGICA DE LA CUENCA DEL VALLEY DE MÉXICO, SRH. 1953-70. Boletín de Mecánica de Suelos del Núm. 1-6. Mexico.

COMISIÓN DE AGUAS DEL VALLE DE MÉXICO, SRH. 1975. Boletin de Mecánica de Suelos Núm. 7, 289 pp.

CORLISS, J. B., and MEADE, R. H. 1964. Clay minerals from an area of land subsidence in the Houston-Galveston Bay area, Texas, in Geological Survey Research 1964. U.S. Geol. Survey Prof. Paper 501-C, p. C79-C81.

DAVIS, G. H., COUNTS, H. B., and HOLDAHL, S. R., 1977. Further examination of subsidence at Savannah, Georgia, 1955-1975. IAHS/AISH Pub. No. 121, p. 347-354.

DAVIS, G. H., and ROLLO, J. R., 1969. Land subsidence related to decline of artesian head at Baton Rouge, Lower Mississippi Valley, USA, in Tison, L. J., ed., Land Subsidence, V. 1. IAHS/AISH Pub. No. 88, p. 174-184.

EDITORIAL COMM. FOR TECHNICAL REPORT ON OSAKA LAND SUBSIDENCE. 1969. Report on land subsidence in Osaka, p. 1-148.

ENSLIN, J. F., KLEYWEGT, R. J., BEUKES, J. H. T., and GORDON-WELSH, J. F., 1977. Artificial recharge of dolomitic ground-water compartments in the Far West Rand gold fields of South Africa. IAHS/AISH Pub. No. 121, p. 495-506.

GABRYSCH, R. K., and BONNET, C. W. 1975. Land-surface subsidence in the Houston-Galveston region, Texas. Texas Water Development Board Report 188, 19 p.

GAMBOLATI, G., and FREEZE, R. A. 1973. Mathematical simulation of subsidence of Venice, 1, Theory. Water Resources Research, v. 9, no. 3, p. 721-733.

GAMBOLATI, G., GATTO, P., and FREEZE, R. A. 1974. Mathematical simulation of subsidence of Venice, 2, Results. Water Resources Research, v. 10, no. 3, p. 563-577.

GLOE, C. S. 1977. Land subsidence related to brown coal open cut operations, Latrobe Valley, Victoria, Australia. IAHS/AISH Pub. No. 121, p. 399-401.

HOWELL, F. T., and JENKINS, P. L. 1977. Some aspects of the subsidences in the rocksalt districts of Cheshire, England. IAHS/AISH Pub. No. 121, p. 507-520.

HWANG, JUI-MING, and WU, CHIAN-MIN. 1969. Land subsidence problems in Taipei Basin, in Tison, L. J., ed., Land Subsidence, V. 1. IAHS/AISH Pub. No. 88, p. 21-34.

IKEBE, N., WATSU, J. I., TAKENAKA, J. 1970. Quaternary geology of Osaka with special reference to land subsidence. Jour. Geosc., Osaka City Univ., 13, p. 39-98.

ISHI, M., KURAMOCHI, F., and ENDO, T. 1977. Recent tendencies of the land subsidence in Tokyo. IAHS/AISH Pub. No. 121, p. 25-34.

KAZMANN, R. G., and HEATH, M. M. 1968. Land subsidence related to ground-water offtake in the New Orleans area. Gulf Coast Assoc. Geological Societies Trans., v. xviii, p. 108-113.

KESSERÜ, ZSOLT. 1970. Felszini süllyedés vizszintsüllyesztés követ-keztében (Land subsidence due to the effect of sinking the ground-water table). Magyar Tudományos Akadémia IV; Bányavizvédelmi Konferencíaja, Budapest IV. Conference of mine-drainage networks, Hungarian Academy of Sciences, Budapest, I.a/Vol. no. 3.

KESSERÜ, ZSOLT. 1972. Forecasting potential building damages due to the effect of sinking the underground-water table. II. International Conference of mining Geodesy, Budapest, Vol. V.

KUMAI, H., SAYAMA, M., SHIBASAKI, T., and UNO, K. 1969. Ground sinking in Shiroishi Plain Saga Prefecture. IAHS/AISH Pub. No. 89, p. 645-657.

KUWAHARA, T., UESHITA, K., and IIDA, K. 1977. Analysis of land subsidence in Nobi Plain. IAHS/AISH Pub. No. 121, p. 55-64.

LANEY, R. L., RAYMOND, R. H., and WINIKKA, C. C. 1978. Maps showing water-level declines, land subsidence, and earth fissures in south-central Arizona. U.S. Geol. Survey Water-Resources Investigations Report 78-83, 2 maps.

LEWIS, R. E., and MILLER, R. E. 1968. Geologic and hydrologic maps of the southern part of Antelope Valley, California. U.S. Geol. Survey report, 13 p.

LOFGREN, B. E. 1975. Land subsidence and tectonism, Raft River Valley, Idaho. U.S. Geol. Survey open-file report 75-585, 21 p.

LOFGREN, B. E. 1976. Land subsidence and aquifer-system compaction in the San Jacinto Valley, Riverside County, California--A progress report. U.S. Geol. Survey Journal of Research, v. 4, no. 1, p. 9-18.

LOFGREN, B. E., and IRELAND, R. L. 1973. Preliminary investigation of land subsidence in the Sacramento Valley, California. U.S. Geol. Survey open-file report, 32 p.

LONGFIELD, T. E. 1932. The subsidence of London. Ordnance Survey, Prof. Papers, new ser., no. 14.

McMILLAN, J. F. 1973. Land subsidence--Antelope Valley area of Los Angeles County. Dept. of County Engineer, Survey Div., Los Angeles, Calif., 11 p.

MALMBERG, G. T. 1964. Land subsidence in Las Vegas Valley, Nevada, 1935-63, in Ground-Water Resources--Information Ser., Rept. 5. Nevada Dept. Conservation and Natural Resources, and U.S. Geol. Survey, 10 p.

MARSAL, RAUL J., and MAZARI, MARCOS. 1959. El Subsuelo de la Ciudad de Mexico. Primer Panamericano, Congreso de Mecanica de Suelos y Cimentaciones, 614 p. (2d ed., 1969, is bilingual in Spanish and English.)

MEADE, R. H. 1967. Petrology of sediments underlying areas of land subsidence in central California. U.S. Geol. Survey Prof. Paper 497-C, 83 p.

MINDLING, ANTHONY, 1971. A summary of data relating to land subsidence in Las Vegas Valley. Nevada Univ. System, Desert Research Inst., Center for Water Resources Research, 55 p.

MISKOLCZI, LÁSZLÓ. 1967. A debreceni mozgásvizgálatok geodéziai tanulságai (Geodetic methodology of land subsidence measurements in Debrecen). Geodézia és Kartográfia v. 19, no. 1.

MIYABE, N. 1962. Studies in the ground sinking in Tokyo. Report Tokyo Inst. Civil Eng., p. 1-38.

MURAKAMI, M., and TAKAHASHI, Y. 1969. Land subsidence research and regional water resource planning of the Nanao Basin. IAHS/AISH Pub. No. 121, p. 211-222.

MURAYAMA, S. 1969. Land subsidence in Osaka. IAHA/AISH Pub. No. 88, p. 105-130.

NAKAMACHI, N. 1977. Land subsidence in Osaka, Japan. Society Soil Mechanics and Foundation Eng., v. 25, no. 6, p. 61-67. (In Japanese)

NEWTON, J. G. 1977. Induced sinkholes--a continuing problem along Alabama highways. Internat. Assoc. Hydrological Sci., Pub. 121, p. 453-463.

ORLÓCZI, ISTVAN. 1969. Water balance investigations based upon measurement of land subsidence caused by ground-water withdrawal. IAHS/AISH Pub. No. 88, p. 224-232.

PIANCHAROEN, CHAROEN. 1977. Ground water and land subsidence in Bangkok, Thailand. IAHS/AISH Pub. No. 121, p. 355-364.

POLAND, J. F. 1968. Compressibility and clay minerals of sediments in subsiding ground-water basins, southwestern United States. Geol. Soc. America 81st Ann. Mtg. Prog., Mexico City (1968), p. 241; 1968, Geol. Soc. America Spec. Paper 121, p. 241.

POLAND, J. F. 1977. Land subsidence stopped by artesian-head recovery, Santa Clara Valley, California. IAHS/AISH Pub. No. 121, p. 124-132.

POLAND, J. P., LOFGREN B. E., and RILEY, F. S. 1972. Glossary of selected terms useful in studies of the mechanics of aquifer systems and land subsidence due to fluid withdrawal. U.S. Geological Survey Water-Supply Paper 2025, 9 p.

POLAND, J. F., LOFGREN, B. E., IRELAND, R. L., and PUGH, R. G. 1975. Land subsidence in the San Joaquin Valley as of 1972. U.S. Geol. Survey Prof. Paper 437-H, 78 p.

ROLLO, J. R. 1966. Ground-water resources of the greater New Orleans area, Louisiana. Louisiana Geol. Survey, Water Resources Bull. No. 9, 69 p.

SCHREFLER, B. A., LEWIS, R. W., and NORRIS, V. A. 1977. A case study of the surface subsidence of the Polesine area. Internat. Jour. for Num. and Analytical Methods in Geomechanics, v. 1, no. 4, p. 377-386.

SCHUMANN, H. H. 1974. Land subsidence and earth fissures in alluvial deposits in the Phoenix area, Arizona. U.S. Geol. Survey Misc. Inv. Ser., Map 1-845-H, 1 sheet.

SCHUMANN, H. H., and POLAND, J. F. 1969. Land subsidence, earth fissures, and ground-water withdrawal in south-central Arizona, USA, in Tison, L. J., ed., Land Subsidence, V. 1. IAHS/AISH Pub. No. 88, p. 295-302.

SHANGHAI HYDROGEOLOGICAL TEAM. 1973. On the control of surface subsidence in Shanghai. Acta Geologica Sinica 2, p. 243-254. (In Chinese)

SMITH, C. G., and KAZMANN, R. G. 1978. Subsidence in the capital area ground-water conservation district--an update. Capital Area Ground-Water Conservation Commission, Bull. no. 2, 31 P.

STILWELL, W. B., HALL, W. K., and TAWHAI, JOHN. 1975. Ground movement in New Zealand geothermal fields. Ministry of Works and Development, Wairakei, Private Bag, Taupo. New Zealand. p. 1427-1434.

SZEKELY, FERENC. 1975. Mathematical model for the cone of depression of waterworks in loose sedimentary basins. International Conference of IAH and IAHS, Hydrogeology of Great Sedimentary Basins, Budapest.

TAKEUCHI, S., KIMOTO, S., WADA, M., MUDAI, K., and HINA, H. 1969. Geological and geohydrological properties of land subsided area--case of Niigata lowland. IAHS/AISH Pub. No. 88, p. 232-241.

TOKYO METROPOLITAN GOVERNMENT. 1969. Land subsidence in Tokyo, p. 1-32.

WATER RESOURCES BOARD. 1972. The hydrogeology of the London Basin. Water Resources Board, Reading, 139 p.

WILSON, GUTHLAC, and GRACE, HENRY. 1942. The settlement of London due to underdrainage of the London Clay. Jour. Inst. Civil Eng., v. 19, no. 2, Paper no. 5294, p. 100-127.

WINIKKA, C. C., and WOLD, D. P. 1977. Land subsidence in central Arizona. IAHS/AISH Pub. No. 121, p. 95-103.

WINTZ, W. A., Jr., KAZMANN, R. G., and SMITH, C. G., Jr. 1970. Subsidence and ground-water off take in the Baton Rouge area. Louisiana State Univ., Louisiana Water Resources Research Inst., Bull. 6, 20 p. W. A. Wintz, Jr., Technical Appendix, 70 p.

WU, CHIAN-MIN. 1977. Ground-water depletion and land subsidence in Taipei Basin. IAHS/AISH Pub. No. 121, p. 389-398.

YAMAMOTO, S. 1977. Recent trend of land subsidence in Japan. IAHS/AISH Pub, No, 121, p. 9-15.

ZAMBON, M. 1967. Abbassamenti del suolo per estrazioni di acqua e gas-Deduzioni ed indirizzi logicamente consequenti per la sistemazione del Delta del diume Po. Atti del XXIII Congresso Naz. delle Bonifiche, Rome, 345-370.

2 Field measurement of deformation, by Joseph F. Poland, Soki Yamamoto, and Working Group

2.1 INTRODUCTION

Decline of the water level in wells causes increase in effective stress--that is, increase in the part of the overburden load that is supported by the sediments being stressed. The resulting strain is primarily expressed as a vertical shortening or compaction of the stressed sediments and consequent subsidence of the land surface. Horizontal displacement also occurs but in a lesser amount.

In this chapter we will describe briefly the methods used for measuring vertical displacement of the land surface (subsidence or uplift), vertical displacement of subsurface deposits (compaction or expansion), horizontal displacement of the land surface, and horizontal displacement of subsurface deposits.

2.2 VERTICAL DISPLACEMENT

2.2.1 Precise leveling by spirit leveling

The elevation of bench marks at land surface commonly is determined by precise leveling, using an engineer’s level and a level rod. This is the most practical method for measuring vertical displacement of bench marks in monitoring subsidence. Equipment and procedures are described briefly in most engineer’s handbooks and in detail in "The Manual of Geodetic Leveling" (Rappleye, 1948). Once a network of bench marks has been established and surveyed by precise leveling, a second survey at some later date will show whether vertical movement has occurred, where, and how much.

The bench-mark net should be designed to cover the area known or suspected to be subsiding, and to extend into a broader regional network at two or three reference bench marks assumed to be stable because they are on bedrock or for some other reason. The bench-mark net can be tied to a tidal bench mark if the subsiding area is near the seacoast. Spacing of bench marks in the net is normally in the range of 400 to 1,000 m, but may be much closer in areas of special interest, such-as ties to structures, or a closely spaced set of bench marks to define movement on surface faults. Bench marks should be placed where danger of destruction is minimal. They are installed as permanent marks that in the past usually have consisted of a brass cap, suitably identified, and grouted into a concrete block or post, into bedrock, or attached securely to the top of a pipe or rod. As the need for greater accuracy and for eliminating surficial disturbances has increased, "deep-seated" bench marks are being installed in increasing numbers. They consist of rods 5 to 10 m long, driven into the ground and protected by an outer sleeve through the top 3-4 m, the zone of surficial disturbances (such as frost-heave, dessication, swelling, oxidation, root growth, and animal burrowing). This type of cased-rod bench mark is particularly well suited for use in monitoring areas of present or potential land subsidence where annual elevation changes of a few mm may be of interest if they represent elastic response of an aquifer system, but should be eliminated if they represent surficial disturbance.

To reduce vandalism, a mark that is less obvious than a brass cap should be used. A convex-headed bolt or pin, projecting a few mm above the concrete or pipe-cap, or a carriage bolt with a nut on the embedded end can be used. The bench-mark designation can be scribed in the concrete before it hardens.[1]

---

[1] Detail on installation and protecting of bench marks is available in a publication of the National Oceanic and Atmospheric Administration (NOAA). Rockville, MD, USA 20852. Entitled Geodetic bench marks, by R. P. Floyd, it is NOAA Manual NOS NGS1, 1978, 50 pages.

Near-surface deposits may contain organic materials subject to bacterial decomposition and consequent settlement of the land surface when the water table is lowered in order to grow crops. Such conditions exist in the peat beds of the Fens in England, in the Florida Everglades (Stephens and Johnson, 1951), and in the Sacramento-San Joaquin Delta in California (Weir, 1950). In such areas, bench marks installed to measure change in elevation of subjacent deposits should be rods or pipes driven firmly into the subjacent deposits and preferably protected from change in the thickness of the overlying organic deposits by an outer pipe sleeve. Furthermore, structures that extend down to the subjacent deposits, such as bridge piers or tidal gages, can serve as sites for the establishment of additional bench marks.

Figure 2.1 shows the network of level lines established by the United States Coast and Geodetic Survey (now National Geodetic Survey) in the subsidence area of the Santa Clara Valley in northern California. This network, which is 400 km long, was first leveled in 1934 and has been releveled 11 times since then. Note that three transverse lines extend southwest into consolidated rock and across the well-known San Andreas fault, and three extend east across the Hayward fault. Both faults are active.

In bench-mark surveys of subsiding areas, the leveling may be of first or second order. First order class I leveling is double run and requires that the allowable discrepancy between duplicate lines does not exceed $3\sqrt{K}$ mm where K is the length of the bench-mark line in kilometres. Second order class I leveling requires a closure of not to exceed $6\sqrt{K}$ mm and costs half to two-thirds as much per kilometre as first order class I. Partly because of the difference in cost between first-order leveling and second-order leveling, it is common practice in resurveying a network in a subsiding area to select principal lines for first-order releveling and secondary lines for second-order releveling. It is extremely important that ties to "stable" ground, to consolidated rock, or to tidal gages, should be included in the first-order leveling.

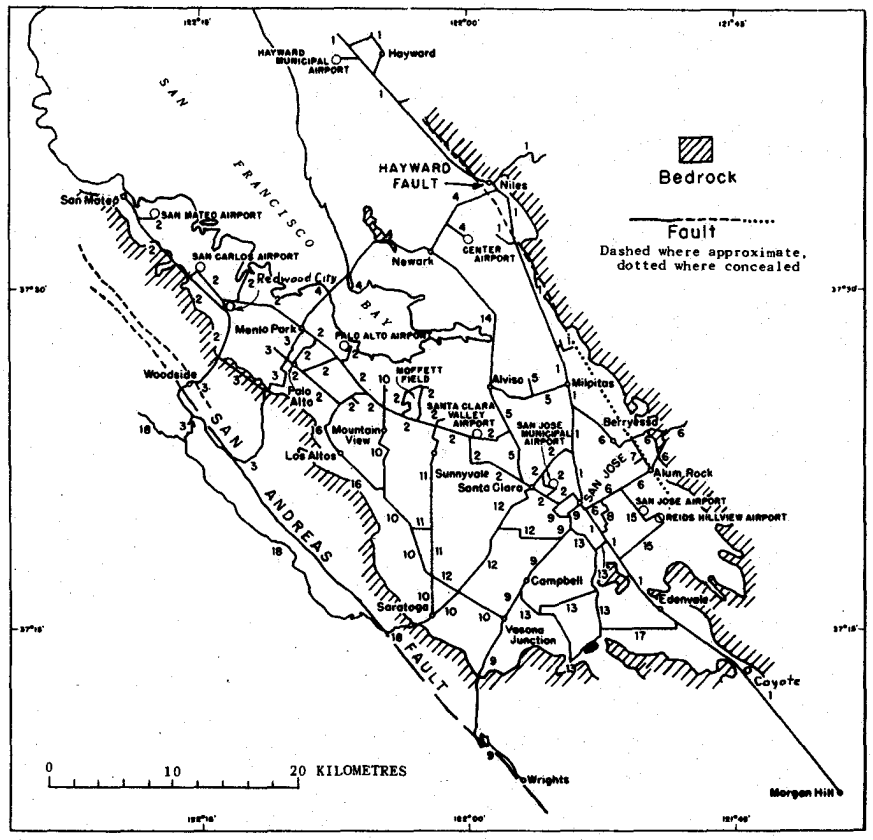

Figure 2.1 Map showing network of level lines in the San Jose subsidence area, Santa Clara Valley, California (modified after National Geodetic Survey; numbers identify level lines).

The releveling pattern at Niigata, Japan, is illustrated in Figure 2.2. The principal first-order leveling lines are identified by the larger circles ("First Class Bench") and those for second-order leveling by the smaller circles. Furthermore, the network is divided into three zones based on rate of subsidence and the economic significance of subsidence: the coastal area northeast of Uchino is releveled every half year, the zone northeast of Yahiko once a year, and the inland zone north of Nagaoka every two years.

Saving time is another reason for using second-order leveling on the secondary lines in a subsiding area. The second-order leveling will cover the distance about twice as fast as first order leveling. In an area that is subsiding 15 to 30 cm per year, a junction point could settle 1 to 3 cm by the time a loop is closed. Any procedures that reduce loop closing time are beneficial. The time of year when the leveling is done is important in a heavily pumped basin, for example, one where the annual fluctuation of artesian head is 10-30 m. Commonly the water level in wells is drawn down in the spring and summer and rises in the autumn and winter when withdrawal is less. Hence, effective stresses are much greater in the summer than in the winter

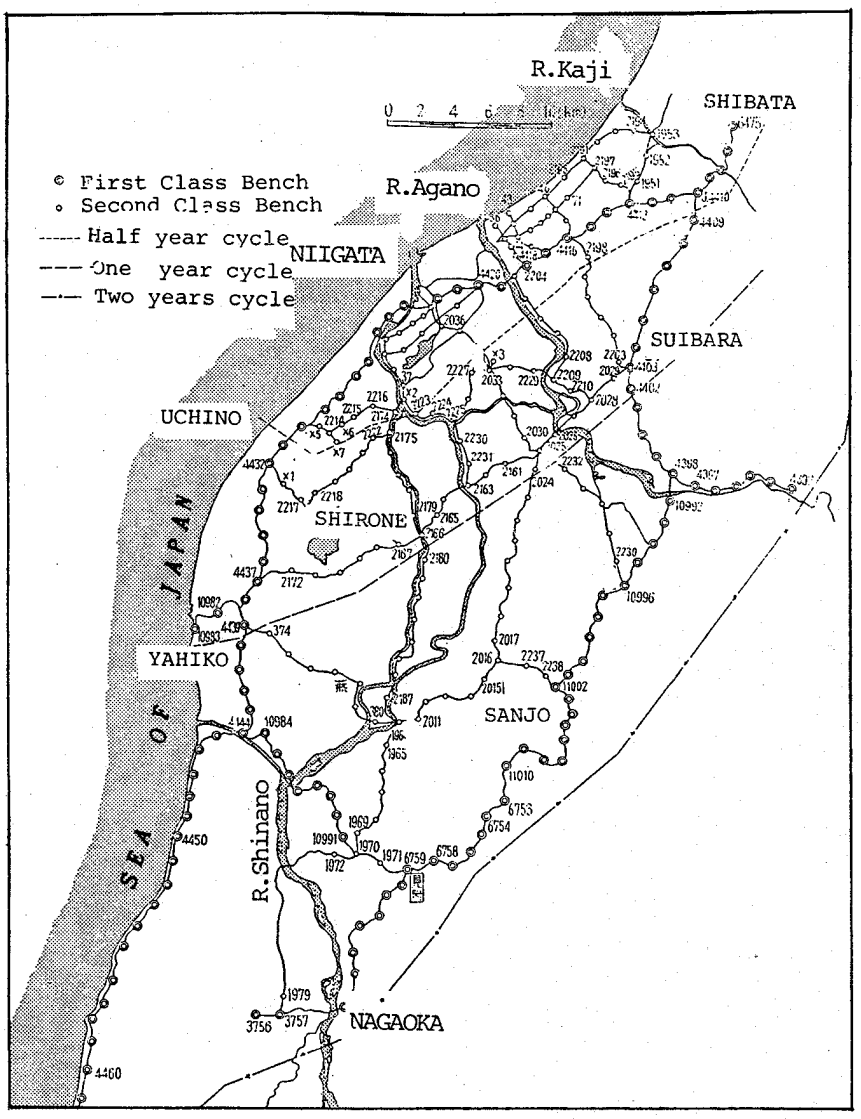

Figure 2.2 Distribution of bench marks in Niigata, Japan.

and the full annual compaction of the aquifer system may occur in 5 to 6 months (see Lofgren, 1968, Figure 3). In such areas, leveling should be accomplished during or immediately following the period of rising water level when compaction and subsidence are minimal.

All the subsidence maps in the case histories of Part II were prepared from change in the elevation of bench marks surveyed at two different times by the leveling procedure. If the bench-mark net has been releveled several times, the magnitude and distribution of subsidence along a line of bench marks can be shown as a series of profiles, one for each releveling, referred to a common base. Figure 9.14.4 is an example of a series of 10 subsidence profiles drawn from surveys from 1919 to 1967, all referred to a 1934 base. 1934 was the first year that the entire line of bench marks was surveyed.

Leveling is a labor-intensive procedure, and as a result the cost has doubled in recent years. The cost of constructing a pipe extensometer that extended to the base of the fresh ground-water reservoir or to the depth tapped by the deepest water wells might well be less than the cost of one releveling of an extensive bench-mark network 300 to 600 km in length. An extensometer placed near the center of a subsidence area could furnish a continuous record of land-surface position and thus would be a subsidence monitor, provided that (1) no compaction of sediments occurred at depths beneath the extensometer footing, and (2) no vertical tectonic movement developed. As a subsidence monitor, it would furnish information needed to decide when to relevel the bench-mark net. Furthermore, under such circumstances, the top of the inner pipe of a pipe extensometer (see Figure 2.5B) would be a reference bench mark of constant elevation and hence a fixed tie for releveling the net. Such a constant reference bench mark near the center of a bench-mark net could eliminate the need for releveling to a regional reference bench mark many kilometres distant.

A guidelines manual for surface monitoring of geothermal areas (Van Til, 1979) was prepared recently to serve as a guide to monitoring the magnitude and direction of land-surface movements prior to, during, and following withdrawal of geothermal fluids from the ground. This manual not only discusses the design of systems and procedures for monitoring subsidence but also describes the capabilities and limitations of instruments available for monitoring purposes. Anyone concerned with the design or operation of a subsidence monitoring system should find the Van Til manual very helpful. Table D-1 from this manual, summarizing instrument capabilities for measuring land-surface displacements, is included as Appendix A in this guidebook.

2.2.2 Other techniques for measuring land-surface displacement

Other instruments utilized in measuring or monitoring differential vertical displacement at land surface are the theodolite with retroreflective targets, capable of measuring vertical angles to 1 second of arc or better, manometers for monitoring settlement of structures or land surface, and tiltmeters for measuring ground tilt. Van Til (1979) has summarized in tabular form the availability, performance characteristics, accuracy, and installation and operating requirements of 8 types of manometers and 6 types of tiltmeters used for monitoring vertical displacements at land surface (see Appendix A). Tide gage records, float measurement on water bodies, and changes in drainage pattern also can be very helpful in defining differential elevation changes or tilting.

2.2.3 Extensometer wells

2.2.3.1 Single and double pipe extensometers

Extensometer wells that have been developed to measure vertical movement or change in thickness of sediments or rocks are similar in principle but vary in detail. Japanese scientists pioneered in the development of this type of observation well. In the early 1930’s they installed the "single pipe well" (also called "single tube well") at several sites in Japan.

The single pipe well (Figure 2.3A), if installed to a shallow depth and passing through soft clay to an aquifer of sand or gravel, may accurately record by increased protrusion of the pipe at land surface the amount of compaction that has occurred in the soft clay. However, at depths greater than 50 to 100 m, the weight of the overlying sediments develops substantial lateral pressure on the pipe. This pressure, which increases with depth, increases the frictional resistance to movement and hence enhances the tendency for the pipe to move vertically in accord with the surrounding sediments. Thus, as the depth to the compacting interval increases, the percentage of the compaction that will appear as increased pipe

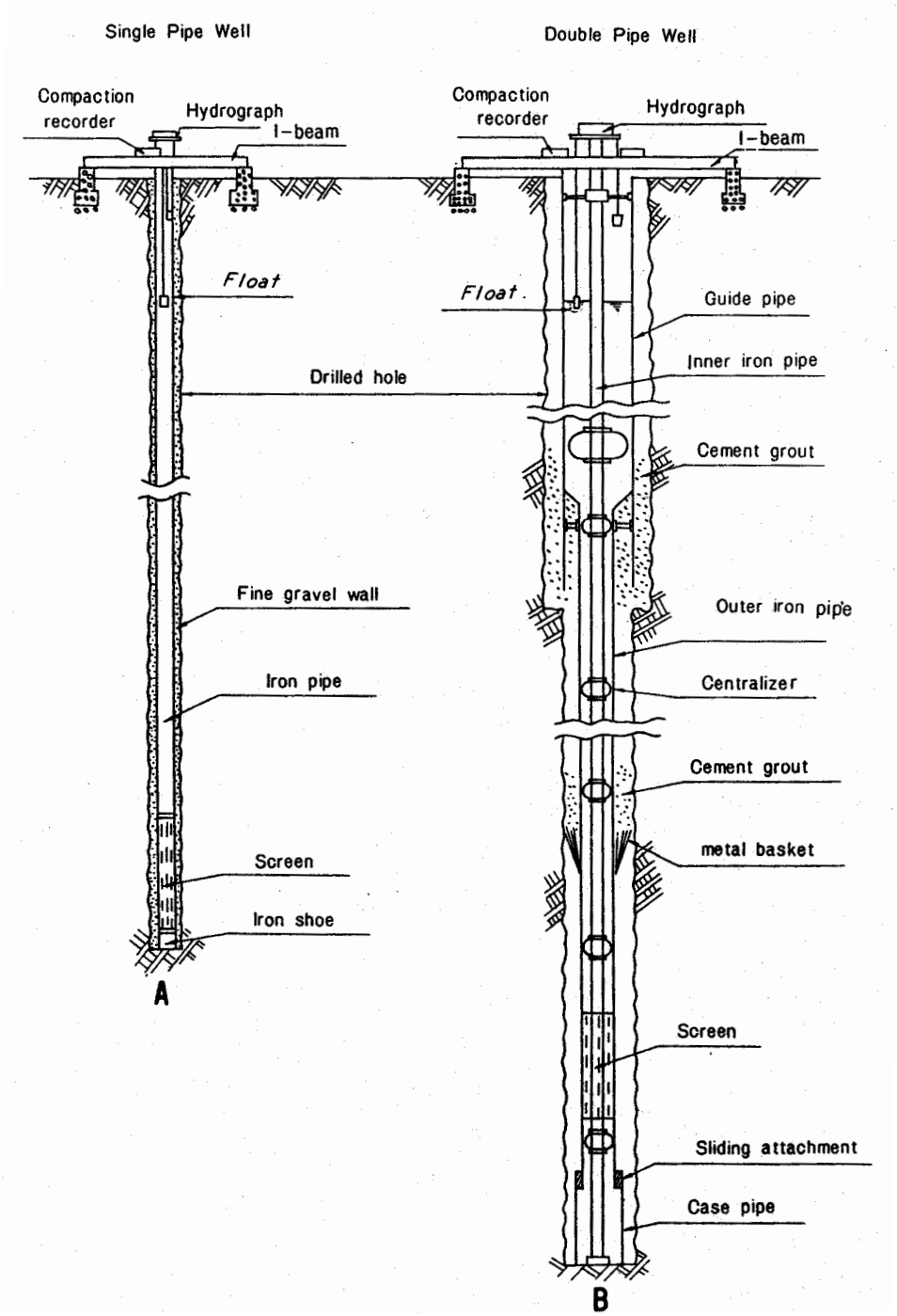

Figure 2.3 Diagram of Japanese extensometers. A, Single pipe well; B, Double pipe well (from Tokyo Metropolitan Gov't, 1969, Fig. 18).

protrusion above land surface decreases and compressional shortening of the pipe at depth increases. Therefore, although increased protrusion of a single pipe well above the land surface is an indicator of subsidence, it should not be considered a reliable measure of the magnitude of compaction for depths greater than 30 to 60 metres.

As demand for ground water increased in Japan and water wells were drilled to greater depths, Japanese scientists designed a "double pipe well" (Figure 2.3B) to measure compaction accurately. A double pipe well was installed at Osaka in 1938. The double pipe well consists

of two concentric iron or steel pipes, inserted into a vertically bored hole. The inner pipe is isolated from the sediments by the outer pipe, and is centered within the outer pipe by centering devices (centralizers). The apparent rising of the inner pipe indicates the relative downward displacement of the I-beam based on the land surface with respect to the top of the inner pipe. Thus, the amount of compaction of the sediments between the land surface and the bottom of the inner pipe can be recorded. The water level in the outer pipe represents the pore-water level or artesian pressure of the aquifer, transmitted through the screen section installed in the outer pipe. This water level is registered by a float-operated water-level recorder when the space between pipes permits.

Note (Figure 2.3B) that the outer pipe is suspended in the well, with a slidable sleeve of oversize casing hanging on the base of the outer pipe and resting on the well bottom. By this means, the weight of the outer pipe is removed from the well bottom and suspended at the land surface.

At the Funabashi-2 well in Chiba (Figure 2.4) the diameter of the outer tube to 60 m depth is 350 mm to accommodate a water-level float, but below that depth is reduced to 200 mm. The diameter of the inner tube is 80 mm. The annulus between the outer tube and the hole wall is cemented at 60 m and 75 m depth. The bottom part of the outer tube has the sliding sleeve ("casing tube") attachment to prevent loading of the well bottom by the weight of the outer tube. The sleeve, closed on the bottom with a bearing plate, is landed on a solid sandy layer and supports the inner tube. Thus, the outer tube can move independently from the inner tube and the sleeve. Figure 2.4 also shows the design of the centralizer--the device centering the inner tube in the outer tube (B)--and details of the instrumentation for recording compaction (or subsidence) and water-level fluctuation (C). If the double tube extensometer well extends through and beneath the base of the compacting sediments, the extensometer records gross compaction, which equals land subsidence if no tectonic movement contributes to the change in land-surface elevation. However, if the bottom of the well is within the compacting interval, the extensometer records compaction--a partial component of the land subsidence.

The validity of the extensometer record depends on the stability of the base of the inner tube with respect to the geologic formation, the stability of the instrument platform with respect to land surface, the degree in which friction between the outer and inner tubes can be minimized, and the accuracy of the measuring apparatus.

The weight of the capped sleeve is composed of its dead weight and the weight of the inner tube. In the Funabashi-2 well, at the bottom plate of the sleeve, the load on the sand-gravel layer is about 2.9 metric tons. Meyerhof (1956) derived a formula to evaluate an ultimate bearing resistance R_u by the number of blows on the sampling spoon during performance of a standard penetration test:

$$R_u = 40\ \bar{N} A_P,$$

where $\bar{N}$ is the average of N blows per foot in a depth interval between 1.0 d downward and 4.0d upward from the base of the tube, A_p is the area of the base of the tube, and d is the diameter of the pile. The diameter of the sliding sleeve (casing tube) in the Funabashi well is 225 mm (Figure 2.4). Thus, $A_p = 0.040\ m^2$. In general, the N value of the sand layer in the Diluvium (Pleistocene) is more than 30. Considering the large factor of safety we can use a reduced formula of

$$R_u = 30\ \bar{N} A_P = 30 \times 30 \times 0.040\ m^2 = 36 \text{ tons}.$$

Then in this case with $0.040\ m^2$ base area, the steel tube of the well can bear about a 36-ton load. According to the above calculation, the Funabashi-2 well will not sink into the sand-gravel layers. Differences between the results of compaction recorders and dial gauges and also differences between the results of water-level recorders and taped measurement are very small. Hence, it is concluded that extensometer wells having the same construction as the Funabashi-2 well should furnish a good record of compaction or subsidence, provided down hole friction is minimal (the well bore is close to vertical).

2.2.3.2 Anchored-cable and pipe extensometers

The United States Geological Survey (USGS) has developed extensometers (compaction recorders) of two types, anchored-cable and free-pipe, both of which are illustrated in Figure 2.5. The anchored-cable extensometer (A) was first installed in 1955 in an unused irrigation well 620 m deep on the west side of the San Joaquin Valley. The extensometer consists of a heavy anchor

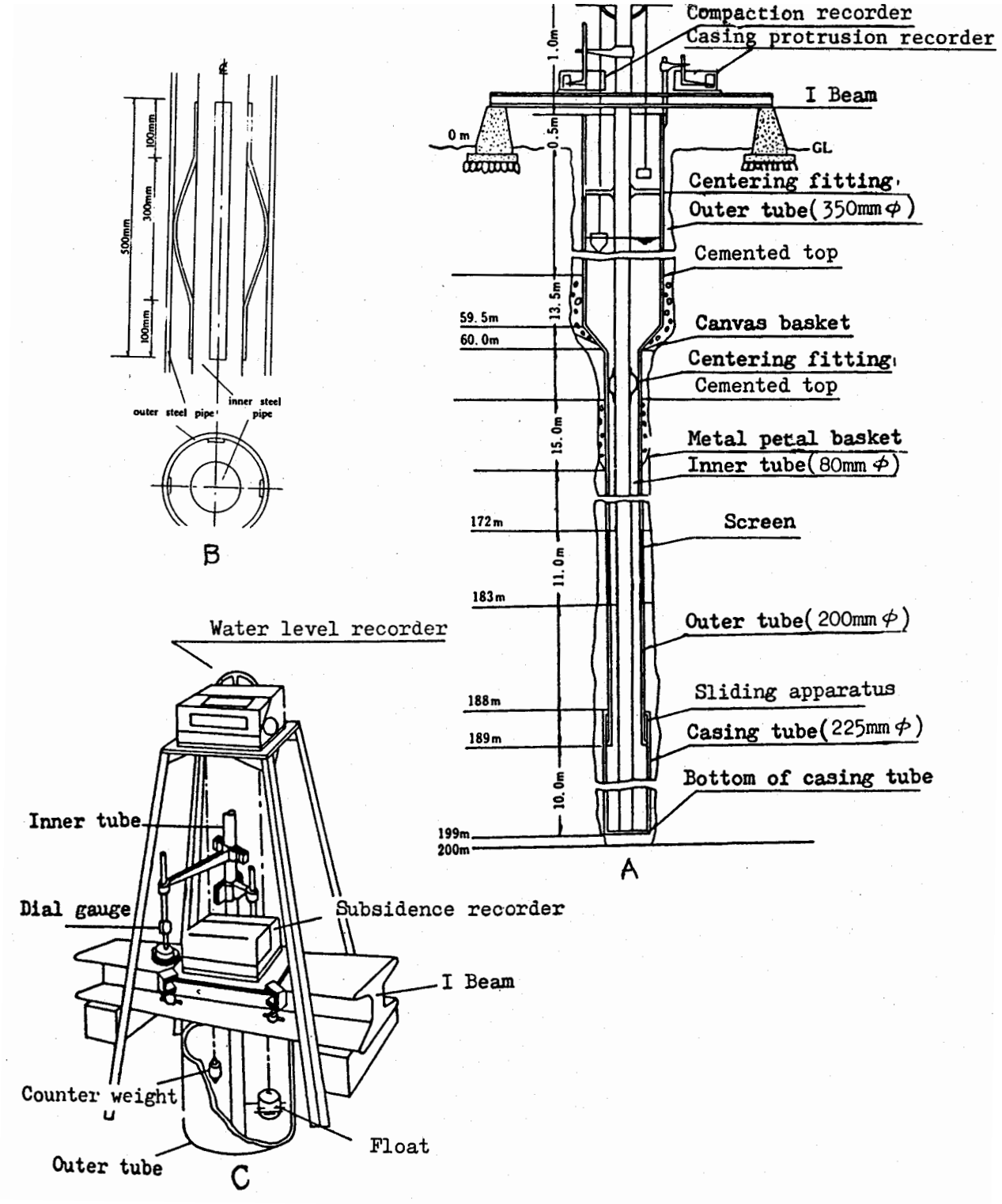

Figure 2.4 Structure of Funabashi observation well (double-tube type). A, Sectional view; B, Centralizer detail; C, Recorder detail.

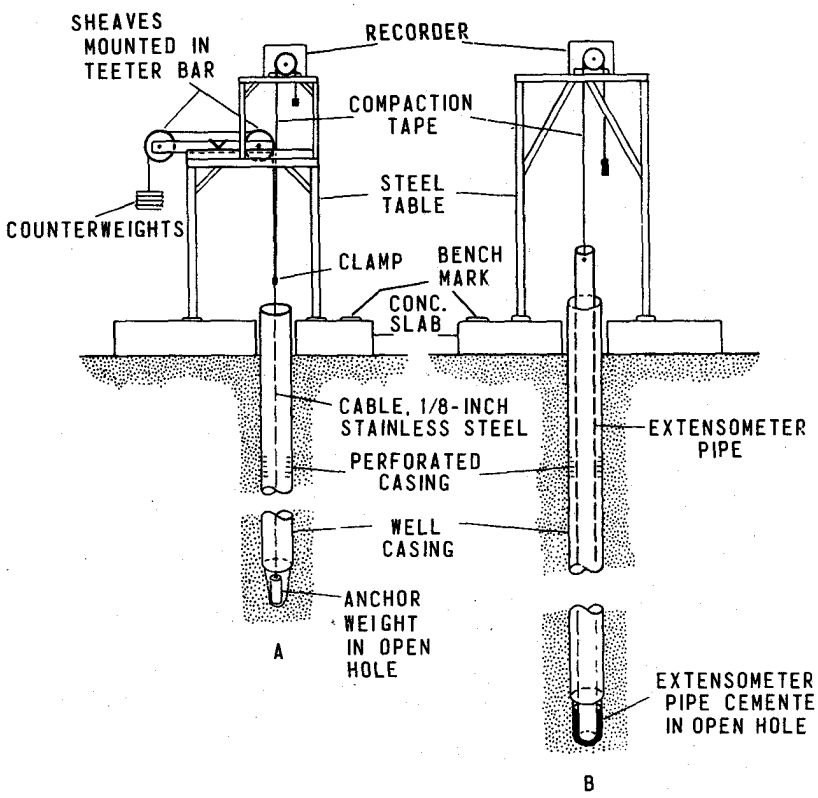

Figure 2.5 Recording extensometer installations. A, Anchored-cable assembly; B, pipe assembly.

(subsurface bench mark) emplaced in the formation beneath the bottom of a well casing; the anchor is attached to a cable that passes over sheaves at the land surface and is counterweighted to maintain constant tension. The cable is connected to a recorder that supplies a time-graph of the movement of the land surface with respect to the anchor--the compaction or expansion of the sediments within that depth range. The inked curve on the recorder chart commonly is amplified 10:1 by suitable gear combinations. The accuracy of the anchored-cable extensometer depends on the plumbness and the straightness of the well casing, the durability and stretch characteristics of the downhole cable, and especially on the success of minimizing cable-casing friction. As pointed out by Lofgren (1969), the cable must remain at constant length during the period of record. If the length changes due to temperature changes, fatigue elongation, or untwisting, the length change is indistinguishable from the record of compaction. The cable now used is a 1/8-inch (3.175 mm) diameter preformed stainless steel, 1 x 19 strand, reverse-lay "aircraft" cable. In order to minimize frictional drag of the surface sheaves, a "teeter bar" on a knife-edge fulcrum (Figure 2.5A and Lofgren, 1969, Figure 8) was designed. Changes as small as 0.1 to 0.2 mm in the thickness of an aquifer system can be recorded with this equipment.

This type of extensometer is being used in California, Nevada, and Arizona in wells as much as 700 m deep. Detailed tests of the accuracy of a similar cable-type extensometer have been made at the Groningen gas field in The Netherlands (de Loos, 1973).

For reasons of economy, most cable extensometers have been installed in unused irrigation wells, after cleaning out the casing and deepening the hole about 10 m below the casing shoe. The anchor weight of roughly 100 kilograms is then lowered into the open hole in the sediments several metres below and independent of the well casing.

To eliminate much of the cable-casing friction problem and thus improve the accuracy of the extensometer record the USGS has installed since 1966 about 30 free-pipe extensometers in California, Arizona, Louisiana, and Texas, to depths as great as 1,000 m. These pipe extensometers (Figure 2.5B) are similar in principle to the Japanese double pipe well. However, they differ in some features. The inside diameter of the well casing (outer pipe) commonly is 4 to 5 inches (10 to 13 cm) and the outside diameter of the couplings on the inner (extensometer)

pipe ranges from 2 to 3.4 inches (5.1 to 8.6 cm). Thus, the space between the casing and the extensometer pipe couplings is only about 2 inches (5 cm); hence, casing centralizers have not been used to center the extensometer pipe. Centralizers have been used, however, in the annulus between the casing and the borehole wall, to center the casing, especially when the law requires cement to be placed in this annulus to protect the ground water of good quality from contamination by water of poor quality at greater depth. Centralizers usually are spaced 15 to 30 m apart.

In about half the installations, a bearing plate on the bottom of the extensometer pipe is landed on the surface of a cement plug (placed in the open hole before the casing is run). In the remainder of the installations, the extensometer pipe is cemented in place in a pocket drilled below the casing shoe. In either case, the top of the cement plug is placed at least three m below the bottom of the casing shoe so that the dead weight of the casing does not stress the extensometer footing. Furthermore, this procedure minimizes the possibility that increasing downward loads, resulting from continuing compaction at shallower depths, will be transmitted through the casing to the extensometer footing. If the cementing of the extensometer footing is accomplished after that pipe has been run into the open-hole pocket, the cement slurry can be pumped into the pocket directly through the extensometer pipe. Care must be exercised, however, in calculating (1) the quantity of cement slurry needed to fill the desired interval of the pocket, and (2) the quantity of followup water needed to displace most of the slurry from the pipe into the pocket without thinning the slurry with water. If the pipe is raised several metres as soon as the followup water has been pumped into the pipe, the water pressure into the pipe and casing can be equalized and the pipe can then be lowered again to rest in the hardening slurry.

Three free-pipe extensometers have been operated since 1975 at a site within a subsiding area in Baton Rouge, Louisiana. These extensometers record compaction of the sediments and water-level change within each of the three depth zones. The extensometer pipes extend to depths of 254, 518, and 914 m. The installations and the record obtained through 1979 have been described by Whiteman (1980). The deepest extensometer indicates an annual land-surface fluctuation of about 4 cm, apparently an elastic response.

The conversion of an abandoned oil-test hole at Westhaven, California, into a dual extensometer and a dual water-level observation well is described in this guidebook because such abandoned oil-test holes are available in many countries, and the cost of conversion is only a small fraction of the cost of drilling and completing one or more new extensometer wells. Figure 2.6 is a diagrammatic sketch of the converted well. This summary of the conversion is condensed chiefly from Poland and Ireland (1965). When the oil-test hole was drilled, a surface string of 11-3/4 inch (29.84 cm) casing was installed from land surface to 611 m. Cement was pumped into the annular space around the casing, from the bottom shoe to land surface, providing a continuous seal to protect the fresh ground water. On abandonment a cement plug was placed in the well between 1930 and 2030 feet (588 and 619 m).

The blank casing was converted to a dual water-level observation well in April 1958. The 11-3/4 inch casing was gun perforated at two depth intervals, near the top and base of the confined aquifer system (see Figure 2.6). To obtain hydraulic separation of the two perforated intervals, a 4-inch diameter pipe with a packer flange at its base was run to a depth of 860 feet (262 m); a cement plug was then placed on top of the packer, thus sealing the annulus between the two casings. Initially, the inner pipe was suspended in tension by a casing hanger resting on the top of the 11-3/4 inch casing. Four months after the inner pipe was installed, the hanger appeared to be rising off the top of the 11-3/4 inch casing, indicating shortening of the casing between land surface and the cemented packer. Beginning in August 1963 the shortening of the full length of casing above the basal cement plug was measured by lowering an anchor weight on top of the cement plug and counterweighting the cable at land surface (see Figure 2.6). Thus the conversion of the oil-test hole provided two water-level observation wells and two extensometers: a pipe-type to 845 feet (258 m) and a cable-type to 1,930 feet (588 m) below land surface.

Monthly measurements from 1964 to the end of 1970, inclusive, indicated compaction from 0-845 ft (0-258 m) was 1.94 ft (0.59 m), and from the land surface to 1,930 ft (0-to-588 m) was 3.57 ft (1.09 m).

These observations at the Westhaven site indicate that even heavy oil-well casing encased in a cement jacket is too weak to resist the compressional force of the compacting sediments. Even in the shallow depth interval from land surface to 845 ft (258 m), the increased protrusion in seven years was only equal to 12 per cent of the subsurface shortening in that interval. It is concluded that in an area subsiding because of sediment compaction due to decrease in fluid pressure, the top of a well casing is not a stable reference bench mark, even if the casing

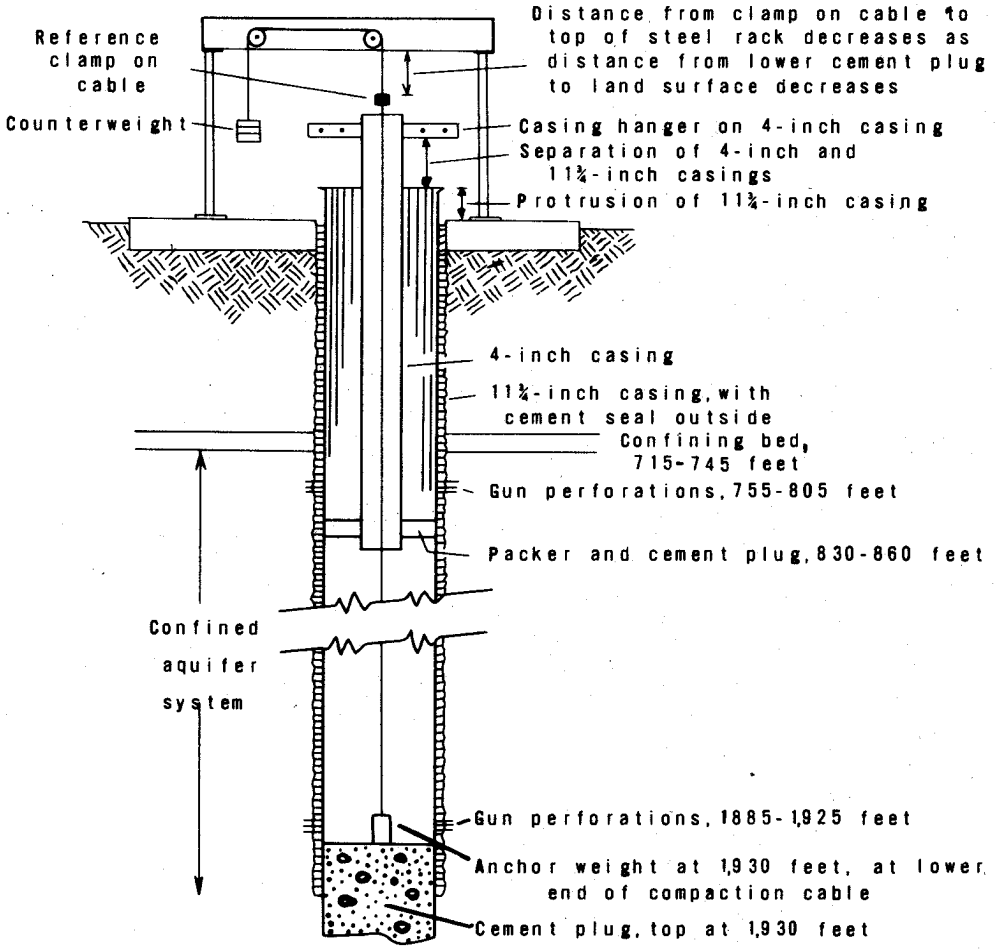

Figure 2.6 Diagrammatic sketch of wells used for measuring water levels and compaction: wells 20/18-1102 and 1103 (from Poland and Ireland, 1965).

extends below the compacting sediments. Also, the evidence is clear that increased protrusion of a casing above the land surface, even though an indicator of land subsidence, is not a reliable measure of either compaction or subsidence. Bull (1975, p. 41-45) cites additional evidence concerning the minor amount of casing protrusion compared to subsurface casing compression in wells on the west side of the San Joaquin Valley.

In Mexico City, however, observed protrusion of some water-well casings has been about the same magnitude as the subsidence. Poland and Davis (1969, p. 225-228 and pl. 6) show graphic pictures taken by Ing. R. Marsal in 1954 of the protrusion of casings of two wells drilled about 1923. They were drilled to a depth of about 100 m but most of the compaction occurs in the highly compressible lake clays in the top 50-60 m. The subsidence at the well sites from 1891 to 1959 was 5.9 m. In 1954, one casing protruded 5.45 m and the second 4.5 m. The protrusion of 5.45 by 1954 is about equal to the subsidence by 1954, proving that essentially all the compaction at the well site is occurring in the top 100 m of sediments, and probably mostly in the top 60 m. The lateral pressure to this depth may not be great enough to compress the outer casing as compaction occurs. However, the excessive protrusion is believed to be due in part to the fact that wells are drilled using more than one casing size.

In evaluating the characteristics of cable and pipe extensometers, the following factors should be considered:

1. If a cased well is available, the cable extensometer costs less to install than the pipe extensometer, chiefly due to the lower unit cost of the cable compared to the pipe.

2. The cable extensometer has minimal cable-casing friction when the well casing is of large diameter (30-40 cm); the friction increases when the well casing is of small diameter (10-15 cm), all other factors being equal.
3. In contrast, the pipe extensometer has minimal pipe-casing friction when the well casing is of small inside diameter (10-15 cm) and the overall space between pipe or pipe couplings and well casing is in the range of 4-6 cm. Alternately, if the well casing is of large diameter, use of pipe centralizers spaced 15 to 30 m apart between casing and pipe, as is done in the Japanese double pipe wells (Figure 2.3B), may produce a record as good as that obtained with the pipe-in-small-casing design. So far as known, no comparative test has been made.
4. The pipe extensometer commonly gives a more accurate record than the cable extensometer, all other conditions being equal.
5. If a well can be drilled so plumb and straight that the departure from verticality at the base does not exceed the inside diameter of the casing, the cable can be positioned to avoid any downhole cable-casing friction. Under such circumstances the cable extensometer is more frictionless than the pipe extensometer. However, a well drilled to a depth of 50 m and with a casing diameter (inside) of 0.3 m would have a departure of 0.3 m from verticality at the bottom if the drift from verticality was 0°20′. For a well 100 m deep, a departure from verticality of 0.3 m at the bottom would require that the drift be held to 0°10′. Thus, it would appear that the chances of drilling a well more than 100 m deep that is sufficiently plumb to eliminate any cable-casing friction are remote. The above discussion does not consider possible cable-casing friction caused by the tendency of rotary-bored holes to develop a spiral pattern.

A cable extensometer at the USGS Cantua site in the San Joaquin Valley, California, installed to a depth of 610 m in a well with 10 cm casing to 595 m, had so much cable-casing friction that the equipment recorded no compaction even when as much as 7.6 cm of compaction had occurred during the prior month. At the time of the monthly visit to service the equipment, the cable was stretched--that is, the counterweight was pushed down about 30 cm and then allowed to rise gently. This operation triggered enough down-hole slippage of the cable at friction points (cable-casing friction) to permit the cable to move upward and record the approximate compaction that had occurred since the last monthly visit. Bull (1975, p. 32 and Figure 25) has discussed the problem and reproduced a part of the stairstepped field record from the extensometer. This extensometer equipment was installed in a corehole. When drilled, the plumbness of the hole was surveyed at 30-metre intervals with a driftmeter. The drift from vertical was 1 degree at 90 m depth and ranged from 5 to 6 degrees between 244 and 580 m depth. In spite of the nonverticality of the hole (and of the casing), an interpolated cumulative compaction curve drawn through the low points of the stepped record produced a reasonably accurate long-term compaction curve for the deep Cantua site extensometer. The compaction plot for well N1 in Figure 9.P.8 is the 13-year record of 3.4 m shortening for sediments between land surface and a depth of 610 m.

At the Terra Bella site on the Friant-Kern Canal in the San Joaquin Valley, casing of 10-5/8 inch (27 cm) diameter was placed in a well to a depth of 377 m and an extensometer pipe of 1-1/2 inch (3.8 cm) diameter was inserted and landed at a depth of 381 m. No centralizers were used. Most of the record in the field compaction charts for this extensometer is composed of a series of stair-step adjustments with individual vertical displacements of 0.15 to 0.3 mm (1-5 to 3 mm at the 10:1 magnification). The overall space between the well casing and the extensometer pipe-couplings is nearly 20 cm, permitting too much flexing of the inner pipe and too many friction points. The compaction record at this site probably could be improved by adding centralizers to center the inner pipe in the casing, by increasing the size of the inner pipe, or by use of a lever and counterweight system at land surface to remove a substantial part of the dead weight of the extensometer pipe. This last procedure should produce the greatest reduction in pipe-casing friction.

Under most favourable conditions, the pipe extensometer as described in this manual will function satisfactorily to depths of 750 to 1,000 m. The most favourable conditions would require straight holes--holes drilled with deviation from the vertical of less than 1/2 degree-and a combination of well casing and extensometer pipe sizes, or use of centralizers, that minimizes pipe-to-casing friction.

The cable extensometer will supply approximate measurements to depths of 600 to 850 m, but the results are less accurate, in general, than with the pipe extensometer.

The depth to which the pipe extensometer equipment is operative--750 to 1,000 m--is adequate for studies of subsidence due to ground-water withdrawal in most of the world. Much ground water is pumped from aquifers less than 300 m deep and most from aquifers less than 600 m deep. However, improvement in the accuracy of compaction measurements at depths greater than 300 m is highly desirable. Furthermore, in connection with the study of subsidence due to other causes, or subsidence due to other types of fluid withdrawal, such as geothermal or oilfield fluids, there is need for improvement of extensometer design to increase the depth of useful measurements. For example, much or nearly all of the dead weight of the inner extensometer pipe can be removed by use of a lever and counterweight system at land surface. Most of the pipe would then be in tension and the frictional stress between pipe and casing should be greatly lessened at the time of compression (or expansion) of the well casing. This method has been applied by Ben E. Lofgren (oral communication, December 1975) to an extensometer 317 m deep in Imperial Valley, California, where more than two-thirds of the pipe weight has been removed by a counterweighted lever designed with a 10-to-1 mechanical advantage. Also, one highly sensitive extensometer was recently constructed in Arizona to a depth of 380 m using this method (F. S. Riley, oral commun., July 1979). In this installation the upper 75 per cent of the extensometer pipe was placed in tension while the lower 25 per cent remained in compression. The neutral point was positioned at a major bend in the casing, as determined by a borehole alignment survey. Before installation of the lever and counterweight this installation had severe friction problems and produced a record characterized by intermittent stair-step movements. After counterweighting the instrument produced a smooth record of continuous compaction.

Research is needed to determine the accuracy of such a lever and counterweight system through a wide span of unloading of the extensometer pipe, say from 25 per cent to 90 per cent. Comparison of simultaneous compaction records from a normally loaded pipe extensometer and a nearby counterweighted extensometer of the same depth and construction, in an area of active subsidence, would be very instructive. Several stages of unloading could be applied to the counterweighted extensometer.

Another way in which the weight of the pipe in a free-pipe extensometer can be reduced is by installing a tapered pipe assembly. For example, the bottom third of the pipe could be 2-1/2 inch, the middle third 2-inch, and the upper third 1-1/2 inch; or the assembly could be 2-inch, 1-1/2 inch, and 1-inch. For an extensometer 750 m deep, a free pipe of 2-1/2 inch constant diameter would weigh 6,580 kg. But if the pipe was installed with equal lengths (250m) of 2-1/2 inch, 2-inch, and 1-1/2 inch pipe, the weight on the bottom joint of the 2-1/2 inch would be decreased about 30 per cent (neglecting buoyancy effects). The decrease in weight should decrease the cost of the installation, and simplify the addition of a lever and counterweight at land surface, if desired.

2.2.3.3 Slip joints

When extensometer or observation wells are being installed in an area that is subsiding at a rapid rate, it is advisable to consider the need for installing a series of slip joints in the casing during construction. When extensometers were being installed on the west side of the San Joaquin Valley of California in 1958-62, the ground-water reservoir was compacting as rapidly as 30 cm per year. Under such circumstances, it was anticipated that the casings of deep extensometers would last longer under severe compressive forces if slip joints were inserted in the well casing. Accordingly, at the Cantua site, for example, eight slip joints were placed at 60-metre intervals in the 4-inch casing 595 metres deep. Figure 2.7 shows details of the slip joint. Each slip joint has about 0.9 m of play between the open and closed position. Since installation in 1958, this extensometer has shortened about 3.5 m. Without slip joints, the elastic compression of the 4-inch (10 cm) casing from full tension when first suspended in the well to the elastic limit in compression would have been about 1.2 m. The additional shortening of 2.3 m beyond the elastic limit of the casing must have resulted from compressional failure of the casing or shortening of the slip joints, or both. Because this equipment is still functioning as an extensometer, we conclude that a major part of the 3.5 m of shortening must have occurred through shortening of slip joints.

2.2.3.4 Telescopic extensometer

An experimental telescopic extensometer, designed by Ignacio Sainz Ortiz, was installed in Mexico City to a depth of 60 m in 1953. Figure 2.8 shows that in the 6-year period 1953-59, 36 cm of shortening occurred in the 60-metre thickness of near-surface deposits. In the first 20-30 m below the land surface lateral stresses against the casing are small. Nevertheless,

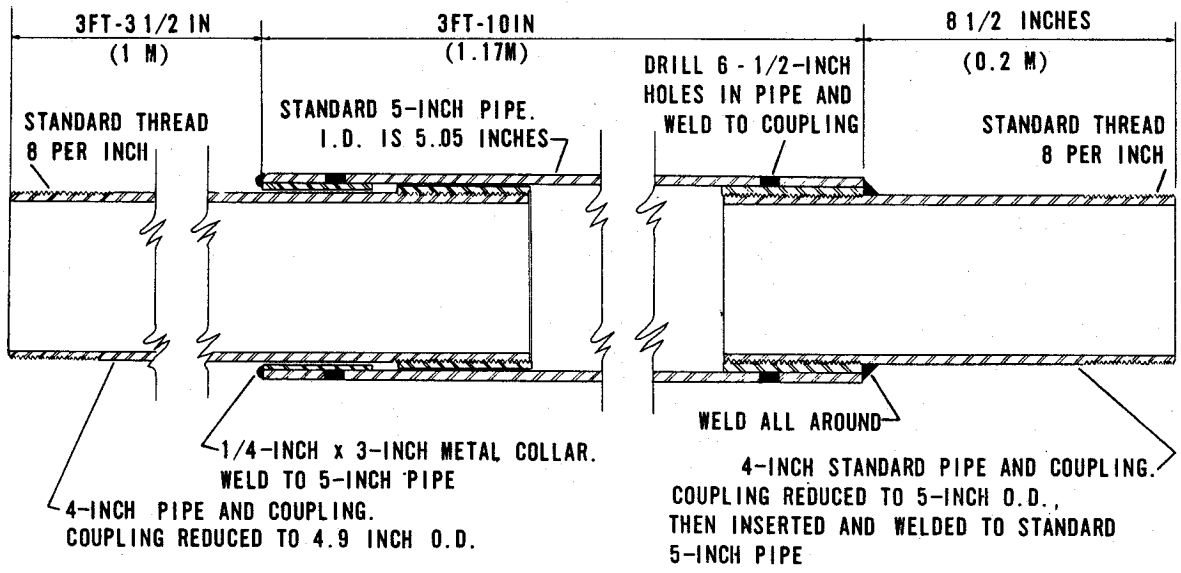

Figure 2.7 Diagram of slip joint.

considering the flexibility of the telescopic construction, the lateral stress should develop enough skin friction to cause the casing to shorten in accord with the surrounding sediments, even at the shallow depth range involved.

2.2.3.5 Extensometer records

Plots of cumulative compaction against time obtained from extensometer records are becoming fairly common in the published record, in connection with field research on land subsidence due to ground-water withdrawal. For example, in Japan, Miyabe (1967, p. 2-3) published compaction plots obtained from extensometers in Tokyo and Hirono (1969) showed plots of compaction from extensometers in Niigata. In the United States, extensometers have been operated for more than 20 years in the San Joaquin and Santa Clara Valleys, California. Computer plots of cumulative compaction through 1970 at 30 sites, together with water-level fluctuations, change in applied stress, and subsidence at most of these sites, have been published (Poland, Lofgren, Ireland, and Pugh, 1975, Figures 53-78).

In the case history for subsidence in the Santa Clara Valley, California, Figure 9.14.5 contains time plots of compaction for 15 years for two depth intervals at the San Jose extensometer site. In Figure 9.14.6 the measured compaction is plotted in annual increments that present a more quantitative picture of the annual change in amount of compaction than does the cumulative plot.

If two or more compaction recorders (extensometers) are installed in adjacent wells of different depths, the record from the multiple-depth installation will indicate the magnitude and rate of compaction (or expansion), not only for total depths of individual extensometers but also for the depth intervals between well bottoms. Figure 9.13.8, discussed in the case history of the San Joaquin Valley, California, is a good example of the record from a multiple-depth installation, and is one of six multiple-depth sites in the valley.

2.2.4 Other techniques of subsurface measurement

2.2.4.1 General

In addition to the pipe-type (double pipe) and anchored-cable extensometers described earlier in this chapter, a number of instruments utilizing similar principles but differing in measurement techniques are being manufactured commercially. O'Rourke and Ranson (1979) have made a summary

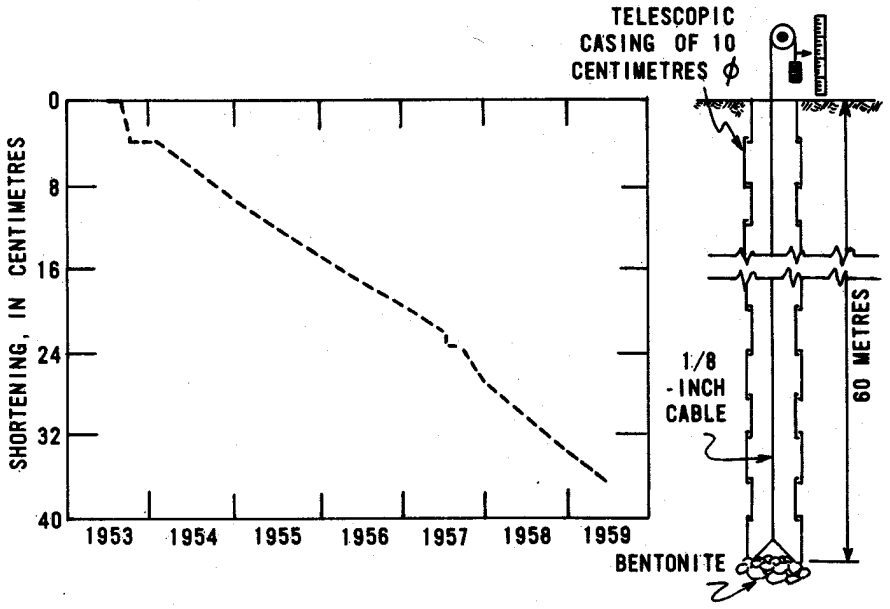

Figure 2.8 Sketch of telescopic extensometer and 6-year record of shortening (compaction of deposits). Redrawn from the Comisión Hydrologica de la Cuenca del Valle de Mexico, 1961, Boletin de Mecanica de Suelos, no. 3, p. 55.

appraisal of the capabilities of existing instruments for monitoring subsurface vertical displacement, examined with respect to availability, performance characteristics, and installation and operating requirements. The summary, reproduced as Appendix B of this guidebook, describes capabilities of 6 wire-type and 6 rod-type extensometers; 1 pipe-type extensometer (the USGS type); 2 multiple base length extensometers with sensors and anchors or magnet markers; 1 chain type extensometer with anchored sensor case; and 6 sonde-type extensometers, including the casing-collar locator and the gamma-ray logger. For details on the various wire-type and rod type extensometers for measuring subsurface vertical displacement, the reader is referred to Appendix B.

The techniques of casing-collar logging and gamma-ray logging with radioactive bullet markers require the use of specialized and expensive equipment. Normally this service would be provided by oil well service companies. In subsidence studies of most ground-water basins, however, the cost of utilizing such expensive equipment on a repeat basis probably would not be economically justified in most cases, when costs were compared with other study techniques. However, because such repeat logging has the decided advantage of indicating the depth range, rate, and magnitude of compaction or expansion of the sediments, a brief statement of the two techniques follows.

2.2.4.2 Casing-collar logging

At Long Beach, California, in the Wilmington oil field, changes in thickness of compacting zones have been measured successfully by running a magnetic collar locator periodically in the same well to determine the change in the distance between casing collars between surveys. According to Allen (1969), the first "collar counting" was in 1949 and more than 200 multiple traverse runs have been made to depths of as much as 1,800 m. These collar logs can be used to measure change in length of individual joints compared to joint length when placed in the well or since a prior logging. They also indicate the depth range, rate, and magnitude of compaction of the sediments if it is assumed that the casing or cement at every point moves in exact accord with contiguous sediments as a result of skin friction produced by lateral stresses. The field evidence at Wilmington from various sources generally supports this assumption for depths greater than 600 m. Collar surveys run five times from 1949 to 1960 in an individual well (Figure 2.9) graphically indicate the depth range, rate, and magnitude of compaction of three

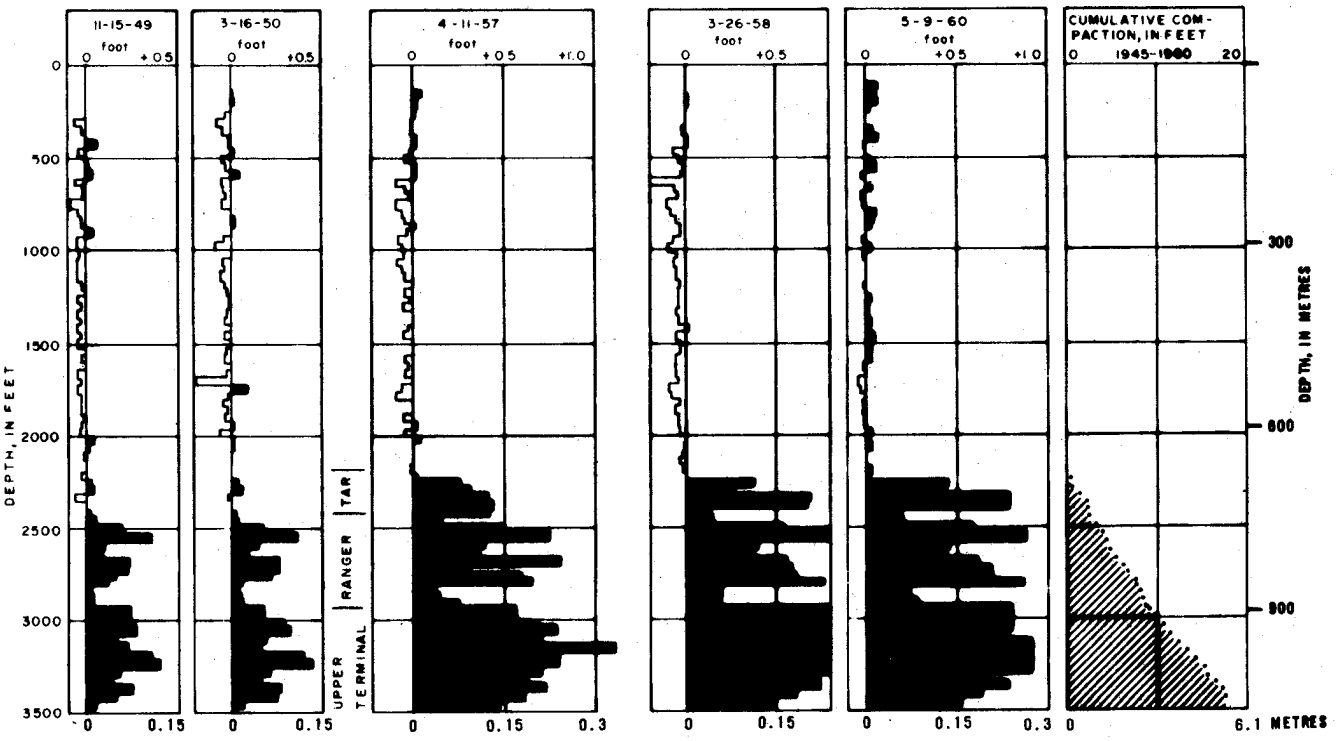

Figure 2.9 Casing collar surveys of a typical well in the Wilmington oil field. Survey on date indicated compared to casing tally of 9-26-45; elongation due to tension shown to left of zero reference, shortening due to compression shown to right (shaded); length of casing joints 12.5 to 13.4 m., in general (data courtesy of Long Beach Harbor Dept.).

oil zones--the Tar, Ranger, and Upper Terminal. The cumulative compaction of these three zones from 1945 to 1960 was 17.6 feet (5.4 m) as summed from the shortening of the casing joints by 1960 compared to their measured length in 1945. Allen and Mayuga (1969, Figure 13) also showed that collar logs can be used to measure oil-zone expansion in an area of rebound by plotting collar-log surveys of wells producing from oil zones that are receiving injection water. According to Allen (oral commun., 1977), recent developments in casing-collar logging at Wilmington provided an accuracy of 9 mm 88.5 per cent of the time for joint lengths of 12.5 to 13.4 m, measured three times. The maximum degree of instrument error is estimated to be 30 mm for each joint length.

Casing-collar logs also have been made in the oil fields on the eastern shore of Lake Maracaibo in Venezuela where maximum subsidence has been about 4 m (Nuñez and Escojido, 1977).

2.2.4.3 Radioactive-bullet logging

At Wilmington, California, at the Lake Maracaibo oil fields in Venezuela, at the methane gas and brine reservoirs of Niigata, Japan, and at the Groningen gas field in The Netherlands, radioactive bullets have been shot into the formation at known depths, and their positions resurveyed later by gamma-ray detectors to measure compaction or expansion. The accuracy of the radioactive-bullet logging equipment used at Wilmington is reported by Allen to be about 3 cm per distance between bullets (at Wilmington 6.1 m) when logging at 7.6 m per minute.

Schoenbeek (1977) reports improvement in the accuracy of measurement at the Groningen gas field. The sandstone reservoir depth is about 2900 m, and the average thickness about 150 m. Radioactive bullets were shot into the formation at 10-m intervals; relative displacement was measured with a gamma-ray sonde containing three detectors. After considerable improvement of technique, the mean error of measurements determined by statistical analysis was reported to be

1 cm in 100 m of measured interval. To achieve this accuracy, however, the logging time had to be slowed to about 20 m per hour. DeLoos (1973) has described in detail the development and testing of logging equipment.

At Niigata, Japan, the radioactive bullet technique was refined by experiments in 1959-60 and the construction of two observation wells (Figure 2.10). According to Sano (1969), the first observation well (Yamanoshita) was completed in 1960 to a depth of 650 m. Four sizes of casing were used, each stage from bottom to top being of larger diameter than the preceding one. The base of each stage was grouted to the contiguous strata and overlapped the head of the stage below it. Sano (1969) states that it was intended that the increase in the overlapped length of each stage should represent the shrinkage between the strata to which the casing was grouted. The system was unsuccessful because the casing contracted with the shrinkage of the formation.

The second well (Uchino) was completed in 1961 to a depth of 950 m. It was constructed with a conductor pipe 100 m long cemented to the surrounding strata through its full length. The main casing 5-1/2 inches in diameter was suspended in the conductor pipe, In effect, this observation well was the single pipe type.

In both observation wells, radioactive bullets were shot into the formation every 40 m and radioactive reference pellets were attached to the casing every 20 m (Figure 2.10). Special logging equipment was designed to improve accuracy. Logging at about 1-year intervals from 1961 to 1966, when the deeper well failed, apparently was reasonably successful in determining location and general magnitude of compaction.

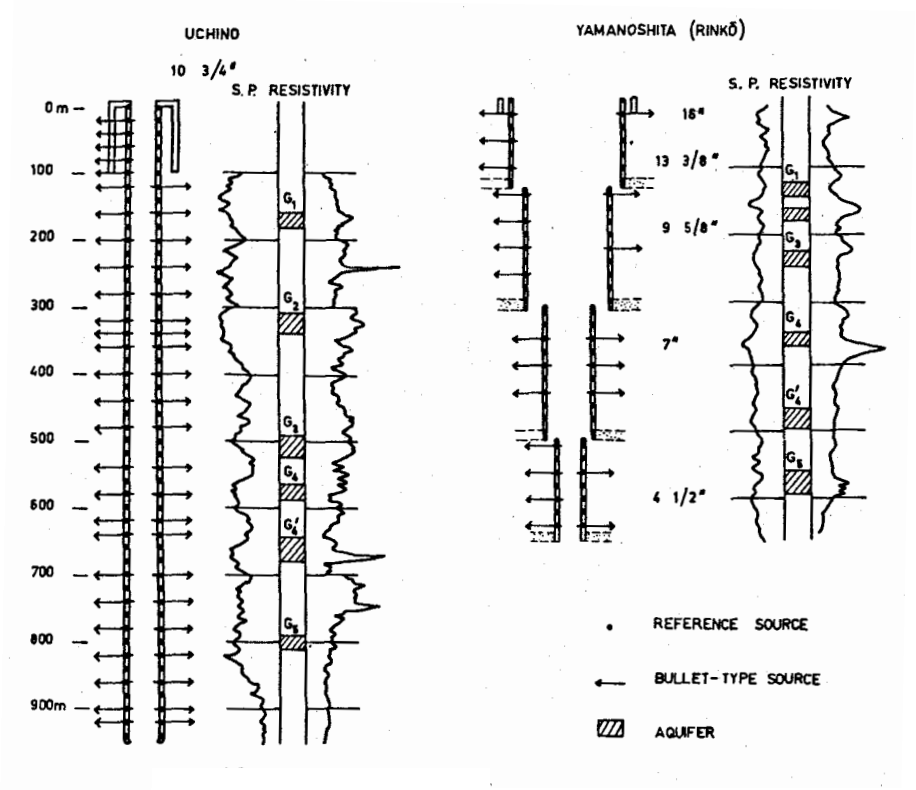

Figure 2.10 Structure of the observation wells in Niigata, Japan (after Sano and Kayana, 1966, Figure 2).

2.3 HORIZONTAL DISPLACEMENT

2.3.1 Land-surface displacement

In areas of subsidence due to fluid withdrawal, horizontal displacement of the land surface has been measured at only a few places. One of those is the Wilmington oil field in Los Angeles County, California, which has experienced as much as nine metres of subsidence. The vertical subsidence has been accompanied by horizontal movement directed inward toward the center of subsidence. This horizontal movement has been measured by surveys of a triangulation network of the Los Angeles County Engineer's office. In 1951, when subsidence at the center was 4.9 m, horizontal movement since 1937 had been as much as 1.9 m (Grant, 1954, Figure 1). By 1962, some points on the east end of Terminal Island had moved as much as 2.7 m, according to the Long Beach Harbor Department.

At Wairakei, New Zealand, Bixley reports that both horizontal and vertical movements have occurred along the steam mains route (see case history 9.9). Maximum movement is near bench mark A97 (Figure 9.9.5), where horizontal movement is about 75 mm/year and vertical movement 130 mm/year.

Until recently, short distances were measured by steel tape and longer distances by triangulation. Triangulation involves the measurement of the angles of a triangle, careful measurement of the length of one side, called the base line, and calculation of the lengths of the other two sides. The process can be extended through angular measurement of many additional triangles.

Within the last decade, however, extremely accurate means have been developed for measuring horizontal distances between points. Electronic Distance Measurement (EDM) equipment permits line-of-sight distance measurement, both rapidly and precisely. Thus, the location of points can now be determined by trilateration, whereby a network of triangles is constructed from one or more known points, with the length of all sides determined directly by use of the EDM equipment. Distance measurements by trilateration have largely replaced measurements by triangulation, especially where extreme accuracy is needed.

The general distance capabilities and accuracy of three types of EDM equipment are as follows:

1. Geodolite, capable of 1 unit in 107 units (laser), 30 km;
2. Electronic EDM, capable of 2 units in 106 (laser), 12 km;
3. Distance meter, capable of 1 unit in 105 (infrared), 3 km.

More information on EDM instruments and other types of equipment to monitor horizontal displacements at land surface are summarized by Van Til (1979, table D-1). Van Til's summary, reproduced in this guidebook as Appendix A, includes a listing of instrument capabilities of steel tapes, EDM instruments, and horizontal extensometers to measure ground strain or crack movement. The appraisal was made with respect to availability, performance characteristics, and installation and operation requirements.

2.3.2 Subsurface displacement

Instruments currently available for the measurement of horizontal displacement at depth are sonde-type borehole inclinometers. Oil-well service companies have equipment to measure both the drift angle (angle of departure from vertical) and the true compass bearing at desired depth intervals to depths as great as 6 km. Most other sonde-type inclinometers have been developed for near-surface geotechnical studies and in general have depth ranges limited to 200-300 m. The availability, operating principles, accuracy, and principal installation and operation features of 10 sonde-type borehole inclinometers and 3 fixed borehole inclinometers are summarized in Appendix B.

2.4 REFERENCES

ALLEN, D. R. 1969. Collar and radioactive bullet logging for subsidence monitoring, Soc. Prof. Well Log Analysts Trans., Paper G, p. 1-19.

ALLEN, D. R., and MAYUGA, M. N. 1969. The mechanics of compaction and rebound, Wilmington oil field, Long Beach, California, USA, in L. J. Tison, ed., Land subsidence, vol. 2, Internat. Assoc. Sci. Hydrology Pub. 89, p. 410-422.

BULL, W. B. 1975. Land subsidence due to ground-water withdrawal in the Los Banos-Kettleman City area, California, Part 2, Subsidence and compaction of deposits, U.S. Geol. Survey Prof. Paper 437-F, 90 p.

FLOYD, R. P. 1978. Geodetic bench marks, National Oceanic and Atmospheric Administration Manual NOS NGS 1, 50 p. NOAA, Rockville, MD, USA 20852

GRANT, U. S. 1954. Subsidence of the Wilmington Oil Field, California, California Division of Mines, Bulletin 170, Chapter X, pp. 19-24.

HIRONO, TAKUZO. 1969. Niigata ground subsidence and ground-water change, in L. J. Tison, ed., Land subsidence, vol. 1, Internat. Assoc. Sci. Hydrology Pub. 88, p. 144-161.

LOFGREN, B. E. 1968. Analysis of stresses causing land subsidence. U.S. Geol. Survey Prof. Paper 600-B, p. 219-225.

LOFGREN, B. E. 1969. Field measurement of aquifer-system compaction, San Joaquin Valley, California, USA, in L. J. Tison, ed., Land subsidence, vol. 1, Internat. Assoc. Sci. Hydrology Pub. 88, p. 272-284.

LOOS de, J. M. 1973. In-situ compaction measurements in Groningen observation wells, Verhandelingen Kon. Ned, Geol. Mijnbouwk. Gen. Volume 28, p. 79-104.

MEYERHOF, G. G. 1965. Penetration test and bearing capacity of cohesionless soils, Proc., American Society of Civil Engineers, Jour. Soil Mech. and Found. Div., vol. 82, SM1 paper no. 866.

MIYABE, NAOMI. 1967. Study of partial compaction of soil layer--in reference to the land subsidence in Tokyo. Tokyo Ins. Civil Eng. Rept. 44, 7 p.

MURAYAMA, S. 1969. Land subsidence in Osaka, in L. J. Tison, ed., Land subsidence, vol. 1, Internat. Assoc. Sci. Hydrology Pub. 88, p. 109-130.

NUÑEZ, 0., and ESCOJIDO, D. 1977. Subsidence in the Bolivar Coast, Internat. Assoc. Sci. Hydrology Pub. 121, p. 257-266.

O'ROURKE, J. E., and RANSON, B. B. 1979. Instruments for subsurface monitoring of geothermal subsidence. Report prepared by Woodward-Clyde Consultants for Lawrence Berkeley Laboratory, Berkeley, Calif., LBL No. 8616, 33 p. and 23 tables.

POLAND, J. P., and DAVIS, G. H. 1969. Land subsidence due to withdrawal of fluids, in Varnes, D. J., and Kiersch, George, eds., Reviews in Engineering Geology, v. 2, Boulder, Colorado, Geol. Soc. America, p. 187-269.

POLAND, J. F., and IRELAND, R. L. 1965. Shortening and protrusion of a well casing due to compaction of sediments in a subsiding area in California, in Geological Survey Research 1965, U.S. Geol. Survey Prof. Paper 525-B, p. B180-B183.

POLAND, J. F., LOFGREN, B. E., IRELAND, R. L., and PUGH, R. G. 1975. Land subsidence in the San Joaquin Valley as of 1972, U.S. Geol Survey Prof. Paper 437-H, 78 p.

RAPPLEYE, H. S. 1948. The manual of geodetic leveling, Special Publication No. 239, NOAA, Rockville, MD, USA. 20852.

SANO, SUN-ICHI. 1969. Observation of compaction of formation in the land subsidence of Niigata City, in L. J. Tison, ed., Land subsidence, vol. 2, Internat. Assoc. Sci. Hydrology Pub. 89, p. 401-409.

SANO, SUN-ICHI, and KANAYA, H. 1966. Observation of partial shrinkage of strata, in Radioisotope instruments in industry and geophysics, Vol. 2, Internat. Atomic Energy Agency, Vienna, p. 279-291.

SCHOONBEEK, J. B. 1977. Land subsidence as a result of gas extraction in Gronigen, The Netherlands, Internat. Assoc. Sci. Hydrology Pub. 121, p. 267-284.

STEPHENS, J. C., and JOHNSON, LAMAR. 1951. Subsidence of organic soils in the Upper Everglades region of Florida, U.S. Dept. Agr., Soil Cons. Service, August, 16 p., 25 figures.

TOKYO METROPOLITAN GOVERNMENT. 1969. Land subsidence in Tokyo, Tokyo, 31 p.

VAN TIL, C. J. 1979. Guidelines manual for surface monitoring of geothermal areas, Report prepared by Woodward-Clyde Consultants for Lawrence Berkeley Laboratory, Berkeley, Calif., LBL report No. 8617, 121 p.

WEIR, W. W. 1950. Subsidence of peat lands of the Sacramento-San Joaquin Delta, California, California Univ. Agr. Exp. Station, Hilgardia, v. 20, no. 3, p. 37-56, June.

WHITEMAN, C. D., Jr. 1980. Measuring local subsidence with extensometers in the Baton Rouge area, Louisiana, 1975-79, Louisiana Department of Transportation and Development, Office of Public Works, Water Resources Technical Report no. 20, 18 p.

3 Mechanics of land subsidence due to fluid withdrawal, by Joseph F. Poland and Working Group

3.1 INTRODUCTION

The three types of fluid withdrawal by man that have caused noticeable subsidence under favorable geologic conditions are (1) the withdrawal of oil, gas, and associated water, (2) the withdrawal of hot water or steam for geothermal power, and (3) the withdrawal of ground water. Each of the three types of withdrawal has produced maximum subsidence of the same order of magnitude. For example, the best known example of oil-field subsidence is the Wilmington oil field in Los Angeles County, California, which has experienced 9 metres of subsidence (Mayuga and Allen, 1969); the withdrawal of hot water for geothermal power at Wairakei, New Zealand, has produced 6-7 metres of subsidence (case history 9.9); and the withdrawal of ground water has produced 9 metres of subsidence in both Mexico City, Mexico, and the San Joaquin Valley of California, USA. (See Table 1.1 and case histories 9.8 and 9.13.) In this guidebook we are concerned with subsidence due to ground-water withdrawal but, regardless of the nature of the fluid removed, the principles involved are the same.

A common understanding of terms is important in discussing the mechanics of land susidence. The reader is referred to three U.S. Geological Survey publications for the definition of many pertinent terms: Water-Supply Paper 494 (Meinzer, 1923) was one of the first comprehensive attempts to define terms used in ground-water studies and has been a much used reference work for the past half century; Water-Supply Paper 1988 (Lohman and others, 1972) contains revised and clarified definitions of selected ground-water terms and stresses the use of consistent units in ground-water flow equations; Water-Supply Paper 2025 (Poland, Lofgren, and Riley, 1972) is a glossary of selected terms useful in studies of the mechanics of aquifer systems and land subsidence due to fluid withdrawal. Principal terms will be defined briefly in this chapter or in an appended glossary, Appendix D.

Figure 3.1 illustrates the terminology for subdivisions of a ground-water reservoir as used in this manual. Case 1, on the left, depicts, from top to bottom, the land surface, a water table, and an unconfined aquifer that functions as an hydraulic unit, a confining bed that functions as a major hydraulic separator; a confined aquifer system that functions approximately as an hydraulic unit; and relatively impermeable bedrock at the base. Case 2 depicts, from top to bottom, the land surface; a water table associated with a semiconfined aquifer system; a confining bed; a confined aquifer system; a second confining bed; a saltwater confined aquifer system; and relatively impermeable bedrock at the base.

Attention is directed to the confined aquifer system that occurs in both cases. Note in particular that aquitards which occur within an hydraulic unit are distinct from a confining bed that serves as an hydraulic separator. For illustrative purposes, the system includes two aquitards (fine-grained compressible interbeds) and three aquifers. Because the aquitards are highly compressible compared to the clastic sand or sand and gravel of the aquifers, they determine by their number and thickness the susceptibility of the aquifer system to compaction in response to increase in stress. In highly compressible confined systems that have experienced several metres of manmade compaction, several tens of aquitards may be interbedded with the aquifers. For example, the microlog of a well drilled through a 400-metre thickness of the confined system on the west side of the San Joaquin Valley, California, displayed 60 aquitards with individual thicknesses ranging from 0.6 m to 15 m and averaging 4.5 m.

In contrast to the large number of aquitards subject to compaction in the San Joaquin Valley, in Mexico City most of the 9 m of compaction has occurred in the top 50 m below land surface, chiefly in two very highly compressible silty clay beds 25-30 and 5-10 m thick. In the upper thicker clay the void ratio averages about 7 and the porosity about 88 per cent; in the lower clay the void ratio averages 4-5 and the porosity about 82 per cent. Figueroa-Vega concludes (case history 9.8, Table 9.8.5) from comparison of casing protrusion and subsidence for 1970-73 that about 75 per cent of the total subsidence was due to compaction of the clayey strata in the top 50 m, and the remainder to compression of the underlying aquifer which is several hundred m thick.

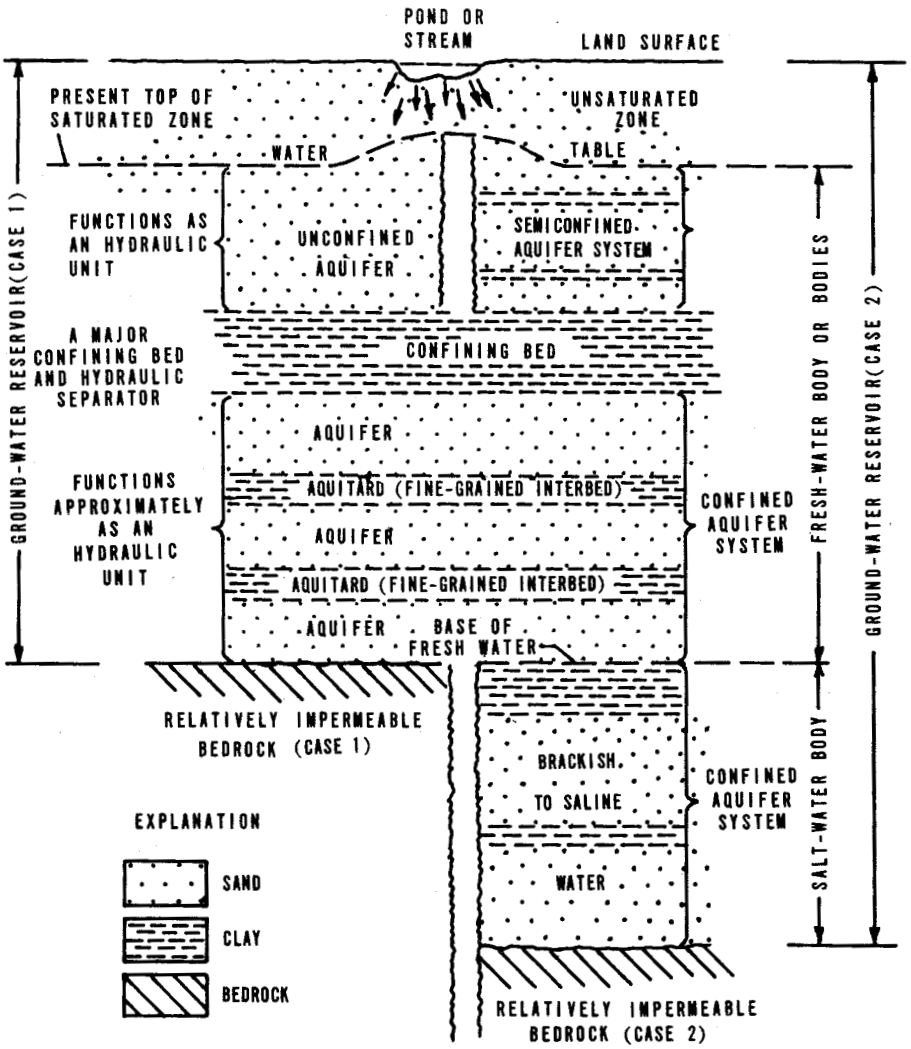

Figure 3.1 Diagram showing terminology for a ground-water reservoir and subdivisions thereof.

In order to count the number and individual thicknesses of the aquitards (or of the aquifers) as displayed in a geophysical bore-hole log, an arbitrary vertical reference, line is drawn on the log. Intervals where the resistivity log lies to the left of the reference line define aquitards; intervals where the resistivity log lies to the right of the reference line define aquifers. Where precisely to draw the reference line becomes a matter of personal judgment. Among the geophysical logs available from oil-field service companies, the microlog of Schlumberger gives considerably more lithologic detail than do the logging devices using a normal electrode configuration. Of these, the short normal with an electrode spacing of about 0.4 metre gives the best detail on thin aquitards.

Figure 9.3.2 is a vertical section of the confined aquifer system beneath Venice, Italy. Using the electric logs and core descriptions from deep test boreholes, the authors of the case history on Venice have divided the confined system into six principal aquifers and a considerable number of aquitards.

3.2 THEORY OF AQUIFER-SYSTEM COMPACTION

In 1925, O. E. Meinzer (Meinzer and Hard, 1925, p. 91) recognized that an artesian aquifer (the Dakota Sandstone) was compressed when the artesian head was decreased. He stated (p. 92) that the overburden pressure of all beds above the confined Dakota aquifer was supported partly by

the fluid pressure at the top of the Dakota and partly by the sandstone itself (grain-to-grain load). He concluded that the grain-to-grain load on the Dakota aquifer at Ellendale, North Dakota, had increased about 50 per cent because of the decline of artesian head.

Meinzer (1928), in a classic paper, discussed the compressibility and elasticity of artesian aquifers in detail. He cited evidence for compressibility and elasticity derived from laboratory tests and from field evidence for confined aquifers and for large artesian basins, notably the Dakota artesian basin. He concluded (p. 289):

> . . . artesian aquifers are apparently all more or less compressible and elastic though they differ widely in the degree and relative importance of these properties. In general the properties of compressibility and elasticity are of the most consequence in aquifers that have low permeability, slow recharge, and high head. In many aquifers these properties are evidently important in supplying water not only by permanent reduction of storage but also by temporary reduction that is replenished when the wells are shut down or during the season of minimum use."

He recognized that water withdrawn from storage was released both by compression of the aquifer and by expansion of the water and that reduction of storage--compression--may be permanent (inelastic) as well as elastic (recoverable).

The next milestone in the understanding of the manner in which artesian aquifers release water from storage was the development by Theis (1935), through analogy with the mathematical theory of heat conduction, of an equation for the non-steady-state flow of ground water to a discharging well. This equation, which for the first time introduced the elements of time and the coefficient of storage (S), subsequently has become the foundation of quantitative ground-water hydrology. Following development of this equation, Theis (1938, p. 894) defined the coefficient of storage as ". . . the volume of water, measured in cubic feet, released from storage in each column of the aquifer having a base one foot square and a height equal to the thickness of the aquifer, when the water table or other piezometric surface is lowered one foot."

Jacob (1940) postulated that when water is removed from and pressure is decreased in an elastic artesian aquifer, stored water is derived from expansion of the confined water, compression of the aquifer, and compression of the adjacent and included clay beds. He concluded that the third source is probably the chief one in the usual case, and he stated (p. 574), ". . . because of the low permeability of the clays (or shales) there is a time lag between the lowering of pressure within the aquifer and the appearance of that part of the water which is derived from storage in those clays (or shales)."

In the field of soil mechanics, Karl Terzaghi (1925; Terzaghi and Peck, 1967) developed the theory of primary one-dimensional consolidation of clays that has served as the basis for solution of most practical soil mechanics and settlement problems in the past half century. This theory commonly is used to estimate the magnitude and rate of settlement or compaction that will occur in fine-grained clayey deposits under a given change in load (stress). According to the theory, compaction results from the slow escape of pore water from the stressed deposits, accompanied by a gradual transfer of stress from the pore water to the granular structure of the deposits. In developing his consolidation theory in 1925, Terzaghi also introduced the basic principle of effective stress that

$$p' = p - u_w, \qquad (3.1)$$

where

p' = effective stress (effective overburden pressure or grain-to-grain load),
p = total stress (geostatic pressure), and
u_w = pore pressure (fluid pressure or neutral stress).

This was the same year that 0. E. Meinzer (Meinzer and Hard, 1925) recognized the principle of effective stress in compression of artesian aquifers.

The application of the time-consolidation theory of soil mechanics to explain the theory of aquifer-system compaction has been summarized lucidly by Riley (1969), as follows:

> "The well-known hydrodynamic (Terzaghi) theory of soil consolidation can provide a semi-quantitative explanation for the phenomenon of repeated permanent compaction during successive cycles of loading and unloading through about the same stress range. In the

context of this problem a central tenet of consolidation theory states that an increase in stress applied to a "clay" stratum (aquitard) becomes effective as a compressive grain-to-grain load only as rapidly as the heads (pore pressures) in the aquitard can decay toward equilibrium with the head in the adjacent aquifer(s). Because of the low permeability and relatively high compressibility of the interbedded aquitards, the consolidation (compaction) of a multi-layered aquifer system in response to increased applied stress is a strongly time-dependent process, and complete or "ultimate" consolidation is not attained until a steady-state vertical distribution of head exists throughout the aquifer system. Transient heads in the aquitards higher than those in the adjacent aquifers (termed residual excess pore pressures) are a direct measure of the remaining primary consolidation that will ultimately occur under the existing stress. When pore-pressure equilibrium is attained throughout the aquitard, it is said to be 100 per cent consolidated for the prevailing stress and no further permanent compaction will occur if the same stress is repeatedly removed and reapplied. The possible role of secondary, or nonhydrodynamic, consolidation in aquifer-system compaction is not well-known, but is assumed in this discussion to be minor.)

"For a single homogeneous aquitard, bounded above and below by aquifers in which the head is instantaneously and equally lowered, the time, t, required to attain any specified dissipation of average excess pore pressure is a direct function of: (1) the volume of water that must be squeezed out of the aquitard in order to establish the denser structure required to withstand the increased stress, and (2) the impedance to the escape of this water. The product of these two parameters constitutes the aquitard time constant. For a specified stress increase, the volume of water is determined by the volume compressibility m_v, of the aquitard, the compressibility, β_w, of the water, and the thickness, b′, of the aquitard. The impedance is determined by vertical permeability, K′, and thickness of the aquitard. Thus, the required time, is a function of the time constant, τ, where

$$\tau = \frac{S'_s(b'/2)^2}{K'} \qquad (3.2)$$

and where S'_S is the specific storage of the aquitard, defined as

$$S'_S = S'_{Sk} + S_{sw} \qquad (3.3)$$

in which

$$S'_{sk} = m_v\gamma_w = \frac{\Delta b'}{b'\Delta h_a} \qquad (3.4)$$

and

$$S_{sw} = n\beta_w\gamma_w \qquad (3.5)$$

S'_{sk} is the component of specific storage due to compressibility of the aquitard, S is the component due to the compressibility of water, h_a is the average head in the aquitard, n is the porosity, and γ_w is the unit weight of water. For consolidating aquitards $S'_{sk} >>> S_{sw}$.

"For convenience, it is customary to define a dimensionless time factor, T, such that

$$T = \frac{t}{\tau'} \qquad (3.6)$$

when T equals unity, t equals the time constant. The degree of consolidation U%, at any time, t, is then expressed as a function of T, the form of the functional relation being determined by the initial conditions of the problem. For the commonly used time-consolidation functions, U% is somewhat more than 90 per cent when T is unity. Detailed development of the time-consolidation theory summarized above may be found in Scott (1963, p. 162-197.)"

3.3 ANALYSIS OF STRESSES CAUSING SUBSIDENCE

3.3.1 Types of stresses

As discussed by Lofgren (1968), three types of stresses are involved in the compaction of an aquifer system:

> "These are closely interrelated, yet of such different nature that a clear distinction is of utmost importance. The first of these is a gravitational stress, caused by the effective weight of overlying deposits, which is transmitted downward through the grain-to-grain contacts in the deposits. The second, a hydrostatic stress due to the weight of the interstitial water, is transmitted downward through the water. The third is a dynamic seepage stress exerted on the grains by the viscous drag of vertically moving interstitial water. The first and third are additive in their effect and together comprise the grain-to-grain stress which effectively changes the void ratio and mechanical properties of the deposit; it is commonly known as the "effective stress." The second type of stress, although it tends to compress each individual grain, has virtually no tendency to change the void ratio of the deposit and is referred to as a neutral stress.
> "Of the various methods used in analyzing the effect of these stresses in a compacting aquifer system (Taylor, 1948, p. 203), only two are considered here. Although they vary in their conceptual approach, these methods give the same mathematical results and can be used to check one another. The classical method, the approach most often used in practical soil-mechanics problems, considers the geostatic load, or combined total weight of grains and water in the system, and the neutral, or hydrostatic, stress. The second method considers the static gravitational stress of the grains, which comprises their true weight above the water table and submerged (buoyed) weight below the water table, and the vertical seepage stresses that may exist in the system. Inasmuch as changes in the effective grain-to-grain stress (both gravitational and stress due to seepage) are directly responsible for the compaction of the deposits and are directly related to changes in head in an aquifer system, this second approach has proved the simplest and clearest in our subsidence investigation."

The definition of seepage stress as a net cumulative difference in hydraulic head is a powerful and useful concept, although the interpretation of seepage stress as being caused by viscous drag may be found to be subject to question in the future. For further discussion of this issue, the reader is referred to Helm (1978) and Helm (1980).

The diagram in Figure 3.2 illustrates the stresses acting at the interface between an artesian aquifer and the overlying confining bed. If we assume that the total load, p, exerted on the aquifer is constant and u_w is reduced as a result of pumping, the load borne by the skeleton of the aquifer, p', is increased by an equal amount. If the artesian head is drawn down to the base of the confining bed (u_w=O), the effective stress, p', on the aquifer skeleton equals the geostatic pressure p.

The idealized pressure diagram of Figure 3.3 utilizes the classical method to illustrate the stresses that cause subsidence. (Also see Poland and Davis, 1969, Figures 1-3.) For the sake of simplicity, pressure is expressed in terms of the height of an equivalent column of water. The geostatic pressure (total stress), p, of sediments and water at some plane of reference below the water table equals the unit weight of moist sediments above the water table, γ_m, times their thickness, plus the unit weight of saturated sediments below the water table, γ, times their thickness. If we assume an average porosity, n, of 40 per cent, an average specific gravity, G, of 2.70 for the grains, an average specific retention, r_s, of 0.20 for the moisture contained above the water table, and let the unit weight of water be unity, then, γ_m equals 1.8 metres of water per metre of thickness:

$$\gamma_m = [G(1-n) + r_s]\gamma_w, \text{ or } [2.7(1-0.4) + 0.20]1 = 1.8, \qquad (3.7)$$

and γ= 2.0 metres of water per metre of thickness:

$$\gamma = [G(1-n) + n]\gamma_w, \text{ or } [2.7(1-0.4) + 0.4]1 = 2.0. \qquad (3.8)$$

Thus the geostatic pressure at depth $z_1 + z_2$ (figure 3.3) is

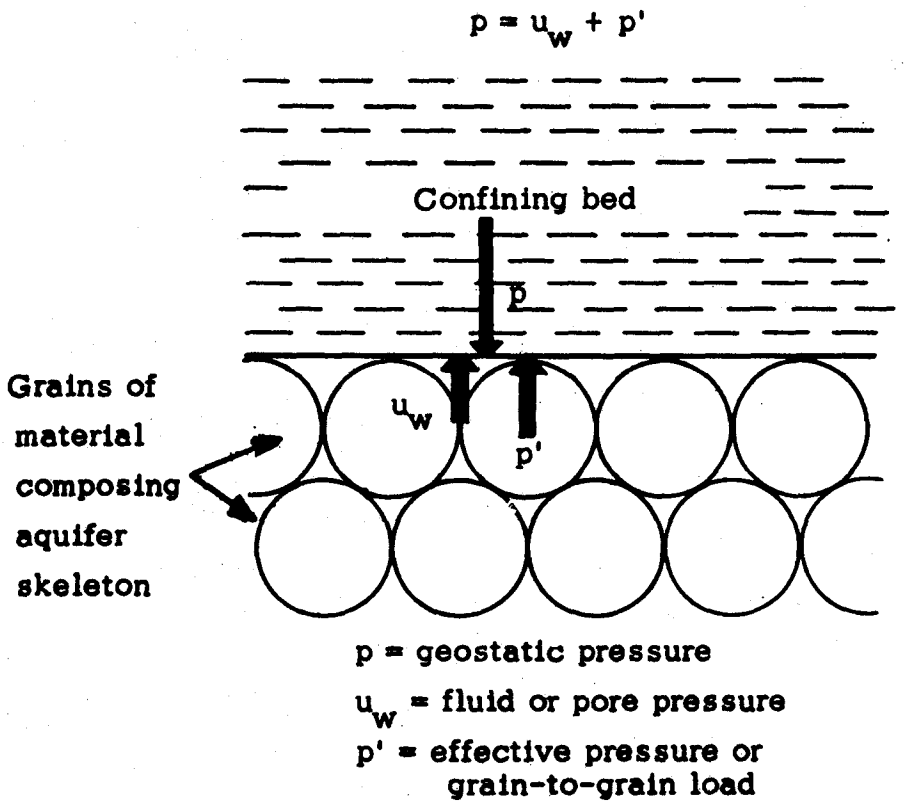

Figure 3.2 Diagrammatic view of stresses acting at interface between artesian aquifer and confining bed (modified from Ferris, Knowles, Brown, and Stallman, 1962, p. 79).

$$p = z_1\gamma_m + z_2\gamma = (50 \times 1.8) + (450 \times 2.0) = 990 \text{ metres of water} \quad (3.9)$$

(a column of water 1 metre high exerts a pressure of 0.1 kg cm^{-2} on its base)

The lowering of artesian head in a confined aquifer system, for example, from depth (Z_1) to (Z_3) in Figure 3.3, does not change the geostatic pressure appreciably. Therefore, the increase in effective stress in the confined aquifers is equal to the decrease in fluid pressure. The compaction in these is immediate and is chiefly recoverable if fluid pressure is restored, but usually it is small.

On the other hand, in the aquitards (fine-grained interbeds) and confining beds, which have low vertical permeability and high specific storage under virgin stressing, the vertical escape of water and the adjustment of pore pressures is slow and time-dependent. Hence, the stress increase applied at the aquifer-aquitard boundaries by the head decline in the confined aquifers becomes effective in these fine-grained beds only as rapidly as pore pressures decay toward equilibrium with those in adjacent aquifers. (See dashed pore-pressure lines of Figure 3.3; where u_t represents the excess pore pressure at time t.) Attainment of pore-pressure equilibrium (dotted lines) may take months or years; the time varies directly as the specific storage and the square of the draining thickness and inversely as the vertical hydraulic conductivity of the aquitard or the confining bed.

Although not illustrated in Figure 3.3, it is readily apparent that increase of fluid pressure from a steady-state condition decreases effective stress and causes expansion of the pressurized sediments (as in subsidence control and underground waste disposal). Fluid pressure cannot exceed geostatic pressures without causing uplift of the overburden.

The stress relations of Figure 3.3 serve to illustrate the principle of effective stress, but do not emphasize the importance of net difference of hydraulic head in causing compaction. Actually, the downward hydraulic gradient developed across the confining bed by the head decline in the confined system induces downward movement of water through the pores that exerts a viscous drag on the clay particles. The stress so exerted on the particles in the confining bed in the direction of flow is a seepage stress.

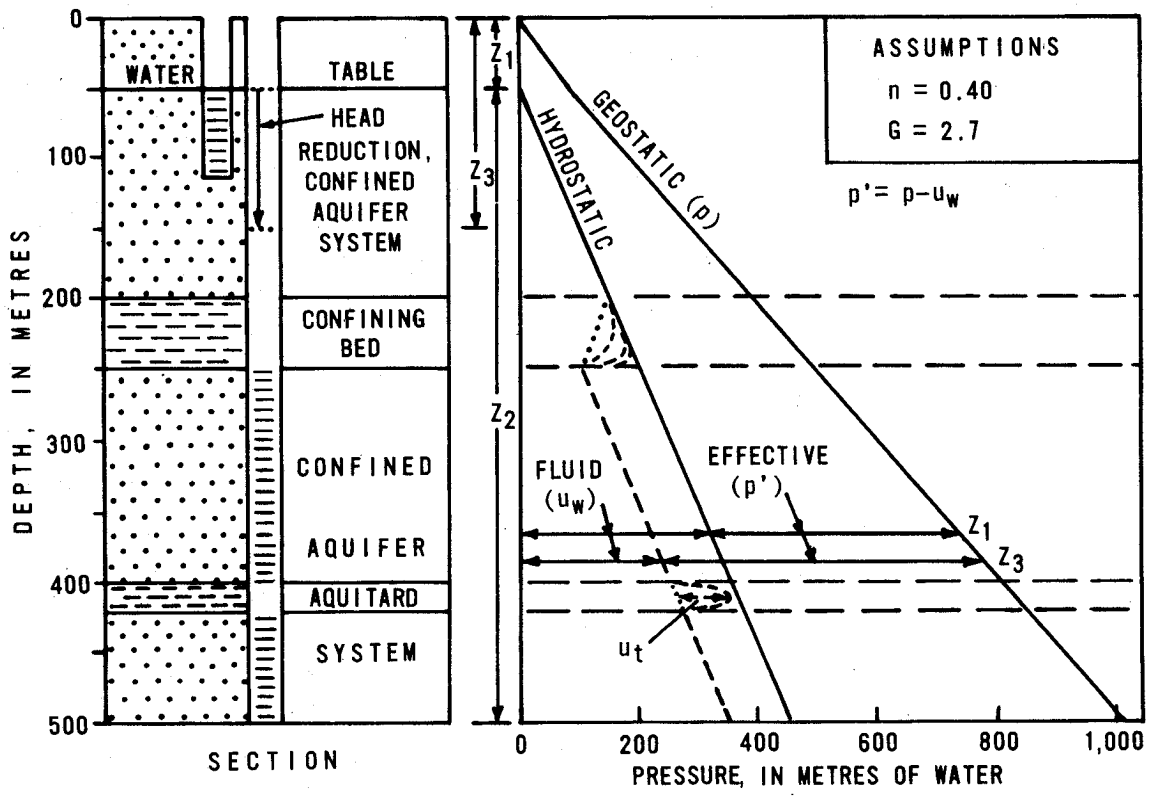

Figure 3.3 Pressure diagram for an unconfined aquifer and a confined aquifer system; head reduction in the confined system only.

3.3.2 Computation of stress change

It is quantitatively convenient in treating complex aquifer systems to compute effective stresses and stress changes in terms of gravitational stress and the vertical normal component of seepage stress, which are algebraically additive. The following brief discussion is summarized from Lofgren (1968) and Poland and others (1975).

Diagram A of Figure 3.4 illustrates part of a confined aquifer system containing an aquitard, overlain by a confining bed and an unconfined aquifer. The water table and the potentiometric surface of the confined system are initially at the same depth; hence, fluid pressure at all depths is hydrostatic. All beds and surfaces within the vertical column are assumed to be horizontal. If we assume the same parameters as for Figure 3.3, and let the unit weight of water be unity, then the effective unit weight of moist deposits above the water table, γ_m, equals 1.8 metres of water per metre of thickness:

$$\gamma_m = [G(1-n) + r_s]\gamma_w, \text{ or } [2.7(1-0.4) + 0.20]1 = 1.8 \qquad (3.7)$$

Also, the effective submerged, or buoyant, unit weight of saturated deposits, γ_b, equals one metre of water per metre of thickness:

$$\gamma_b = (1-n)\,(G-1)\gamma_w, \text{ or } (1-0.4)\,(2.7-1)1 = 1.0 \qquad (3.10)$$

If these gravitational stresses Are expressed in metres of water (one metre of water is equivalent to 0.1 kg cm^{-2}), they can be added directly to hydraulic stresses.

Vectors to the right of diagram A (Figure 3.4) represent the two components of effective gravitational stress at three depths. At the 400-metre depth, for example, the stress due to the unsaturated deposits, s, equals 200 metres of thickness times 1.8, or 360 metres of water; the stress due to the buoyant weight of submerged deposits, b, equals 200 x 1.0, or 200 metres of water. The sum of s + b, 560 metres of water, is the grain-to-grain stress at this plane of

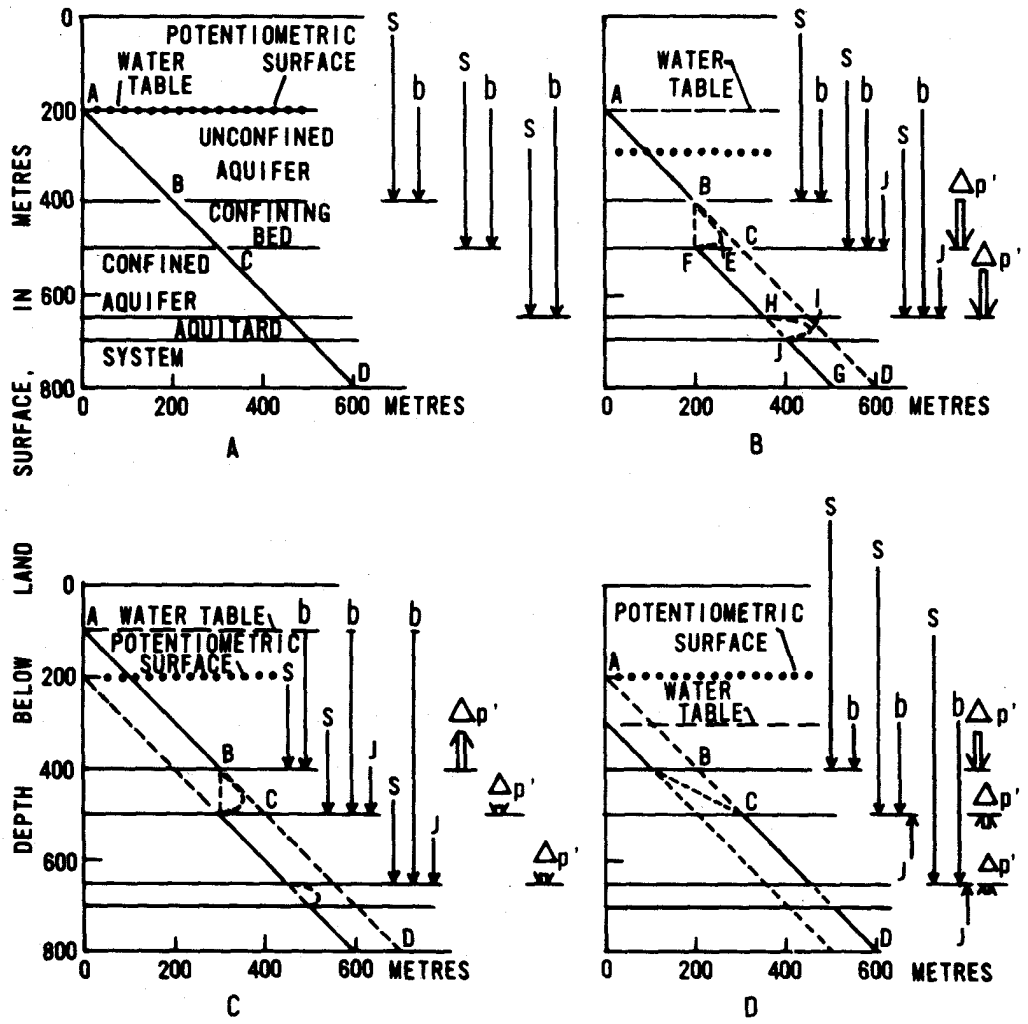

Figure 3.4 Effective stress diagrams for a confined aquifer system overlain by an unconfined aquifer. A, water table and potentiometric surface common. B, water table constant, potentiometric surface lowered. C, water table raised, potentiometric surface constant. D, water table lowered, potentiometric surface constant. Stresses in metres of water; based on assumed porosity = 0.40, specific gravity of solids = 2.7, and specific retention = 0.20. S = effective stress due to weight of unsaturated deposits; b = effective stress due to buoyant weight of submerged deposits; J = seepage stress; $\Delta p'$ = change in total effective stress from condition A.

reference. The effective stress of the saturated deposits increases directly with depth below, the water table, as indicated by the increasing vector lengths, b, at the base of the confining bed and the top of the aquitard.

If the potentiometric surface of the confined aquifer system is drawn down 100 metres as in diagram B, gravitational stresses remain as in A because the water table is unchanged. However, a downward component of hydraulic gradient is developed across the confining bed, which induces downward movement of water through the pores and exerts a viscous drag on the grains. The net force transferred to the grains between any two depths is measured by the head loss between those depths. The stress so exerted on the grains is called a seepage stress. This third effective stress component is represented by vector J on a horizontal plane. Its vertical component is algebraically additive to the gravitational stresses and is transmitted downward through the confined aquifer system. The wide arrows to the right of diagram B indicate within a vertical column the net change in the vertical normal component of effective stress at the base of the confining bed and below, from the hydrostatic condition of diagram A.

Because the water table is unchanged the net change is the change in seepage stress, which is equal to the decrease in fluid (neutral) pressure represented by line C-F (base of confining bed).

The increase in effective stress in the permeable aquifers occurs simultaneously with decrease in head, but decrease of pore pressure in the aquitards and confining beds is delayed because of their high compressibility and low vertical permeability. The reduction in head in the permeable aquifers creates a two-directional hydraulic gradient outward from the center of the aquitard and consequently induces two-directional drainage from the aquitard. Thus, although upward and downward seepage forces occur within the aquitard during this adjustment, internal stresses have no net external effect on the rest of the aquifer system. During this period of transient pressures, the effective stress can increase only as rapidly as the excess pore-pressure decreases. The general pattern of decay is illustrated in diagram B of Figure 3.4 in the confining bed by dashed line B-E-F and in the aquitard by dashed line H-I-J. Full dissipation of excess pore pressures to equilibrium (dashed lines B-F and H-J) may require months or years. Note that water drains through both boundaries of the aquitard, but only through the lower boundary of the confining bed under the specified conditions.

If the potentiometric surface of the confined aquifer system remains constant and the water table is raised or lowered, both gravitational and seepage stresses change, but with opposite sign. For example, if the water table is raised 100 m (diagram C) and the parameters are as assumed earlier, the change in gravitational stress is -0.8 metre of water per metre of rise; however, the unit change in seepage stress (differential between water table and potentiometric surface of confined system) is +1.0 metre. Hence, the net unit change in applied stress in the confined system is +0.2 metre of water. Conversely, if the water table is lowered (diagram D), the net change in applied stress is -0.2 metre per metre of decline.

In summary, water-level fluctuations change effective stresses in the following two ways:

1. A rise of the water table provides buoyant support for the grains in the zone of the change, and a decline removes the buoyant support; these changes in gravitational stress are transmitted downward to all underlying deposits.
2. A change in position of either the water table or the potentiometric surface of the confined aquifer system, or both, may induce vertical hydraulic gradients across confining or semiconfining beds and thereby produce a seepage stress. The vertical normal component of this stress is algebraically additive to the gravitational stress. A change in effective stress results if preexisting seepage stresses are altered in direction or magnitude.

The change in applied stress within a confined aquifer system, due to changes in both the water table and the artesian head, may be summarized concisely (Poland and others, 1972, p. 6) as

$$\Delta p_a = -(\Delta hc - \Delta h_u y_s), \qquad (3.11$$

where p_a is the applied stress expressed in metres of water, h_c is the head (assumed uniform) in the confined aquifer system, h_u is the head in the overlying unconfined aquifer, and y_s is the average specific yield (expressed as a decimal fraction) in the interval of water-table fluctuation.

In the San Joaquin Valley, California, the areas in which subsidence has been appreciable coincide generally with the areas in which ground water is withdrawn chiefly from confined aquifer systems. (See Chapter 9.13, Figure 9.13.2.) Furthermore, the great increases in stress applied to the sediments in the ground-water reservoir by the intensive mining of ground water developed chiefly as increased seepage stresses on the confined aquifer systems.

3.4 COMPRESSIBILITY AND STORAGE CHARACTERISTICS

3.4.1 Stress-strain analysis

Field measurements of compaction and correlative change in water level may serve as continuous monitors of subsidence and indicators of the response of the system to change in applied stress. They also can be utilized to construct stress-strain curves from which, under certain favourable conditions, one can derive storage and compressibility parameters of the aquifer system, as first demonstrated by Riley (1969) for the Pixley site in the southern part of the San Joaquin valley, California.

Thirteen years of measured water-level change and compaction at Pixley are shown in Figure 3.5. They have been utilized to derive a computer plot of stress change versus strain (Figure 3.5, E) for a 101-metre thickness of the confined aquifer system. The change in stress (B) applied to all strata within the depth interval is calculated from the hydrographs (A) of wells 16N4 (water table) and 16N3 (confined system). This stress-change graph is plotted with stress increasing downward to emphasize the close correlation with declining artesian head. The compaction within the 131-232-metre depth interval (D) is obtained as the difference between the two extensometer plots on graph C. The stress-strain diagram (E) represents the mechanica1 response (change in thickness) of the 131-232-metre depth interval to change in effective stress. It is plotted from the calculated data of graphs B and D. For convenience, the stress-change plot of graph B is expressed in equivalent units of water head (1 ft of water head is equivalent to 0.4333 lb in^{-2}; 1 m of head is equivalent to 0.1 kg cm^{-2}).

Attention is directed to (1) the annual depth-to-water pattern for the confined aquifer system (see hydrograph for well 16N3) in response to the characteristic seasonal pumping for irrigation--the main seasonal decline occurs in spring to late summer followed by recovery of water level to a peak late in the winter; (2) the reduced rate of compaction during years of small seasonal drawdown of water level in well 16N3, such as 1962, 1963, 1967 and 1969; (3) the small but definite expansion of the deposits (D) in most winters, accompanying the water-level recovery; and (4) the series of annual stress-strain loops (E), formed by the yearly cycles of stress increase and decrease.

As discussed by Riley (1969):

> "The descending segments of the annual loop are of particular interest since the represent the resultant of two opposing tendencies--one toward continuing compaction and one toward elastic expansion in response to decreasing applied stress. Expansion of the more permeable strata of the aquifer system must be essentially concurrent with the observed rise in head in wells. However, the first reduction of stress may produce only a slight reduction in compaction rate. Evidently, initial expansion of the aquifers is concealed by continuing compaction of the interbedded aquitards as water continues to be expelled under the influence of higher pore pressures remaining within the medial regions of the beds.
>
> "Consolidation theory requires that the maximum excess pore pressure, which is in the middle of a doubly-draining aquitard, be related to the same parameters . . . . . that control the time-consolidation function. It is, therefore, inevitable that there be, at the end of a relatively short pumping season, a large range of maximum excess pore pressures in a sequence of aquitards of widely varying thicknesses and physical properties. Thus, as head in the aquifers rises and stress declines, the thinnest and (or) most permeable aquitards, containing the least excess pore pressure, will quickly assume an elastic response; but the thickest and (or) least permeable beds may continue to compact at diminishing rates through most or perhaps all of the period of head recovery and stress relief.
>
> "Evidence for this type of behavior is contained in the continuously curving stress strain line characteristic of much of the descending portions of the annual loops."

If in Figure 3.5E the lower part of the descending curve approximates a straight line with a positive slope, as it does, for instance, in 1968 and 1970, we can assume that essentially all excess pore pressures have been exceeded by the rising heads and that the entire aquifer system is expanding in accordance with its elastic modulus.

The lower parts of the descending segments of the annual loops for the winters of 1968-69 1969-70, and the latter part of 1970 are approximately parallel straight lines, as shown by the upward projection of the dotted lines. The reciprocal of the slope of the dotted lines is realistic estimate of the component of the storage coefficient, S, attributable, to the elastic or recoverable deformation of the aquifer system skeleton, S_{ke}:

$$S_{ke} = \frac{\Delta b}{\Delta h} = 6.4 \times 10^{-4} \qquad (3.12)$$

where b is the thickness of the aquifer-system segment being measured, Δb is compaction, h is applied stress, and Δh is change in applied stress. The component of average specific storage due to elastic deformation is S_{ske}:

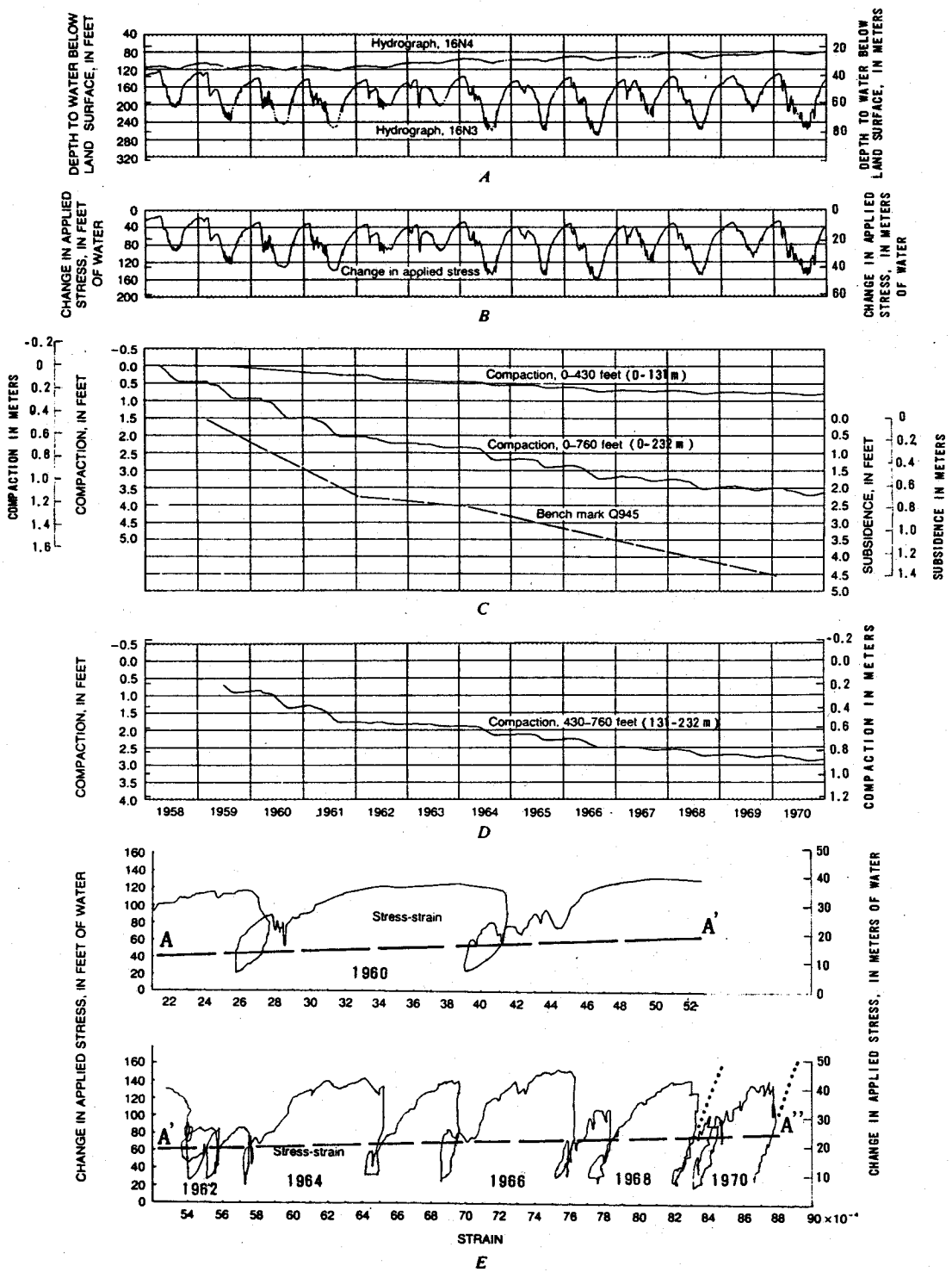

Figure 3.5 Hydrographs, change in applied stress, compaction, subsidence, and stress-strain relationship, 23/25-16N. A, Hydrographs of wells 23/25-16N4, perforated 61-73 m depth, and 23/25-16N3, perforated 110-128 m depth. B, Change in applied stress. C, Compaction to 131-metre depth in well 23/25-16N3 and to 232-metre depth in well 23/25-16N1 and subsidence of bench mark Q945 at well 23/25-16N1. D, Compaction in 131-232-metre depth interval. E, Stress change versus strain (101-metre thickness). (Modified from Poland, Lofgren, Ireland, and Pugh, 1975, Fig. 70.)

$$S_{ske} = \frac{\Delta b}{b} / \Delta h = \frac{S_{ke}}{b} = \frac{6.4 \times 10^{-4}}{101 m} = 10^{-6} m^{-1} \quad (3.13)$$

where $\Delta b/b$ represents strain in Figure 3.5E and can be considered a conservative estimate of bulk volume strain, $\Delta V/V$, in the field. The compressibility of the aquifer-system skeleton in the elastic range of stress is α_{ke}:

$$\alpha_{ke} = \frac{S_{ske}}{\gamma_w} = \frac{6.3 \times 10^{-6} m^{-1}}{0.1 kg cm^{-2} m^{-1}} = 6.3 \times 10^{-5} cm^2 kg^{-1} . \quad (3.14)$$

However, if stresses are expressed in metres of water, and if γ_w (the unit weight of water) equals unity, α_{ke} is equal numerically to S_{ske}. It is of interest to note that the compressibility of water, β_w, at 20° C, is 4.7 x 10^{-5} $cm^2 kg^{-1}$. Hence, the average elastic compressibility of the aquifer-system skeleton is about 1.3 times as large as the compressibility of water.

On the other hand,

$$S_{sw} = n\beta_w\gamma_w, \quad (3.5)$$

If the average porosity, n, equals 0.4, then

$$S_{sw} = (0.4)(4.7 \times 10^{-5} cm^2 kg^{-1})(0.1 kg cm^{-2} m^{-1}) = 1.9 \times 10^{-6} m^{-1} \quad (3.15)$$

Therefore, for the 101-metre thickness of the measured interval, the ratio of specific storage values for the elastic deformation of the aquifer system and for the elastic expansion of water is

$$\frac{S_{ske}}{S_{sw}} = \frac{6.3 \times 10^{-6} m^{-1}}{1.9 \times 10^{-6} m^{-1}} = 3.3 . \quad (3.16)$$

This means that for each unit of change in head, the volume of water released from or taken into storage per unit volume of the porous medium by elastic (recoverable) deformation of the medium is more than three times the volume released by elastic deformation of the interstitial water

Elastic storage and compressibility parameters have been derived from two other stress-strain plots described in the case histories. One is for a well in western Fresno County, illustrated in Figure 9.13.9. The depth interval measured is 70-176 m below land surface. At this site, S_{ke} = 1.2 x 10^{-3} and S_{ske} = 1.1 x $10^{-5} m^{-1}$. This stress-strain plot (Figure 9.13.9) is of interest also because the lower parts of both the descending and ascending segments of the annual "hysteresis loops" form essentially a common straight line, indicating almost no time delay in adjustment of the aquifer-system skeleton to change in stress in the elastic range of stress.. Of this 106-m thickness of aquifer system, the sum of the aquifers is 71 m or two-thirds of the total and the sum of the aquitards is only one-third of the total. The electric log suggests the aquitards are largely silt and hence relatively permeable compared with clay.

The other plot is for a well in San Jose, California, illustrated in Figure 9.14.7. The depth interval measured is 244 m thick, 61-305 m below the land surface, representing the full thickness of the confined aquifer system. The stress-compaction plot indicates that S_{ke} 1.5 x 10^{-3} and $S_{ske} = S_{ke}/244m$ = 6.15 x $10^{-6} m^{-1}$. In these computations I have assumed that in the range of stresses less than preconsolidation stress, the compressibility of the aquitards and the aquifers is the same. Therefore, the full thickness of the confined aquifer system, 244 m, was used to derive the specific storage component, S_{ske}, in the elastic range of stress.

For stresses exceeding past maximum (preconsolidation) stresses, virgin specific storage and compressibility parameters can be approximated from Figure 3.5. Straight line A-A′-A" is drawn through the annual hysteresis loops approximately at the level at which the rising elastic compaction curve crosses over the descending expansion curve. The reciprocal of the slope of line A-A′-A" is the component of the storage coefficient, S, attributable to the inelastic (nonrecoverable) deformation of the aquifer-system skeleton, S_{kv}:

$$S_{kv} = \frac{\Delta b}{\Delta h} = 6.8 \times 10^{-2} \tag{3.17}$$

The component of specific storage due to inelastic (nonrecoverable) deformation of the aquifer system skeleton is S_{skv}:

$$S_{skv} = \frac{S_{kv}}{b} = \frac{6.8 \times 10^{-2}}{101\text{m}} = 6.7 \times 10^{-4}\text{m}^{-1} \tag{3.18}$$

Relation 3.18 is an average value for the entire system. It is reasonable to assume, however, that only the clay interbeds deform inelastically. To obtain the average nonrecoverable specific storage of the aquitards in accordance with this convention, S_{kv} is divided by the aggregate thickness, b′, of aquitards, which is 70 metres:

$$S'_{skv} = \frac{S_{kv}}{b'} = \frac{6.8 \times 10^{-2}}{70\text{m}} = 9.7 \times 10^{-4}\text{m}^{-1} \tag{3.19}$$

The average aquitard compressibility

$$\frac{S'_{skv}}{w} = \frac{9.7 \times 10^{-4}\text{m}^{-1}}{0.1\text{kgcm}^{-2}\text{m}^{-1}} = 9.7 \times 10^{-3}\text{cm}^2\text{kg}^{-1} \tag{3.20}$$

The average compressibility of the aquifer-system skeleton in the virgin range of stressing is α_{kv}:

$$\alpha_{kv} = \frac{S_{skv}}{\gamma_w} = \frac{6.7 \times 10^{-4}\text{m}^{-1}}{0.1\text{kgcm}^{-2}\text{m}^{-1}} = 6.7 \times 10^{-3}\text{cm}^2\text{kg}^{-1} \tag{3.21}$$

Thus, from the appraisal of Figure 3.5, and the comparison of α_{ke} of 3.14 to α_{kv} of 3.21, we can conclude that at Pixley, the compressibility of the measured interval of the aquifer system in the virgin range of stressing is about 100 times as great as the compressibility in the elastic range of stressing. Hydrologists should be aware that in multiaquifer systems the values of the compressibility and storage parameters may be 10 to 100 times greater when total applied stresses are in the virgin range of stressing than when they are in the elastic range. This fact must be kept in mind in the interpretation of aquifer tests and when making estimates of the usable storage capacity of a confined-aquifer system.

3.4.2 Soil-mechanics techniques

Compressibility characteristics of fine-grained compressible layers or lenses (aquitards) can be obtained by making one-dimensional consolidation tests of "undisturbed" cores in the laboratory. These tests are described in soil mechanics textbooks and briefly in Chapter, 4 of this manual. The plot of void ratio against the logarithm of load (effective stress) is known as the e-log p plot. Three parameters that can be obtained from this plot are (1) the compression index, C_c, a measure of the nonlinear compressibility of the sample, (2) the coefficient of consolidation, C_v, a measure of the time rate of consolidation, and (3) the approximate value of the preconsolidation load, determined graphically (see Figure 4-9). The preconsolidation load or stress is the maximum prior effective stress to which a deposit has been subjected and which it can withstand without undergoing additional permanent deformation. Most of the compacting deposits in the subsiding areas of Table 1.1 are of late Cenozoic age and before disturbance of equilibrium conditions by man were normally consolidated or slightly overconsolidated (1 to 4 kg cm^{-2}).

For effective stress changes in the stress range less than preconsolidation stress, the compaction or expansion of both aquitards and aquifers is elastic--that is, approximately proportional to change in effective stress over a moderate range in stress, and fully recoverable if the stress reverts to the initial condition.

For increase in effective stress in the range of loading that exceeds preconsolidation stress, the "virgin" compaction of aquitards is chiefly inelastic--that is, not recoverable upon decrease in stress. However, this virgin compaction includes a recoverable elastic component

that is small compared to the nonrecoverable component. The virgin compaction usually is roughly proportional to the logarithm of effective stress.

The compaction of aquifers, in contrast to that of aquitards, is chiefly elastic (recoverable) but it may include an inelastic component. In poorly sorted and angular sands and especially in micaceous sands, the inelastic component may dominate.

A semilogarithmic plot of void ratio, e, versus the logarithm of load (effective stress p', shown in Figure 3.6, illustrates a graphic method of computing compressibility. The coefficient of volume compressibility, m_v in soil-mechanics terminology,

$$m_v = \frac{e_0 - e_1}{(1 + e_0)\Delta p'}$$

(Terzaghi and Peck, 1967). It represents the compression of the clay, per unit of initia1 thickness, per unit increase in load (for effective stress change in the range exceeding pre-consolidation stress). Utilizing the laboratory virgin compression curve, which is a straight line on the semilogarithmic plot, we see that for a load change $\Delta p'$, from 100 to 200 lbs in^{-2}

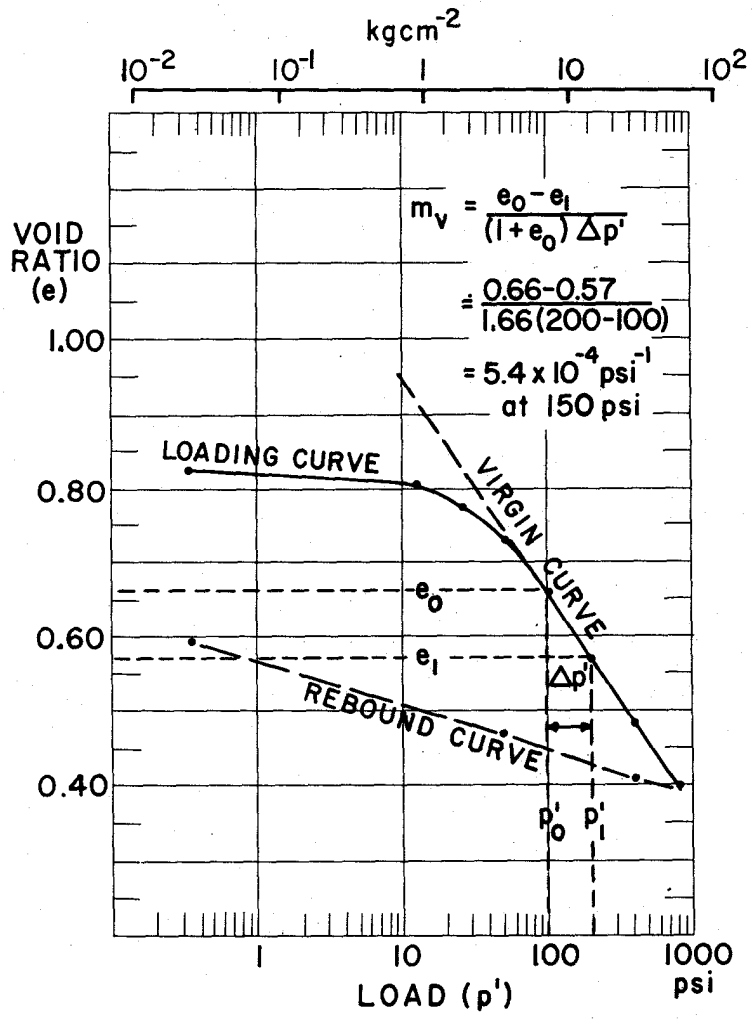

Figure 3.6 Deriving m from e-log p' plot.

(7 to 14 kg cm^{-2}), the void ratio, e, decreases from 0.66 to 0.57. The decrease in volume or length of the sample, $e_0 - e_1$, divided by the initial volume, $1 + e_0$, and by the change in load for the values given, supplies an approximation of compressibility at the midpoint of $\Delta p'$. Thus, the compressibility at 150 lbs in^{-2} (10.5 kg cm^{-2}) is approximately 5.4×10^{-4} $in^2 lb^{-1}$ (7.7×10^{-3} cm kg^{-1}). The compressibility decreases markedly with increase in effective stress. Repeating the computation, for several increments of load increase furnishes the data for plotting compressibility for the pertinent range in effective stress.

Figure 3.7 is a logarithmic plot showing the principal range in compressibility of tested cores from four core holes tapping alluvial and minor lacustrine deposits in southwestern United States, as well as the compressibility of pure clays made by Chilingar and Knight (1960).

The four core holes are spaced from California to Texas, as follows:

Core hole	Location	Depth (m)
A	Santa Clara Valley, California, in San Jose	305
B	San Joaquin Valley, California, in western Fresno County	610
C	Pinal County, Arizona, near Eloy	592
D	Harris County, Texas, at Clear Lake	294

The graph summarizes the compressibility range for 30 samples from the four core holes for effective stresses between 8 and 100 kg cm^{-2}. If we consider these samples under a common effective stress of 70 kg cm^{-2} (note the vertical dashed line), the range in compressibility of

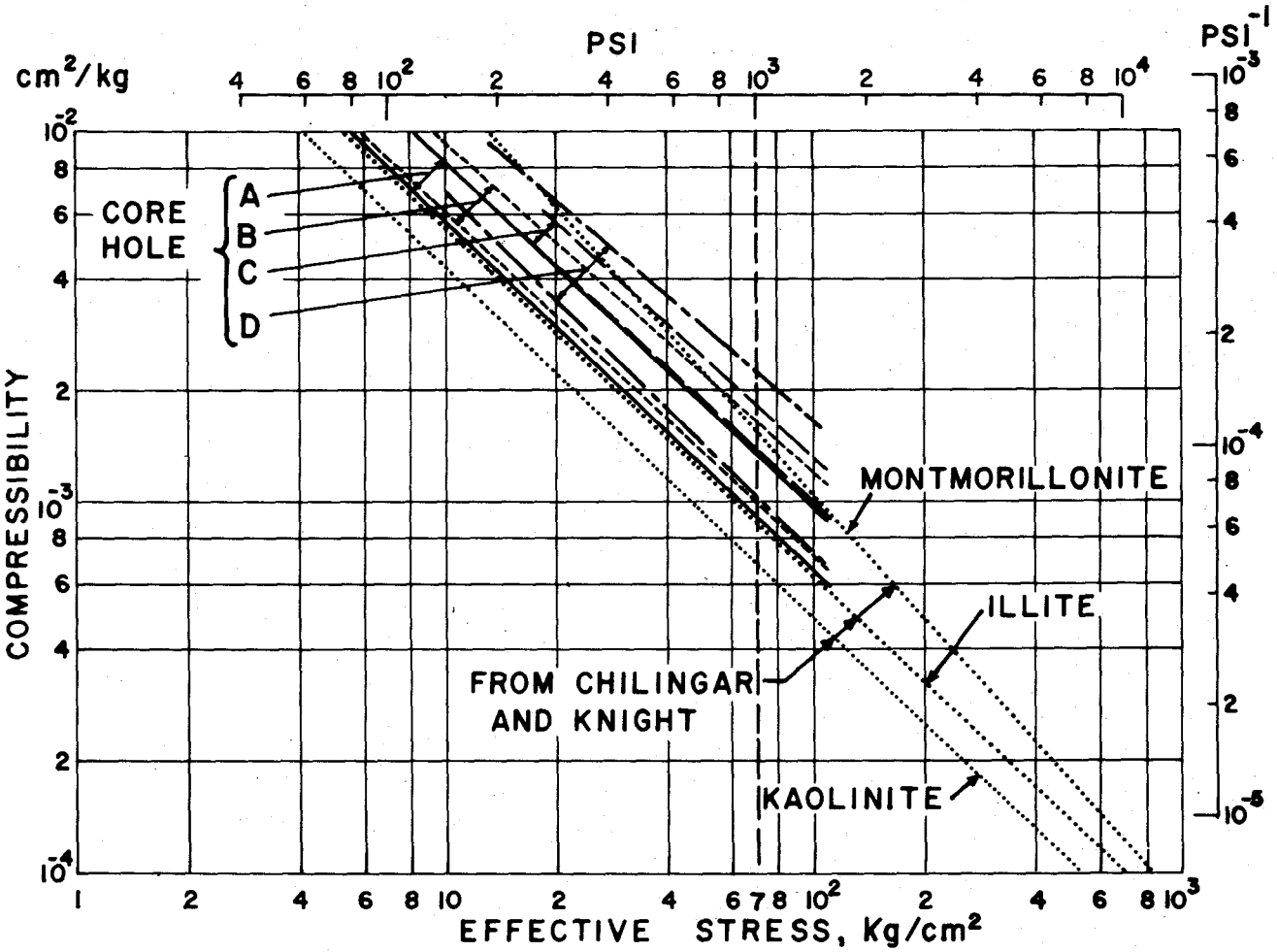

Figure 3.7 Compressibility plots for fine-grained samples from four core holes in southwestern United States and for pure clays tested by Chilingar and Knight (1960).

the 30 cores is about 9 x 10^{-4} to 2.3 x 10^{-3} cm^2 kg^{-1}, a range by a factor of nearly three.

Experimental compaction studies by Chilingar and Knight (1960), made on kaolinite, illite, and montmorillonite clays at pressures from 3 to 14,000 kg cm^{-2} afford an opportunity to compare compressibilities of the fine-grained corehole samples with those of pure clays. The standard clay-mineral samples tested were described by Chilingar and Knight (1960, p. 103) as follows:

Montmorillonite No. 25, Upton, Wyoming
Illite No. 35, Fithian, Illinois
Kaolinite No. 4, Macon, Georgia

The results of their tests, which they expressed in moisture content in per cent (dry weight) versus the logarithm of pressure, have been converted to compressibility versus effective stress and are shown as dotted lines in Figure 3.7. Kaolinite has the lowest compressibility, illite the intermediate, and montmorillonite has the highest. The compressibilities of all 30 corehole samples are higher than those of the standard illite throughout the stress range tested. Furthermore, the compressibilities of all the samples from core holes A and B (central California) fall between the standard illite and montmorillonite curves. X-ray diffraction analysis of the clay-mineral assemblages at all four sites indicated that montmorillonite is the predominant clay mineral, ranging from 6 to 8 parts in 10.

Compressibility tests have been made on many samples of fine-grained sediments taken from a deep (950m) borehole in Venice, Italy, in 1971. Values of m_v versus depth for more than 50 samples are plotted in Figure 9.3.3 of the Venice case history. The compressibilities were computed at the actual "in situ" pressures for both the loading and unloading curves. Ricceri and Butterfield (1974) made a detailed analysis of the compressibility data from the deep borehole. If the compressiblities for samples from 120-220 m depth, computed from the loading curve (m_{vl} points in Figure 9.3.3), are plotted in Figure 3.7, most points fall on or just to the right of the illite curve. Compressibilities average about 3 x 10^{-3} cm^2kg^{-1} for effective stresses in the range of 12 to 22 kg cm^{-2} (120-220 m depth). The highest compressibilities fall within the range of compressibilities for samples from corehole A (Santa Clara Valley, Calif.).

3.4.3 The compressibility environment

Effective stresses, including the increase applied by pumping, are in the range of 10 to 100 kg cm^{-2} for aquifer systems tapped by water wells within depths of 60 to 900 m. This depth range includes about all the stressed sediments of Table 1.1. Within this stress range sands in general are much less compressible than clays. However, at effective stresses of 100 to 200 kg cm^{-2}, evidence is accumulating to show that some sands may be as compressible as clays or siltstones.

Roberts (1969) made a laboratory study of the compressiblity of sands and clays as determined from one-dimensional consolidation tests at stresses up to 700 kg cm^{-2}. The tests showed that in the range of effective stresses from 100 to 200 kg cm^{-2}, some sands were as compressible as typical clays. Roberts noted that sands are relatively incompressible at low pressures (<100 kg cm^{-2})--the compression is due to particle rearrangement. At higher pressures fracturing of the grains develops. He concluded that factors affecting the pressures at which fracturing begins include the initial density of the sample, angularity of the grains, and grain-size distribution.

In a study of subsidence of oil fields bordering Lake Maracaibo in Venezuela, van der Knapp and van der Vlis (1967) made one-dimensional consolidation tests on cores of uncemented sand and clay, taken from depths of 900 to 1050 m. Compressibility was computed from the virgin compression curve of the e-log p’ plot. The composite graphs of compressibility of the sand and clay samples showed that the two materials have comparable compressibilities. For example, at 140 kg cm^{-2} of effective stress, the mean sand compressibility (8 samples) is about 5.7 x 10^{-4} cm kg^{-1} and the mean clay compressibility (11 samples) is about 4.5 x 10^{-4} cm^2kg^{-1}.

The principal oil zones at the Wilmington oil field in Los Angeles and Long Beach, California, that compacted to cause as much as 9 m of subsidence are at depths of 600 to 1200 m. When fluid pressures in the zones were depleted in the late 1950’s prior to repressuring, effective stresses were 100 to 200 kg cm^{-2} According to Allen and Mayuga (1969), axial loading tests on the reservoir sands and siltstones showed the sands to be as compactible, or more so, than the siltstones at the field effective stresses. From the laboratory tests, reservoir calculations, and casing-collar measurements, they concluded that about two-thirds of the compaction

had occurred in the sands and one-third in the siltstones. The sands are composed of about 35-70 per cent quartz, 12-40 per cent feldspar, and 8-12 per cent silt and clay minerals. Above the 1,220 m depth, the sands are uncemented and loose, and they grade in grain size from fine to coarse. Roberts' (1969) findings that some sands fracture appreciably in the stress range of 100-200 kg cm^{-2} suggest that the high compressibility of the feldspathic Wilmington "oil sands" in this same effective-stress range is due chiefly to fracturing.

For additional information on the compressibilities of unconsolidated sands and clays, the reader is referred to Roberts (1969), Meade (1968), Grim (1962), Allen and Chilingarian, in Chilingarian and Wolf (1975, p. 43-77), and Rieke and Chilingarian (1974, p. 173-217).

3.5 REFERENCES

ALLEN, D. R., and MAYUGA, M. N. 1969. The mechanics of compaction and rebound, Wilmington oil field, Long Beach, California, USA, in L. J. Tison, ed., Land Subsidence, v. 2, Internat. Assoc. Sci. Hydrology Pub. 89, p. 410-422.

CHILINGAR, G. V., and KNIGHT, LARRY. 1960. Relationship between pressure and moisture content of kaolinite, illite, and montmorillonite clays. Bull. Am. Assoc. Petroleum Geologists, v. 44, no. 1, p. 101-106.

CHILINGARIAN, G. V., and WOLF, K. H., eds. 1975. Compaction of coarse-grained sediments, I. Elsevier Scientific Publishing Company, Amsterdam, 552 p.

FERRIS, J. G., KNOWLES, D. B., BROWN, R. H., and STALLMAN, R. W. 1962. Theory of aquifer tests. U.S. Geol. Survey Water-Supply Paper 1536-E, p. 69-174.

GRIM, R. E. 1962. Applied clay mineralogy. McGraw-Hill Book Company, Inc. New York, 422 p.

HELM, D. C. 1978. A postulated relation between granular movement and Darcy's law for transient flow. Proceedings of Conference on Evaluation and Prediction of Subsidence, S. K. Saxena, ed., American Soc. Civil Engineers, p. 417-440.

HELM, D. C. 1982. Conceptual aspects of subsidence due to fluid withdrawal, in Recent trends in hydrogeology, Geological Society of America Special Paper in press.

JACOB, C. E. 1940. On the flow of water in an elastic artesian aquifer. Am. Geophys. Union Trans., pt. 2, p. 574-586.

LOFGREN, B. E. 1968. Analysis of stresses causing land subsidence. U.S. Geol. Survey Prof. Paper 600-B, p. B219-B225.

LOHMAN, S. W., and others. 1972. Definitions of selected ground-water terms--Revisions and conceptual refinements. U.S. Geol. Survey Water-supply Paper 1978, 21 p.

MAYUGA, M. N., and ALLEN, D. R. 1969. Subsidence in the Wilmington oil field, Long Beach, Calif., USA, in L. J. Tison, ed., Land subsidence, v. 1. Internat. Assoc. Sci. Hydrology Pub. 88, p. 6C6-79.

MEADE, R. H. 1968. Compaction of sediments underlying areas of land subsidence in central California. U.S. Geol. Survey Prof. Paper 497-D, 39 p.

MEINZER, 0. E. 1923. outline of ground-water hydrology with definitions. U.S. Geol. Survey Water-Supply Paper 494, 71 p.

MEINZER, 0. E. 1928. Compressibility and elasticity of artesian aquifers. Econ. Geology, v. 23, no. 3, p. 263-291.

MEINZER, 0. E., and HARD, H. A. 1925. The artesian-water supply of the Dakota sandstone in North Dakota with special reference to the Edgeley quadrangle. U.S. Geol. Survey Water-Supply Paper 520-E, p. 73-95.

POLAND, J. P. 1972. Subsidence and its control. Am. Assoc. Petroleum Geologists Underground Waste Management and Environmental implications, Memoir No. 18, p. 50-71.

POLAND, J. F., and DAVIS, G. H. 1969. Land subsidence due to withdrawal of fluids, in Varnes, D. J., and Kiersch, G., eds. Reviews in engineering geology, v. 2. Geol. Soc. America, p. 187-269.

POLAND, J. P., LOFGREN, B. E., IRELAND, R. L., and PUGH, R. G., 1975. Land subsidence in the San Joaquin Valley, California, as of 1972. U.S. Geol. Survey Prof. Paper 437-H, 77 p.

POLAND, J. F., LOFGREN, B. E., and RILEY, F. S., 1972. Glossary of selected terms useful in the studies of the mechanics of aquifer systems and land subsidence due to fluid withdrawal. U.S. Geol. Survey Water-Supply Paper 2025, 9 p.

RICCERI, G., and BUTTERFIELD, R. 1974. An analysis of compressibility data from a deep borehole in Venice. Geotechnique, no. 2, p. 175-192.

RIEKE, H. H., III, and CHILINGARIAN, G. V. 1974. Compaction of argillaceous sediments. Elsevier Scientific Publishing Company, Amsterdam, 424 p.

RILEY, F. S. 1969. Analysis of borehole extensometer data from central California, in Tison, L. J., ed., Land subsidence, v. 2. Internat. Assoc. Sci. Hydrology Pub. 89, p. 423-431.

ROBERTS, J. E. 1969. Sand compression as a factor in oil field subsidence, in Tison, L.J., ed., Land subsidence, v. 2. Internat. Assoc. Sci. Hydrology Pub. 89, p. 368-376.

SCOTT, R. F. 1963. Principles of soil mechanics. Addison-Wesley Pub. Co., Palo Alto, California, 550 p.

TAYLOR, D. W. 1948. Fundamentals of soil mechanics. New York, John Wiley and Sons, Inc., 700 p

TERZAGHI, KARL. 1925. Principles of soil mechanics: IV, Settlement and consolidation of clay. Eng. News-Rec., p. 874-878.

TERZAGHI, KARL, and PECK, R. B. 1967. Soil mechanics in engineering practice. New York, John Wiley and Sons, Inc. 2d ed., 729 p.

THEIS, C. V. 1935. The relation between the lowering of the piezometric surface and the rate and duration of discharge of a well using ground-water storage. Am. Geophys. Union Trans., v. 16, p. 519-524.

THEIS, C. V. 1938. The significance and nature of the cone of depression in ground-water bodies. Econ. Geology, v. 33, no. 8, p. 889-902.

VAN DER KNAPP, W., and VAN DER VLIS, A. C. 1967. On the cause of subsidence in oil-producing area, in Drilling and production. Mexico City, 7th World Petroleum Cong. Proc., v. 3, p. 85-95.

4 Laboratory tests for properties of sediments in subsiding areas, by A. I. Johnson and Working Group

4.1 INTRODUCTION

Laboratory tests of core samples are made to determine their physical, hydrologic, and engineering properties and their consolidation and rebound characteristics. The laboratory test results then are utilized, along with the observed changes in artesian head, to compute compaction of the aquifer system on the basis of soil mechanics theory. In addition, the mineralogy and petrography of samples is determined in the laboratory in order to study these properties with special reference to the environment of deposition.

This chapter briefly describes some of the test methods used in the laboratory and presents examples of the tables and graphs summarizing the properties for compacting sediments in the specific study area--primarily the San Joaquin Valley, with some reference to the Santa Clara Valley, both in central California. The physical and geologic characteristics and the subsidence problems for these areas are described in Case Histories 9.13 and 9.14 and all laboratory methods and data are presented in more detail in the report by Johnson, Moston, and Morris (1968). The laboratory analyses that were used directly in this case study were primarily the particle-size distribution, specific gravity and unit weight, porosity and void ratio, and the consolidation and rebound tests. The tests of Atterberg limits and indices were not used quantitatively in the central California study but provided supplementary data that furnish at least a qualitative index to the compressibility characteristics of the sediments. For example, in the Unified Soil Classification system, the liquid limit is used to distinguish between clay of high compressibility and clay of low compressibility. The tests of permeability were useful in related studies. The tests comparing permeability parallel and normal to the stratification gave some data on the relative ease of movement of water in the two directions, and thus were of use in studies of leakage through confining beds.

Applications of laboratory-test data may be found in chapters 3 and 5 and in some case histories in Chapter 9 (such as 9.3, 9.13 and 9.14).

4.2 FIELD SAMPLING

The samples for which test results are discussed later in this chapter were obtained from core holes in the San Joaquin and Santa Clara Valleys, in Central California. Eight core holes were drilled to depths as great as 620 m and samples were collected from these core holes for analysis in the laboratory.

The core holes were drilled by a rotary-drilling rig, utilizing core barrels of the double-tube type, which have an outer rotating barrel and an inner stationary barrel. The inside diameter of the core barrel was nominally 7.6 cm and the average diameter of core recovered was about 7 cm. In most of the work, a core barrel capable of taking a core 3 m long was used. A 6-m core barrel was tried but did not give as good core recovery.

Above the Corcoran Clay Member of the Tulare Formation in the Los Banos-Kettleman City area, (Figure 4.1) a 3-m interval was cored after each 9-m of drilling. Below the top of the Corcoran Clay Member, coring was generally continuous to the bottom of the hole. Core recovery was excellent for unconsolidated to semiconsolidated alluvial deposits of sand, silt, and clay. For example, at core hole 14/13-llDl, the accumulated cored interval was 302 m and the aggregate core footage brought to land surface was 211 m, an average core recovery of 70 per cent. Core recovery was as high as 80 per cent and as low as 30 per cent. The lowest recovery was in the coarse, loose water-bearing material. Hence, the core suite obtained did not contain a representative sampling of the coarser, most permeable layers.

At each of the drilling sites, cores were laid out in sequence in 1.2-m wooden core boxes and properly labelled for future reference. From each 3-m interval cored, the following samples were collected:

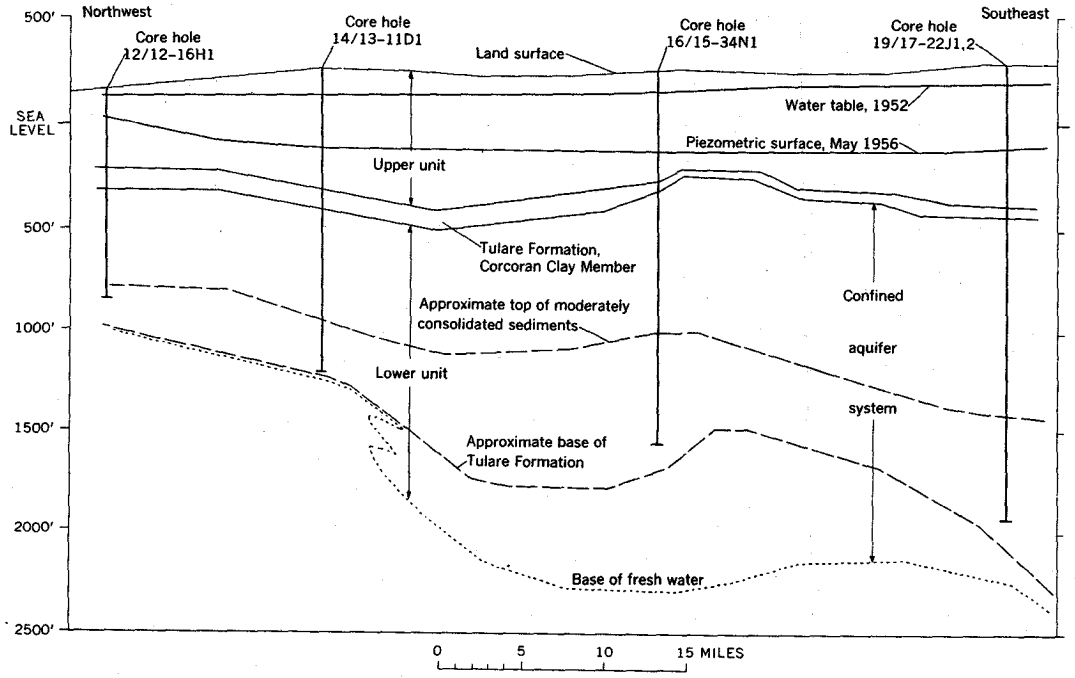

Figure 4.1 Simplified geologic section through core holes in the Los Banos-Kettleman City area, San Joaquin Valley, California.

1. Physical and engineering properties sample.--One litre-sized sample (about 15 cm long), taken from the most representative materials of the cored interval, was sealed in wax in a cardboard container to preserve the natural moisture content insofar as practicable and to prevent disturbance of the core.
2. Petrographic samples.--One or more samples, taken from the same materials and contiguous to the physical characteristic samples, were collected and sealed in wax in a 0.5 litre cardboard container and retained for petrographic examination. For paleontologic examination, samples also were taken of fossiliferous beds encountered in several of the core holes; they were not sealed in wax.
3. General purpose samples.--Two or more 0.25 litre samples were collected for general reference, one representing the fine-textured materials and one representing the coarse-textured layers; they were retained in cardboard cartons but not sealed in wax.

In addition, undisturbed samples of representative fine-grained deposits were collected for consolidation tests. Litre-sized samples were carefully selected and then sealed in wax in metal containers to keep them in an undisturbed condition.

4.3 COMPOSITE LOGS OF CORE HOLES

An electric log was obtained for each core hole after coring was completed. Graphic logs and generalized lithologic descriptions were prepared from the geologists' logs made at the drill site, supplemented by interpretation of the electric log in zones not cored or of poor recovery. These three elements were combined to give a composite log for each core hole. The depths of the samples tested also are plotted on the composite logs. Figure 4. 2 is an example of a composite log for one of the core holes.

The interpretation of electric logs is based on the principle that, in fresh-water-bearing deposits such as those penetrated in this area, high resistivity values are indicative of sand and low resistivity values are indicative of clay and silty clay. Intermediate values are indicative of clayey silt, silt, silty sand, and other sediments classified texturally between sand and clay. Resistivity is indicated by the right-hand curve of the electric log; it increases toward the right. Thus, the Corcoran Clay Member of the Tulare Formation is indicated

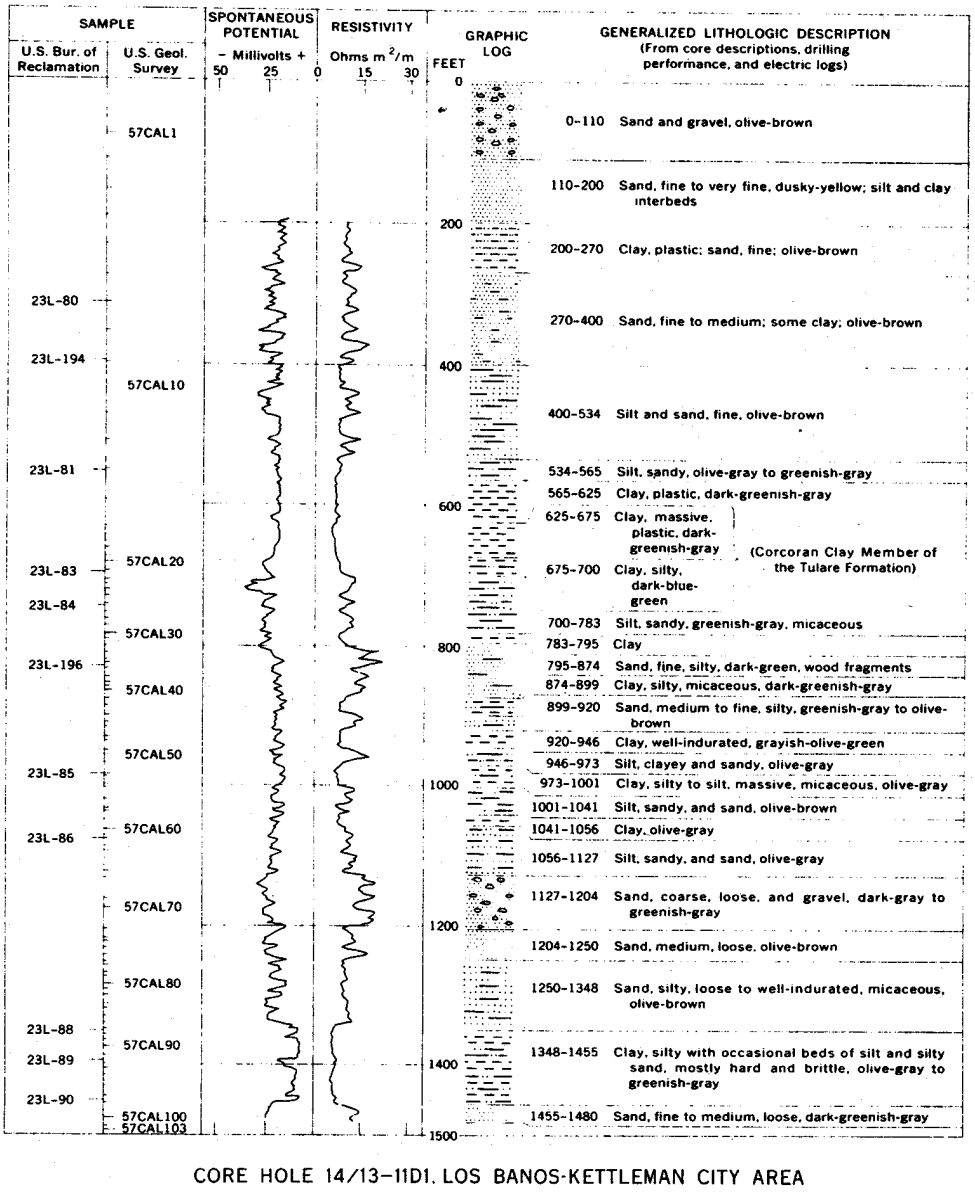

Figure 4.2 Example of a composite log of a core hole.

by a curve segment of uniformly low resistivity (Figure 4.2). The electric logs of the core holes can be compared with the physical and hydrologic properties of the samples plotted according to depth, as in Figures 4.3 and 4.4.

4.4 METHODS OF LABORATORY ANALYSIS

Utilizing a hydraulic-press assembly in the laboratory, cores 5 cm in diameter by 5 cm long were obtained by forcing thin-wall brass cylinders into the larger core--one in a direction at right angles to the bedding (vertical) and the other parallel to the bedding (horizontal). These small cores were used for permeability tests and for determining unit weight and porosity.

The rest of the large core was prepared and used for determination of specific gravity, particle-size distribution, and Atterberg limits and indices. Sample preparation for these analyses began with the air-drying of chunks of the large core. These chunks of material were

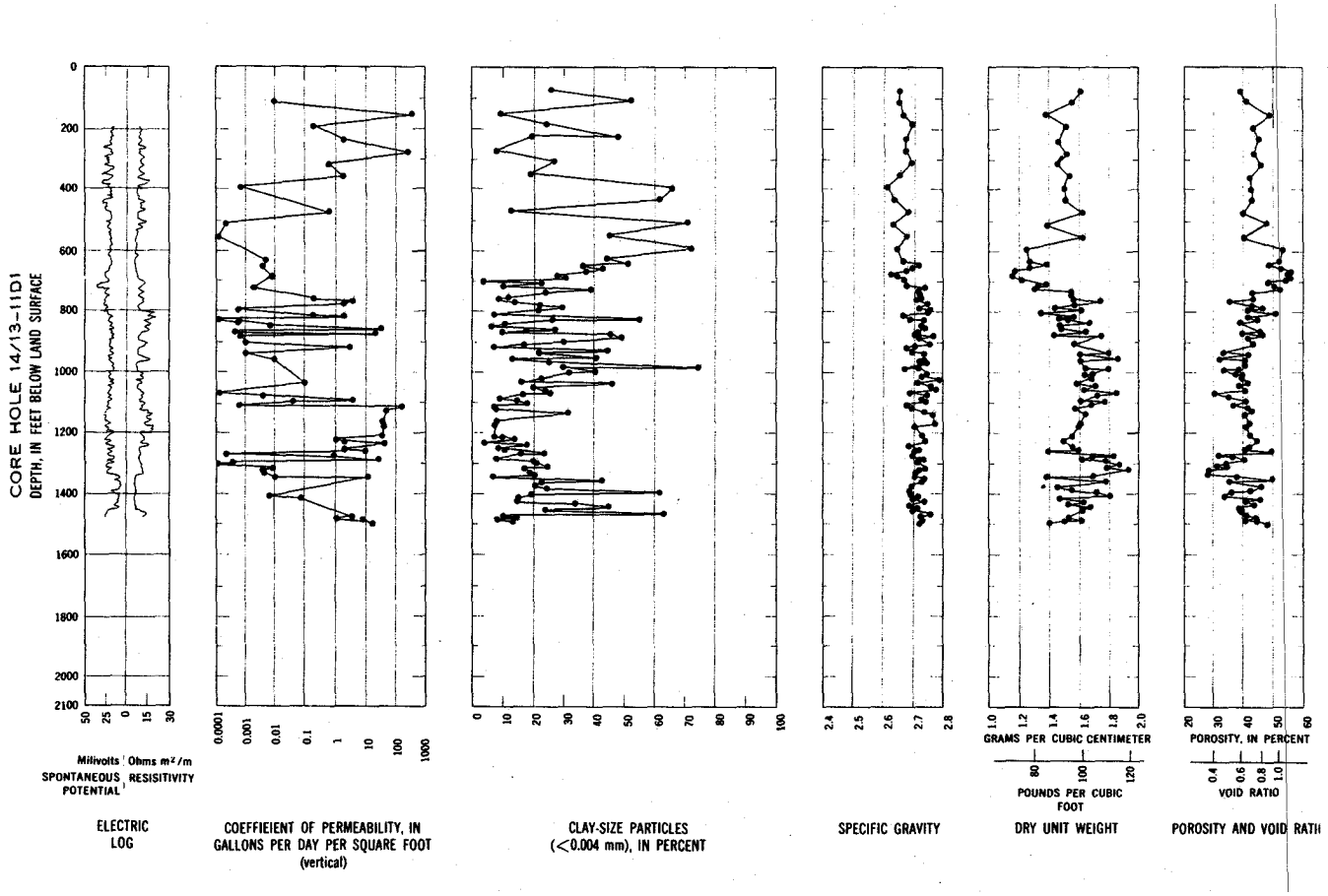

Figure 4.3 A graph of physical properties from core hole 14/13-llDl in the San Joaquin Valley, California.

then gently but thoroughly separated into individual particles in a mortar with a rubber-covered pestle. Care was taken to prevent crushing of the individual particles.

Core samples were analyzed by use of the standard methods described briefly in the following paragraphs. Additional information on the theory and methods of analysis is available in Meinzer (1923, 1949), Wenzel (1942), Taylor (1948), U.S. Bureau of Reclamation (1974, p. 407-508) and the American Society for Testing Materials (1980). Results of the laboratory analyses were reported in tables. The first page of each of the tables is shown as tables 4.1 through 4.5 at the end of this chapter as an example of the format and type of the data reported. The tables were published in inch-pound units, thus readers interested in metric units may refer to the metric conversion table, Appendix E.

4.4.1 Particle-size distribution

Particle-size analysis, also termed a "mechanical analysis," is the determination of the distribution of particle sizes in a sample. Particle sizes smaller than 0.0625 mm were determined by the hydrometer method of sedimentation analysis, and sizes larger than 0.0625 mm were determined by wet-sieve analysis.

The hydrometer method of sedimentation analysis consisted of (1) dispersing a representative part of the prepared sample with a deflocculating agent, sodium hexametaphosphate, in one litre of water and (2) measuring the density of the suspension at increasing intervals of time with a soil hydrometer. At given times, the size of the largest particles remaining in suspension at the level of the hydrometer was computed by use of Stokes' law, and the weight of particles finer than that size was computed from the density of the suspension at the same level.

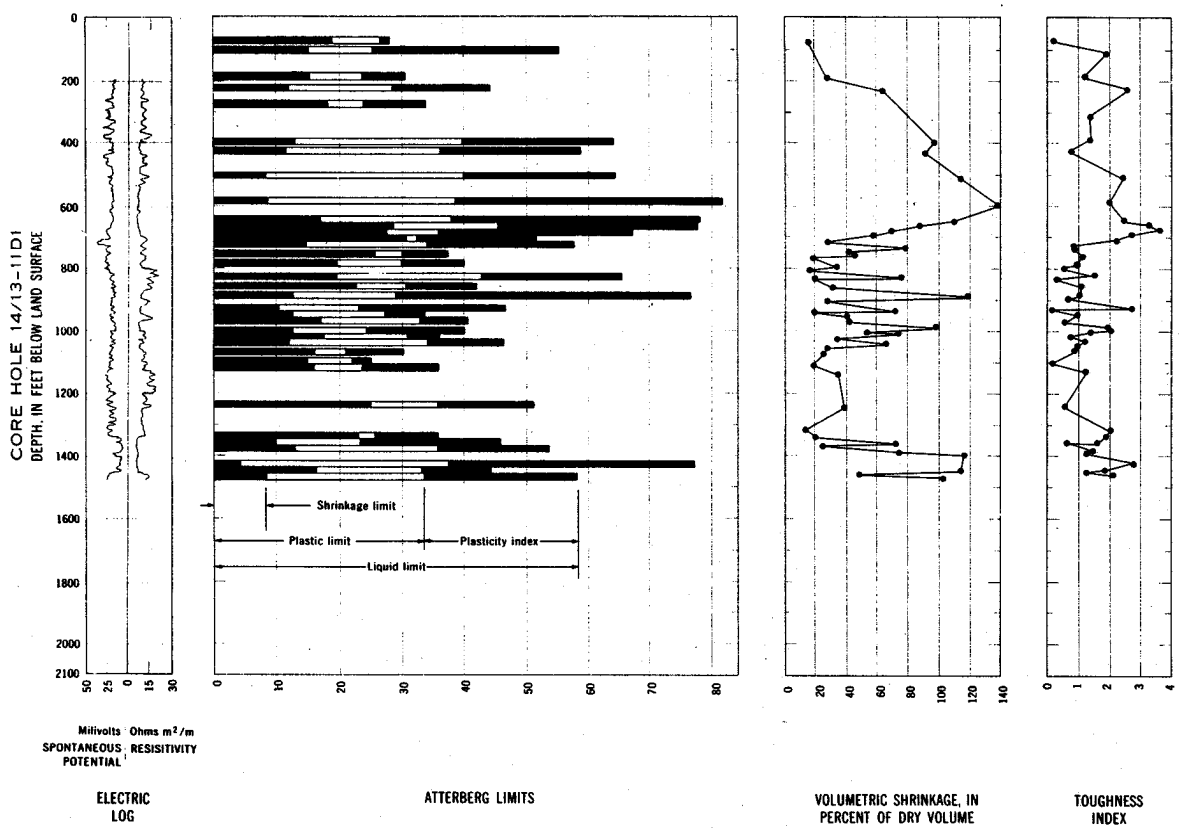

Figure 4.4 Continuation of a graph of properties from core hole 14/13-llDl in the San Joaquin Valley, California.

After the hydrometer analysis, the sample suspension was poured into a sieve which had openings of 0.0625 mm. The sample then was gently agitated and washed over the sieve. The material retained was carefully dried and placed in a set of standard 20-cm sieves which were shaken for a period of 15 minutes on a Ro-tap mechanical shaker. The fraction of the sample remaining on each sieve was weighed on a balance.

From the hydrometer analysis and the sieve analysis, the percentage of the particles smaller than a given size was calculated and plotted as a cumulative distribution curve. The particle sizes, in millimeters, were plotted as abscissas on a logarithmic scale and the cumulative percentages of particles smaller than the size shown, by weight, as ordinates on an arithmetic scale. The percentage in each of several size ranges was then determined from this curve.

The size ranges were identified according to the following particle sizes:

	Diameter (mm)
Gravel	>2.0
Very coarse sand	1.0 -2.0
Coarse sand	.5 -1.0
Medium sand	.25 - .5
Fine sand	.125 - .25
Very fine sand	.0625- .125
Silt-size	.004 - .0625
Clay-size	<0.004

This size classification system is used by the Water Resources Division, U.S. Geological Survey, and is essentially the same as classifications proposed by Wentworth (1922) and the National Research Council (Lane, 1947), except that those authors proposed further subdivisions of gravel, silt, and clay. Subsequent references to sand, silt, and clay in this report will relate to sand-,silt-, and clay-size particles as specified in the foregoing table.

4.4.2 Permeability

Permeability is the capacity of rock or soil to transmit fluid under the combined action of gravity and pressure. It can be determined in the laboratory by observing the rate of movement of fluid through a sample of known length and cross-sectional area, under a known difference head.

The basic law for flow of fluids through porous materials was established by Darcy who demonstrated experimentally that the rate of flow of water was proportional to the hydraulic gradient. Darcy's law may be expressed as

$$Q = KiA, \tag{4.l}$$

where Q is the quantity of water discharged in a unit of time, A is the total cross-sectiona1 area through which the water flows, i is the hydraulic gradient (the difference in head, h, divided by the length of flow, L), and K is the hydraulic conductivity (occasionally known as the coefficient of permeability) of the material for water, or

$$K = \frac{Q}{iA} = \frac{QL}{hA} \tag{4.2}$$

Because the water is assumed to be relatively pure, density is ignored.

Hydraulic conductivity is determined in the laboratory in constant-head or variable-head permeameters or is computed from consolidation-test results. The permeameters used for the tests discussed in this chapter are described in detail by Johnson, Moston, Morris (1968).

Entrapped air in a sample may cause plugging of pore space and thus reduce the apparent hydraulic conductivity. Therefore, a specially designed vacuum system provided the de-aired tapwater used as the percolation fluid.

The chemical character of the water used for the permeability tests of fine-grained silty or clayey materials should be compatible with the chemical character of the native pore water. If the test water is not compatible, the clay-water system and the permeability values obtained will be affected. The chemical character of the native pore water in the fine-grained sediment was not known at the time of the test and Denver tapwater therefore was used in the permeability tests.

The 5-cm-diameter "undisturbed" cores cut from the larger original core were retained in their cylinders. These cylinders were installed directly in the permeameter to serve as the percolation cylinder of the apparatus. The reported hydraulic conductivity was the maximum value obtained after several test runs and represents saturation permeability.

4.4.3 Unit weight

For reference in developing some of the equations used in following sections of this chapter, it is useful to study the relations found in a unit soil mass, as seen in Figure 4 5. The concepts and symbols shown in that figure will be used in development of equations related to the properties of compacting sediments. Other useful definitions and symbols can be found in the publication of the American Society for Testing and Materials (1980).

The dry unit weight is the weight of solids per unit of total volume of oven-dry rock or soil mass. It normally is reported in grams per cubic centimeter or kilograms per cubic metre. Void space as well as solid particles are included in the volume represented by the dry unit weight. The dry unit weight divided by the unit weight of distilled water at a stated temperature (usually 4° C) is known occasionally as the apparent specific gravity, which is dimensionless.

The volume of the small cores, cut previously from the large cores, was obtained by measurement of the cylinder dimensions. This volume and the ovendry weight of the contained sample were then used to calculate the dry unit weight as follows:

$$\gamma_d = \frac{W_s}{V}, \tag{4.3}$$

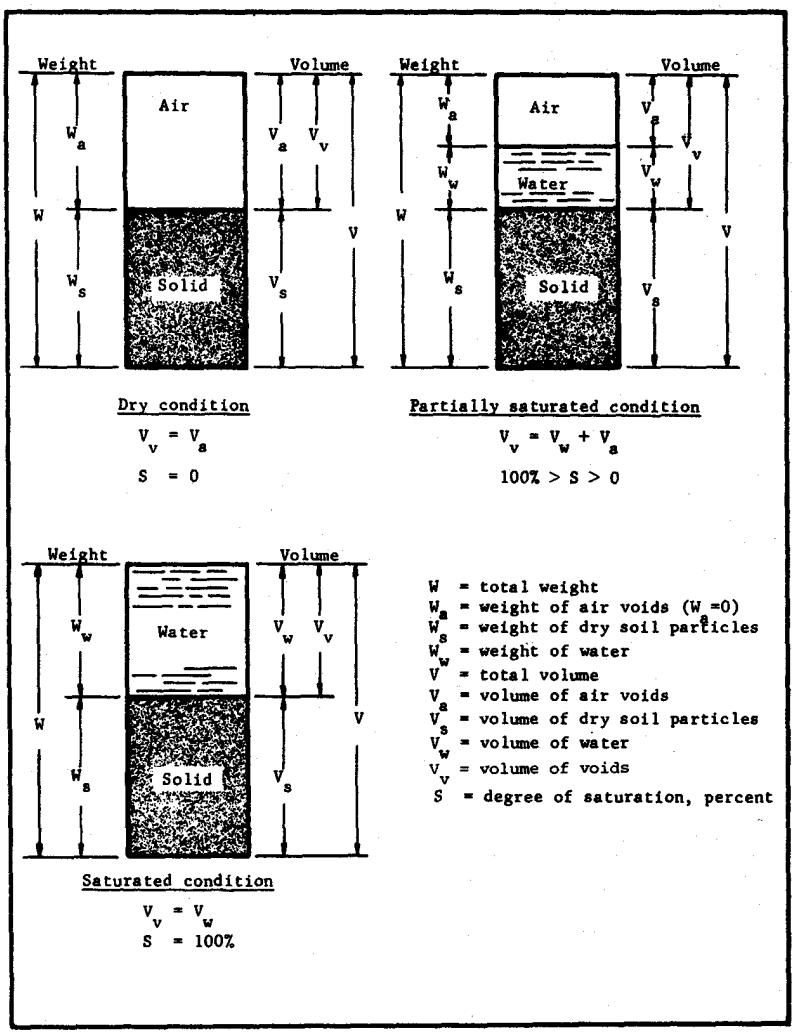

Figure 4.5 Principal phases of a unit soil mass.

where

γ_d = dry unit weight, in grams per cubic centimetre,
W_S = weight of ovendry sample, in grams,
V = total mass volume of sample, in cubic centimetres.

4.4.4 Specific gravity of solids

Specific gravity of solids, G, is the ratio of (1) the weight in air of a given volume of solids at a stated temperature (unit weight of solid particles or particle density) to (2) the weight in air of an equal volume of distilled water at stated temperature (usually 4° C), or

$$\gamma_S = \frac{W_S}{V_S} \quad \text{and} \quad \gamma_W = \frac{W_W}{V_W} ,$$

so

$$G = \frac{\gamma_S}{\gamma_W} \tag{4.4}$$

where

γ_S = unit weight of solids, in grams per cubic centimetre,
V_S = volume of solids, in cubic centimetres,
γ_W = unit weight of water, in grams per cubic centimetre,
W_W = weight of water, in grams,
V_W = volume of water, in cubic centimetres, and
G = specific gravity, a ratio.

The volumetric-flask method was used for determining the specific gravity of solids. A weighed oven-dry part of the sample was dispersed in water in a calibrated volumetric flask. The volume of the particles was equivalent to the volume of displaced water. The unit weight of the solid particles was obtained by dividing the dry weight of the sample by the volume of the solid particles. Because the density of water at 4° C is unity in the metric system, the specific gravity is numerically equivalent to this unit weight.

4.4.5 Porosity and void ratio

Porosity, n, is defined as the ratio of (1) the volume of the void spaces to (2) the tota1 volume of the rock or soil mass. It normally is expressed as a percentage. Therefore,

$$n = \frac{V_v(100)}{V} = \frac{V - V_S(100)}{V}, \qquad (4.5)$$

then as

$$\gamma_d = \frac{W_S}{V}$$

and

$$\gamma_s = \frac{W_S}{V_s},$$

$$n = \frac{W_S/\gamma_d - W_S/\gamma_s}{W_S/\gamma_d}(100),$$

or

$$n = \frac{\gamma_S - \gamma_d}{\gamma_S}(100) \qquad (4.6)$$

where

n = porosity, in per cent,
V_v = volume of voids, in cubic centimetres,
V = total mass volume, in cubic centimetres,
W_S = weight of oven-dry particles, in grams,
γ_S = unit weight of particles, in grams per cubic centimetre (equal numerically to specific gravity of solids in metric system),
γ_d = dry unit weight of sample, in grams per cubic centimetre, and
V_S = volume of solid particles, in cubic centimetres.

After the dry unit weight and the specific gravity of solids had been determined for the sample, the porosity was calculated from the above equation. The relation among these three properties is illustrated in Figure 4.6.

The void ratio is defined as the ratio of (1) the volume of voids to (2) the volume of solid particles in a soil mass, or

$$e = \frac{V_V}{V_S} \qquad (4.7)$$

Its relation to porosity is expressed by

$$e = \frac{n}{1-n}, \qquad (4.8)$$

where e = void ratio, and n = porosity, in per cent.

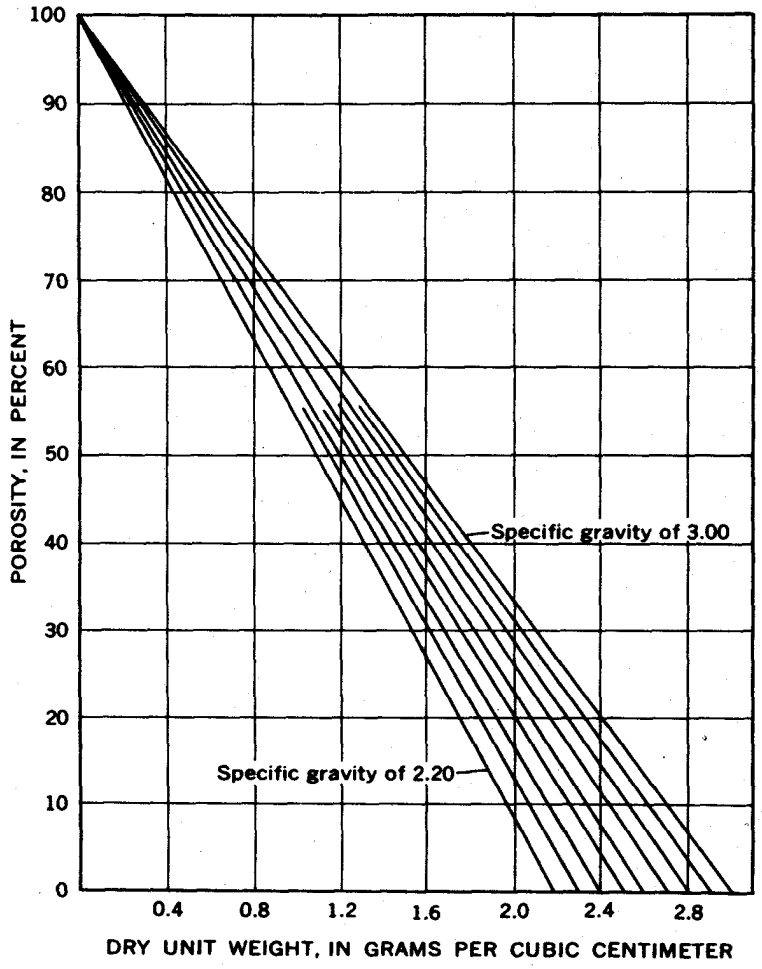

Figure 4.6 Relation of porosity to dry unit weight for various specific gravities of solids.

The relation between void ratio and porosity is illustrated in Figure 4.7.

4.4.6 Moisture content

The moisture content of rock or soil material is the ratio of the weight of water contained in a sample to the oven-dry weight of solid particles, expressed as a percentage, or

$$w = \frac{W_W}{W_S}(100), \tag{4.9}$$

where

w = moisture content, in per cent of dry weight,
W_W = weight of water, in grams, and
W_S = weight of oven-dry sample (dry solids), in grams.

Usually, samples in moisture-proof containers, are weighed to obtain their wet weight. They are oven-dried to constant weight at 110°C and reweighed. The loss of weight (the amount of contained water) divided by the dry weight of the sample equals the moisture content.

4.4.7 Atterberg limits

Atterberg (1911), a Swedish soil scientist, suggested a series of arbitrary limits for indicating the effects of variations of moisture content on the plasticity of soil materials.

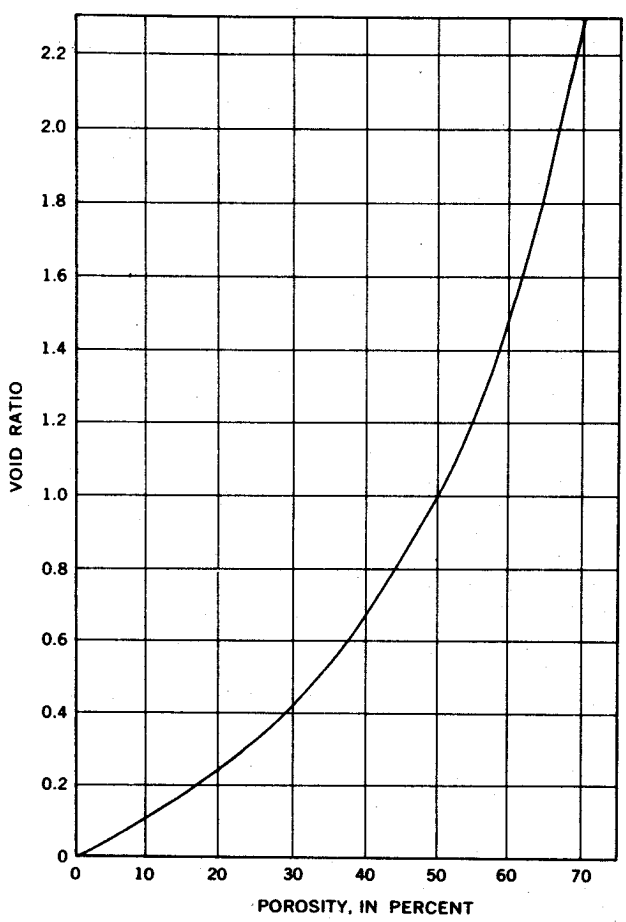

Figure 4.7 Relation of void ratio to porosity.

The most commonly used Atterberg limits, sometimes referred to as limits of consistency, are the liquid and plastic limits. Among a number of indices, the plasticity index is most commonly determined.

The moisture contents at which fine-textured sediments pass from one state of consistency to another are governed by the texture and composition of the sediments. Atterberg (1911), Terzaghi (1926), and Goldschmidt (1926) found that plasticity is a function of the amount of fine platelike particles in a sediment mass. Thus, the Atterberg consistency limits and indices are influenced by the clay content of the sediments tested.

Although the Atterberg limits are somewhat empirical, most soil investigators believe that they are valuable in characterizing the plastic properties of fine-textured sediment, (Casagrande, 1932).

Only the smaller size particles of a given sample, those passing a U.S. Standard No. 40 sieve (finer than 0.42 mm in diameter) are used for Atterberg tests. Although limits and indices are calculated as moisture content, in per cent of dry weight, (W_W/W_S) , all values are usually reported as numbers only.

4.4.7.1 Liquid limit

The liquid limit, w_L, is the moisture content, expressed as a percentage of the oven-dry weight, at which any particular soil material passes from the plastic to the liquid state. It is that moisture content at which a groove of standard dimensions cut in a pat of soil will close for a distance of 1/2 in. (1.3 cm) under the impact of 25 shocks in a standard liquid-limit apparatus. The moist sample was placed in the round-bottomed brass cup of the mechanical liquid-limit device and was divided into two halves by a V-shaped grooving tool. A cam on the device raised the cup and let it drop against the base of the machine until the two edges of the groove flowed

together for the specified half an inch. The number of taps, or shocks, were recorded, and the moisture content of a part of the sample was determined. This process was repeated three times at different moisture contents. These data are plotted as a "flow curve" on a semilogarithmic graph, the number of shocks plotted as abscissa on the logarithmic scale and the moisture content as ordinates on the arithmetic scale. The moisture content corresponding to the intersection of the flow curve with the 25-shock line was taken as the liquid limit of that soil material.

4.4.7.2 Plastic limit

The plastic limit, w_P, is the minimum moisture content, expressed as a percentage of the oven-dry weight, at which soil material can be rolled into 1/8-in. (0.3-cm) diameter threads without the threads breaking into pieces. This moisture content represents the transition point between the plastic and semisolid states of consistency. The moist sample was rolled between the hand and a glass plate until a thread 0.3 cm in diameter was formed. The sample was then kneaded together and again rolled out. This process was continued at slowly decreasing water contents until crumbling prevented the formation of the thread. The pieces of the crumbled sample were then collected together and the moisture content was determined. This moisture content was considered to be the plastic limit.

4.4.8 Consolidation

When a saturated soil sample is subjected to a load, that load initially is carried by the water in the voids of the sample because the water is incompressible in comparison with the sample's structure. If water can escape from the sample voids as a load is continually applied to the sample, an adjustment takes place wherein the load is gradually shifted to the soil structure. This process of load transference is generally slow for clay and is accompanied by a change in volume of the soil mass. Consolidation is defined as that gradual process which involves, simultaneously, a slow escape of water, a gradual compression, and a gradual pressure adjustment. This use of the term should not be confused with the geologists' definition which refers to the processes by which a material becomes firm or coherent (Am. Geol. Inst., 1957, p. 62). The theory of consolidation is discussed in detail by Terzaghi (1943, p. 265-297).

To determine the rate and magnitude of consolidation of sediments, a small-scale laboratory test known as a one-dimensional consolidation test is used. The test and apparatus, described in detail by the U.S. Bureau of Reclamation (1974), are discussed briefly in the following paragraphs for the benefit of the reader. The application of one-dimensional consolidation test data to a foundation-settlement analysis has been described by Gibbs (1953). The apparatus (consolidometer) used by the Bureau of Reclamation (1974) is shown in Figure 4.8. In addition to the unit shown, a means of loading is required--usually a platform scale with a weighing beam attached to the connecting rods of the consolidometer.

Normally, the sample is trimmed to the size of the specimen rings, which are 4-1/4 in. (10.8 cm) in inside diameter and 1-1/4 in. (3.2 cm) high. Samples must be in as near an undisturbed condition as possible. Because of the small size of the cores collected for the subsidence studies, however, consolidation specimens of standard size could not be used, and the core diameter had to be trimmed to fit 2 in. (5-cm) rings.

Loads are applied to the specimen in increments, but the minimum number of increments is usually four-- 12, 25, 50, and 100 per cent of the maximum desired load. Increments are usually selected so that each succeeding load is double that of the previous load. Each load is applied to the consolidometer while dial readings of consolidation are taken and recorded for 4, 10, 20 seconds, and other time intervals up to 24 hours. Additional readings are taken at 24-hour intervals until the consolidation is virtually complete for that load.

The percentage of consolidation of the specimen is computed, and a curve of consolidation versus time is obtained for each load increment. The final stress-strain relations are presented as a curve showing the void ratio versus log of pressure (load), the final condition for each increment of load being a point on the curve (Figure 4.9).

Two important soil properties furnished by a consolidation test are the coefficient of consolidation and the compression index. The coefficient of consolidation, C_V, represents the rate of consolidation for a given load increment. It is determined by use of the 50-percent point on the time consolidation curve in the equation

$$C_v = \frac{T_{50} T_{50}^2}{t_{50}}, \qquad (4.10)$$

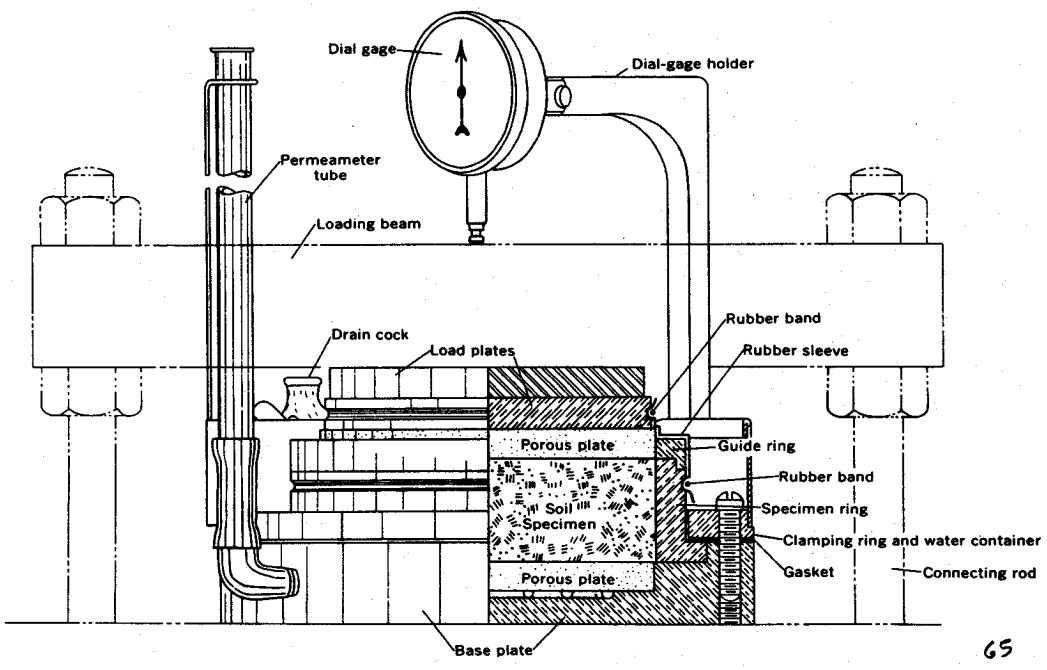

Figure 4.8 One-dimensional consolidometer specimen container (from U.S. Bureau of Reclamation, 1960, p. 495).

where

T_{50} = time factor at 50-per-cent consolidation = 0.20,
H_{50} = one half the specimen thickness at 50-per-cent consolidation, and
t_{50} = time required for specimen to reach 50-per-cent consolidation. The coefficient of consolidation is usually reported in square centimetres per second or in square inches per second.

The compression index, C_C, represents the compressibility of the soil samples. It is the slope of the straight-line portion of the void ratio-log of pressure (load) curve. The compression index can be determined from the equation

$$C_c = \frac{e_o - e}{\log \frac{P_o + \Delta P}{P_o}} \quad \text{(see Figure 4.9 for symbols).} \qquad (4.11)$$

When the consolidation is complete under maximum loading, the consolidometer can be used as a variable-head permeameter, and the hydraulic conductivity can be determined directly. The mechanical procedure is similar to that described previously (section 4.4.2). The consolidation data also can be used for computing the hydraulic conductivity. The equation utilizing time-consolidation characteristics is

$$K = \frac{C_v(\gamma_w)(e_o - e)}{\Delta_P(1 + e_o)} \qquad (4.12)$$

where

C_V = coefficient of consolidation,
γ_W = unit weight of water,
e_0 = void ratio at start of load increment,
e = final void ratio, and
Δ_P = increment of load.

Although the example in Table 4.4 shows feet per year for the permeability (standard inch-pound system units), cm per sec is the commonly reported unit for K.

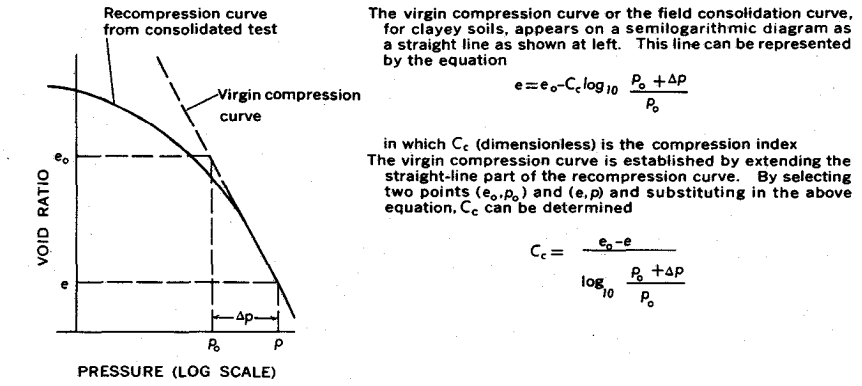

A. METHOD OF DETERMINING THE COMPRESSION INDEX (C_c)

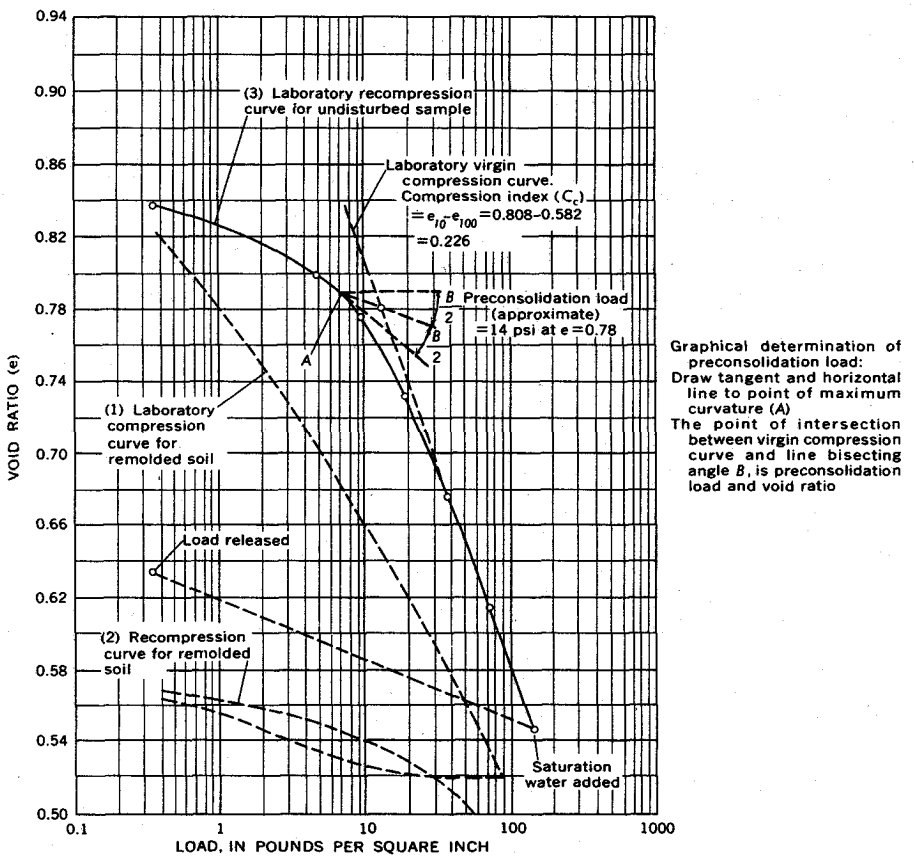

B. VOID RATIO–LOAD CURVES AND PRECONSOLIDATION LOAD

Figure 4.9 Void ratio-load curve, compression index, and preconsolidation load (modified from U.S. Bureau of Reclamation, 1960, p. 58).

4.5 RESULTS OF LABORATORY ANALYSES

4.5.1 Particle-size distribution

An example of particle-size distribution data from central California is presented in Table 4.1. The percentage of gravel-, sand, silt-, and clay-size particles were shown in such tables for each of the 549 samples from seven core holes analyzed in the laboratory. Particle-size distribution curves for all of the samples were plotted on figures similar to Figure 4.10. An example of the size-distribution (gradation) for samples tested for consolidation is given in Table 4.3.

Table 4.1 Physical and hydrologic properties of samples from core holes.

Hydrologic laboratory sample	Sample depth (feet)	Particle analysis, percentage of—					Median diameter, D_{50} (mm)	Geometrical quartile deviation (sorting coefficient), So	Log quartile deviation (log sorting coefficient), $\log_{10} So$	Sediment class (Shepard system)	Specific gravity of solids	Dry unit weight		Total porosity (percent)	Void ratio	Coefficient of permeability (gp per sq ft at 60°F)	
		Gravel	Sand	Silt	Clay <0.004 mm	Clay <0.002 mm						G per cc	Lb per cu ft			Vertical	Horizontal
Core hole 14/13-11D1																	
57CAL1	77.0- 77.5		24.8	49.5	25.7	18	0.024	4.04	0.606	Sand-silt-clay	2.66	1.60	99.8	39.9	0.66		
2	110.5- 111.0		10.7	37.3	52.0	44	.0034			Silty clay	2.66	1.56	97.3	41.4	.71	0.01	0.03
3	153.0- 153.5		87.1	3.7	9.2	9	.19	1.46	.164	Sand	2.67	1.37	85.5	48.7	.95	360	
4	191.5- 192.0		29.0	46.8	24.2	20	.028	3.92	.593	Sand-silt-clay	2.70	1.52	94.8	43.7	.78	.2	.2
5a	232.5- 233.0		21.6	30.4	48.0	39	.0045			do	2.68	1.47	91.7	45.1	.82	2	
5b	232.5- 233.0		61.6	18.9	19.5	16	.092	3.16	.500	Clayey sand	2.64	1.64	102.3	37.9	.61	4	
6	277.1- 277.6	1.3	89.0	1.9	7.8	7	.25	1.59	.201	Sand	2.68	1.52	94.8	43.3	.76	270	
7	314.0- 314.5		22.3	51.0	26.7	22	.019	4.12	.615	Sand-silt-clay	2.70	1.46	91.1	45.9	.85	.6	
8	353.0- 353.5		47.0	34.3	18.7	16	.060	3.37	.528	Silty sand	2.66	1.54	96.1	42.1	.73	2	10
9	398.0- 398.5		.6	33.4	66.0	56	.0010			Silty clay	2.62	1.51	94.2	42.4	.74	.0007	.002
10	432.0- 432.5		7.0	31.2	61.8	50	.0020			do	2.64	1.51	94.2	42.8	.75	.00007	
11	471.5- 472.0		47.3	40.0	12.7	11	.059	2.00	.301	Silty sand	2.69	1.63	101.7	39.4	.65	.7	
12	510.3- 510.8	.6	8.9	19.5	71.0	61				Silty clay	2.64	1.39	86.7	47.3	.90	.0002	
13	552.5- 553.0		22.0	33.0	45.0	36	.0062			Sand-silt-clay	2.68	1.63	101.7	39.2	.65	.0001	
14	594.0- 594.5		8.8	19.7	71.5	59	.0012			Silty clay	2.65	1.25	78.0	52.8	1.12		
15	631.0- 631.5		19.2	36.3	44.5	34	.0057	5.68	.754	do	2.67	1.28	79.9	52.1	1.09	.005	
16	646.6- 647.1		1.0	47.5	51.5	40	.0036			do	2.72	1.39	86.7	48.9	.96		
17	652.3- 652.8		23.3	40.1	36.6	26	.0096	5.20	.716	Sand-silt-clay	2.70	1.28	79.9	52.6	1.11	.004	
18	662.1- 662.6		.8	56.2	43.0	30	.0058	3.26	.513	Clayey silt	2.68	1.18	73.6	56.2	1.28		
19	674.0- 674.5		1.0	61.5	37.5	25	.0068	2.61	.417	do	2.63	1.18	73.6	55.1	1.23		
20	682.5- 683.0		26.8	45.2	28.0	20	.013	5.06	.704	Sand-silt-clay	2.65	1.17	73.0	55.8	1.26	.008	
21	697.0- 697.5		.6	68.4	31.0	20	.0082	2.51	.400	Clayey silt	2.67	1.23	76.8	54.1	1.18		
22	707.0- 707.5		80.2	16.1	3.7	3	.26	1.68	.225	Sand	2.67	1.38	86.1	48.3	.94		
23	713.0- 713.5		.2	76.8	23.0	14	.010	2.00	.301	Silt	2.68	1.33	83.0	50.4	1.02		
24	721.5- 722.0		4.0	86.0	10.0	7	.012	1.48	.170	do	2.74	1.31	81.7	52.2	1.09	.002	
25	731.0- 731.5		1.6	59.4	39.0	26	.0067	2.99	.476	Clayey silt	2.72	1.55	96.7	42.8	.75		
26	743.0- 743.5		6.0	70.0	24.0	17	.013	2.57	.410	do	2.72	1.55	96.7	42.9	.75		
27	757.0- 757.5		50.2	38.1	11.7	8	.062	3.06	.486	Silty sand	2.73	1.57	98.0	42.7	.75	.2	
28	764.9- 765.4		77.4	13.9	8.7	7	.34	2.42	.384	Sand	2.71	1.75	109.2	35.4	.55	4	
29	773.0- 773.5		38.2	48.0	13.8	11	.050	2.22	.346	Sandy silt	2.75	1.57	98.0	42.9	.75	2	2
30	784.5- 785.0		16.2	61.8	22.0	14	.020	2.94	.468	Clayey silt	2.72	1.45	90.5	46.7	.88		
31	791.0- 791.5		26.0	44.2	29.8	26	.026	5.89	.770	Sand-silt-clay	2.76	1.62	101.1	41.3	.70	.0006	
32	802.0- 802.5		35.4	43.0	21.6	16	.040	3.56	.551	do	2.75	1.35	84.2	50.9	.04		
33	812.0- 812.5		80.2	11.8	8.0	8	.25	2.36	.373	Sand	2.67	1.57	98.0	41.2	.70	.2	
34	813 - 821	.3	91.7	1.0	7.0	7	.21	1.27	.104	do	2.69	1.47	91.7	45.4	.83	2	
35	826.0- 826.5		1.0	44.0	55.0	38	.0033	2.72	.435	Silty clay	2.74	1.53	95.5	44.2	.80	.0001	
36	831.5- 832.0		12.2	61.3	26.5	20	.020	3.46	.539	Clayey silt	2.74	1.68	104.8	38.7	.63	.0006	
37	843.5- 844.0		69.0	20.0	11.0	9	.12	1.91	.281	Silty sand	2.73	1.48	92.4	45.8	.85	.007	
38	853.0- 853.5		83.2	10.6	6.2	5	.12	1.31	.117	Sand	2.74	1.49	93.0	45.6	.84	33	
39	860.0- 860.5		2.4	70.4	27.2	21	.145	3.01	.479	Clayey silt	2.74	1.62	103.0	39.8	.66		
40	867.0- 867.5		54.2	27.8	18.0	16	.010			Silty sand	2.72	1.64	102.3	39.7	.66	.0005	
41	871.0- 871.5		70.0	19.8	10.2	9	.099	1.73	.238	do	2.71	1.44	89.9	46.9	.88	22	
42	877.0- 877.5		4.5	49.5	46.0	34	.0050	4.24	.627	Clayey silt	2.77	1.76	109.8	36.5	.57	.0007	
43	887.5- 888.0		.8	49.7	49.5	37	.0041	3.16	.500	Silty clay	2.72	1.59	99.2	41.5	.71		
44	901.0- 901.5		8.6	61.2	30.2	19	.011	2.97	.473	Clayey silt	2.76	1.57	98.0	43.1	.76	.001	
45	911.5- 912.0		48.4	34.6	17.0	16	.056	3.52	.547	Silty sand	2.71						
46	917.2- 917.7		80.0	13.0	7.0	7	.22	1.58	.199	Sand	2.68					3	
47	932.0- 932.5		8.0	47.3	44.7	37	.0064			Clayey silt	2.70	1.80	112.3	33.2	.50		
48	936.5- 937.0		12.6	65.4	22.0	14	.016	2.60	.415	do	2.74	1.61	100.5	41.2	.70	.001	
49	951.0- 951.5		4.6	54.4	41.0	33	.0082	5.10	.708	do	2.74	1.87	116.7	31.8	.47		
50	957.5- 958.0		39.4	47.4	13.2	11	.044	2.34	.369	Sandy silt	2.72	1.62	101.1	40.4	.68	.01	
51	968.5- 969.0		6.0	68.8	25.2	20	.016	2.86	.456	Clayey silt	2.75	1.63	101.7	40.7	.69		
52	984.0- 984.5		2.2	23.1	74.7	58	.0015			Silty clay	2.67	1.65	103.0	38.2	.62		
53	987.6- 988.0		27.2	43.0	29.8	26	.026	6.57	.818	Sand-silt-clay	2.72	1.80	112.3	33.8	.51		
54	1,000.5-1,001.0		4.2	54.8	41.0	32	.0068	4.42	.645	Clayey silt	2.75	1.72	107.3	37.5	.60		
55	1,005.1-1,005.6		2.8	65.2	32.0	22	.0090	2.79	.446	do	2.73	1.65	103.0	39.8	.66		
56	1,010.8-1,021.3		11.4	65.8	22.8	16	.024	2.83	.452	do	2.79	1.69	105.5	39.4	.65		
57	1,033.8-1,034.2		52.0	32.0	16.0	13	.070	4.39	.642	Silty sand	2.72	1.58	98.6	41.9	.72	.1	
58	1,039.5-1,040.0		1.8	52.2	46.0	36	.0048			Clayey silt	2.76	1.71	106.7	38.0	.61		
59	1,051.5-1,052.0		12.4	67.6	20.0	15	.025	2.51	.400	do	2.78	1.64	102.3	41.0	.70		
60	1,063.5-1,064.0		35.6	40.4	24.0	20	.026	6.14	.788	Sand-silt-clay	2.69	1.86	116.1	30.9	.45	.0001	
61	1,070.8-1,071.3		19.5	54.5	26.0	21	.020	3.67	.565	Clayey silt	2.75	1.73	108.0	37.1	.59		
62	1,075.0-1,075.5		55.6	27.2	17.2	14	.079	3.02	.480	Silty sand	2.75	1.77	110.4	35.6	.55	.004	
63	1,088.5-1,089.0		81.6	9.4	9.0	8	.18	1.67	.223	Sand	2.73	1.62	101.1	40.7	.69	42	
64	1,092.0-1,092.5		35.4	49.6	15.0	12	.042	3.16	.500	Sandy silt	2.75	1.78	111.1	35.3	.55	.04	
65	1,104.6-1,105.1		38.0	44.0	18.0	15	.037	1.15	.061	do	2.68	1.69	105.5	36.9	.59	.0006	
66	1,113.5-1,114.0		91.2	1.6	7.2	7	.23	1.23	.090	Sand	2.70	1.58	98.6	41.5	.71	174	
67	1,123.5-1,124.0		84.2	7.8	8.0	7	.16	1.38	.140	do	2.74	1.57	98.0	42.7	.75	50	

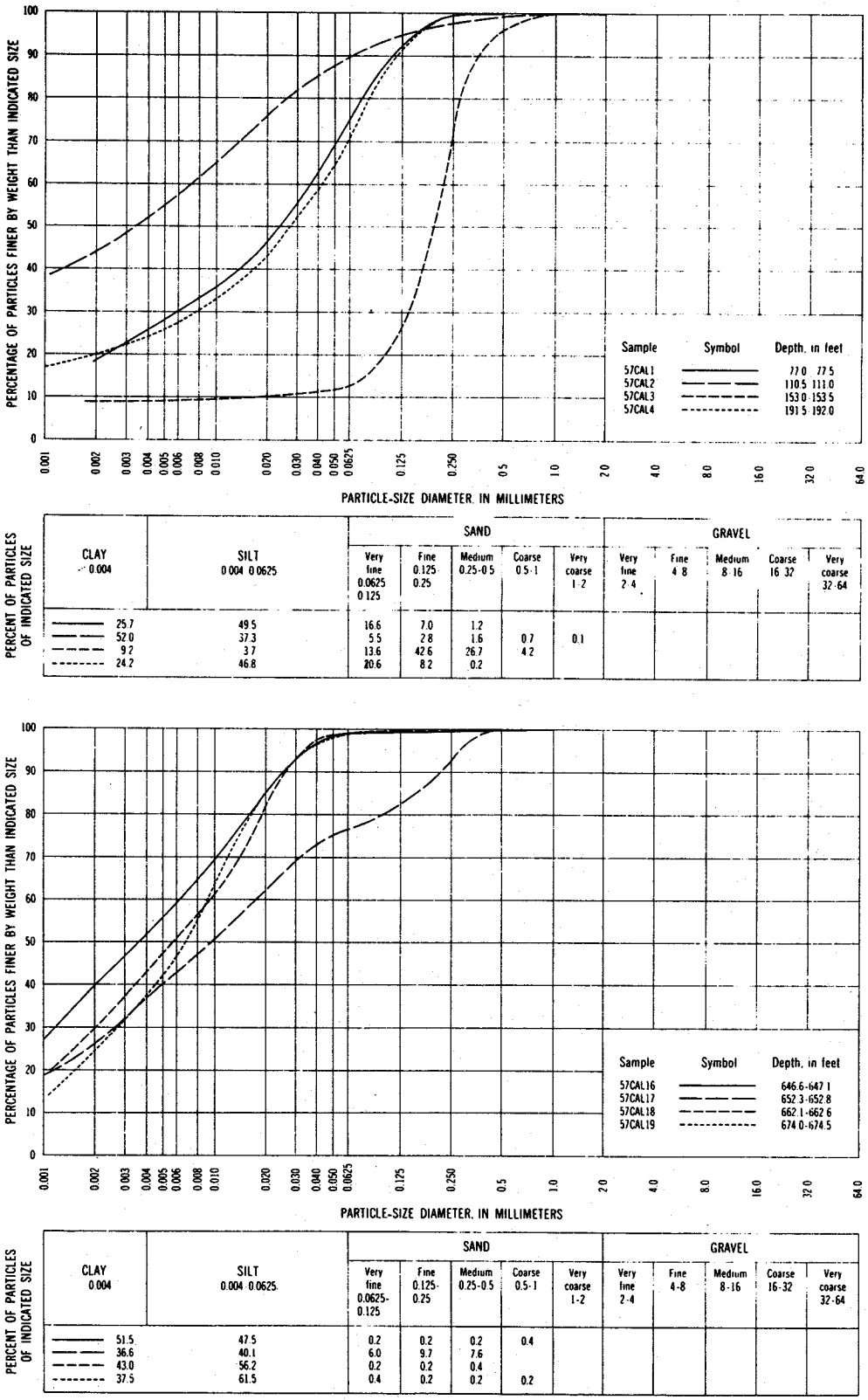

PERCENT OF PARTICLES OF INDICATED SIZE

	CLAY 0.004	SILT 0.004-0.0625	SAND Very fine 0.0625-0.125	SAND Fine 0.125-0.25	SAND Medium 0.25-0.5	SAND Coarse 0.5-1	SAND Very coarse 1-2	GRAVEL Very fine 2-4	GRAVEL Fine 4-8	GRAVEL Medium 8-16	GRAVEL Coarse 16-32	GRAVEL Very coarse 32-64
57CAL1	25.7	49.5	16.6	7.0	1.2							
57CAL2	52.0	37.3	5.5	2.8	1.6	0.7	0.1					
57CAL3	9.2	3.7	13.6	42.6	26.7	4.2						
57CAL4	24.2	46.8	20.6	8.2	0.2							

PERCENT OF PARTICLES OF INDICATED SIZE

	CLAY 0.004	SILT 0.004-0.0625	SAND Very fine 0.0625-0.125	SAND Fine 0.125-0.25	SAND Medium 0.25-0.5	SAND Coarse 0.5-1	SAND Very coarse 1-2	GRAVEL Very fine 2-4	GRAVEL Fine 4-8	GRAVEL Medium 8-16	GRAVEL Coarse 16-32	GRAVEL Very coarse 32-64
57CAL16	51.5	47.5	0.2	0.2	0.2	0.4						
57CAL17	36.6	40.1	6.0	9.7	7.6							
57CAL18	43.0	56.2	0.2	0.2	0.4							
57CAL19	37.5	61.5	0.4	0.2	0.2	0.2						

Figure 4.10 Some graphs of particle-size distribution curves for core hole 14/13-llDl in the San Joaquin Valley, California.

Because clay content has an important influence on many of the properties of sediments, the clay content for all the samples was plotted to facilitate comparison with the other properties (see example, Figure 4.3). In Table 4.1, the percentage of particles smaller than 2-μm (0.002-mm) clay, as well as smaller than 4- μm (0.004-mm) clay, has been reported. When the 4-μm rather than the 2-μm size was used as the criterion, 78.5 per cent of the samples showed 1ess than 10 per cent greater clay content. In addition, 20.9 per cent of the samples showed 10-20 per cent greater clay content and 0.6 per cent of the samples showed more than 20 per cent greater clay content for the 4-μm than for 2-μm size criterion.

4.5.2 Sediment classification triangles

Most clastic sediments are a mixture of sand-, silt-, and clay-size particles in varying proportions. A suitable nomenclature for sediments is therefore important to describe the approximate relations among these three main constituents. Because sediment classification is often based on the relative percentages of sand-, silt-, and clay-size particles, it is convenient to plot these three constituents on a triangular chart.

A large number of triangular classification systems have been devised over the years. Some were developed primarily for the use of geologists in relating classification to sedimentation characteristics, and others were developed for the use of soils engineers in relating classification to the engineering properties of the sediments. Shepard (1954) developed a sediment classification triangle based on the needs of sedimentologists for studying mode of transport and environment of deposition of sediments. Shepard's classification gives equa1 importance to sand-, silt-, and clay-size particles (Figure 4.11).

Because the mode of transport and environment of deposition of the sediments were being studied, as well as the engineering properties, Shepard's classification was used in the centra1 California study to determine the sediment class name listed for each sample in Table 4.1. For classification of sediments in the lower Mississippi Valley, the U.S. Army Corps of Engineer (Casagrande, 1948) developed a triangle which emphasizes the importance of clay-size particle content. To assist soils engineers in relating the classification of samples to their engineering properties, a transparent overlay of the Mississippi valley classification triangle could be placed over the plots in Figure 4.11 to determine the classification name under that system.

The textural classification used in Table 4.1, based on the Shepard system, is a laboratory classification derived from particle-size distribution graphs. It departs substantially from the field description made from examination of cores and drill cuttings by geologists especially for the fine-textured materials. In the field examination, material containing more than 30-40 per cent of clay-size particles has sufficient clay content to give it the physical properties of clay, such as plasticity. Therefore, the textural description of cores or samples in the field by geologists is not directly comparable to the laboratory textural classification by the Shepard system. Field examination by the geologists results in a textural description much closer to that of the Mississippi Valley classification than to that of the Shepard classification.

4.5.3 Statistical measures

For comparison and statistical analysis, it is convenient to have characteristics of particle-size distribution (mechanical analysis) curves expressed as numbers.

The measure of central tendency is the value (size of particle) about which all other values (sizes) cluster. One such measure is the median diameter, D_{50}, which is defined as that particle diameter which is larger than 50 per cent of the diameters and smaller than the other 50 per cent. It is determined by reading, from the particle-size distribution curve, the particle diameter at the point where the particle-size distribution curve intersects the 50-percent line.

The quartile deviation is a measure of spread of particle sizes. Quartiles are the particle-diameter values read at the intersection of the curve with the 25- (Q_1), 50-(Q_2), and 75- (Q_3) per-cent lines. By convention, the third quartile (Q_3) is always taken as the larger value, regardless of the manner of plotting. The geometrical quartile deviation, or the "sorting coefficient," S_o of Trask (1932, p. 70-72), is represented by the equation

$$S_o = \sqrt{Q_3/Q_1} \qquad (4.13)$$

An S_o value of less than 2.5 indicates a well-sorted sediment, of 3 a normally sorted sediment, and of 4.5 a poorly sorted sediment.

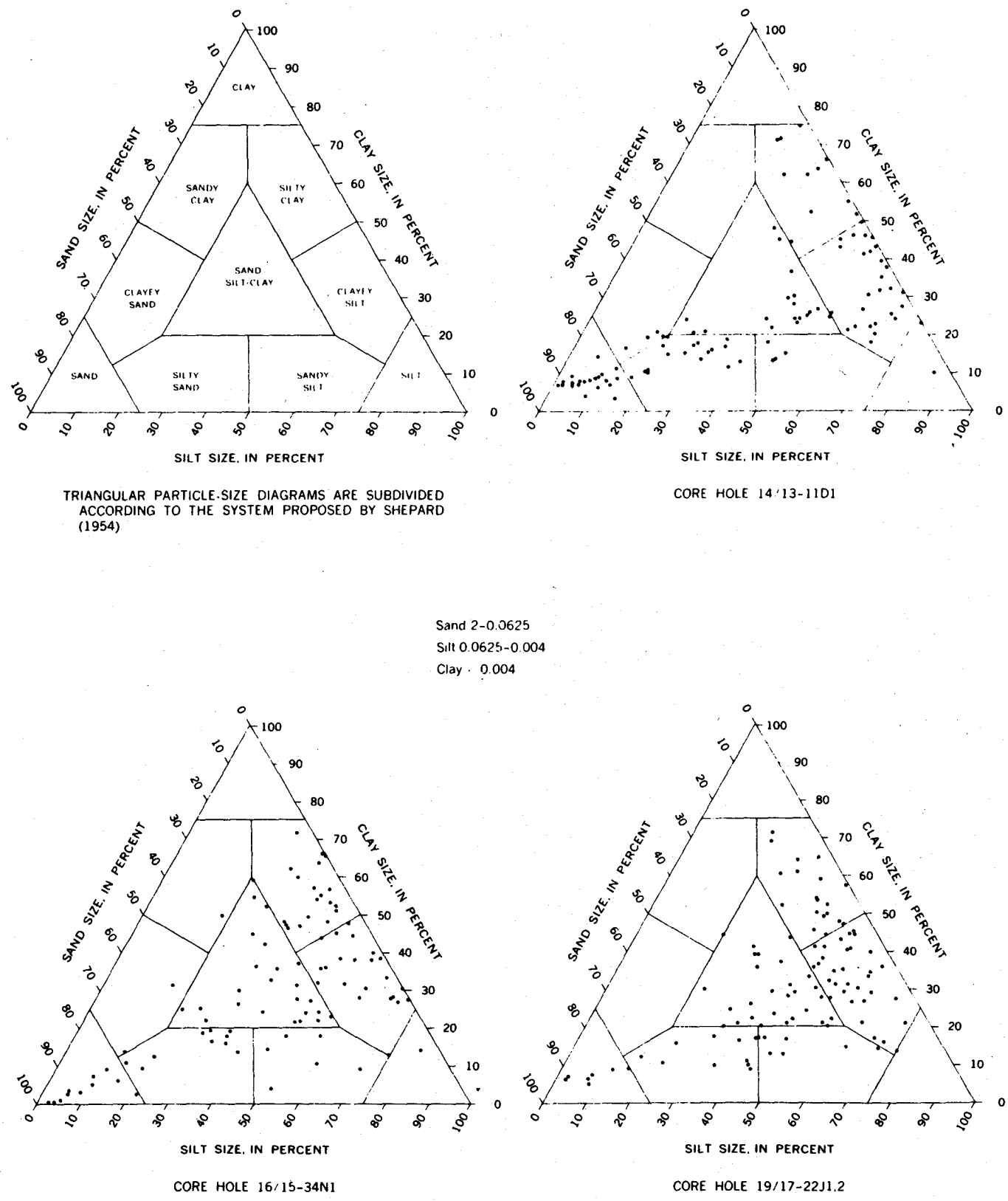

Figure 4.11 Sediment classification triangles for samples from core holes in the Los Banos-Kettleman City area, California.

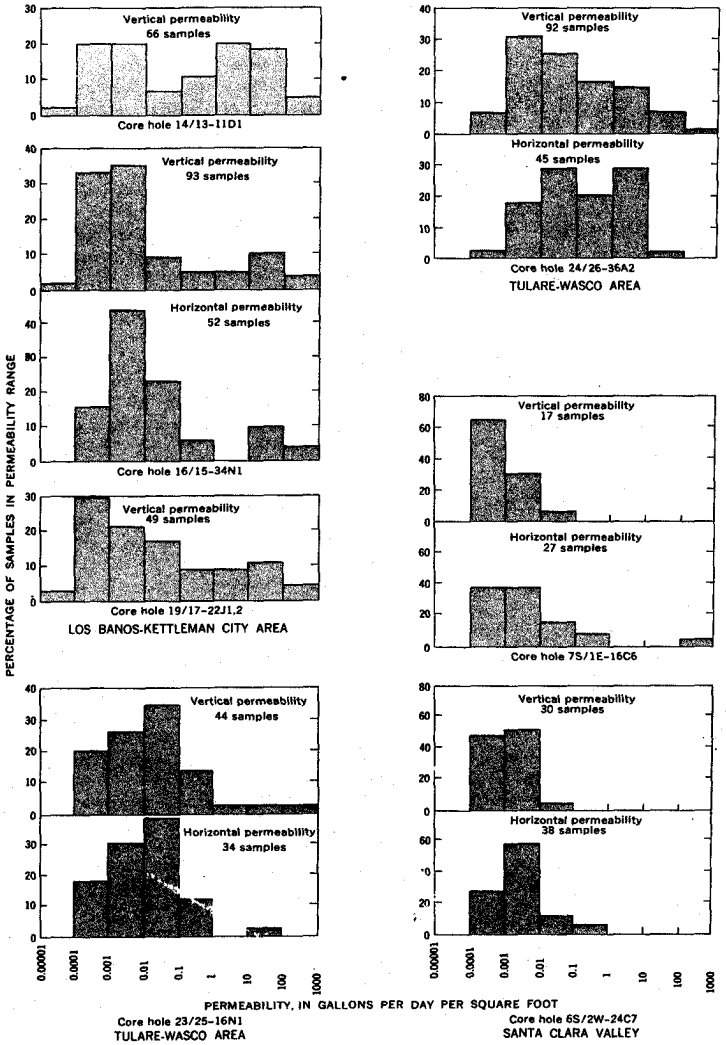

Figure 4.12 Range in permeability of samples from core holes.

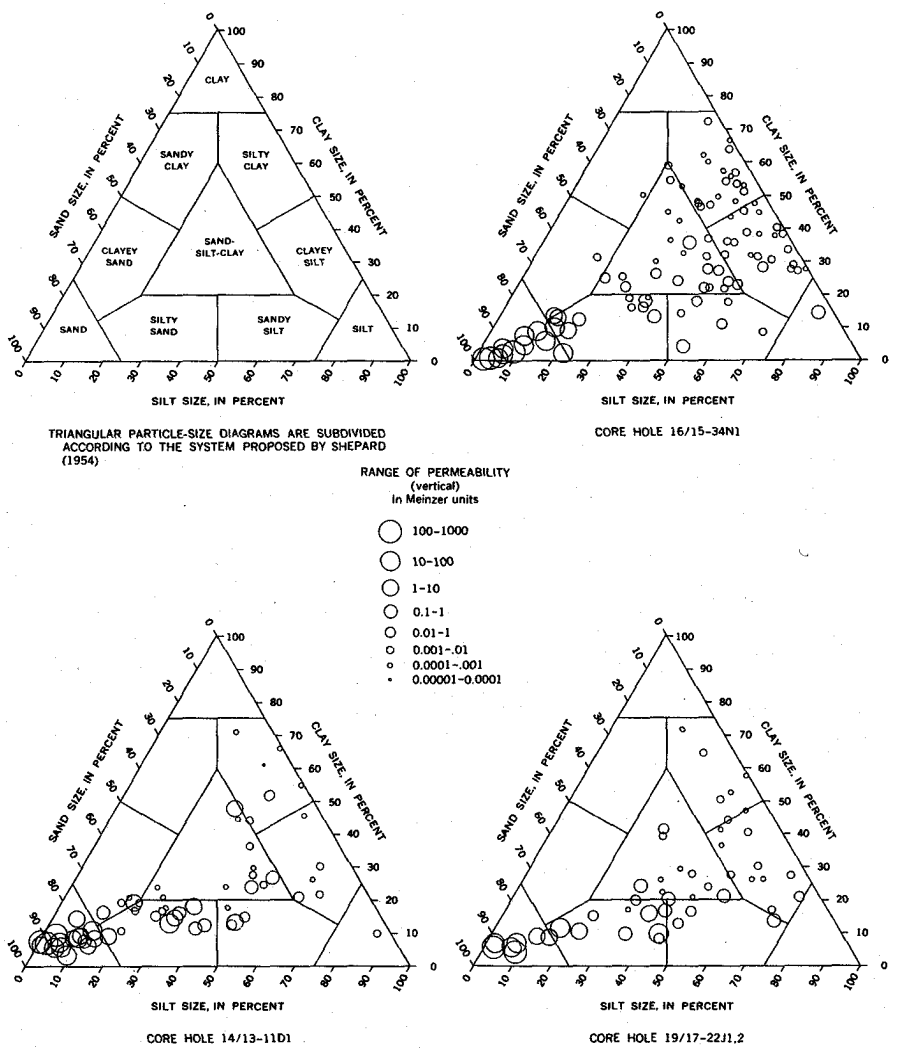

Figure 4.13 Relation between permeability and texture for samples from core holes in the Los Banos-Kettleman City area, California.

The log quartile deviation is the log of the geometrical quartile deviation, or sorting coefficient, S_0, and is represented by the equation

$$\text{Log } S_0 = (\log Q_3 - \log Q_1)/2 \qquad (4.14)$$

The log S_0 can be expressed to the base 10 (Krumbein and Pettijohn, 1938, p. 232) and is so tabulated in this report.

As noted by Krumbein and Pettijohn (1938, p. 232), the geometric quartile measures are ratios between quartiles and thus have an advantage over the arithmetic quartile measures in that they eliminate both the size factor and the unit of measurement. They do not, however, give a direct comparison because the log S_0 (the log quartile deviation) increases arithmetically. Thus, a sediment having log S_0 = 0.402 is twice as widely spread between Q_1 and Q_3 as one having log S_0 = 0.201.

Many sedimentologists now use a $\varnothing$ scale in which

$$\varnothing = -\log_2 d, \qquad (4.15)$$

in which d is the diameter of the particle in millimetres. This scale has certain advantages over the $\log_{10}$ scale for expressing quartile deviation and other statistical parameters (Krumbein and Pettijohn, 1938, p. 233-235). Therefore, statistical parameters were listed in terms of the $\varnothing$ scale in the report by Meade (1967) on the petrology of sediments in subsiding areas of central California.

4.5.4 Permeability

The hydraulic conductivity depends in general on the degree of sorting and upon the arrangement and size of particles. It is usually low for clay and other fine-grained or tightly cemented materials and high for clean coarse gravel. In general, the hydraulic conductivity in a direction parallel to the bedding plane of the sediments (referred to in the data tables as horizontal permeability) is greater than the permeability perpendicular to the bedding plane (referred to as vertical permeability in the tables in this chapter). Most water-bearing materials of any significance as sources of water to wells have hydraulic conductivities above 5×10^{-3} cm per sec.

For central California, the hydraulic conductivities (coefficients of permeability) were presented in tables similar to Table 4.4, and in graphical form such as in Figures 4.12 and 4.13. Figure 4.12 shows the relation of horizontal and vertical hydraulic conductivity for many paired samples. Horizontal hydraulic conductivity was as much as 200 times greater than vertical hydraulic conductivity, with an average ratio of horizontal to vertical permeability of about 3.

Figure 4.14 shows the relation between vertical hydraulic conductivity and texture for samples from core holes in central California. Hydraulic conductivities have been grouped into eight ranges; a symbol representing the proper range for each sample is plotted in the appropriate textural location on the triangle, which is subdivided according to the system proposed by Shepard (1954). Although the highest hydraulic conductivity naturally occurs in the coarse-textured and well-sorted samples, conductivities within each textural classification vary considerably.

The vertical hydraulic conductivities for the clayey sediments tested in the variable-head permeameter under no load (Table 4.1) in general appear to be in a considerably higher range than those in Table 4.4 (ft per yr $\times$ 9.7 $\times$ 10^{-7} = cm per sec) which were computed from the consolidation tests for samples of similar texture. There are at least three reasons for this difference:

1. The permeability of a clayey sediment decreases markedly with decrease in void ratio (or porosity). The hydraulic conductivities given in Table 4.4 (in feet per year) are computed from time-consolidation data derived from test loads ranging from 7 to 112 kg per cm^2 and thus represent conditions of substantially reduced void ratios from those of the samples tested in an unloaded condition in the variable-head permeameter. For sample 23L-207 (Table 4.4), the computed coefficient of vertical hydraulic conductivity for the load range 7 to 14 kg per cm^2 is about 50 times as high as that for the load range 56 to 112 kg per cm^2.
2. For a clayey sediment, the water used for testing permeability in the variable-head permeameter, if not chemically compatible with the pore water, may affect the

results substantially. In the water used in the Hydrologic Laboratory for the variable-head tests, calcium was the predominant cation; however, sodium is the predominant cation in the pore water of the sediments beneath the Corcoran Clay Member in the San Joaquin Valley area. The use of water in which the calcium ion is predominant in testing cores of such sediments would tend to increase the value of the hydraulic conductivity obtained in the variable-head tests. The consolidation test, however, did not involve the passage of water through the sample, only the squeezing out of native pore water.

3. For a sample of very low hydraulic conductivity tested under no load in a variable-head permeameter, the disturbed condition of the sample at and near the container wall creates a boundary region which may produce a zone of appreciably higher permeability than that of the undisturbed sample matrix. Tests in a consolidometer, however, create lateral pressure against the container walls and thus tend to reduce the permeability of the disturbed boundary region to approximately that of the sample matrix.

For these three reasons, the coefficients of permeability of the clayey sediments as derived from the unloaded variable-head permeameter tests (Table 4.1) are not directly comparable to those computed from the time-consolidation data (Table 4.4). Coefficients from the consolidation tests are considered more reliable for samples taken as deep as these, but, to be meaningful for field applications, the coefficients would have to be computed at the void ratio or porosity, existing under the overburden (effective) stress conditions in the field.

4.5.5 Specific gravity, unit weight, and porosity

The specific gravity of a sediment is the average of the specific gravities of all the constituent mineral particles. The specific gravity of most clean sands is usually near 2.65, whereas that of clays ranges from 2.5 to 2.9. Organic matter in the sediment will lower its specific gravity.

The dry unit weight of a sediment is dependent upon the shape, arrangement, and mineral composition of the constituent particles, the degree of sorting, the amount of compaction, and the amount of cementation. Dry unit weights of unconsolidated sediments commonly range from 1.3 to 1.8 g per cm^3.

Because porosity is calculated from the dry unit weight and specific gravity of the sediment, it is dependent upon the same factors. Most natural sands have porosities ranging from 25 to 50 per cent, and soft clays from 30 to 60 per cent. Compaction and cementation tend to reduce these values. In general, porosities decrease with depth below land surface, and dry unit weights increase with depth. Athy (1930) described just such a progressive compaction of sediments as the load of overlying material increased with deposition.

The general trends discussed previously are complicated by other factors which affect the unit weight and porosity of individual samples. These factors are (1) differences in particle sizes or in particle-size distribution, (2) differences in type of clay mineral, (3) exposure to atmosphere and pre-consolidation, such as by dessication, during their depositional history (4) differences in intergranular structure as originally deposited, and (5) change in volume and structure of the core during and subsequent to the sampling operations.

The first four factors are natural phenomena, whereas the last one, the change in volume and structure of the core during and subsequent to the sampling operation, is introduced by man in his disturbance of the natural state in order to procure the sample. The sediments cored in the holes of the San Joaquin Valley ranged in depth from 21 to 630 m below the land surface. The effective stress, or grain-to-grain load, of the overburden on these materials in place increased from about 3 to 70 kg per cm^2 in this depth range. While the core was being cut, additional load was placed on the material by the core barrel and drill pipe, especially near the outer edge of the core. As soon as the materials were encased in the core barrel, however, the effective stress of the overburden was removed and they expanded elastically. Thus, the change in volume (porosity and unit weight) from the natural to the laboratory condition is a function of several variables:

1. Compacting effect produced by displacement of the material by the cutting edge, the inside-wall friction, or by overdriving of the core barrel.
2. Expanding effect of removal of the effective stress of the overburden load at the time the core enters the barrel; the magnitude depends on the elasticity of the material and on the amount of the effective stress removed (increasing with depth).

3. Disturbing effects of mechanical rotation of core-barrel teeth and core catcher while cutting the core, removal of core from barrel, packing, shipping, unpacking, and processing.

The net effect of this sampling process is believed to be an expansion of the sediments as tested in the laboratory, thus providing values that are higher for porosity and lower for unit weight than exist in the natural state. On the basis of a study of the consolidation and rebound data, the laboratory-determined porosity of the fine-textured materials from the San Joaquin Valley was estimated to be as much as 2-3 per cent higher than the in-place field porosity (J. F. Poland, written commun., 1963).

4.5.6 Atterberg limits and indices

The Atterberg limits and indices determined for selected fine-textured samples from the core holes are presented in Tables 4.2 and 4.3. Predominantly fine-textured samples to be tested were selected by visual inspection. Because the Atterberg limits describe properties of the fine part of a sample, presenting Atterberg limit data for samples which are predominantly coarse textured could be misleading. When the influence which the limits of consistency have on the behavior of a sample is being judged, the percentage of the sample tested must be considered. Table 4.2 includes a column which lists the per cent (by weight) of the total sample that passed a No. 40 sieve (0.42-mm openings) and was therefore the part of the sample tested for Atterberg limits.

Most of these Atterberg limits and indices are not directly applicable to the study of subsidence and compaction of sediments under increased effective overburden load, but they do furnish a rough comparative measure of the way in which fine-grained sediments respond to a decrease in moisture content as they pass from the liquid to the solid state. Because the values of these indices are related to texture, composition, clay content, and type of clay minerals present, they may be of qualitative use in comparing the fine-textured clayey deposits in different areas to each other and to fine-textured sediments in other areas for which Atterberg indices have been obtained but for which the clay content, the compression index (C_C), and the type of clay minerals present are not known.

The liquid and plastic limits (moisture content, in per cent by weight) for samples from all core holes in the central California subsidence areas are plotted against percentage of clay-size particles in figure 4.14. As shown by the trend lines, both limits tend to increase with an increase in clay content, the liquid limit increasing at a greater rate than the plastic limit.

The trend lines shown in Figure 4.14 were plotted from equations derived by computer. The equations are of the form $y = a + bx$, in which y represents the moisture content (w), x represents the clay content (C), both in per cent, and a and b are constants. In Figure 4.14A the equation of the liquid-limit trend line is w_L - 13.5 + 1.3C and that of the plastic-limit trend line is w_P = 17.3 + 0.54C. In Figure 4.14C the equation of the liquid-limit trend line is w_L = 14.0 +0.72C and that of the plastic-limit trend line is w_P = 14.7 + 0.22C. The equations of all these trend lines are for samples having clay content based on the percentage of particles less than 0.004 mm in size.

Figure 4.14D shows trends which are composites of all the samples shown in Figures 4.14A-C. The equation of line 1, the liquid-limit trend line for clay sizes less than 0.002 mm, is W_L = 27.8 + 0.71C. The equation of line 2, the liquid-limit trend line for clay sizes less than 0.004 mm, is w_L - 25.8 + 0.60C. The equation of line 3, the plastic-limit trend line for clay sizes less than 0.002 mm is w_P = 25.6 + 0.21C. The equation of line 4, the plastic-limit trend line for clay sizes less than 0.004 mm is w_P = 24.5 + 0.19C. Lines 1 and 3 are included to show the relation between liquid and plastic limits and per cent of clay-size particles if 0.002 mm is chosen as the upper limit of the clay-size range.

The value of the standard error for each trend line was obtained by computer. The pairs of dashed lines which parallel each trend line designate two standard errors on either side of the trend line. The probability is 19 to 1 that, for a given value of clay content (in per cent), the observed liquid limit or plastic limit will lie within the interval between the dashed lines.

The difference between the liquid and plastic limits, or the plasticity index, represents the range of moisture content within which a sediment mass will remain in the plastic state. The moisture content difference between the liquid-limit trend line and the plastic-limit trend line in each part of Figure 4.14 represents the average plasticity index for different clay contents.

Table 4.2 Atterberg limits and indices of samples from core holes.

Hydrologic Laboratory sample	Depth (feet)	Percent passing No. 40 sieve	Liquid limit	Plastic limit	Shrinkage limit	Plasticity index	Flow index	Toughness index	Shrinkage index	Shrinkage ratio	Volumetric shrinkage	Linear shrinkage
Core hole 14/13-11D1												
57CAL1	77.0- 77.5	100	28	27	19	1	6	0.2	8	1.7	15	4
2	110.5- 111.0	99	56	26		30	16	1.9				
4	191.5- 192.0	100	33	24	15	9	8	1.1	9	1.8	32	8
5a	232.5- 233.0	100	44	29	12	15	6	2.5	17	2.0	64	15
7	314.0- 314.5	100	34	24	18	10	8	1.3	6	1.7	27	8
9	396.0- 396.5	100	64	40	13	24	19	1.3	27	1.9	97	20
10	432.0- 432.5	100	59	36	12	23	28	.8	24	1.9	89	19
12	510.3- 510.8	97	65	40	8	25	11	2.3	32	2.0	114	22
14	594.0- 594.5	100	82	39	9	43	22	2.0	30	1.9	139	25
16	646.6- 647.1	100	78	38	17	40	17	2.4	21	1.8	110	22
18	662.1- 662.6	100	80	44	24	36	11	3.3	20	1.6	90	19
19	674.0- 674.5	100	78	46	28	32	9	3.6	18	1.4	70	16
21	697.0- 697.5	100	67	36	28	31	11	2.8	8	1.5	58	14
23	713.0- 713.5	100	52	33	31	19	9	2.1	2	1.4	29	8
25	731.0- 731.5	100	58	34	15	24	26	.9	19	1.8	77	17
26	743.0- 743.5	100	46	28	21	18	19	.9	7	1.6	40	11
27	757.0- 757.5	98	30		27		11			1.5	4	1
28	764.9- 765.4	65	38	30	26	8	6	1.3	4	1.6	19	5
31	791.0- 791.5	100	40	30	20	10	10	1.0	10	1.7	34	9
32	802.0- 802.5	100	34	26	24	8	13	.6	2	1.7	17	5
35	826.0- 826.5	100	65	43	20	22	14	1.6	23	1.7	77	17
36	831.5- 832.0	100	31	26	19	5	25	.2	7	1.7	20	6
39	860.0- 860.5	100	42	31	23	11	10	1.1	8	1.6	30	8
43	887.5- 888.0	100	76	29	13	47	42	1.1	16	1.9	120	23
44	901.0- 901.5	100	40	30	23	10	15	.7	7	1.6	27	8
47	932.0- 932.5	99	47	23	10	24	9	2.7	13	2.0	74	17
48	936.5- 937.0	100	33	29	20	4	16	.2	9	1.7	22	6
49	951.0- 951.5	100	34	27	13	7	6	1.2	14	1.9	40	11
51	968.5- 969.0	100	41	33	17	8	12	.7	16	1.8	43	11
52	984.0- 984.5	100	59	29	10	30	15	2.0	19	2.0	98	20
54	1,000.5-1,001.0	100	40	24	12	16	8	2.0	12	1.9	53	14
55	1,005.1-1,005.6	100	50	29	11	21	14	1.5	18	2.0	78	17
56	1,020.8-1,021.3	100	36	31	17	5	7	.7	14	1.8	34	9
58	1,039.5-1,040.0	100	47	34	12	13	10	1.3	22	1.9	67	16
59	1,051.5-1,052.0	100	33	24	17	9	10	.9	7	1.8	29	8
61	1,070.8-1,071.3	100	30	21	16	9	11	.8	5	1.8	25	7
65	1,104.6-1,105.1	88	25	22	15	3	15	.2	7	1.8	18	5
66	1,133.0-1,133.5	100	36	24	16	12	10	1.2	8	1.8	36	10
75	1,242.0-1,242.5	100	51	36	25	15	26	.6	11	1.5	39	11
83	1,312.0-1,312.5	98	26	18	18	8	4	2.0	0	1.8	14	4
86	1,339.5-1,340.0	100	36	26	23	10	6	1.7	3	1.6	21	6
88	1,357.0-1,357.5	100	46	23	10	23	14	1.6	13	2.0	72	17
89	1,362.5-1,363.0	100	32	21	18	11	16	.7	3	1.7	24	7
91	1,385.0-1,385.5	100	54	36	13	18	12	1.5	23	1.8	74	17
92	1,397.0-1,397.5	98	61	41	5	20	17	1.2	36	2.1	118	23
96	1,432.5-1,433.0	100	77	38	4	39	14	2.8	34	2.3	168	28
97	1,446.0-1,446.5	100	56	28	5	28	15	1.9	23	2.2	112	22
98	1,454.5-1,455.0	100	44	33	16	11	9	1.2	17	1.7	48	13
99	1,465.0-1,465.5	100	58	34	8	24	11	2.2	26	2.1	105	21
Core hole 16/15-34N1												
58CAL2	298.2- 298.7	98	38	30	13	8	11	0.7	17	1.9	48	13
3	332.4- 332.9	98	40	26	12	14	14	1.0	14	1.9	53	14
5	418.5- 419.0	100	44	30	13	14	11	1.3	17	1.9	59	15
6	454.3- 454.8	99	54	37	8	17	23	.7	29	2.0	92	20
9	509.5- 510.0	100	46	35	15	11	18	.6	20	1.8	56	14
11	532.4- 532.9	97	42	34	12	8	9	.9	22	1.9	57	14
12	552.8- 553.2	100	45	32	11	13	8	1.6	21	1.9	65	16
13	563.7- 564.2	100	56	46	12	10	13	.8	34	1.9	84	18
14	570.7- 571.2	100	70	58	9	12	18	.7	49	2.0	122	23
19	636.4- 636.9	99	61	52	20	9	14	.6	32	1.6	66	16
20	643.2- 643.7	99	31	25	22	6	19	.3	3	1.6	14	4
21	652.6- 653.1	96	32	26	12	6	12	.5	14	1.8	36	10
22	666.0- 666.5	100	55	43	15	12	15	.8	28	1.8	72	17
24	683.7- 684.2	100	36	30	19	6	16	.4	11	1.7	29	8
25	696.6- 697.1	100	59	42	12	17	8	2.1	30	1.8	85	18
26	701.8- 702.4	100	42	32	17	10	18	.6	15	1.7	43	11
27	713.4- 713.9	99	61	40	7	21	16	1.3	33	2.0	108	22
29	732.0- 732.6	100	39	28	18	11	12	.9	10	1.7	36	10
31	753.8- 754.3	100	41	30	14	11	17	.6	16	1.8	49	13
32	762.4- 762.9	100	46	33	7	13	14	.9	26	2.0	78	17
33	773.3- 773.8	100	30	26	19	4	10	.4	7	1.7	19	5
36	806.1- 806.6	100	55	40	12	15	15	1.0	28	1.8	77	17
38	822.1- 822.6	98	60	49	10	11	12	.9	39	1.9	95	20
39	827.8- 828.2	100	47	33	13	14	20	.7	20	1.8	61	15
40	837.7- 838.2	100	58	43	14	15	17	.9	29	1.8	79	18
42	860.1- 860.6	100	31	24	22	7	13	.5	2	1.6	14	4
43	866.7- 867.3	100	30	23	18	7	7	1.0	5	1.7	20	6
45	891.6- 892.1	100	53	41	11	12	15	.8	30	1.9	80	18
48	922.6- 923.1	100	46	35	13	11	14	.8	22	1.8	59	15
49	931.2- 931.7	100	35	28	15	7	12	.6	13	1.8	36	10
50	940.6- 941.1	100	46	36	9	10	8	1.2	27	2.0	74	17
51	946.3- 946.8	100	63	43	7	20	22	.9	36	2.0	112	22
52	963.7- 964.2	100	37	28	16	9	14	.6	12	1.8	38	10
53	971.5- 972.0	100	57	46	16	11	20	.6	30	1.7	70	16
54	980.6- 981.1	100	35		27		14			1.5	12	3
58	1,042.8-1,043.3	100	51	45	14	6	13	.5	31	1.8	67	16
61	1,189.5-1,190.0	100	47	34	16	13	24	.5	18	1.8	56	14
63	1,225.0-1,225.5	100	38	34	25	4	14	.3	9	1.6	21	6
64	1,238.1-1,238.6	100	47	36	17	11	16	.7	19	1.7	51	13
66	1,254.9-1,255.4	100	41	36	30	5	7	.7	6	1.4	15	4

Table 4.3 Visual classification, Atterberg limits, and specific gravities of samples tested for consolidation.

[Data from Earth Laboratory, U.S. Bureau of Reclamation, Denver, Colo.]

Earth Laboratory sample	Depth (feet)	Gradation (estimated)				Color (wet)	Soil classification and description	Unified Soil Classification symbol	Atterberg limits			Specific gravity of solids
		Maximum size (U.S. Standard sieve No.)	Gravel >4.76 mm (percent)	Sand, 4.76–0.074 mm (percent)	Silt and clay <0.074 mm (percent)				Liquid limit (percent)	Plastic limit (percent)	Plasticity index	
Core hole 12/12–16H1												
23L91	84.3– 84.6	30	0	10	90	Brown	Clay, containing some fine sand; medium plasticity; slight dilatancy; medium dry strength; no reaction to HCl; trace of gypsum.	CL	31	14	17	2.80
92	159.4– 159.8	100	0	10	90	do	Clay, containing some fine sand; medium to high plasticity; slow dilatancy; medium reaction to HCl.	CL–CH	50	19	31	2.74
93	230.8– 231.2	50	0	10	90	Tan to brown	Clay, lean; low plasticity; slight dilatancy; low dry strength; slight reaction to HCl.	CL	33	11	22	2.73
94	324.5– 324.9	100	0	20	80	Gray	Clay, containing fine sand; low plasticity; medium dilatancy; ome micaceous material present; no reaction to HCl.	CL	29	19	10	2.68
95	374.0– 374.5	200	0	0	100	do	Clay, fat; high plasticity; no dilatancy; no reaction to HCl	CH	54	23	31	2.73
96	425.0– 425.3	100	0	10	90	do	Clay, fat, containing fine sand lenses; high plasticity; no dilatancy; no reaction to HCl; moist, and firm.	CH	76	27	49	2.67
97	471.2– 471.5	100	0	5	95	do	Clay, fat; high plasticity; no dilatancy; lensed with fine sand	CH	58	20	38	2.68
98	516.5– 516.9	50	0	75	25	Gray to black	Sand, fine, no plasticity; fast dilatancy; strong organic odor present; soft and loosely cemented.	SM				2.70
99	579.0– 579.3	100	0	35	65	Tan	Clay, silty containing fine sand; medium plasticity; slight dilatancy.	CL	32	14	18	2.69
100	625.0– 625.4	200	0	0	100	Gray	Clay, fat; high plasticity; no dilatancy; firm; numerous planes containing some silt.	CH	59	19	40	2.79
101	675.9– 676.2	50	0	45	55	do	Clay, silty containing fine sand, medium plasticity, slow dilatancy; clay on outer surface; sand in center, angular.	CL	45	14	31	2.72
102	722.0– 722.3	100	0	5	95	do	Clay, fat; high plasticity; no dilatancy, blocky structure; fractures contain silt.	CH	70	20	50	2.69
103	773.0– 773.4	50	0	60	40	Brown to gray	Sand, fine containing silt; no plasticity; fast dilatancy; lensed with clay and silt; medium cementation; no reaction to HCl.	SM				2.77
104	821.4– 821.8	50	0	55	45	Gray	Sand, fine containing silt; no plasticity; fast dilatancy; organic odor present; no reaction to HCl.	SM				2.74
105	877.4– 877.8	30	0	65	35	Brown	Sand, fine, uniform; no plasticity; fast dilatancy; free water present; no reaction to HCl.	SM				2.71
106	926.8– 927.2	50	0	20	80	Gray	Clay, silty; medium plasticity; slow dilatancy; no reaction to HCl; top of sample contained sand of No. 30 size; rest of sample was silt and clay lensed.	CL	47	32	15	2.72
107	972.0– 972.4	30	0	75	25	do	Sand, fine: no plasticity; fast dilatancy; slight binder	SM				2.70
108	998.6– 999.0	50	0	40	60	Brown	Clay containing fine sand; medium plasticity, slow dilatancy; sample lensed with clay and fine sand.	CL	37	20	17	2.68

Casagrande (1948, P. 919) devised a chart on which the liquid limit is plotted against the plasticity index and used it for rough classification of soils. Points representing different samples from the same stratum or fine-grained deposit plot as a straight line that is rough1y parallel to an "A" line, an empirical boundary between typically inorganic clays above and plastic organic soils below the line. The higher a sample plots on this chart at a given liquid limit, the greater its toughness and dry strength and the lower its permeability and rate of volume change. Figure 4.15 shows plasticity charts of the Casagrande type on which the data for all samples tested from the central California subsidence areas have been plotted.

4.5.7 Consolidation

As one phase of the research on subsidence and compaction of aquifer systems in central California, laboratory consolidation tests were made on representative cores from eight core holes. The results of these consolidation tests were utilized in interpretive reports of the Geological Survey to compute compaction in the confined aquifer system in response to the known decline in artesian head. The method has been described by Miller (1961); it is a refinement of a technique outlined by Gibbs (1959, p. 4-5) based upon Terzaghi's (1943) theory of consolidation and the use of one-dimensional consolidation tests. The consolidation test results are summarized as in Table 4.4.

Consolidation-test curves representative of samples from various depths in one of the San Joaquin valley core holes are shown in Figure 4.16. The curves show, in general, that the Corcoran Clay Member has a greater unit consolidation potential than any of the other sediments. The compaction of the Corcoran Clay Member, however, has contributed very little to the total subsidence to date (Miller, 1961, p. B57) because, where the Corcoran is thick, water moves out very slowly, owing to the formation's low vertical permeability. Where the Corcoran is thin and more permeable, it forms only a small percentage of the water-bearing section. Consolidation curves for the Corcoran Clay Member are generally steep in the load range 14-70 kg per cm^2 and indicate that the clay is normally loaded and has not been precompressed. Therefore the clay has only partly completed its potential consolidation at the present time and at the present artesian pressure.

4.5.7.1 Estimating the compression index

Terzaghi and Peck (1948, p. 66), in a continuation of work begun by Skempton (1944, p. 126), state that the compression indices for clays in a remolded state (C'_C) increase consistently with increasing liquid limit (w_L). Using data from approximately 30 samples selected at random from different parts of the world and representing both ordinary and extra-sensitive clays, Terzaghi and Peck (1948) state that the data on compression indices and liquid limits for these clays plot on a graph within ± 30 per cent of a line representing the equation

$$C'_C = 0.007\ (w_L - 10 \text{ per cent}). \qquad (4.16)$$

They state further that for an ordinary clay of medium or low sensitivity tested in the undisturbed state, the value of C_C corresponding to field consolidation is approximately equal to 1.30 C'_C; thus,

$$C_C = 0.009\ (w_L - 10 \text{ per cent}). \qquad (4.17)$$

Hence, these authors conclude that for normally loaded clays with low or moderate sensitivity the compression index, C_C can be estimated approximately from knowledge of the liquid limit and use of equation 4.17. However, Terzaghi and Peck do caution that this approximate method of computation may furnish merely a lower limiting value for the compression index of an extra-sensitive clay. Later papers by Nishida (1956), and Roberts and Darragh (1963), showed exceptions to the compression index-liquid limit relationships described by Terzaghi and Peck (1948) and indicated a wide scattering of data. Furthermore, they found no simple correlation between these factors for the sample data they studied.

Figure 4.17 shows the relationship between liquid limit and compression index for core samples from test holes in subsiding areas of central California. Although the liquid limit is calculated as moisture content in per cent of dry weight, values usually are reported as numbers only and are reported thus in Figure 4.17 and henceforth in this section. The compression indices used in these graphs were obtained from consolidation tests, not by calculation from the

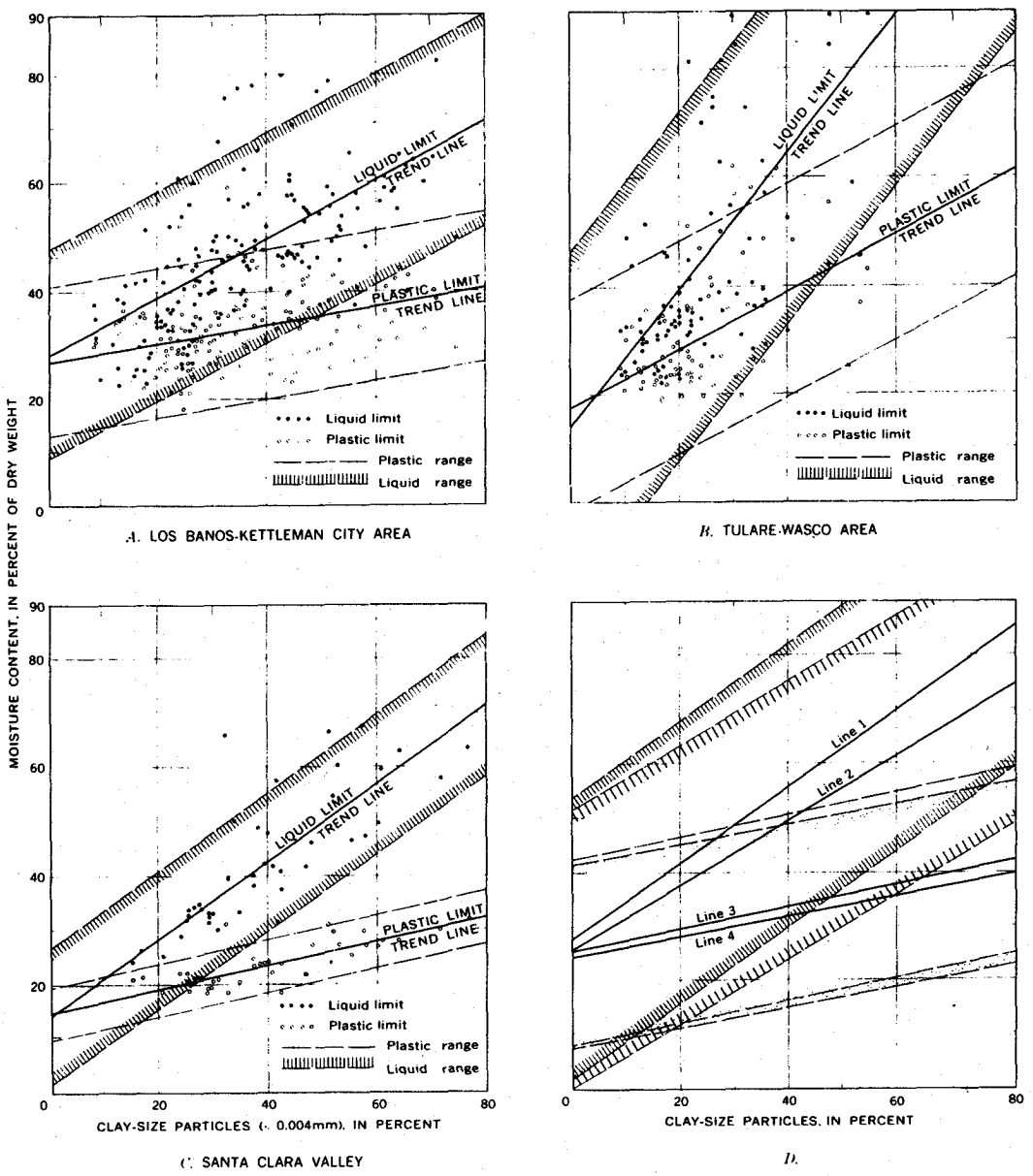

Figure 4.14 Effect of clay content on liquid limit; D, composite of all samples tested.

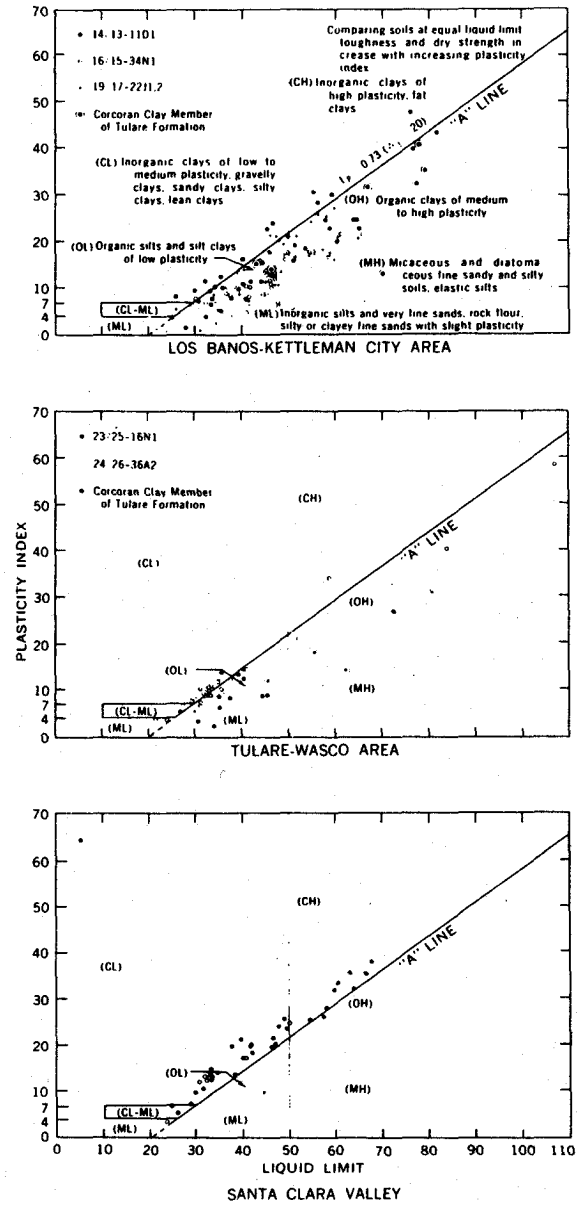

Figure 4.15 Unified soil classification for core-hole samples (ASTM, 1980).

Table 4.4 Consolidation test summaries.

[Data from Earth Laboratory, U.S. Bureau of Reclamation, Denver, Colo.]

Earth laboratory sample	Depth (feet)	Compression index, C_c		Time-consolidation data					Unified soil classification symbol
		From consolidation curve	From Atterberg test	Load range (psi)	Coefficient of consolidation, C_v		Coefficient of permeability		
					Sq in. per sec	Sq ft per yr	Calculated (ft per yr)	From test (ft per yr)	
Core hole 12/12-16H1									
23L91	84.3- 84.6	0.12	0.19	100- 200	3.3×10^{-4}	72.5	8.5×10^{-3}		CL
				200- 400	1.5×10^{-4}	31.8	2.0×10^{-3}		
92	159.4- 159.8	.22	.36	100- 200	9.2×10^{-5}	20.1	2.8×10^{-3}		CL-CH
				200- 400	5.1×10^{-5}	11.2	1.3×10^{-3}		
93	230.8- 231.2	.21	.21	200- 400	1.7×10^{-4}	37.2	4.0×10^{-3}		CL
94	324.5- 324.9	.11	.17						CL
95	374.0- 374.5	.32	.39	200- 400	1.5×10^{-5}	3.3	2.9×10^{-4}		CH
				400- 800	1.0×10^{-5}	2.2	1.5×10^{-4}		
96	425.0- 425.3	1.13	.59	200- 400	4.2×10^{-6}	0.92	3.2×10^{-4}		CH
				400- 800	3.2×10^{-6}	.70	1.2×10^{-4}		
97	471.2- 471.5	.90	.43	200- 400	1.3×10^{-4}	28.5	8.0×10^{-3}		CH
				400- 800	1.3×10^{-4}	28.5	3.6×10^{-3}		
98	516.5- 516.9	.41						5.7	SM
99	579.0- 579.3	.23	.20	200- 400	5.6×10^{-4}	122.0	7.2×10^{-3}		CL
				400- 800	3.8×10^{-4}	83.2	4.4×10^{-3}		
				800-1, 600	2.5×10^{-4}	54.8	1.5×10^{-3}		
100	625.0- 625.4	.34	.44	400- 800	1.7×10^{-5}	3.7	2.6×10^{-4}		CH
				800-1, 600	8.0×10^{-6}	1.8	6.0×10^{-5}		
101	675.9- 676.2	.27	.32	400- 800	1.1×10^{-3}	232.1	1.2×10^{-2}		CL
				800-1, 600	6.9×10^{-4}	151.1	4.8×10^{-3}		
102	722.0- 722.3	.34	.54	400- 800	2.7×10^{-5}	5.9	3.3×10^{-4}		CH
				800-1, 600	6.0×10^{-6}	1.3	5.0×10^{-5}		
103	773.0- 773.4	.33		800-1, 600	4.3×10^{-5}	9.4	3.5×10^{-4}		SM
104	821.4- 821.8	.20						14.2	SM
105	877.4- 877.8	.18						33.9	SM
106	926.8- 927.2	.68	.34	400- 800	1.6×10^{-4}	35.0	3.7×10^{-3}		CL
				800-1, 600	8.5×10^{-5}	18.6	1.2×10^{-3}		
107	972.0- 972.4	.33						38.4	SM
108	998.6- 999.0	.30	.24					1.4	CL
Core hole 14/13-11D1									
23L80	315.0- 315.3							25.3	SP
194	397.0- 397.3	0.36		200- 400	1.8×10^{-4}	39.4	4.0×10^{-3}		CL
				400- 800	5.1×10^{-5}	11.2	8.1×10^{-4}		
				800-1, 600	1.2×10^{-5}	2.6	9.0×10^{-5}		
81	554.0- 554.4	.22		200- 400	6.8×10^{-5}	15.0	9.5×10^{-4}		CL
				400- 800	2.2×10^{-5}	4.9	2.2×10^{-4}		
				800-1, 600	4.1×10^{-5}	9.0	1.8×10^{-4}		
83	699.0- 699.4	.97		400- 800	5.8×10^{-5}	12.8	2.1×10^{-3}		CL
				800-1, 600	3.2×10^{-5}	7.1	5.0×10^{-4}		
84	746.0- 746.4	.30		200- 400	1.7×10^{-4}	37.4	2.6×10^{-3}		
				400- 800	1.2×10^{-4}	26.9	1.5×10^{-3}		
				800-1, 600	6.6×10^{-5}	14.5	5.5×10^{-4}		
196	832.2- 832.7	.36		200- 400	2.0×10^{-4}	43.8	3.6×10^{-3}		CL
				400- 800	6.7×10^{-5}	14.7	9.4×10^{-4}		
				800-1, 600	4.5×10^{-5}	9.9	3.7×10^{-4}		
85	983.6- 984.0	0.35		200- 400	1.2×10^{-4}	2.6	2.1×10^{-4}		CL
				400- 800	1.0×10^{-4}	2.2	1.1×10^{-4}		
				800-1, 600	1.2×10^{-5}	2.6	1.2×10^{-4}		
86	1,076.0-1,076.4							1.7	SM
88	1,350.5-1,350.8							19.3	SP
89	1,395.0-1,395.3			200- 400	1.0×10^{-4}	21.8	1.2×10^{-3}		CL
				400- 800	1.7×10^{-5}	3.6	1.5×10^{-4}		
				800-1, 600	1.1×10^{-5}	2.4	8.0×10^{-5}		
90	1,450.0-1,450.3	.29		800-1, 600	3.9×10^{-5}	8.4	2.4×10^{-4}		CL
Core hole 16/15-34N1									
23L197	299.1- 299.5	0.34	0.38	200- 400	3.4×10^{-4}	74.9	1.1×10^{-2}		CH
198	418.1- 418.5	.32	.31	100- 200	1.7×10^{-3}	361.4	6.3×10^{-2}		CL
				200- 400	5.0×10^{-4}	109.5	1.3×10^{-2}		
				400- 800	1.4×10^{-4}	30.7	2.1×10^{-3}		
200	538.9- 539.2	.30	.42	200- 400	3.4×10^{-4}	74.5	6.3×10^{-3}		CH
				400- 800	1.3×10^{-4}	28.5	2.1×10^{-3}		
201	571.2- 571.6		.65						CH
202	636.9- 637.3	.70	.63	400- 800	1.8×10^{-5}	3.9	4.0×10^{-4}		CH
				800-1, 600	8.1×10^{-6}	1.8	1.3×10^{-4}		
204	713.1- 713.4	.31	.46	200- 400	3.3×10^{-4}	72.3	3.6×10^{-3}		CH
				400- 800	7.0×10^{-5}	15.3	8.9×10^{-4}		
				800-1, 600	5.0×10^{-5}	11.0	4.1×10^{-4}		
206	859.7- 860.1		.19	800-1, 600	5.6×10^{-4}	122.6	4.6×10^{-3}		SC
207	901.7- 902.1	.29	.55	100- 200	1.4×10^{-4}	30.7	3.0×10^{-3}		CH
				200- 400	3.1×10^{-5}	6.6	4.9×10^{-4}		
				400- 800	1.6×10^{-5}	3.5	2.0×10^{-4}		
				800-1, 600	7.5×10^{-6}	1.6	6.1×10^{-5}		
208	972.0- 972.4	.42	.53	200- 400	2.3×10^{-4}	50.4	3.1×10^{-3}		CH
				400- 800	2.2×10^{-5}	4.8	3.6×10^{-4}		
				800-1, 600	6.5×10^{-6}	1.4	7.0×10^{-5}		
210	1,153.6-1,154.0	.21	.23	400- 800	6.2×10^{-4}	135.8	5.1×10^{-3}		CL
				800-1, 600	3.2×10^{-4}	70.0	2.2×10^{-3}		
212	1,237.7-1,238.1			400- 800	3.7×10^{-5}	8.1	2.7×10^{-4}		CH

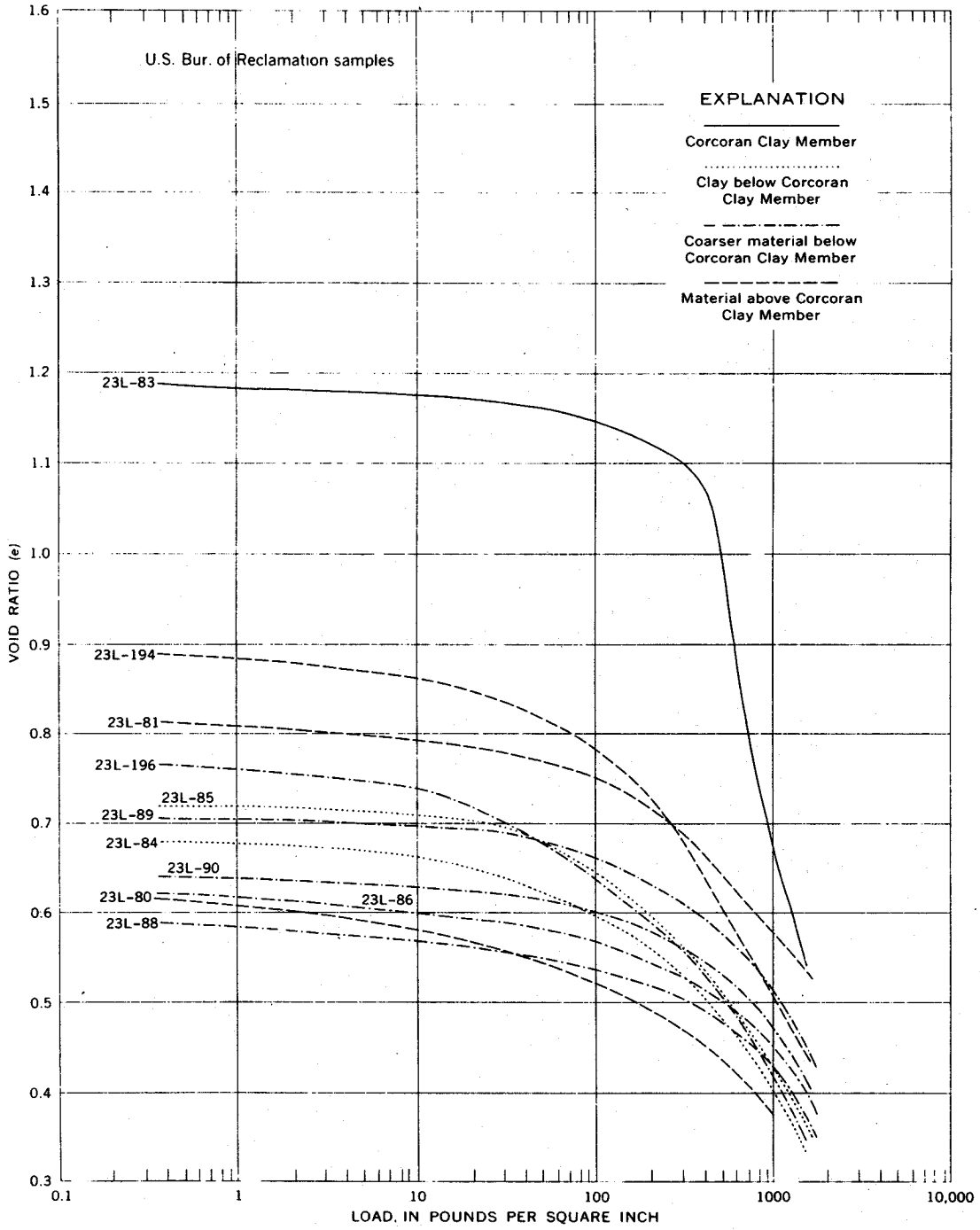

Figure 4.16 Void ratio/load curves for selected samples from core hole 14/13-llDl in the San Joaquin Valley, California.

Terzaghi and Peck equation. The solid line in each of the parts of Figure 4.17 represents the regression line for the Terzaghi and Peck equation, $C_C = 0.0009 (w_L - 10)$.

The data in Figure 4.17 show that 10 of the 22 samples from the Los Banos-Kettleman City area, 11 of the 12 samples from the Tulare-Wasco area, and 4 of the 21 samples, from the Santa Clara Valley, lie outside the ± 30 per-cent limits of scatter about the regression line for the Terzaghi and Peck equation, $C_C = 0.0009 (w_L - 10)$. Three samples of clay in the Los Banos-

Kettleman City area have compression indices approximately twice as large as would be predicted from the Terzaghi-Peck equation. The void ratio-load curves for these three samples suggest that they are extrasensitive clays and, if so, they would be expected to plot well above the equation line. However, even if these samples are excluded, the data of Figure 4.17 show that the relationship between liquid limit and compression index for fine-textured sediments on the west side of the San Joaquin Valley does not fit the Terzaghi-Peck equation as closely as might be expected from the discussion by those authors (Terzaghi and Peck, 1948), p. 66).

Regression lines were determined by computer for the liquid limit-compression index relationship for samples from core holes in the San Joaquin and Santa Clara Valleys. Table 4.5 presents the equations of the regression lines for data from the central California area so they can be compared with the regression line for the Terzaghi and Peck equations, $C'_C = 0.0007\ (w_L - 10)$ and $C_C = 0.0009\ (w_L - 10)$. The table shows that only the equation for core hole 16/15-34N1 is approximately equivalent to either equation discussed by Terzaghi and Peck. Figure 4.17, part D, and Table 4.5 show that the equation of the regression line for 11 samples from the San Joaquin Valley (except the three samples with the exceptionally high compression indices) is $C_C = 0.014\ (w_L - 22)$ and the equation for the Santa Clara Valley is $C_C = 0.003\ (w_L + 35)$.

4.5.7.2 Correlation of compression indices

Figure 4.18 demonstrates the correlation between compression indices estimated from liquid-limit tests and those determined from consolidation curves such as are shown in Figure 4.16. In Figure 4.18 the heavy line passing through the origin at an angle of 45 degrees to the x and y axes represents absolute correlation between the values represented by the two axes. The compression indices estimated from liquid limits for the Los Banos-Kettleman City area and Santa Clara Valley generally are higher than those determined from consolidation curves and those for the Tulare-Wasco area are lower.

The data in Figure 4.18 also show that the sediments of marine origin have much higher compression indices when determined from consolidation curves than when estimated from liquid limits. Furthermore, sediments of lacustrine origin have somewhat lower compression indices when determined from consolidation curves than when estimated from liquid limits. Again, the explanation may be due to the difference in load conditions, the marine sediments being the deepest and the alluvial sediments being the shallowest.

4.5.7.3 Estimating coefficients of consolidation

Figure 4.19 shows the computed coefficient of consolidation for 1 to 4 different load ranges plotted against liquid limit for samples from the central California areas. Although the coefficient of consolidation shows a general decrease for increasing values of liquid limit, Figure 4.17 indicates that the coefficient of consolidation for any particular load range can vary through more than one order of magnitude for any given liquid limit. Terzaghi and Peck (1948, pp. 76-77) described a similar relationship for data from about 30 samples and noted that the relationship is different for each core hole as well as for each area.

4.5.7.4 Effect of soil classification

Information in Figures 4.17 and 4.18 indicates the effect of particle size and texture on the consolidation characteristics and the liquid limit. The Unified Soil Classification (Am. Soc. Testing Materials, 1964, pp. 208-220) designation, which is based on texture, is indicated at the top of Figure 4.17.

In general, those samples with a classification of CH-MH have the largest liquid limits and compression indices, and the smallest coefficients of consolidation. Samples with a classification of SC and SM have the smallest liquid limits and compression indices, and the largest coefficient of consolidation. Samples with a classification of ML, CL and CH have values somewhere between these two extremes. Samples of sediments of alluvial origin tended to be classified as CL and CH; and those of marine origin were classified primarily as CH-MH.

4.5.7.5 Relationship of consolidation characteristics and liquid limits

Data presented in this chapter show that the equations presented by Terzaghi and Peck (1948) (equations 4.16 and 4.17) do not apply to the relationship between compression index and liquid limit for sedimentary deposits tested from the central California subsidence areas.

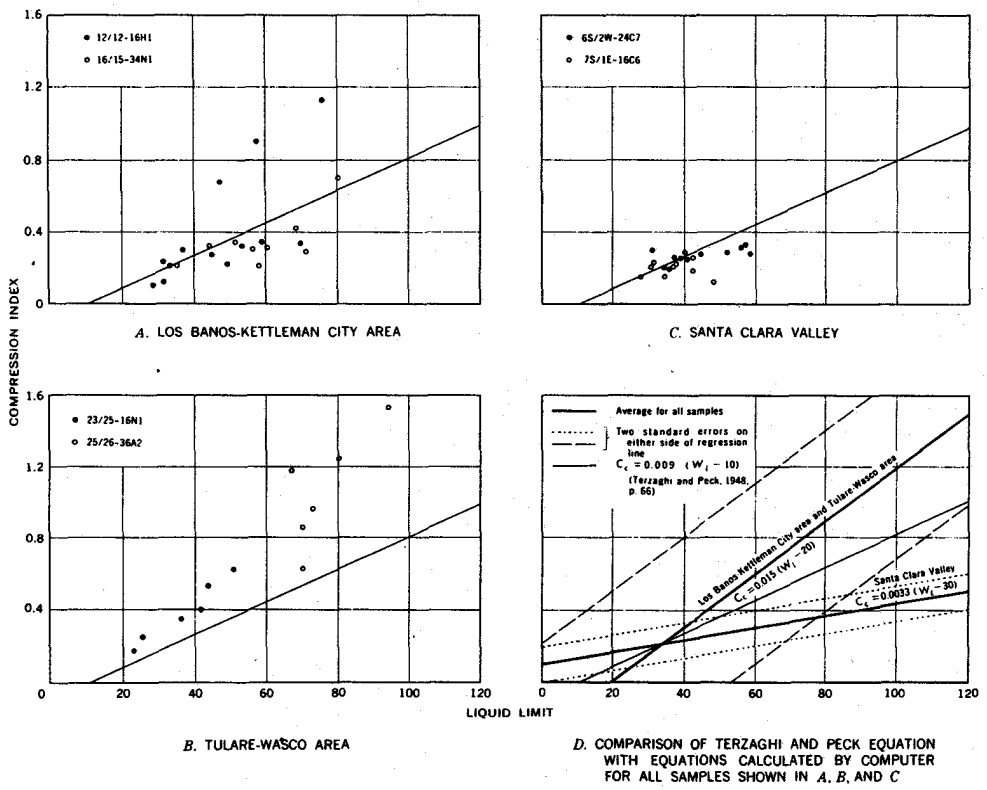

Figure 4.17 Relation between liquid limit and compression index for selected samples from core holes in San Joaquin and Santa Clara Valleys, California.

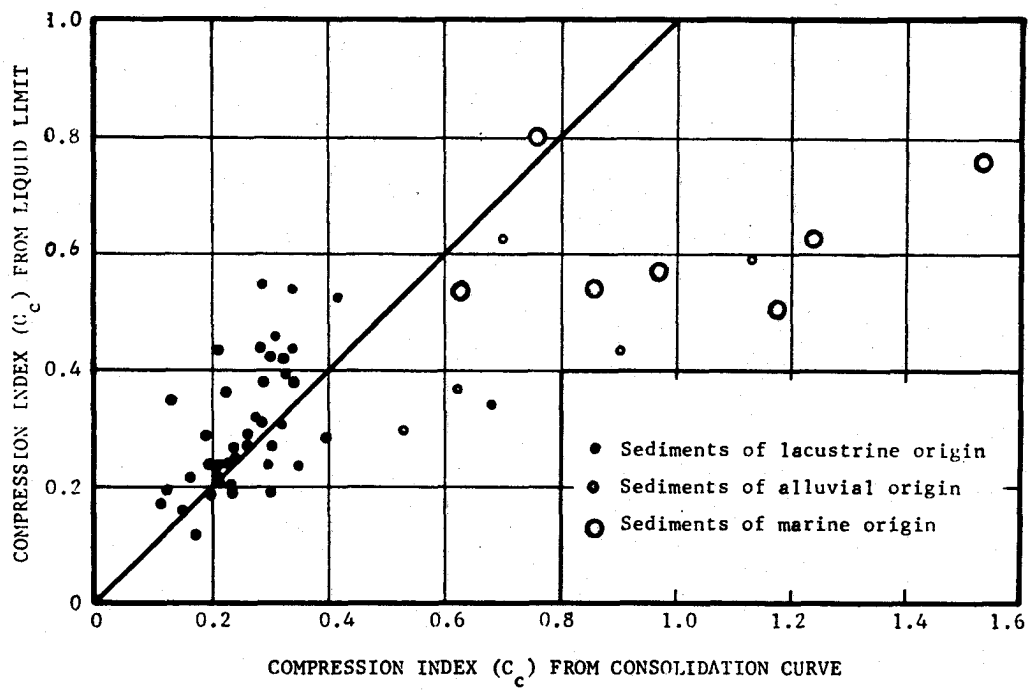

Figure 4.18 Comparison of two methods for determination of compression index for all samples from subsidence areas in the San Joaquin and Santa Clara Valleys, California.

Table 4.5 Equations for regression lines for various groups of data from subsiding areas in central California

Data used	Equation
Los Banos-Kettleman City area	
Core hole 12/12-16Hl, exclusive of the 3 samples with exceptionally high compression indices	$C_C = 0.005 (w_L=6)$
Core hole 16/15-34N1	$C_C = 0.007 (w_L-12)$
All samples in area, exclusive of 3 samples with exceptionally high compression indices	$C_C = 0.006 (w_L-3)$
Tulare-Wasco area	
Core hole 23/25-16Nl	$C_C = 0.015 (w_L-l$
Core hole 24/26-36A2	$C_C = 0.024 (w_L-32)$
All samples in area	$C_C = 0.018 (w_L-16)$
San Joaquin Valley, exclusive of 3 samples with exceptionally high compression indices	$C_C = 0.014 (w_L-22)$
Santa Clara Valley	
Core hole 6S/2W-24C7	$C_C = 0.003 (w_L-47)$
Core hole 7S/lE-16C6	$C_C = 0.0005 (W_L+370)$
All samples in area	$C_C = 0.003 (w_L+35)$

Furthermore, the data show that no single equation applies to the relationship for all areas studied, with the following equations being obtained for the two valleys:

San Joaquin Valley: $C_C = 0.014 (w_L - 22);$ (4.18)

Santa Clara Valley: $C_C = 0.003 (w_L + 35).$ (4.19)

In essentially every case, the equations of the regression lines represent only general trends because there is considerable scatter of data for all core holes. The trend line for data from the Santa Clara Valley is so nearly horizontal that a rather narrow range of compression indices could be obtained over a wide range of liquid limits. Compression indices estimated from liquid limits, however, showed better correlation with indices determined from consolidation curves when the sediments were of alluvial or lacustrine origin than when they were of marine origin.

All coefficients of consolidation showed a general decrease for increasing values of liquid limit. However, because the coefficients for any particular load range could vary through more than one order of magnitude for any given liquid limit, the relationship could not be estimated with reasonable accuracy. In fact, the general trend for the relationship even varies, for each subsidence area and for each core hole.

At least for the areas studied in central California, the consolidation characteristics of the undisturbed sediments in the field cannot be closely approximated by liquid limits, which are made on disturbed samples of those sediments. The studies also indicate that the equations reported by Terzaghi and Peck (1948) must be used with extreme caution to estimate the consolidation characteristics of sediments in areas of subsidence--especially if the compacting sediments are at considerable depth.

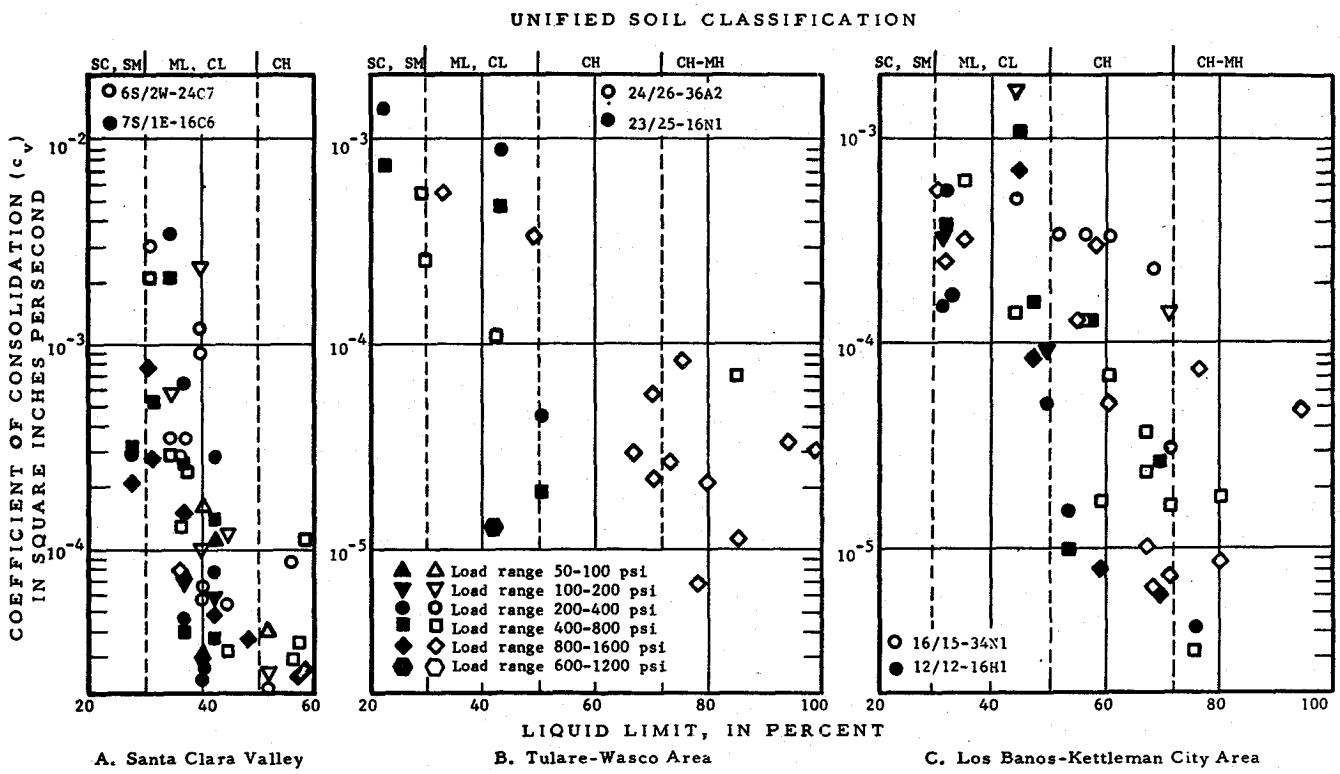

Figure 4.19 Relation of coefficient of consolidation to liquid limit for samples from core holes in the San Joaquin and Santa Clara Valleys, California.

4.6 REFERENCES

AMERICAN GEOLOGICAL INSTITUTE. 1960. Glossary of geology and related sciences, 2d ed. Washington, 397 p.

AMERICAN SOCIETY FOR TESTING MATERIALS. 1980. Annual Book of Standards, Part 19. Philadelphia, 654 p.

ATHY, L. P. 1930. Density, porosity, and compaction of sedimentary rocks. Am. Assoc. Petroleum Geologists Bull., v. 14, pt. 1, no. 1, p. 1-24.

ATTERBERG, A. 1911. Über die physikalische bodenuntersuchung, und Über die plastizitat der tone. Internat. Mitt. Bodenkunde, v. 1, p. 10-43.

BULL, W. B. 1961. Causes and mechanics of near-surface subsidence in western Fresno County, California, in Short papers in the geologic and hydrologic sciences. U.S. Geol. Survey Prof. Paper 424-B, p. B187-B189.

BULL, W. B. 1964. Alluvial fans and near-surface subsidence, western Fresno County, California. U.S. Geol. Survey Prof. Paper 437-A, p. Al-A71.

CALIFORNIA STATE WATER RESOURCES BOARD. 1955. Santa Clara Valley investigation, Sacramento, Bull., 7, 154 p.

CASAGRANDE, ARTHUR. 1932. Research on the Atterberg limits of soils. Public Roads, v. 13, no. 9, p. 121-136.

CASAGRANDE, ARTHUR. 1948. Classification and identification of soils. Am. Soc. Civil Engineers Trans., v. 113, p. 901-930.

CLARK, W. 0. 1924. Ground water in Santa Clara Valley, California. U.S. Geol. Survey Water Supply Paper 519, 209 p.

DAVIS, G. H., and POLAND, J. F. 1957. Ground-water conditions in the Mendota-Huron are Fresno and Kings Counties, California. U.S. Geol. Survey water-Supply Paper 1360-G, 409-588.

GIBBS, H. J. 1953. Estimating foundation settlements by one-dimensional consolidation test Denver, Colo. U.S. Bureau of Reclamation Eng. Mon. 13, 24 p.

GIBBS, H. J. 1959. A laboratory testing study of land subsidence. Pan-Am. Conf. Soil Mech Found. Eng., lst, Mexico City, 1959, Proc., p. 3-36.

GOLDSCHMIDT, V. M. 1926. Undersokelser over lersedimenter. Beretning om Nordiske Jordbrugs forskeres Kongress i Osla, Copenhagen Nordisk Jordsbrugsforskning, v. 4, no. 7, p. 434-445.

INTER-AGENCY COMMITTEE ON LAND SUBSIDENCE IN THE SAN JOAQUIN VALLEY. 1955. Proposed program for investigating land subsidence in the San Joaquin Valley, California. Sacramento, Calif., 60 P.

INTER-AGENCY COMMITTEE ON LAND SUBSIDENCE IN THE SAN JOAQUIN VALLEY. 1958, Progress report on land-subsidence investigations in the San Joaquin Valley, California, through 1957. Sacramento, Calif., 160 p. 45 p1s., 5 tables.

JOHNSON, A. I., and MORRIS, D. A. 1962a. Physical and hydrologic properties of water-bearing deposits from core holes in the Los Banos-Kettleman City area, California. U. S. Geological Survey open file report, 182 p.

JOHNSON, A. I., and MORRIS, D. A. 1962b. Relation of volumetric shrinkage to clay. content of sediments from the San Joaquin Valley, California, in Short papers in geology, hydrology, an topography. U.S. Geol. Survey Prof. Paper 450-B, p. B43-B44.

JOHNSON, A. I., and MOSTON, R. P. 1969. Relationship of consolidation characteristics an Atterberg limits for subsiding sediments in Central California, U.S.A. Internat. Symposium on Land Subsidence, Tokyo, IAHS, p. 579-587.

JOHNSON, A. I., MOSTON, R. P., and MORRIS, D. A. 1968. Physical and hydrologic properties of water-bearing deposits in subsiding areas in central California. U.S. Geol. Survey Prof. Paper 497-A, 71 p., 14 p1s.

KRUMBEIN, W. C., and PETTIJOHN, F. J. 1938. Manual of sedimentary petrography. New York, Appleton-Century-Crofts, Inc., 549 p.

LANE, E. W., Chairman. 1947. Report of the Subcommittee on Sediment Terminology. Am. Geophys. Union Trans., v. 28, p. 936-938.

LOFGREN, B. E. 1960. Near-surface land subsidence in western San Joaquin Valley, California. Jour. Geophys. Research, v. 65, no. 3, p. 1053-1062.

LOFGREN, B. E. 1963. Land subsidence in the Arvin-Maricopa area, San Joaquin Valley, California, in Short papers in geology and hydrology. U.S. Geol. Survey Prof. Paper 475-B, p. B171-175.

LOFGREN, B. E. 1969. Field measurement of aquifer-system compaction, San Joaquin Valley, California.Internat. Symposium on Land Subsidence, Tokyo--1969, I.A.S.H. Pub. 88, p. 272-284.

MEADE, R. H. 1964. Removal of water and rearrangement of particles during the compaction of clayey sediments--review. U.S. Geol. Survey Prof. Paper 497-B. 23 p.

MEADE, R. H. 1967. Petrology of sediments underlying areas of land subsidence in central California. U.S. Geol. Survey Prof. Paper 497-C, 83 p.

MEINZER, 0. E. 1923. The occurrence of ground water in the United States, with a discussion of principles. U.S. Geol. Survey Water-Supply Paper 489, 321 p.

MEINZER, 0. E., ed. 1949. Hydrology, in Physics of the Earth. New York, Dover Pubs., Inc., 712 p.

MILLER, R. E. 1961. Compaction of an aquifer system computed from consolidation tests and decline in artesian head, in Short papers in the geologic and hydrologic sciences. U.S. Geol. Survey Prof. Paper 424-B, p. B54-58.

MORRIS, D. A., and JOHNSON, A. I. 1959. Correlation of Atterberg limits with geology of deep cores from subsidence areas in California. Am. Soc. Testing Materials Spec. Tech. Pub. 254, p. 183-187.

NISHIDA, YOSHICHIKA. 1956. A brief note on compression index of soil. Am. Soc. Civil Engineers, Soil Mech. Found. Div. Jour., vol. 82, SM 3, Paper 1027, 14 p.

POLAND, J. P. 1960. Land subsidence in the San Joaquin Valley, California, and its effect on estimates of ground-water resources, in International Association of Scientific Hydrology Commission of Subterranean Waters. I.A.S.H. pub. 52, p. 324-335.

POLAND, J. P. 1969. Land subsidence and aquifer system compaction, Santa Clara Valley, Calif. Internat. Symposium on Land Subsidence, Tokyo 1969, I.A.S.H. pub. 88, p. 285-294.

POLAND, J. F., and DAVIS, G. H. 1956. Subsidence of the land surface in the Tulare-Wasco (Delano) and Los Banos-Kettleman City areas, San Joaquin Valley, California. Am. Geophys. Union Trans., v. 37, no. 3, p. 287-296.

POLAND, J. F., and GREEN, J. H. 1962. Subsidence in the Santa Clara Valley, California--A progress report. U.S. Geol. Survey Water-Supply Paper 1619-C, 16 p.

REITEMEIER, R. F. 1946. Effect of moisture content on the dissolved and exchangeable ions of soils of arid regions. Soil Sci., v. 61, p. 195-214.

RILEY, F. S. 1969. Analysis of bore-hole extensometer data from Central California. Internat. Symposium on Land Subsidence, Tokyo 1969, I.A.S.H. pub. 89, p. 423-431.

ROBERTS, D. V., and DARRAGH, R. D. 1962. Areal fill settlements and building foundation behavior at the San Francisco airport, in Field testing of soils. Am. Soc. Testing materials Spec. Tech. Pub. 322, p. 211-230.

SHEPARD, F. P. 1954. Nomenclature based on sand-silt-clay ratios. Jour. Sed. Petrology, v. 24, no. 3, p. 151-158.

SKEMPTON, A. W. 1944. Notes on the compressibility of clays. Geol. Soc.--London Quart. Jour., vol. C, p. 119-135.

TAYLOR, D. W. 1948. Fundamentals of soil mechanics. New York, John Wiley & Sons, Inc., 700 p.

TERZAGHI, KARL. 1926. Simplified soil tests for subgrades and their physical significance. Public Roads, v. 7, p. 153-162.

TERZAGHI, KARL. 1943. Theoretical soil mechanics. New York, John Wiley & Sons, Inc., 510 p.

TERZAGHI, KARL, and PECK, R. B. 1,948. Soil mechanics in engineering practice. New York, John Wiley & Sons, Inc. 566 p.

TRASK, P. D. .1932. Origin and environment of source sediments of petroleum, Houston. Gulf Publishing Co., 323 p.

TWENHOFEL, W. H., and TYLER, S. A. 1941. Methods of study of sediments. New York, McGraw-Hill Book Co., Inc., 183 p.

U.S. BUREAU OF RECLAMATION. 1974. Earth manual. Denver, 751 p.

WENTWORTH, C. K. 1922. A scale of grade and class terms for elastic sediments. Jour. Geology, v. 30, p. 377-392.

WENZEL, L. K. 1942. Methods for determining permeability of water-bearing materials. U.S Geol. Survey Water-Supply Paper 887, 192 p.

5 Techniques for prediction of subsidence, by Germán Figueroa Vega, Soki Yamamoto, and Working Group (Section 5.3.6 by Donald C. Helm)

It is very important to predict the amount of subsidence and to estimate the subsidence rate in the near future. There are many methods for predicting the amount of land subsidence due to the overdraft of fluids from aquifers. Some methods are simple and others are complex. It is preferable to use several methods whenever possible and to reach a conclusion based on the overall judgment.

Both adequate and accurate data are required to obtain useful results, although these depend on the purpose, time length of the forecast, and cost. The methods used may be classified into the following categories: (1) Empirical methods; (2) semi-theoretical approach; (3) theoretical approach.

5.1 EMPIRICAL METHODS

This is the method of extrapolating available data to derive the future trend. It is a time series model. The amount of subsidence, the amount of compaction, and sometimes tidal height near the sea coast, are available to plot against time. In this method, the amount of subsidence is considered a function of time, ignoring causality of land subsidence.

5.1.1 Extrapolation of data by naked eye

No explanation of this procedure is needed except that a smooth curve with a natural trend should be obtained.

5.1.2 Application of some suitable curve: Nonlinear extrapolation

1. Fitting of quadratic function (Figure 5.1):
   The following function is used and the least squares method is applied:

   $s = ax^2 + bx + c$, or $s = ax + b$, (5.1)

   where
   s = subsidence amount,
   x = time, and
   a, b, and c are constants.

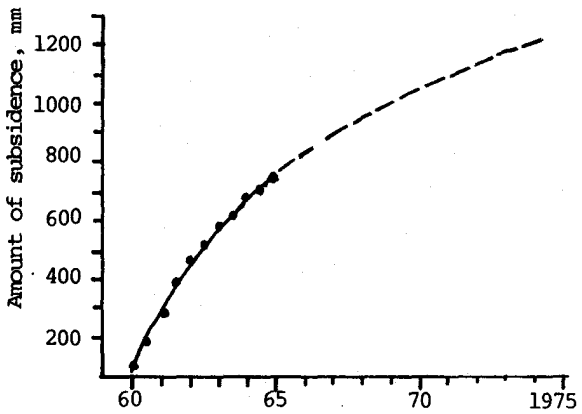

Figure 5.1 Fitting of quadratic curve (bench mark no. 2179, Niigata).

2. Fitting of exponential or logarithmic function (Figures 5.2 and 5.3):
   The following function is applied and the least squares method is used:

   $s = ax^b$, $\log s = \log a + b \log x$, or(5.2)

   $s = ae^{bx}$,

   where
   s = amount of subsidence,
   x = time, and
   a and b are constants.

Many data correlating land subsidence and water level have been published. Figures 5.4 through 5.7 are four examples of such correlations.

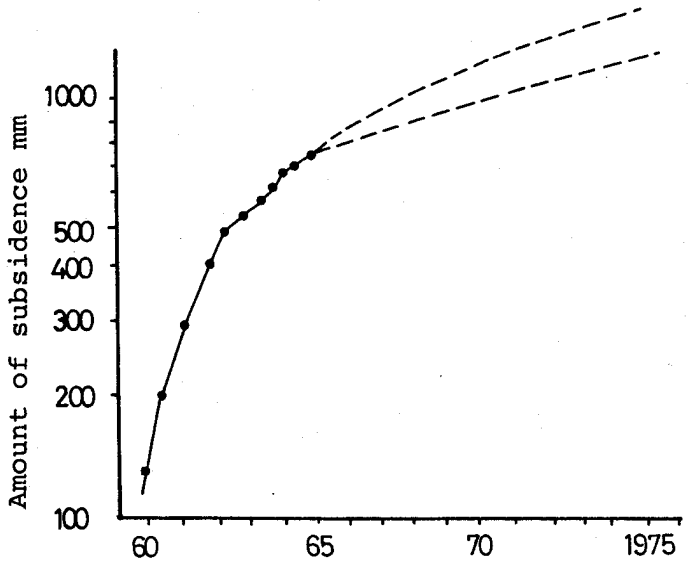

Figure 5.2 Fitting of exponential curve (bench mark no. 2179, Niigata)

.

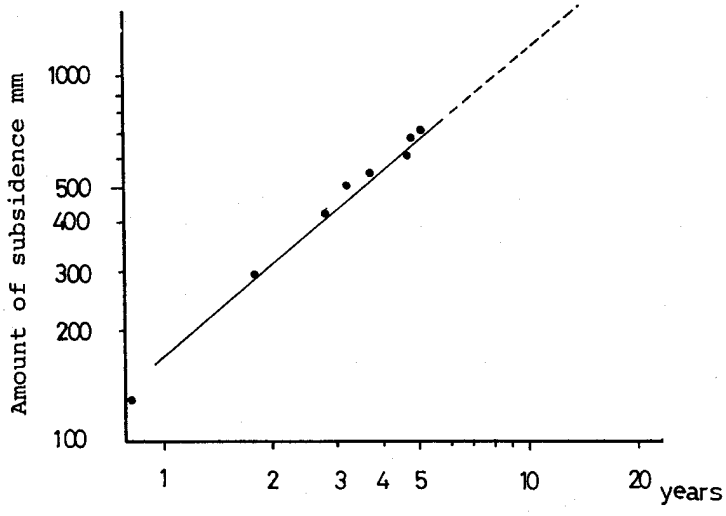

Figure 5.3 Log-log relation between subsidence and years.

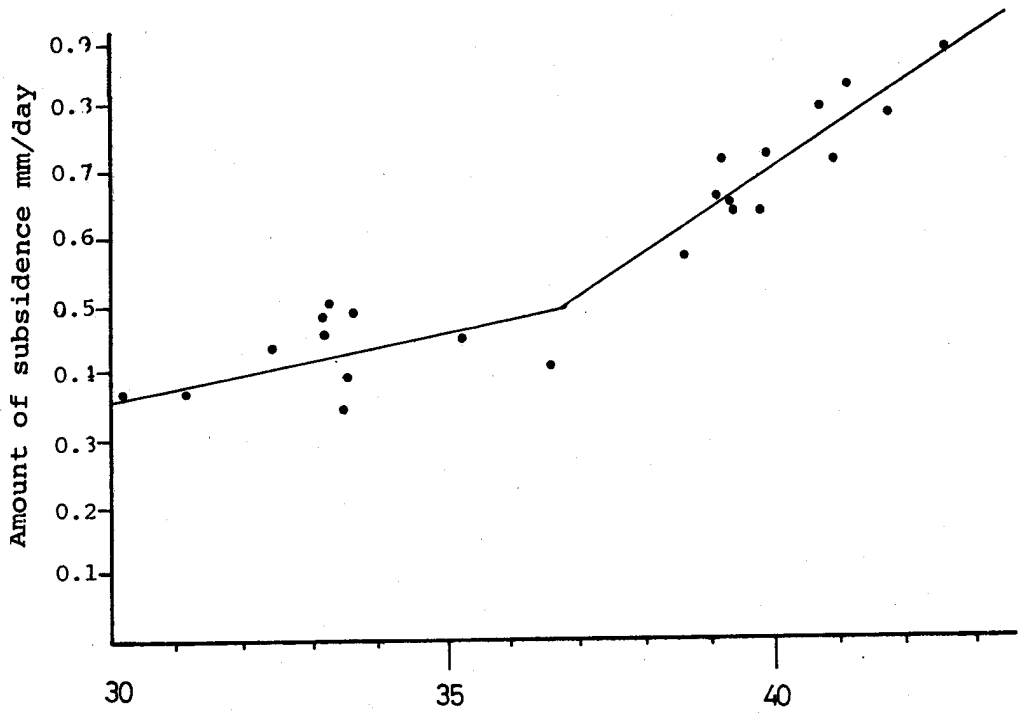

Figure 5.4 Correlation of land subsidence and water level in well 610 metres deep, Tokyo, Japan.

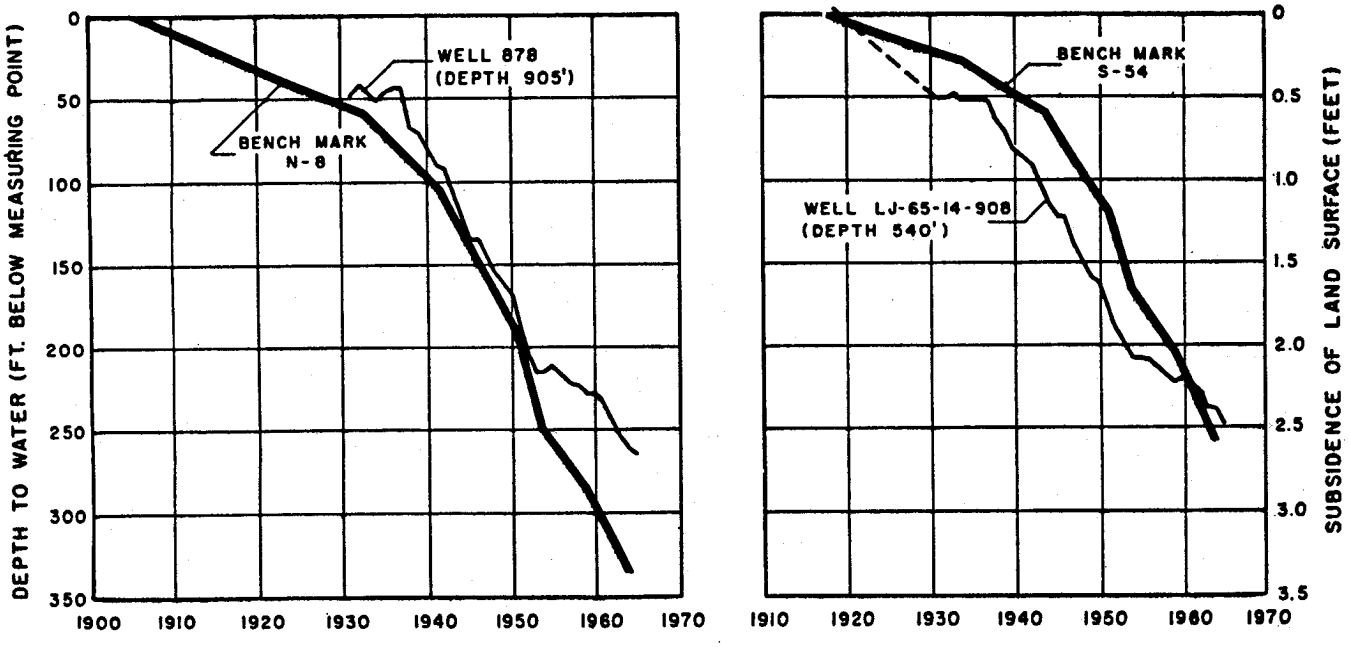

Figure 5.5 The relation between water-level declines and land-surface subsidence in the Houston area, Texas (Gabrysch, 1969).

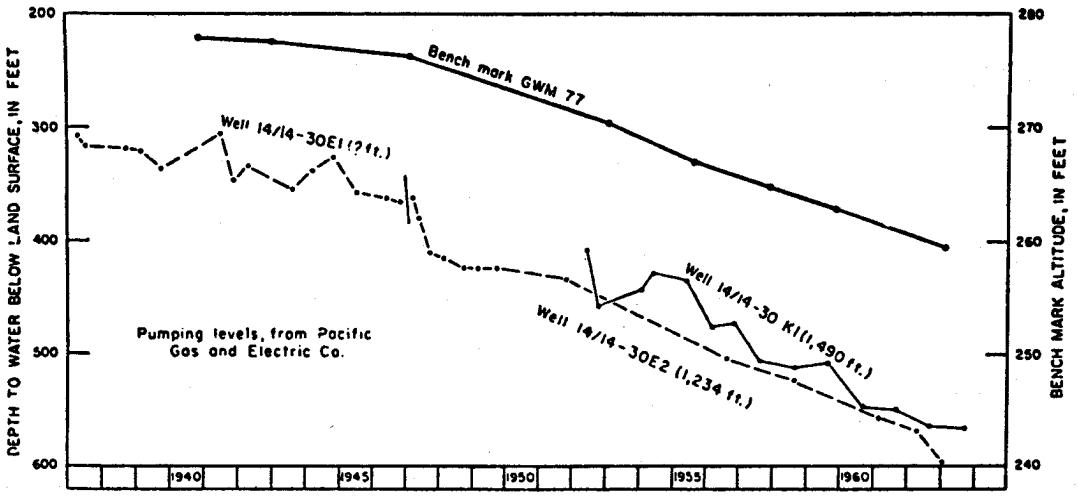

Figure 5.6 Correlation between subsidence and change in artesian head near center of subsidence west of Fresno, California (Lofgren, 1969).

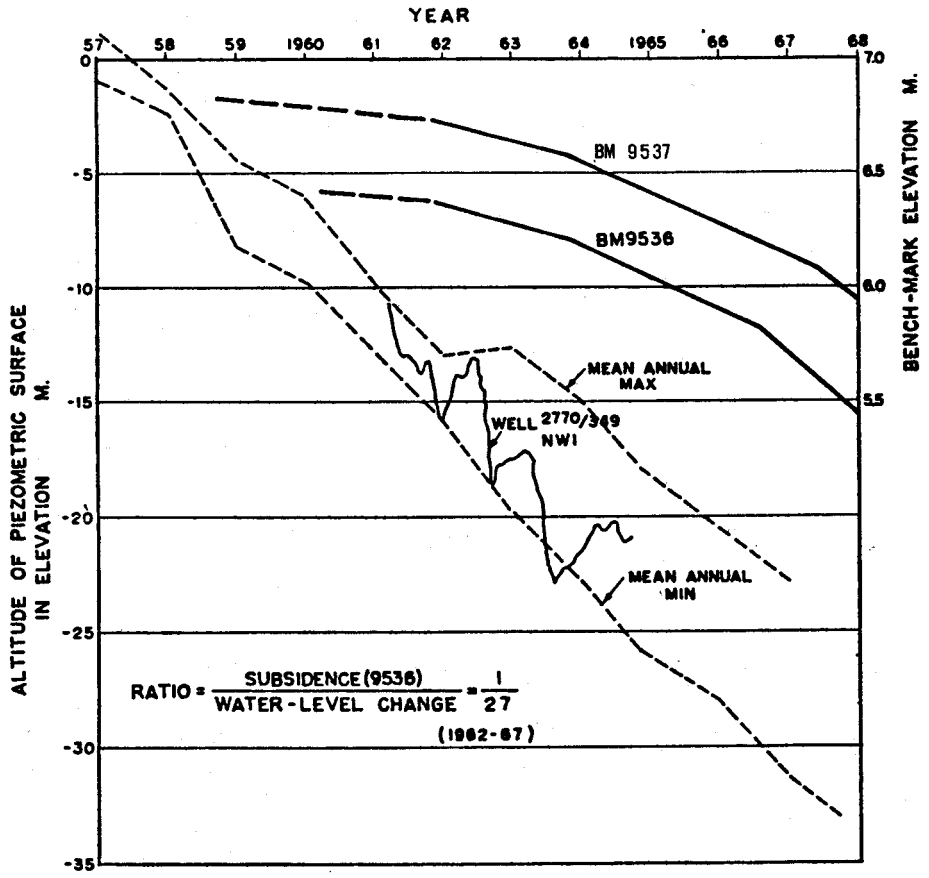

Figure 5.7 Change in altitude at BM9536, -37 and change in artesian head in nearby wells (Hwang and Wu, 1969).

5.2 SEMI-THEORETICAL APPROACH

This method utilizes the relation between subsidence and related phenomena. Although the relation is not strictly theoretical but rather an apparent one, still it can be used to estimate future trend.

5.2.1 Wadachi's (1939) model

Wadachi (1940) pointed out that the rate of subsidence, not the amount of subsidence itself, is proportional to the water-level change (Figure 5.8) and proposed the following equation:

$$\frac{dH}{dt} = k(p_0 - p) \tag{5.3}$$

where

$\frac{dH}{dt}$ = of subsidence,
p_0 = reference water level,
p = water level, and
k = a constant

This suggests that there exists a reference water level. That is to say, if the water level p recovers to the reference water level p_0, no subsidence occurs. But according to Yamaguchi's recent study (1969) there is no such reference water level. In place of Wadachi's equation, he proposed the following one:

$$\frac{ds}{dt} = ks_c\left\{(p_0 - p)t - \frac{dp}{dt}\right\}\exp\{-k(p_0 - p)t\}, \tag{5.4}$$

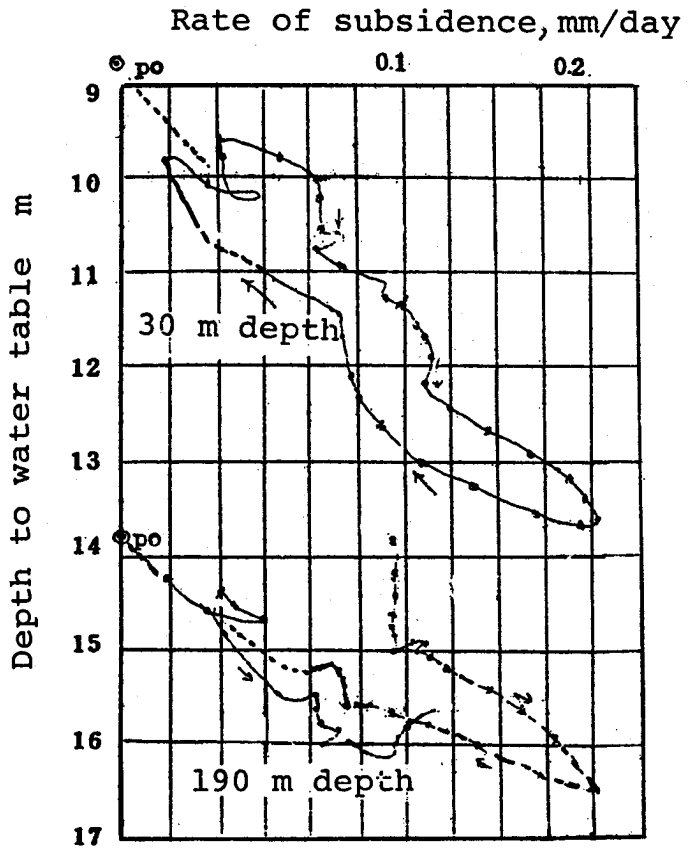

Figure 5.8 Relation between water level and rate of subsidence.

where

$\frac{ds}{dt}$ = rate of subsidence,
s_c = final subsidence amount,
P_0 = initial water level,
p = water level,
k = constant, and
t = time.

On solving this equation, the quantities

$$Y = \log\left[\frac{ds}{dt} \Big/ \left\{(p_0 - p)t - \frac{dp}{dt}\right\}\right] \text{ and } x = (p_0 - p)$$

are plotted on the respective axes as in Figures 5.9a and 5.9b and s_c can be obtained.

5.2.2 Ratio of subsidence volume to liquid withdrawal

According to Yamamoto (personal communication), the relation between liquid production and subsidence in the Niigata gas field (case history 9.7) has been expressed by the following equations, with fair results:

$$s = aQ + b, \text{ or } s = a\sqrt{Q} + b, \tag{5.5}$$

where
s = subsidence,
Q = amount of liquid production, and
a and b are constants.

Castle, Yerkes, and Riley (1969) stated that direct comparisons between the various measures of liquid production and subsidence in six oil fields showed a close relation. Correlation between production and subsidence has varied approximately linearly with net production (Figure 5.10).

The following relation has also been established but not yet published (Yamamoto, personal communication):

$$s = C/m_v \tag{5.6}$$

where
s = subsidence,
m_v = coefficient of volume compressibility, and
C = $\Delta H/\Delta Q$, where ΔH and ΔQ are the change of bench-mark elevation and the amount of production per unit area, respectively.

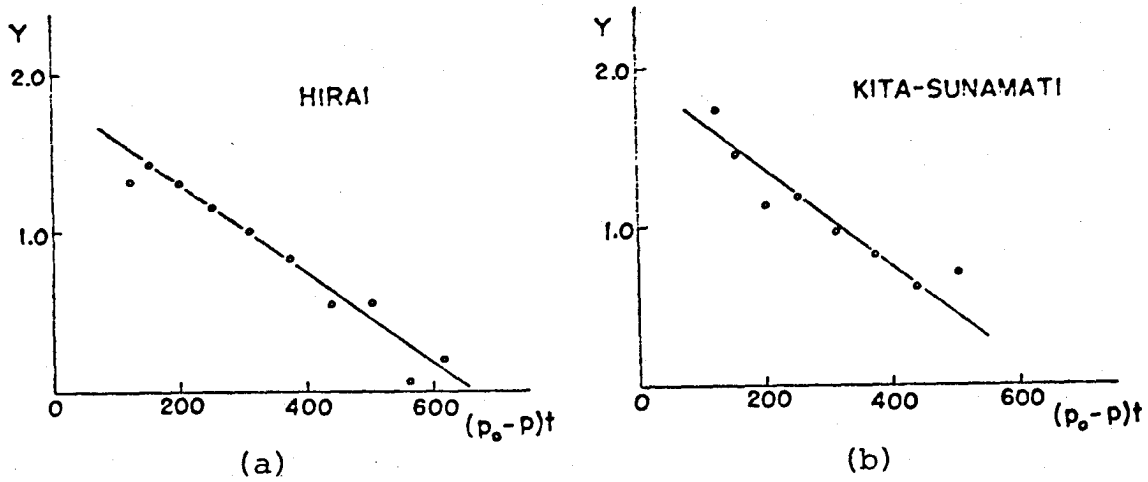

Figure 5.9 Relation between Y and $(p_o - p)t$.

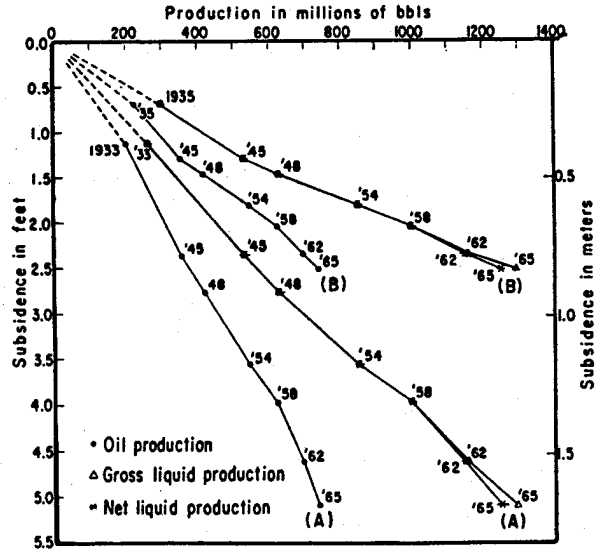

Figure 5.10 Cumulative oil, gross-liquid, and net-liquid production from the Huntington Beach oil field plotted against subsidence at bench marks located (A) near the center of subsidence and (B) midway up the southeast limb of the subsidence bowl. Prepared from production statistics of the California Division of Oil and Gas and elevation data of the U.S. Coast and Geodetic Survey and the Orange County Office of County Surveyor and Road Commissioner. Easily related elevation measurements have been available only since 1933; estimates of subsidence since 1920 shown by dashed lines (Castle, Yerkes, and Riley, 1969).

In one region in Japan, the change of the computed leakage rate, L, plotted against the measured volumetric land-subsidence rate, V_S, showed a close correlation (Figure 5.11).

On the Shiroishi Plain, Kyushu, Japan, Shibasaki et al (1969) proposed the following simple relationship for the data in the three-year period 1963 to 1966:

$$V_S = 0.27\ L + 0.25, \tag{5.7}$$

where each unit is expressed in $10^6 m^3$/mo (cubic metres per month) (Figure 5.12).

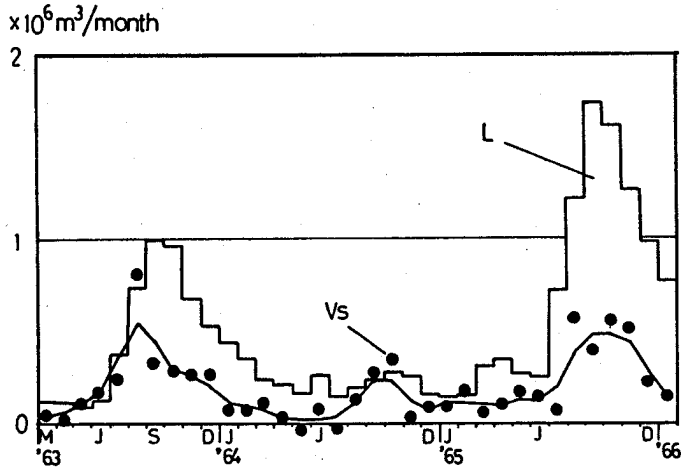

Figure 5.11 Changes of leakage rate, L, and volumetric land subsidence rate, V_S, both in m^3/month, over Shiroishi basin (Shibasaki, Kamata, and Shindo, 1960).

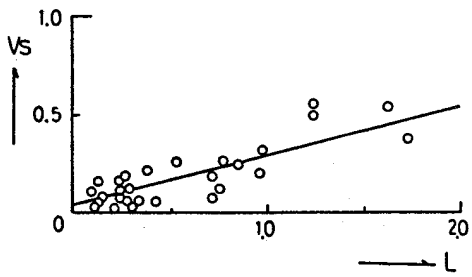

Figure 5.12 Simple relationship between leakage rate and volumetric subsidence rate over Shiroshi basin (Shibasaki, et al., 1969).

Although Castle, Yerkes, and Riley (1969) found that subsidence in six oil fields varied approximately linearly with net liquid production, the correlation between reservoir-pressure decline and subsidence was poor. Their explanation for this is as follows:

> "The general theory advanced in explanation of reservoir compaction and resultant oil-field subsidence (Gilluly and Grant, 1949) is, in its broad outlines, beyond challenge. Thus Terzaghi's principle, which relates increased effective stress directly to fluid pressure decline, probably is validly applied to the multifluid-phase system. Yet in seeming opposition to this generalization, measured reservoir pressure decline within the Vickers zone was disproportionately high with respect to surface subsidence during the early production years (Figure 2a and d); a similar situation is believed to have prevailed in the Wilmington field (City of Long Beach, 1967, unpublished data). Whatever the relationship, then, between measured reservoir pressure decline and compaction, the two are certainly not directly proportional.
> "The most likely explanation for the poor correlation between reservoir-pressure decline and subsidence (or compaction) is that pressure decline as measured at individual producing wells is generally non-representative of the average or systemic decline over the field as a whole. Thus in examining this problem in the Wilmington field, Miller and Somerton (1955, p. 70) observed that 'reductions in average pressure in the reservoir are virtually impossible to determine with a satisfactory degree of accuracy.' This deduction, coupled with the observed linearity between net-liquid production and subsidence, suggests that the liquid production may constitute a better index of average reservoir-pressure decline than that obtained through down-hole measurements."

Figures 5.13, 5.14, and 5.15 present additional examples illustrating the relation between fluid withdrawal and subsidence. Figure 5.13 shows the relation between land subsidence in mm/year and annual discharge in 106m3/year on the Shiroishi Plain in Japan (From Kumai, et al., 1969). Figure 5.14 illustrates the stress-strain relation obtained by plotting discharge in $10^3 m^3$/month against land subsidence in mm/month in Osaka, Japan, for the five years 1954-1958. Figure 5.15 shows the consistent relationship between the cumulative volumes of subsidence and ground-water pumpage in the Los Banos-Kettleman City area, California, from 1926 to 1968. The volume of subsidence was equal to one-third the volume of pumpage consistently through the 42-year period.

5.2.3 Ratio of subsidence to head decline

The subsidence/head-decline ratio is the ratio between land subsidence and the head decline in the coarse-grained permeable beds of the compacting aquifer system, for a common time interval. It represents the change in thickness per unit change in effective stress ($\Delta b/\Delta p'$). This ratio is useful for predicting a lower limit for the magnitude of subsidence in response to a step increase in virgin stress (stress exceeding past maximum). If pore pressures in the compacting aquitards reach equilibrium with those in adjacent aquifers, then compaction stops and the subsidence/head-decline ratio is a true measure of the virgin compressibility of the system. Until or unless equilibrium of pore pressures is attained, the ratio of subsidence to head decline is a transient value.

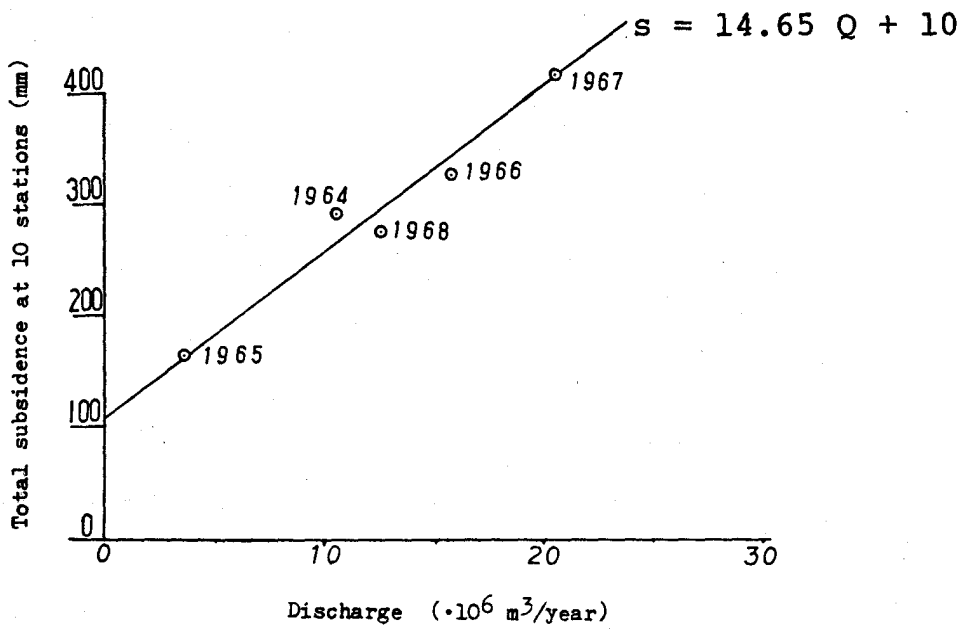

Figure 5.13 Simple relationship between annual land subsidence and corresponding discharge (Kumai, et al., 1969).

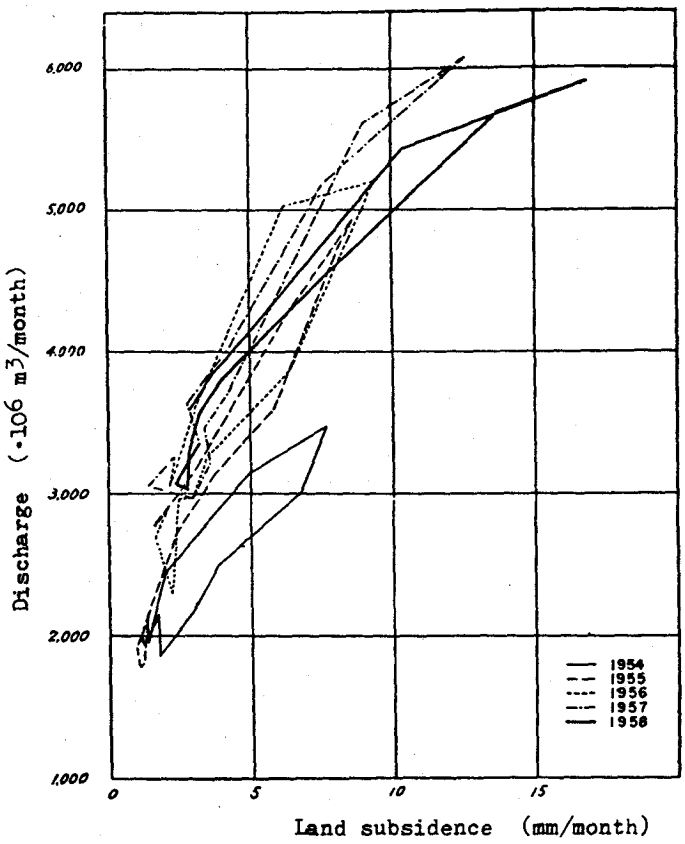

Figure 5.14 Correlation between subsidence and discharge of ground water (Editorial Committee for Land Subsidence in Osaka, 1969).

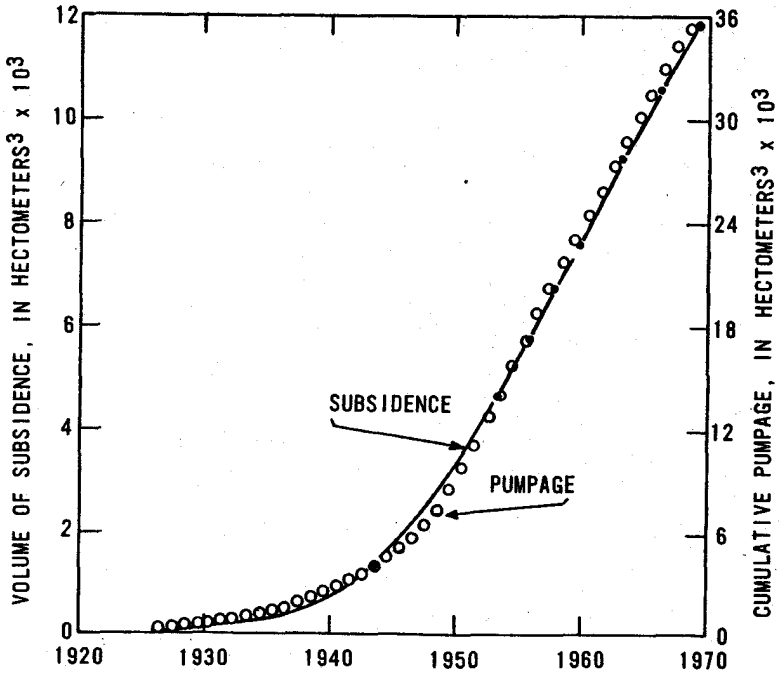

Figure 5.15 Cumulative volumes of subsidence and pumpage, Los Banos-Kettleman City area, California. Points on subsidence curve indicate times of leveling control (from Poland, et al., 1975).

Subsidence/head-decline ratios can be derived at a point if the water-level change for the compacting system and the periodic surveys of the elevation of a nearby bench mark are available for a common time period. For example, Figure 5.5 illustrates the subsidence and head-decline records for a pair of bench marks and nearby wells in Houston, Texas. At plotting scales of 1 (subsidence) to 100 (water level), the plots are roughly coincident. The indicated subsidence/ head-decline ratio is approximately 1/100.

Figure 5.6 is another example of close correlation between subsidence and head decline. The intensive pumping of ground water for more than two decades caused an artesian-head decline of about 300 ft (90m), producing a subsidence of about 18 ft (5.5 m). The indicated subsidence/ head-decline ratio is 1/16 (Lofgren, 1969). Although the ordinate scales in figures 5.5 and 5.6 are in feet, the ratio is dimensionless and hence would be identical in the metric system.

From the subsidence and head-decline record for Figure 5.7, Hwang and Wu (1969) derived a subsidence/head-decline ratio of 1/27 for the period 1962-67. Note, however, that although the mean annual minimum water-level trend is approximately a straight line, the rate of subsidence accelerated sharply in 1967. Hence, a ratio derived from the subsidence rate and water-level change in 1967 would be much larger, roughly about 1/12.

For all three of the examples discussed (Figures 5.5-5.7) it should be emphasized that the ratios are reliable only if the water levels are representative of the average artesian head in the aquifers (coarse-grained beds) of the compacting system.

If maps of subsidence and head decline are available for a common period of time during which both subsidence and head decline continued without interruption, the ratio of subsidence to head decline can be plotted on a map as lines of equal ratio. Figure 5.16 is such a ratio map, plotted from maps showing subsidence and head decline from 1943 to 1959 in an area of 4000 km^2 on the west side of the San Joaquin Valley, California (after Bull and Poland, 1975, Figure 32). The ratios on this map range from 0.08 to 0.01, indicating that the head decline required to produce 1 m of subsidence has ranged from 12 to 100 m, depending on the location. In addition to their use in prediction, the ratios in Figure 5.16 represent a minimum value of the storage coefficient component for virgin compaction of the aquifer-system skeleton.

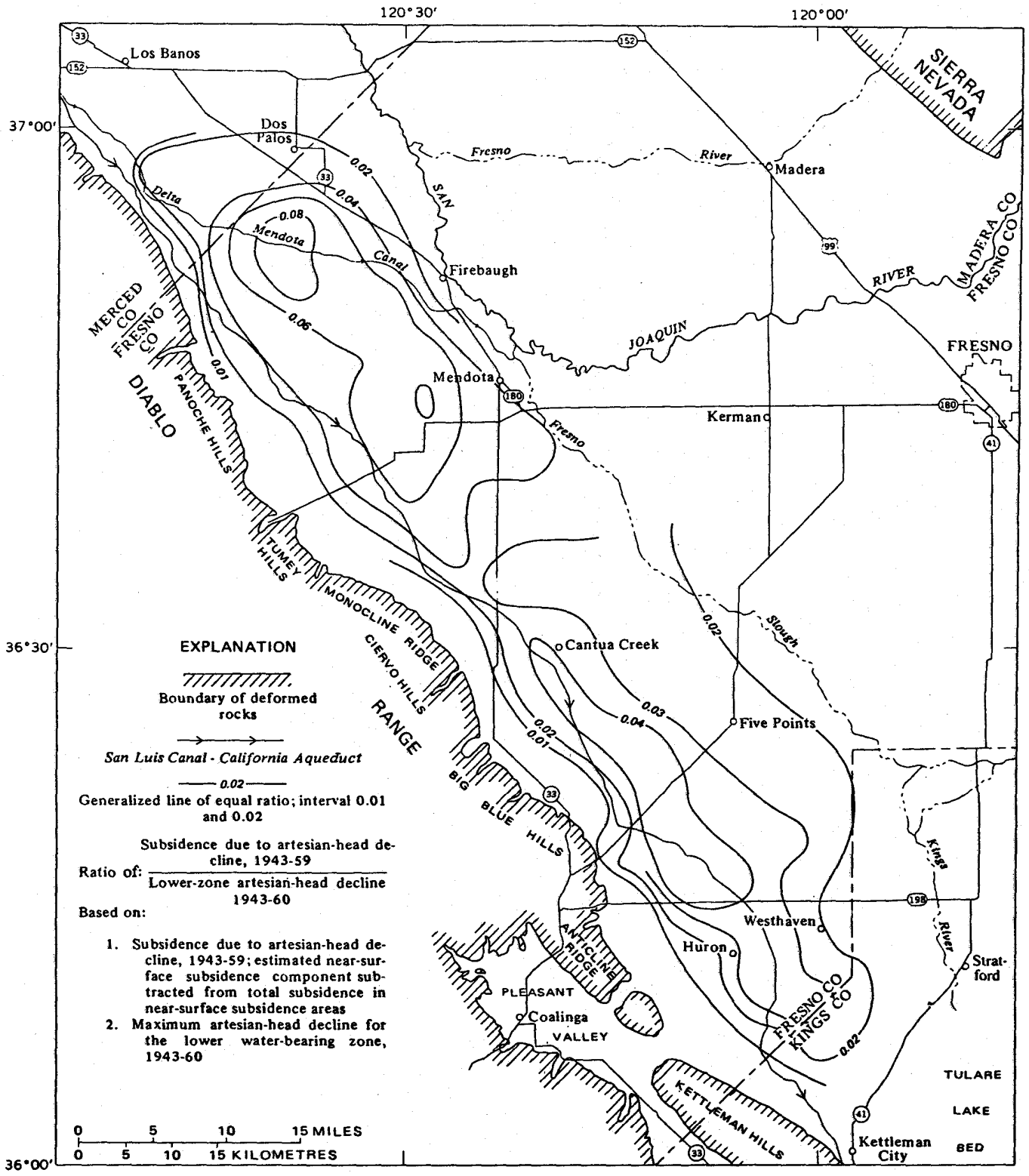

Figure 5.16 Ratio of subsidence to head decline, west side of San Joaquin Valley, California, 1943-59 (Bull and Poland, 1975, Figure 32).

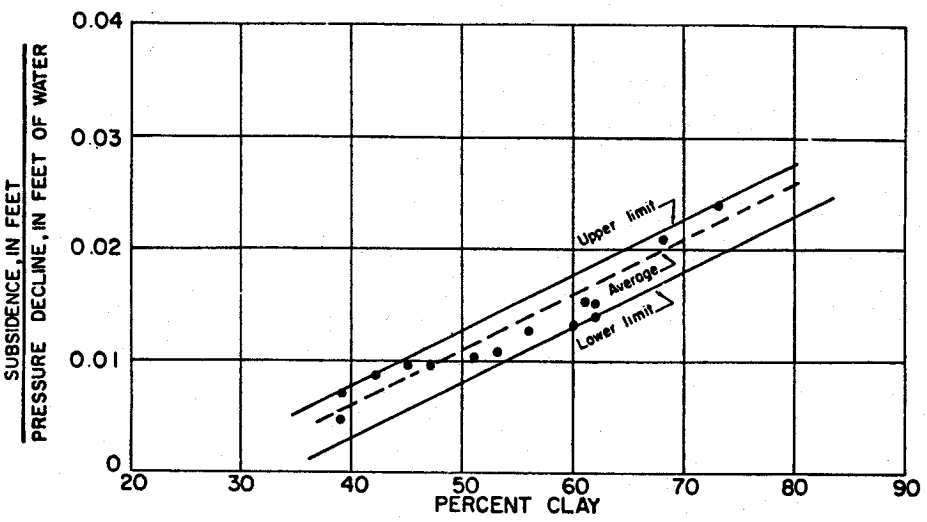

Figure 5.17 Relation between per cent clay and subsidence due to pressure decline (Gabrysch, 1969).

5.2.4 Clay content-subsidence relation

Figure 5.17 shows the general relationship in the Houston-Galveston area, Texas, between the percentage of clay beds and the subsidence head-decline ratio. According to Gabrysch (1969), the percentage of clay beds was determined from interpretation of electrical logs; the pressure-head decline was determined from measured water levels in wells; and subsidence values were taken from changes in nearby bench-mark elevations.

5.3 THEORETICAL APPROACH

5.3.1 General remarks

Regional subsidence due to ground-water extraction is a complex phenomenon which may be roughly "felt" in an intuitive fashion very difficult to explain quantitatively, due to the complexities of the materials involved.

Basically, the extraction of ground water reduces the interstitial water pressure (neutral pressure) which, according to the well-known "effective-pressure principle" of Terzaghi, means a transference of load to the soil skeleton (effective pressure) and its subsequent volume reduction (i.e., surface subsidence).

From a qualitative standpoint there is no "mystery" at all. However, in trying to explain the phenomenon both qualitatively and quantitatively, a series of unsuspected problems arise originating mainly from the elusive mechanical properties of soils.

Soils are complex multiple-phase systems constituted by solids, liquids, gases, and other substances like organic matter, ions, etc., which form, from a mechanical standpoint, a highly hyperstatic system whose properties must be inferred, at best, through statistical averages or "representative" tests.

As a result, soils incorporate into their mechanical properties all the behavioral aspects of their components, i.e. elasticity and plasticity of solids; viscosity of liquids; compressibility of gases; decay properties of organic matter; attraction and repulsion of ionic charges, etc., in a much more involved fashion.

This type of material has non-linear elastic, plastic, and viscous properties whose mechanical parameters are anisotropic and are history-, stress-, and time-dependent.

Such material is very difficult--if not impossible--to handle in any kind of a theoretical model of subsidence and this explains why the different approaches described in the scientific literature for that purpose, resort to many simplifications and idealizations in order to obtain some kind of a model that allows a more or less correct interpretation of past events, prediction of future ones, and decisions to be made about them. The questions are: What to simplify? How to idealize soils?

Unfortunately, there is no general rule, because the dominant feature in one case may be negligible in another and therefore, judgment and expertise must be exercised for best results. As general information, the more common simplifications regarding soil properties are listed here:

1. No organic matter present;
2. Only two phases present (solid-liquid);
3. No viscous properties;
4. No plastic properties;
5. Newtonian behavior of liquid phase;
6. No anisotropy;
7. Linear elastic properties of soil structure;
B. Constant parameters or, at least, one set for virgin compression and another for expansion and recompression.

Additionally, other simplifications regarding the system of aquifers and aquitards may be introduced, such as

9. Horizontal strata;
10. Horizontal flow in aquifers and vertical flow in aquitards;
11. Subsidence due mainly to aquitard consolidation;
12. No free surface of flow in the aquifers.

and so on.

As might be expected, the larger the number of simplifications made, the more restricted the nature of the resultant model and the more specific its applicability.

However, it should be remembered that, in practice, simplifications must be made according to the nature and volume of the available information and that the best way of modeling a given case may be to begin with the simpler models first, advancing later to the more involved ones, up to the highest level justified by the existing data.

In the remainder of this chapter an insight will be given on the details of several types of subsidence models (Figueroa Vega, 1973, 1977).

5.3.2 Compressibility relationships and total potential subsidence

The traditional laboratory test employed to disclose the compressibility relationships of soils is the consolidation test (odometer test) developed by Karl Terzaghi. The test is discussed in Chapter 4.

In this test, soils exhibit a more or less linear relationship between e (void ratio) and log p'/p_0', effective intergranular pressure) of the type

$$e = e_0 - C_C \log \frac{p'}{p_0'}, \tag{5.8}$$

(a slightly modified form of equation 4.14 shown in Chapter 4), where Cc is the "compression index" and eo and pol are initial reference values. This relationship is valid for increasing values greater than the maximum intergranular pressure the soil has supported in the past (pol, preconsolidation pressure). For discharge or recharge at pressures lower than the preconsolidation pressure (i.e.: within preconsolidation range) the relationship is similar, with a lower Cc value (Cc), which means that only part of the total deformation of a soil is recoverable and also that the compressibility parameters of a soil are history dependent.

In the soil mechanics field, it is customary to define the "coefficient of volume compressibility," m_V, as

$$m_V = \frac{\frac{de}{dp'}}{1 + e_0} = \frac{a_V}{1 + e_0}, \tag{5.9}$$

where a_V stands for the coefficient of compressibility, such that, within a small increment of pressure, the total settlement of a column of soil of thickness, H_0, may be computed as

$$\Delta H = m_V \, \Delta p' H_0. \tag{5.10}$$

As may be noted in equation (5.9), m_v, is stress dependent and therefore its value must be estimated for the proper e_0 and $\Delta p'$ values. Otherwise, equation (5-10) may lead to serious errors.

Equation (5.10) may be applied directly--as in the soil mechanics field--as a first approximation, whenever the strata thickness sequence is known (H_{01}, H_{02}, ..., H_{0i}) as well as the corresponding neutral pressure reductions due to water extraction (taken initially as the effective pressure increments) and their estimated coefficients of volume compressibility (m_{v1}, m_{v2},....,m_{vi}). The total subsidence in this case would be approximately

$$\overline{\Delta H} \approx \sum_{1}^{i} m_{vi} \Delta P_i' H_{oi} . \qquad (5.11)$$

When all the involved strata remain saturated and the total relative shortening of the column is small, the foregoing calculations may be accepted as sufficiently good for practical purposes. In other cases, they must be taken only as giving approximate values and subsequent calculations must be made utilizing these values to estimate the total initial and final column loads at each level, the initial and final effective pressures (vertical pressure due to total load) and applying again equation (5.11) and repeating the process iteratively, until final results take account properly of both effects.

5.3.3 Differential equations of ground-water flow in an aquifer-aquitard system

Steady laminar flow of interstitial water within any portion of saturated soil obeys two basic laws--the mass conservation law:

$$\mathrm{div}(\gamma \bar{v}) = 0 , \qquad (5.12)$$

where "div" stands for the divergence operator, "γ" for density of water, "v" for flow velocity vector, and Darcy's Law:

$$\bar{v} = -K \ \mathrm{grad}\ h, \qquad (5.13)$$

where K is the hydraulic conductivity of the soil and "h" the hydraulic head.

Combining these laws into a single equation and neglecting the variability of γ and K gives

$$\nabla^2 h = \frac{\partial^2 h}{\partial x^2} + \frac{\partial^2 h}{\partial y^2} + \frac{\partial^2 h}{\partial z^2} = 0 , \qquad (5.14)$$

the well-known Laplace equation. Therefore, h must be an harmonic variable satisfying the existing boundary conditions.

Equation (5.12) simply states that the mass of water within the portion of saturated soil remains constant. When the flow is unsteady, this does not hold anymore and some water is stored in or extracted from a specified elemental volume of soil and equation (5.14) must be modified accordingly, resulting in

$$K\nabla^2 h = S_s \frac{\partial h}{\partial t} , \qquad (5.15)$$

where "S_S" is the specific storage and a linear compressibility relationship is assumed both for water and soil structureo.

In a homogeneous horizontal aquifer of constant thickness "b" with horizontal flow, equation (5.15) reduces to

$$\frac{\partial^2 h}{\partial x^2} + \frac{\partial^2 h}{\partial y^2} = \frac{S_s}{K}\frac{\partial h}{\partial t} = \frac{S}{T}\frac{\partial h}{\partial t} = \frac{1}{\nu}\frac{\partial h}{\partial t} , \qquad (5.16)$$

where

$$S = bS_S;\ T = bK;\ \text{and}\ \nu = \frac{T}{S} \qquad (5.17)$$

are the storage coefficient, transmissivity and hydraulic diffusivity respectively. In a compressible aquitard with vertical flow, equation (5.15) reduces simply to

$$\frac{\partial^2 h}{\partial z^2} = \frac{1}{\nu}\frac{\partial h}{\partial t}\,. \tag{5.18}$$

These equations may also be written in terms of "s" (drawdown) instead of "h" (hydraulic head).

Equation (5.16) is the classical aquifer differential equation due to Theis (Theis, 1935) and equation (5.18) is the classical consolidation equation due to Terzaghi (Terzaghi, 1923). Both equations must be solved subject to their proper initial and boundary conditions.

In a system with aquifer(s) and aquitard(s), the mathematical problem to solve is made up of one equation of the type (5.16) for each aquifer including some additional terms to take account of vertical inflows or outflows, if any, and one equation of the type (5-18) for each aquitard, plus the adequate initial and boundary conditions and additional conditions stating equality of hydraulic heads in any plane of contact of any two of the existing aquifer(s) and aquitard(s). This is referred to as a "quasi three-dimensional model." The final result is a complex coupled system which may be solved with the help of numerical methods (finite differences or finite elements). The assumption of vertical flow in aquitards and horizontal flow in aquifers is only justified when the permeability of the latter is much higher than that of the former (say tenfold or more). Otherwise, it is necessary to resort to a truly three dimensional model, where all the second order partial derivatives are kept for all the strata.

The solution of the coupled system implies advancing numerically and simultaneously the solution for all the involved strata through each time increment, and this may represent a large number of calculations which might eventually overflow the working capability of the available computer. Models of this kind have been developed and published elsewhere (Carrillo, 1950; Gambolati, 1972).

An interesting alternative solution, for quasi three dimensional models, as applied to the Mexico City case (Figueroa V, 1973), is to depart from a coupled system to reduce the problem's complexity via integrodifferential equations. This will be outlined in the next section.

5.3.4 Uncoupling the system and solving a simpler problem

For a system made up of one aquifer underlain and overlain by consolidating aquitards, several mathematical formulations are possible in accordance with the upper and lower boundary conditions type (constant head or null flow). In any case, the mathematical formulation is made up, in terms of drawdowns, as explained before, by one equation of the type (5.16), including in its left side two terms of the form

$$\mp\frac{K_i}{T}\frac{\partial}{\partial z}s_i(x, y, 0, t) \tag{5.19}$$

to take account of vertical flow into the main aquifer, through the aquifer-aquitard common boundaries, plus two equations of the type (5.18) also in terms of drawdowns, plus the corresponding initial and boundary conditions.

For all the resulting cases of this system it has been shown (Herrera and Figueroa, 1969) that the problem was equivalent to

$$\frac{\partial^2 s}{\partial x^2} + \frac{\partial^2 s}{\partial y^2} + \int_0^t \frac{\partial}{\partial t}s(x, y, \beta)G(t-\beta)\partial\beta = \frac{1}{\nu}\frac{\partial s}{\partial t}\,, \tag{5.20}$$

where the convolution term includes the vertical inflows to the aquifer, and

$$G(t) = \frac{K_1}{T}\frac{\partial}{\partial z}A_1(0, t) - \frac{K_2}{T}\frac{\partial}{\partial z}A_2(0, t) \tag{5.21}$$

in which G(t) is the zero elevation at the aquifer-aquitard contacts and A_1 and A_2 the basic

solutions of classical consolidation theory corresponding to the particular boundary conditions present in each case. Additionally, in general

$$G(t) = -C - F(t) \tag{5.22}$$

where "C" is a constant depending on the system's parameters which incorporates the vertical inflows coming from the exterior boundaries of the system in the cases of constant head boundary conditions, and the function F (t) incorporates the vertical inflows released from aquitards by consolidation.

Equation (5.20) may be reduced to

$$\frac{\partial^2 s}{\partial x^2} + \frac{\partial^2 s}{\partial y^2} - C_s - \int_0^t \frac{\partial}{\partial \beta} s(x, y, \beta) \bullet F(t-\beta) \partial \beta = \frac{1}{\nu} \frac{\partial s}{\partial t} . \tag{5.23}$$

Furthermore, the integral term may be approximated by

$$\int_0^t \frac{\partial}{\partial \beta} s(x, y, \beta) \bullet F(t-\beta) \partial \beta = I \frac{\partial}{\partial t} s(x, y, t) \tag{5.24}$$

when $\partial s / (\partial \beta)$ has a slow variation, being

$$I = \int_0^\infty F(\beta) \partial \beta , \tag{5.25}$$

a constant. Under these conditions, the problem further reduces to

$$\frac{\partial^2 S_c}{\partial x^2} + \frac{\partial^2 S_c}{\partial y^2} = \frac{1}{\nu_c} \frac{\partial S_c}{\partial t} , \tag{5.26}$$

where

$$S_c = s e^{c \nu_c t} \tag{5.27}$$

and

$$\nu_c = \frac{\nu}{1 + I_\nu} . \tag{5.28}$$

This is the "correspondence principle" (Herrera and Figueroa, 1969). It means that the original coupled system is equivalent, under the already stated conditions, to an equivalent confined aquifer system.

For the case of a single aquifer and a single aquitard, the applicable expressions are

$$G(t) = -\frac{K_1}{T b_1} 1 + 2 \sum_{n=1}^{\infty} \exp - \frac{n^2 \pi^2 \nu_1}{b_1^2} t , \tag{5.29}$$

$$I = \frac{S_1}{3T} ; C = \frac{K_1}{T b_i} ; \nu_c = \frac{3T}{3S + S_1} \tag{5.30}$$

for the constant head external boundary condition and

$$G(t) = -\frac{2K_1}{Tb_1}\sum_{n=0}^{\infty}\exp\left(-\frac{\left(n+\frac{1}{2}\right)^2\pi^2 v_1}{b_1^2}t\right), \tag{5.31}$$

$$I = \frac{S_1}{T}; C = 0; v_c = \frac{T}{S+S_1}, \tag{5.32}$$

for the zero gradient external boundary condition. In all these formulas, the index 1 refers to the aquitard.

Both the integrodifferential equation and the correspondence principle have been applied to the Mexico City case, with some additional considerations which will be mentioned later, with reasonably good results. As a general comment, the applicability of the above-mentioned simplifications of the correspondence principle is much greater than it seems, for the following reasons.

Apparently, the correspondence principle would be applicable whenever $\partial s/\partial t$ "has a slow variation" as stated before. However in the extreme case of constant drawdown the right part of equation (5.24) equals zero for $t \neq 0$, which means that there is no consolidation except at $t = 0$, where the subsidence cause is concentrated. So, the former condition should read "has a slow variation everywhere."

It must be noted that equation (5.24) simply removes the lag-effects of the consolidation process and therefore it may work only if the drawdown is gradual. The more $\partial s/\partial t$ departs from a constant value the more the results depart from reality.

However, the consolidation process compensates this situation somehow, because while at any time increment, the subsidence increment includes some subsidence due to the preceding drawdowns, also part of the subsidence due to its own drawdown increment is transferred to future time increments. In any case, a short consolidation time may improve the results.

It is possible that an integration by parts of the memory term could lead to a better approximation, and this is a question which must be explored.

Another reason which supports the correspondence principle is the remarkably good correlation found between total drawdown and total subsidence.

According to the experience gained in the Mexico City case, from a practical standpoint there seems to be no strong reason to use equation (5.26) instead of equation (5.23) as there is not a big difference in computing time or computer memory requirements. So, its use seems to be more practical in non-computer modeling, as described in the next section.

In applying equation (5.23), some aspects must be considered:

1. Additional terms must be included to take into account infiltration or pumpage.
2. Compressibility parameters must distinguish between virgin compression and elastic recompression.
3. The storage coefficient in the main aquifer must be changed in those cells of the model where drawdowns are such that ground-water flow changes from confined to unconfined.
4. The aquifer compaction itself, if considered relatively important, may be added, computing it as an instant response to drawdown, thus taking care of point (b), above.

The procedures described herein may be incorporated in any of the existing types of ground-water models.

5.3.5 Simplified subsidence modeling

In some cases it may be desirable to have a fast estimate of the probable order of magnitude of subsidence versus time due to regional pumpage in some selected site(s) and this may be done through (1) estimating future drawdowns in the site(s) and (2) estimating future subsidence in the site(s).

The first part may be achieved by simple superposition of the Theis equation or by the application of the Influence Diagram (Figueroa Vega, 1971), together with the application of the aforementioned Correspondence Principle (equations 5.26, 5.27 and 5.28).

The superposition of the Theis equation needs no further comment. It may be advisable when the number of wells is not too large.

When there are many wells and their distribution is fairly uniform with an average pumpage of "q" units of volume per unit of time, it is much more practical to apply the influence diagram mentioned before, which is a diagram similar to that developed by Newmark (1942) in the soil mechanics field to integrate vertical stresses due to a distributed surcharge.

By means of it, drawdown "s" at the site and at time "t," due to a distributed pumpage of intensity "q" in any area is simply

$$s = \frac{qt}{S}(0.0025N_i + 0.001N_e), \tag{5.33}$$

where "S" is the storage coefficient and "N_i" and "N_e" are the internal and external "squares" covered by the pumping area drawn at a proper scale.

The application of equation (5.33) for several times makes it possible to plot estimated future drawdowns versus time.

The next step is to estimate the future subsidence, the time derivative of which is T (transmissibility) times the convolution term of the left side of equation (5.23), i.e.:

$$\frac{\partial h}{\partial t} = T\int_0^t \frac{\partial}{\partial \beta} s(x, y, \beta) \bullet F(t-\beta)\partial\beta \, . \tag{5.34}$$

This expression may be easily approximated by numerical methods with the help of a pocket programmable calculator and the total subsidence for each time is the area under the curve versus t.

Equation (5.34) takes only into account the consolidation of the clay strata. Compression of the aquifer may be included, as an instant response for each increment of time, using equation (5.11).

The former procedure, though simple and lacking precision, may be used as a basis for preliminary decision-making in many cases of regional subsidence due to ground-water extraction, while a more precise digital computer model is elaborated and validated.

5.3.6 Other types of subsidence models, by Donald C. Helm[2]

A variety of prediction techniques have been discussed--empirical, semi-theoretical, and theoretical. The empirical and semi-theoretical techniques require induced subsidence to have already begun. Empirical and semi-theoretical methods offer reasonable parameters that link subsidence to some other measurable phenomenon in the field. The theoretical techniques which have been discussed to this point require the results of laboratory tests in order to predict subsidence.

Two other techniques for subsidence prediction will now be discussed. This will be followed by a discussion of the role of the unpumped overburden. One technique, which uses a depth-porosity model, is too primitive to require induced subsidence to have already begun. This is its power; it can give a rough approximation of potential ultimate subsidence of an area where the local confined aquifer system has not yet been stressed. The second technique that will be discussed uses an aquitard drainage model. In contrast to the depth-porosity model, this second technique requires compressible beds to be stressed in the field. It is sufficiently sophisticated not to require laboratory tests on soil specimens. Neither the depth-porosity model nor the aquitard-drainage model requires laboratory tests; each uses its own independent field-based method for parameter evaluation. They are both useful techniques.

The parameter found by using the depth-porosity model is a generalized depth-dependent approximation for a coefficient of volume change, m_v, of equation 5.10 which corresponds to nonrecoverable specific storage, S'_{skv}, of equations 3.4 and 3.19. This parameter controls the ultimate response to stress of a specified bed. The parameters found by using the aquitard drainage model are site-specific average values of specific storage, S'_{skv}, and the vertical component of hydraulic conductivity, K'. These parameters control the time-delayed response to

---

[2] Work performed under auspices of the U.S. Department of Energy by the Lawrence Livermore National Laboratory under contract No. W-7405-ENG-48.

stress of compressible interbeds within a confined system. They appear directly in equation 3.2 and indirectly in equation 5.15.

5.3.6.1 Depth-porosity model

Porosity of sedimentary materials is known to decrease in general with depth (Figure 5.18). Based on empirical data for shale and mudstone, Athy (1930) and Magara (1978) suggest that a relation between porosity and depth can be found from an exponential expression

$$n + n_0 e^{-cz} \tag{5.35}$$

for conditions of compaction equilibrium where n is porosity at a specified depth z, n_0 is an extrapolation of n to land surface (z = 0), and c is an empirically determined constant. For Athy's data of shale porosities from Oklahoma, n_0 equals 0.48 and c equals 0.0014 when z is expressed in metres. Schatz, Kasameyer, and Cheney (1978) suggest using equation 5.35 for site-specific values for n_0 and c as a means of approximating S'_{skv} as a function of depth, z, for all compressible sedimentary material including shale, mudstone, sandstone, and clay. They tacitly argue that decreasing fluid pressure due to producing an artesian aquifer system has an

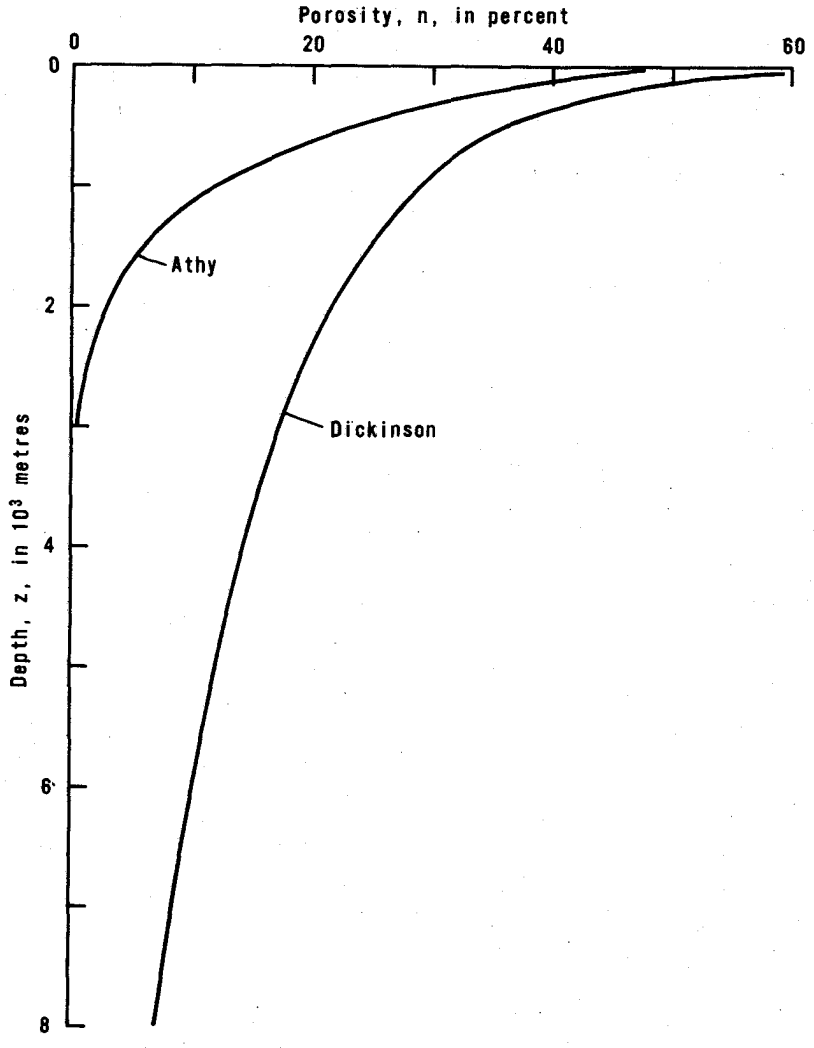

Figure 5.18 Two examples of decrease of porosity with depth.

equivalent effect on porosity that lowering the bed to a greater depth would have. Hence the curves in Figure 5.18 are treated by them to represent a type of ultimate stress/strain relation for equilibrium compaction.

Unfortunately, not all empirical depth-porosity curves follow an exponential relation as expressed by equation 5.35. A notable exception (Magara, 1978, p. 93) is Dickinson's (1953) data for shale porosities from the Gulf of Mexico coast. Helm (1980, unpublished manuscript) has found that Dickinson's shale porosities follow a logarithmic relation with depth, namely

$$\Delta n = -a\ \Delta \ln x, \tag{5.36}$$

$$n = n_{ref} - a\ \ln(z/z_{ref}), \tag{5.37}$$

where n_{ref} and z_{ref} are reference values for porosity and depth and a is an empirical constant. If a is interpreted as a type of compression index, equations 5.36 and 5.37 approximate the type of stress-strain relation one would anticipate from standard soil mechanics interpretation of laboratory consolidation data. For Dickinson's field data from the Gulf Coast, a equals 0.103 and n_{ref} is found to equal 0.05 for an arbitrary reference depth z_{ref} of 10^4 m.

It is now possible to get two depth-dependent theoretical values of S'_{skv} based on equations 5.35 and 5.37. Recalling equation 3.10, we can express how lithostatic effective stress, p', due to submerged weight of overlying material changes with depth, z, by the gradient

$$\frac{dp'}{dz} = (1-n)(G-1)\gamma_w = \frac{G-1}{1+e}\gamma_w . \tag{5.38}$$

According to the left-hand equality of equation 3.4 and equation 5.9, we write

$$S'_{skv} = -\frac{1}{1+e}\frac{de}{dp'}\gamma_w = -(1-n)\frac{de}{dp'}\gamma_w . \tag{5.39}$$

Equation 5.39 can be written

$$S'_{skv} = -(1-n)\frac{de}{dn}\frac{dn}{dz}\frac{dz}{dp'}\gamma_w = -\frac{\gamma_w}{1-n}\frac{dn}{dz}\frac{dz}{dp'}, \tag{5.40}$$

which, in accordance with equation 5.38, becomes

$$S'_{skv} = -\frac{1}{(1-n)^2(G-1)}\frac{dn}{dz} . \tag{5.41}$$

It now becomes necessary to determine dn/dz from Figure 5.18. For Athy's curve, equation 5.41 becomes

$$S'_{skv} = \frac{c}{(G-1)}\frac{n}{(1-n)^2}, \tag{5.42}$$

where we have used equation 5.35. For Dickinson's curve, however, equation 5.41 becomes

$$S'_{skv} = \frac{a}{(G-1)z(1-n)^2} \tag{5-43}$$

where we have used equation 5.37.

Figure 5.19 shows the relation of S'_{skv} and depth z in accordance with Athy's data (dashed line) and Dickinson's data (solid line). The dashed line in Figure 5.19 was found by substituting equation 5.35 into the right-hand side of equation 5.42 and assuming n_0 to equal 0.48 and c to equal 0.0014. The solid line in Figure 5.19 was similarly found by substituting equation 5.37 into the right-hand side of equation 5.43 and assuming n_{ref} to equal 0.05, Z_{ref} to equal 10^4 m, and a to equal 0.103.

The marks on Figure 5.19 indicate a selection of S'_{skv} values determined by other methods. The X's in the upper right-hand corner of Figure 5.19 represent values of S'_{skv} calculated from results (Marsal and Graue, 1969, Table 5, p. 190) of standard laboratory consolidation tests on soil samples near Mexico City. The symbols X_{SC}, X_T, and X_W represent values of S'_{skv} calculated from results of standard laboratory consolidation tests on soil samples taken respectively from the Santa Clara Valley, California (Poland, written communication, 1978), from near Seabrook,

Texas (Gabrysch and Bonnet, 1976, Table 3), and a composite of values from the Wilmington Oil Field, California (Allen and Mayuga, 1969). Subsidence is known to have occurred at all these sites. The circles represent values of S_{skv} determined from simulating observed compaction and expansion in California by means of a digital computer code. This computer simulation technique uses the aquitard-drainage model and is discussed in the next section.

It is evident from Figure 5.19 that within 1000 metres of land surface, Dickinson's curve gives a high, but reasonable, estimate of S'_{skv}. Helm (1980, unpublished manuscript) suggests the use of the solid curve in Figure 5.19 as a first approximation of S'_{skv}, For example, assume a confined aquifer has not been developed and hence no field-based compaction records are available. However, suppose one knows that an areally extensive confined aquifer system lies at a depth between roughly 100 and 300 metres. Within this 200-metre interval there is found to exist about 100 metres of fine-grained compressible interbeds. Hence the thickness of compressible beds, b′, is about 100 m, the average depth is about 200 m, and in accordance with Dickinson's curve in Figure 5.19 we can estimate S'_{skv} to approximate $10^{-3}m^{-1}$. Using equation 3.4, we find

$$\Delta b'/\Delta h_a = S'_{skv}b' \cong 10^{-3} \times 10^{2} = 10^{-1}. \qquad (5.44)$$

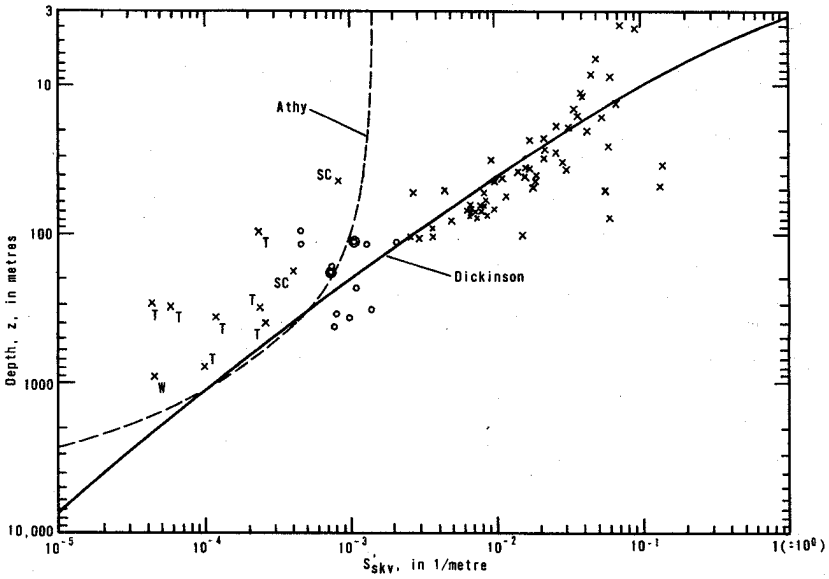

Figure 5.19 Specific storage for nonrecoverable compaction, S'_{skv}, as a function of depth, z.

Equation 5.44 tells us, as a first approximation, that for every foot of long-term drawdown, one can expect about one-tenth of a foot of ultimate compaction.

Let us interpret equation 5.44 in a somewhat broader time frame. One would expect a time lag of decades before compaction in the field would reach its ultimate value (equation 5.44) even under conditions of no recovery of artesian head. If at any time artesian head recovers above a transient critical elevation, ongoing residual subsidence will stop.

Predicting this critical elevation of head is discussed in the next section. Equation 5.44 and use of Dickinson's curve in Figure 5.19 tacitly requires sedimentary material within a con-

fined system initially to be normally consolidated. Another tacit assumption of equation 5.44 is that volume strain expresses itself entirely in vertical compression. For a confined aquifer system whose volume strain is isotropic, the vertical component of strain is one-third the volume strain. Whenever in situ strain is actually isotropic, use of Dickinson's curve (Figure 5.19) in equation 5.44 would thereby automatically give an estimate of vertical compression three times too large.

Methods for approximating a regional distribution of Δh_a, which appears in the left-hand side of equation 5.44, are available (e.g., Figueroa Vega, 1971). Discussion of these methods is beyond the scope of the present section.

5.3.6.2 Aquitard-drainage model

Tolman and Poland (1940) suggested that subsidence in the Santa Clara Valley, California, is caused not simply by declining artesian heads and the resulting compaction of permeable sands, but primarily by the nonrecoverable compaction of slow-draining clay layers within the confined system. This marks the conceptual birth of the aquitard-drainage model (Figure 5.20). Riley (1969) applied Terzaghi's (1925) theory of one-dimensional consolidation quantitatively to the aquitard-drainage model. Helm (1972, 1975, 1976) borrowed Riley's insights to develop a

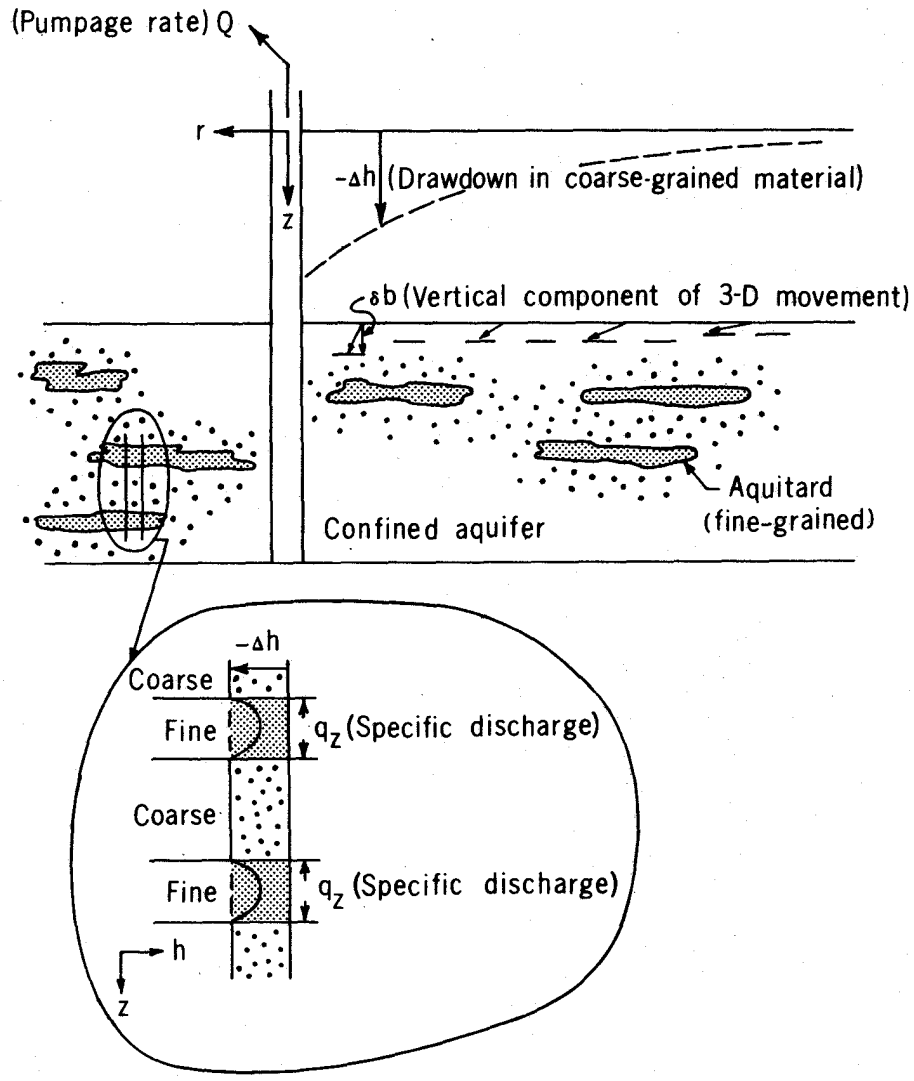

Figure 5.20 Aquitard-drainage model (modified from Helm, 1980, Figure 4).

one-dimensional computer code to simulate time-delayed aquitard compression and expansion in response to arbitrary fluctuations of hydraulic head within the coarse-grained portion of a confined aquifer system. In turn, Freeze (Witherspoon and Freeze, 1972; Gambolati and Freeze, 1973) and Narasimhan (Narasimhan and Witherspoon, 1977) borrowed Helm's insights for developing their own one-dimensional computer codes for aquifer-system compaction and expansion. Digitalizing the aquitard-drainage model led directly to a powerful predictive technique (Helm, 1978; Pollard and others, 1979) for land subsidence caused by water-level fluctuations within a confined aquifer system.

The aquitard-drainage model (Figure 5.20) represents the confined aquifer system as containing two basic types of porous material: a group of (i) fine-grained interbeds each of which is completely surrounded by a hydraulically connected system of (ii) coarse-grained material. The fine-grained interbeds (aquitards) are considered much less permeable than the interconnected coarse-grained portion of the confined aquifer system. Because slow-draining aquitards are interbedded within an aquifer, they are conceptually distinct from caprock, confining bed, or semi-confining bed that serves as a confined aquifer's upper boundary. The aquitard-drainage model conceptually attributes the observed time-lag (of compaction response to stress change) to the vertical component of fluid flow from one idealized material (aquitard) to another (aquifer) within the two-material system itself. The slow vertical drainage, q_z, from highly compressible aquitards to the less compressible aquifer material serves a somewhat similar rheological function in this model that a viscous "dashpot" serves in a viscoelastic reservoir model that has only one idealized undifferentiated material (Corapcioglu and Burtsaert, 1977).

In conjunction with appropriate field data, the model predicts (1) residual nonrecoverable compaction within a system, (2) time-dependent in situ preconsolidation pressure (a critical depth to water at which non-recoverable compaction is stopped during the unloading phase and is triggered during the reloading phase of a specified unloading-reloading cycle), and (3) a timeconstant, τ, for a confined system at a site of interest. According to Terzaghi's theory of consolidation, τ can be interpreted to represent the length of time required for initially unstressed aquitards to reach a 93 per-cent nonrecoverable compaction if water levels in adjacent aquifers (of a confined system) are instantaneously lowered a specified amount and then held constant.

By simulating field compaction and expansion at 8 sites in the Santa Clara Valley and 7 sites in the San Joaquin Valley, California, Helm (1978, Table 2) estimated that in 1978 residual compaction in the Santa Clara Valley ranged from a minimum of 0.52 m at one site to a maximum of 2.53 m at another. Among the analyzed sets of field data collected in the San Joaquin Valley, calculated residual compaction ranged from a minimum of 0.85 m at one site to a maximum of 9.75 m at another. In the early 1970's the critical depth to water was calculated site by site to range from a few to several tens of metres above a local past maximum depth to water. Time constants also were estimated from site-specific field data. In the Santa Clara Valley, τ was calculated to range from a minimum of 13 years at one site to 125 years at another. In the San Joaquin Valley τ was calculated to range from 5 years at one site to 1350 years at another.

Figures 5.21 and 5.22 illustrate the use of a one-dimensional computer simulation based on the aquitard-drainage model. Using the stress curve shown in the upper graph of Figure 5.21 as input values, parameter values within the mathematical model are calibrated in order to make calculated compaction (dotted line in the lower graph of Figure 5.21) be as close an approximation to observed compaction (solid line in the lower graph of Figure 5.21) as possible. Using these parameter values and the input stress curve shown in the upper graph of Figure 5.22, a predicted compaction curve is calculated for the period 1921-74. This prediction is shown by the solid line in the lower graph of Figure 5.22. Actual compaction is estimated as a portion of subsidence measured at bench mark J111 and is plotted as solid circles in the lower graph of Figure 5.22. The excellent agreement between predicted and observed compaction in Figure 5.22 confirms the parameter values found during the calibration process (Figure 5.21). This result increases one's confidence in the residual compaction, preconsolidation stress, and time constants that are estimated from this procedure.

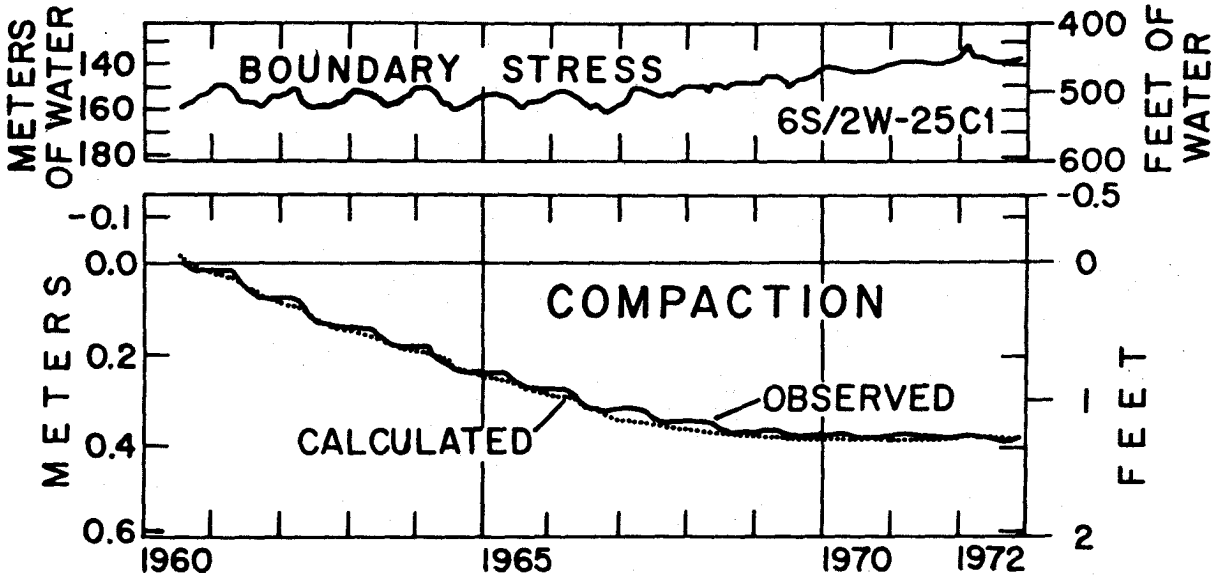

Figure 5.21 Simulation of compaction based on water-level data for well 6S/2W-25Cl (1960-72) and compaction data observed in well 24C3.

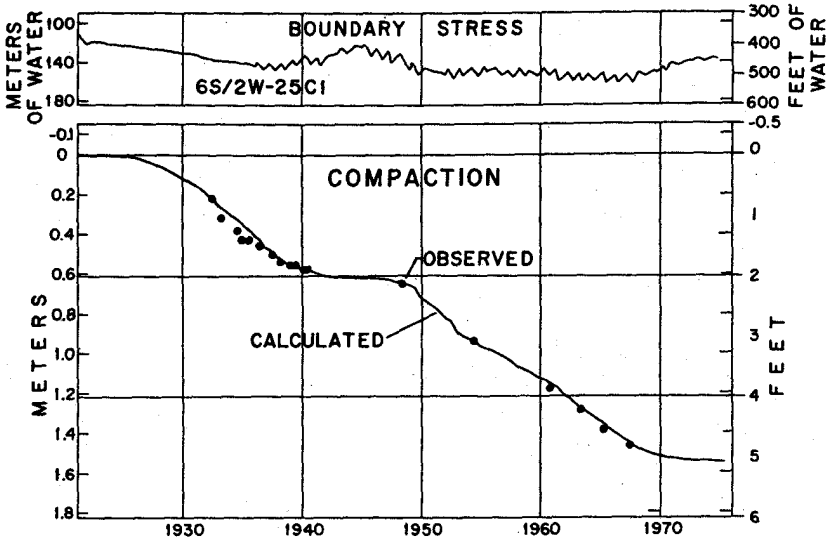

Figure 5.22 Simulation of compaction based on water-level data for well 6S/2W-25Cl (1921-74) and on compaction estimated as a portion of subsidence measured at bench mark

5.3.6.3 Influence of material within the unpumped overburden

Subsidence due to fluid withdrawal is the expression at land surface of the compression at depth of a stressed artesian aquifer system. Material within the intervening unpumped overburden may possibly play a role in mitigating land surface effects. Geertsma (1957, 1973) has in effect discussed quantitatively the role of the overburden. His equation for ultimate vertical displacement, U_z, directly over the center of an axially symmetric confined aquifer system (Figure 5.23) is

$$U_z(0, 0) = - 2((1-\nu)c_m b\Delta p \{1-[C/(1+C)^2]\}, \quad (5.45)$$

where

ν is Poisson's ratio,
b is thickness of compressing bed(s),
p is pressure change,
C is D/R,
D is depth to compressing bed(s), and
R is radius of stressed system.

For highly compressible poro-elastic bulk material, Geertsma's coefficient of uniaxial compaction, c_m, becomes

$$C_m = (1-2\nu)(1+\nu)/E(1-\nu), \tag{5.46}$$

where E is Young's modulus.

Equation 5.45 should be used with caution for the following reasons. Due to gravitational body forces on submerged solids, it is reasonable to assume that the base of a depressured aquifer system does not move upward. Unfortunately, Geertsma neglects such body forces in his analysis with the unrealistic result that under some circumstances the base of his idealized reservoir (confined aquifer system) mathematically moves upward a significant amount. This physically unlikely upward movement can mathematically nearly equal the total compaction of the stressed system. Hence there may mathematically be no downward movement of the top of the idealized reservoir. Correspondingly under these circumstances there would mathematically be no subsidence at land surface whatsoever. This questionable aspect of Geertsma's analysis reflects itself in equation 5.45.

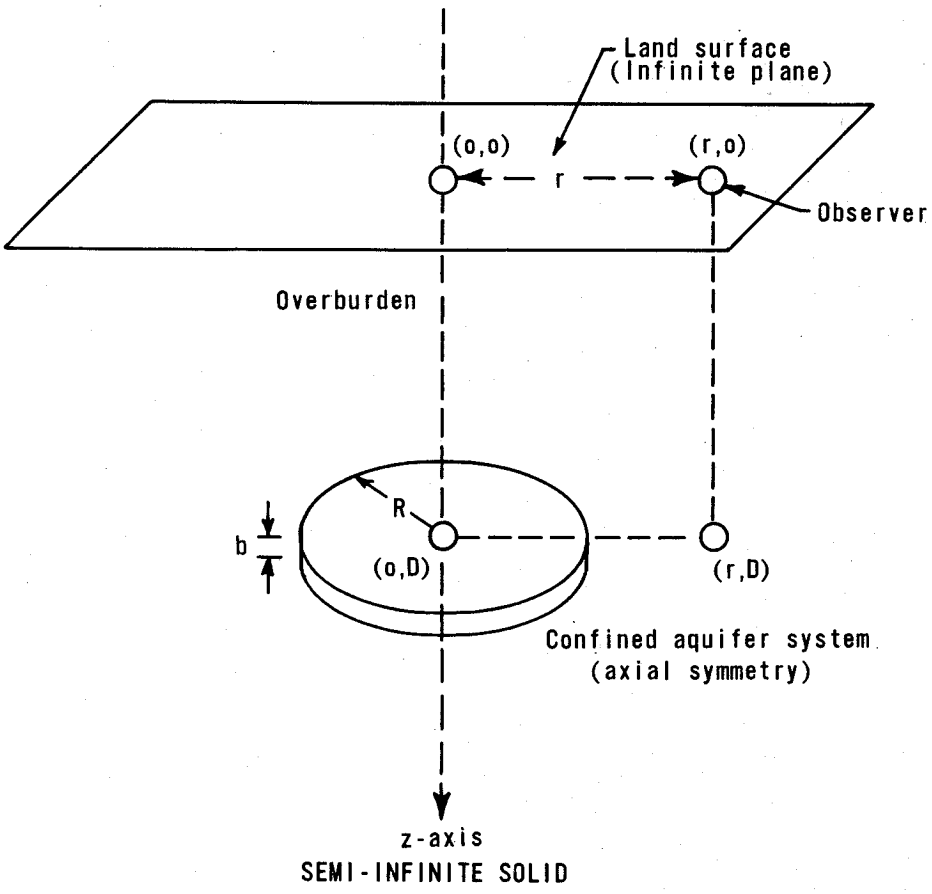

Figure 5.23 Half-space model (modified from Helm, 1980, Figure 2).

It is more reasonable to assume that the volume of compaction of a compressible aquifer system expresses itself eventually by an equal volume of subsidence at land surface. Whenever the upper boundary of a compacting aquifer system moves downward in response to compression of underlying sediments, Geertsma (1973) himself points out that the volume which this upper surface moves is preserved at land surface. When the vertical movement of the base of a confined aquifer system can realistically be considered negligible, land subsidence, according to Geertsma, equals volumetrically the total compaction of the confined aquifer system.

The areal distribution of subsidence is somewhat influenced, however, by the ratio of depth D to radius R (Figure 5.23) of the depressured confined aquifer system. The effect of compaction of an aquifer system with a large D/R ratio may be spread over a large area at land surface and hence minimize the vertical component of volumetric subsidence. The limit, however, would not be zero (which is erroneously implied by equation 5.45) but some finite fraction of b', of equation (5.44). For most ground-water systems the D/R ratio is sufficiently small that the overburden's spreading effect can be completely ignored. This implies the direct applicability of a depth-porosity model (Section 5.3.6.1).

The conceptual model used by many investigators, including Geertsma, will now be described. It is a variation of what can more generally be called a half-space model (Figure 5.23). The earth is represented as a homogeneous, isotropic, semi-infinite elastic (or poro-elastic) medium. Land surface is represented as a flat upper surface that is free to move. Neither calculated surface movement nor topographic relief affects the essential flatness of the idealized surface. Although a depressured zone at depth D below land surface with a center at radial distance r from an observer on land surface is represented by an idealized spherical tension center by Carrillo (1949), by vertical pincers by McCann and Wilts (1951), and by a radially symmetric group of strain nuclei by Geertsma (1957), the various representations are conceptually similar. Gambolati (1972) has discussed the major conceptual distinctions between the tension-center representation (Carrillo, 1949; McCann and Wilts, 1951) and the strain-nucleus representation (Mindlin and Cheng, 1950; Sen, 1950; Geertsma, 1957, 1966, 1973; Finol and Farouq Ali, 1975). Briefly, a tension center model tacitly requires an infinitely compressible reservoir within an elastic half-space. The strain-nucleus model requires the confined aquifer system's compressibility to equal the compressibility of the surrounding elastic halfspace. Finite heterogeneity between the compressing system and the surrounding half-space was introduced to the model by Gambolati (1972).

The question of finite heterogeneity deserves some comment. A confined aquifer system by definition yields fluid to a discharging well and experiences a pressure loss. The surrounding material by definition does not yield fluid. Hence porosity within a compressible confined aquifer system decreases. Porosity does not necessarily decrease within the surrounding halfspace. This distinction is analogous to the distinction in soil mechanics between drained and undrained compression. Decrease in porosity as a source for fluid discharge inherently introduces an extra component into a compressibility term for a confined aquifer system. This extra component does not appear in a corresponding compressibility term for the undrained surrounding half-space. Specifically, only S_{SW} of equation 3.3 is appropriate to use for the surrounding half-space whose individual grains are considered incompressible,, whereas the sum of S'_{SK} and S_{SW} is appropriate to use for the aquifer system itself. S'_{SK} is a function of porosity loss whereas S_{SW} is a function of the expansion of interstitial water. Hence, the hydraulics of underground fluid flow alone helps dictate the apparent heterogeneity of compressibilities between a compressing aquifer system and the surrounding half-space. This apparent or in situ hydraulic heterogeneity is distinct from standard differences in material properties which are tested and recorded in the laboratory.

5.4 REFERENCES

ALLEN, D. R., and MAYUGA, M. N. 1969. The mechanics of compaction and rebound, Wilmington oil field, Long Beach, California, USA, in Tison, L. J. (ed.), Land subsidence, Vol. 2. Internat. Assoc. Sci. Hydrology, Pub. 89, p. 4710-423.

ATHY, L. F. 1930. Density porosity, and compaction of sedimentary rocks. Bull. American Assoc. Petroleum Geologists, v. 14, p. 1-24.

BULL, W. B., and POLAND, J. F. 1975. Land subsidence due to ground-water withdrawal in the Los Banos-Kettleman City area, California, Part 3. Interrelations of water-level change, change in aquifer-system thickness, and subsidence. U. S. Geological Survey Professional Paper 437-G, 62 p.

CARRILLO, NABOR. 1949. Subsidence in the Long Beach-San Pedro area. Stanford Research Institute, p. 67-69.

CASTLE, R. 0., YERKES, R. F., and RILEY, F. S. 1969. A linear relationship between liquid production and oil-field subsidence, in Tison, L. J. (ed.), Land subsidence, Vol. 1. Internat. Assoc. Sci. Hydrology Pub. 88, p. 162-173.

CORAPCIOGLU, M. Y., and BRUTSAERT, W. 1977. Viscoelastic aquifer model applied to subsidence due to pumping. Water Resources Research, v. 13, p. 597-604.

DICKINSON, G. 1953. Geological aspects of abnormal reservoir pressures in Gulf Coast Louisiana. Bull. American Assoc. Petroleum Geologists, v. 37, no. 2, p. 410-432.

FIGUEROA VEGA, GERMÁN E. 1971. Influence chart for regional pumping effects. Water Resources Research, v. 7, no. 1, p. 209.

FIGUEROA VEGA, GERMÁN E. 1973. Aquifer and subsidence model for Mexico City. 85th Annual Meeting of The Geological Society of America, v. 5, no. 7, p. 620.

FIGUEROA VEGA, GERMÁN E. 1977. Subsidence of the City of Mexico; a historical review. Second Internat. Symposium on Land Subsidence Proc., IAHS-AISH Pub. 121, p. 35.

FINOL, A., and FAROUQ ALI, S. M. 1975. Numerical simulation of oil production with simultaneous ground subsidence. Jour. Soc. Petroleum Eng., p. 411-422.

GABRYSCH, R. K. 1969. Land surface subsidence in the Houston-Galveston region, Texas, in Tison, L. J., ed., Land subsidence, Vol. 1. Internat. Assoc. Sci. Hydrology, Pub. 88, p. 43-54.

GABRYSCH, R. K., and BONNET, C. W. 1976. Land-surface subsidence at Seabrook, Texas. U.S. Geological Survey Water-Resources Investigation 76-31, 53 p.

GAMBOLATI, G. 1972. A three dimensional model to compute land subsidence. Bull. Internat. Assoc. Hydrol. Sci., v. 17, no. 2, p. 219-226.

GAMBOLATI, G., and FREEZE, R. A. 1973. Mathematical simulation of the subsidence of Venice, 1, Theory. Water Resources Research, v. 9, no. 3, p. 721-733.

GEERTSMA, J. 1957. The effect of fluid pressure decline on volumetric changes of porous rocks. Trans. Amer. Soc. Mech. Engrs., AIME v. 210, p. 331-340.

GEERTSMA, J. 1966. Problems of rock mechanics in petroleum production engineering. Proc. First Cong. of the Internat. Soc. of Rock Mech., Lisbon, v. 1, p. 585-594.

GEERTSMA,J. 1973. A basic theory of subsidence due to reservoir compaction: the homogeneous case. Verhandeliger Kon. Ned. Geol. Mijhbouwk, v. 28, p. 43-62.

HELM, D. C. 1972. Simulation of aquitard compaction due to changes in stress [abs.]. EOS Trans. American Geophys. Union, v. 53, no. 11, p. 979.

HELM, D. C. 1975. One-dimensional simulation of aquifer system compaction near Pixley, Calif. 1, Constant parameters. Water Resources Research, v. 11, no. 3, p. 465-478.

HELM, D. C. 1976. One-dimensional simulation of aquifer system compaction near Pixley, Calif. 2, Stress-dependent parameters. Water Resources Research, v. 1, no. 3, p. 375-391.

HELM, D. C. 1978. Field verification of a one-dimensional mathematical model for transient compaction and expansion of a confined aquifer system, in Verification of mathematical and physical models in hydraulic engineering. Proc. 26th Hydraul. Div. Specialty Conf., College Park, Maryland, American Soc. Civil Eng., p. 189-196.

HERRERA, I., and FIGUEROA, G. E. 1969. A correspondence principle for the theory of leaky aquifers. Water Resources Research, v. 5, no. 4, p. 900-904.

HWANG, JUI-MING, and WU, CHIAU-MIN. 1969. Land subsidence problems in Taipei Basin, in Tison, L. J., ed., Land Subsidence, Vol. 1. Internat. Assoc. Sci. Hydrology, Pub. 88, p. 21-734.

IIDA, K. 1976. Land subsidence in Nobi Plain and change of water level. Rept. Commission on Environmental Protection, Nobi Area (Japan).

KUMAI, H., SAYAMA, M., SHIBASAKI, T., and UNO, K. 1969. Land subsidence in the Shiroishi Plain Kyushu, Japan, in Land Subsidence, Vol. 2. Internat. Assoc. Sci. Hydrology, Pub. 89, p. 645-657.

LOFGREN, B. E. 1969. Field measurement of aquifer-system compaction, San Joaquin Valley, California, USA, in Land Subsidence, Vol. 1. Internat. Assoc. Sci. Hydrology, Pub. 88, p. 272-284.

McCANN, G. D., and WILTS, C. H. 1951. A mathematical analysis of the subsidence in the Long Beach-San Pedro area. Calif. Inst. Technology, Tech. Rept., 117 p.

MAGARA, KINJI. 1978. Compaction and fluid migration. Elsevier Scientific Pub. Co., New York, 319 p.

MARSAL, R. J., and GRAUE, R. 1969. The subsoil of Lake Texcoco, in Carillo, Nabor, The subsidence of Mexico City and Texcoco Project. Secretaria de hacienda y credito publico fiduciarie, Mexico, p. 167-202.

MINDLIN, R. D., and CHENG, D. H. 1950. Thermoelastic stress in the semi-infinite solid. Jour. of Appl. Phys., v. 21, p. 931.

NARASIMHAN, T.N., and WITHERSPOON, P. A. 1977. Numerical model for land subsidence in shallow ground-water systems, Internat. Assoc. Sci. Hydrology Pub. 121, p. 133-144.

NEWMARK, N. M. 1942. Influence charts for computation of stresses in elastic foundations. University of Illinois, Bull. 40(12).

POLAND, J. F., LOFGREN, B. E., IRELAND, R. L., and PUGH, R. G. 1975. Land subsidence in the San Joaquin Valley, California, as of 1972. U.S. Geological Survey Professional Paper 437-H, 77 p.

POLLARD, W. S., HOLCOMBE, R. F., and MARSHALL, A. P. 1979. Subsidence cause and effect. Harris-Galveston Coastal Subsidence District Phase 1-A study, McClelland Engineers, Inc., Houston, Texas, 2 vols.

RILEY F. S. 1969. Analysis of borehole extensometer data from central California, in Tison, L. J., ed., Land subsidence, Vol. 2. Internat. Assoc. Sci. Hydrology, Pub. 89, p. 423-431.

SCHATZ, J. F., KASAMEYER, P. W. and CHENEY, J. A. 1978. A method of using in situ porosity measurements to place an upper bound on geothermal reservoir compaction, in Proc. Second Invit. Well Testing Symp., Berkeley, Calif. Lawrence Berkeley Laboratory.

SEN, B. 1950. Note on the stresses produced by nuclei of thermoelastic strain in a semi-infinite elastic solid. Quart. Appl. Math., v. 8, p. 635.

SHIBASAKI, T., KAMATA, A., and SHINTO, S. 1969. Hydrologic balance in the land subsidence phenomena, in Tison, L. J., ed., Land Subsidence, Vol. 2. Internat. Assoc. Sci. Hydrol. Pub. 88, p. 201-214.

TERZAGHI, KARL. 1923. Die Berechnung der Durchlassigkeitsziffer des Tones aus dem Verlauf der hydrodinamischen Spannungserscheinungen. Sitzber, Akad. Wiss. Wien, Abt. IIa, v. 132.

TERZAGHI, KARL. 1925. Settlement and consolidation of clay. Eng. News-Rec., McGraw-Hill, New York, p. 874-878, Nov. 26

THEIS, C. V. 1935. The relation between the lowering of piezometric surface and the rate and duration of discharge of a well using ground-water storage. Trans. American Geophys. Union, v. 16, p. 519-524.

TOLMAN, C. F., and POLAND, J. F. 1940. Ground-water, salt-water infiltration, and groundsurface recession in Santa Clara Valley, Santa Clara County, California. Trans., American Geophys. Union, pt. 1, p. 23-34.

WADACHI, K. 1940. Ground sinking in west Osaka (second rept.) Rept. Disaster Prevention Research Institute, No. 3.

WITHERSPOON, P. A., and FREEZE, R. A. 1972. The role of aquitards in a multiple-aquifer system. Penrose Conf. of the Geological Society of America, 1971, Geotimes, v. 17, no. 4, p. 22-24.

YAMAGUCHI, R. 1969. Water level change in the deep well of the University of Tokyo. Bull. Earthquake Research Institute, No. 47.

6 Economic and social impacts and legal considerations, by Joseph F. Poland, Laura Carbognin, Soki Yamamoto, and Working Group

6.1 GENERAL COMMENTS

Land subsidence induces very serious economic and social problems, which unfortunately appear later than the commencement of the subsidence event and when most damages are irreversible.

Because intensive ground-water withdrawals often occur in urbanized and/or industrial areas, the subsidence effects are widespread and affect not only the natural structures but also the man-made ones. In general, and sad to say, damages may be recorded but it is nearly impossible to establish their actual cost.

The physical environment is a principal determining factor in the severity of economic and social impacts as a result of land subsidence due to ground-water withdrawal. Coastal-plain areas, initially 1 to 5 metres above mean sea level, are susceptible to severe impact if appreciable subsidence develops. The severity of the damage and the social problems to be anticipated are greatly increased if the subsiding area lies in a region subject to typhoons or hurricanes. Furthermore, the greater or more calamitous is the actual, anticipated, or potential damage, the greater is the likelihood that legal decisions may develop to modify the doctrine of absolute ownership or the doctrine of "correlative rights," with respect to liability for subsidence of the lands of others due to pumping of ground water.

Table 1.1 lists 42 subsidence areas worldwide. Of these, at least 19 border the ocean or a bay and 2 others are crossed by tidal rivers. In this casebook it is not practicable to discuss economic problems and legal considerations for all the subsiding areas. Therefore, in this chapter we will limit the discussion to a few significant socioeconomic problems and legal developments in Italy, Japan, and the United States.

6.2 ITALY

Reported cases of subsidence in Italy due to ground-water withdrawal are few because not all the occurrences have been identified and classified as of yet.

Venice and Ravenna cases (case histories 9.3 and 9.15) must be included among the more serious; the former for its precarious environmental setting in which the phenomenon occurs even if at low rates, the latter for its areal extent and intensity.

Both cases were brought about by the intensive exploitation of underground fluids, occurring with the Italian post-war industrial boom during the 50’s and the 60’s. in both cases exploitation occurred without taking into account possible consequences to the subsoil equilibrium.

After 20 years of continuous ground-water withdrawal, subsidence has by now greatly affected the environment and its consequences are dramatic and even more serious for the irreversible effects.

Both Ravenna and Venice are located in shallow coastal zones so that the well-known subsidence effects are worsened because the land-sea interaction is considerably reduced.

Ravenna, about 7 km from the coast, is periodically flooded because its defences are no Longer sufficient against seasonal stormy seas. Venice, built in a lagoonal environment, has a close relationship with its waters and even with just normal tidal events the city becomes partially submerged and socioeconomic activity nearly stops.

Whereas Ravenna’s historical center is somewhat protected from marine aggression, Venice is continually exposed to sea domination, thus assuming a dismal appearance which naturally conflicts with the goal of the picturesque tourist attraction. Damages are enormous for both the artistic patrimony and the normal life activity (ruined merchandise, failures in heating systems, short circuits in electrical systems, etc.).

These inconveniences are a menace to the increasingly unstable socioeconomic life because of the frequently occurring flooding paralyzing the city, for health reasons (a very humid environment), for sanitary purposes (faulty sewage system), etc.

All this and other social reasons contribute to the Venetian exodus. For this reason, the city is witnessing a rapid decline in population, especially of its poorer working classes which suffer more than the others for their ghetto-like living conditions.

Depopulation occurs even in the islands and in the least defended littorals (ex. Pellestrina). The closer and more modern industrial area (Marchera) is the greatest attraction for more modern living conditions even if there are more psychosociological stresses.

At Ravenna subsidence affects especially the littoral zones (beach regression) where the largest resorts are located, and the widespread land fills where the usable soil thickness for cultivation is reduced and the types of cultivation must be diversified. Moreover subsidence causes considerable hydraulic problems in river flow in the delta zone, facilitates salt-water intrusion at the river's mouth, and produces problems to inland navigation, in the sewage system, etc.

Although at Ravenna, the damages are very serious and economically severe they are not as dramatic as at Venice where subsidence becomes a factor of survival.

At Ravenna the hydraulic problem would almost be permanently resolved after constructing suitable sea defences and restoring older hydraulic structures. The irreversible sinking of the area greatly affects only the littorals which are diminished in their width.

In Venice the sluice gates proposed to be constructed at the inlets to control the lagoon's water level would only partially resolve Venice's complex problem; resulting changes in the lagoon ecosystem would necessitate heavy commitments for a solution.

Even if subsidence is not the main factor responsible for the slow death of Venice, without a doubt its effects have indirectly determined this evolution. This leads to the necessity of concrete interventions.

The two worst Italian cases of subsidence just described involve two very important cities because of their unusual environments and artistic patrimonies. In these cases, as well as in many other Italian cases, the cause should be sought in the haphazard territorial planning in overestimating the possibility of utilizing ground-water resources.

Strict legislation for control and regulation of environmental use plus an efficient supervising organ for the development of underground waters would have safe-guarded the areas. Unfortunately, in Italy, public institutions and laws for territorial protection against subsidence effects due to ground-water withdrawal do not exist. Underground water management is still governed by an old law of 1933, which is only effective in a few municipalities. Furthermore, such legislation deals only with the authorization to search for water and, then, the declaration of finding it.

After the 1933 law, there has been no legislation which establishes any control on artesian pumping for the defense of the territory against subsidence. Only in recent years has government's attitude changed mainly due to the alarming situations which arose in Venice and Ravenna.

So far no specific norms or restrictions have been adopted: Italian government policy leaves preventive measures restricting ground-water exploitation to the local authorities.

6.3 JAPAN

6.3.1 Socioeconomic impacts

Land subsidence has been reported in more than 40 areas in Japan; most of these areas are subsiding because of excessive ground-water withdrawal and consequent declining artesian head. Many of the large cities in Japan are built on low flat alluvial plains underlain by unconsolidated water-bearing deposits of Quaternary age. The 10 chief subsidence areas due to ground-water withdrawal (shown in Figure 1.1 and described in Table 1.1) all border the ocean; in several of these areas subsidence has lowered the land surface below sea level, creating a hazardous situation. Yamamoto (1977) reports that as of 1975 the areas of land subsidence in Japan totaled 7,380 km^2, of which about 1,200 km^2 was below mean sea level.

The prolonged subsidence since 1920 in the Koto district in the eastern part of Tokyo developed the most serious environmental subsidence problem in Japan and probably in the entire world. The artesian head in the confined aquifers, initially above sea level, declined to as much as 60 m below sea level by 1965. The long-continued head decline, due to excessive withdrawal of ground water for industrial plants, caused the subsidence. As a result, 80 km^2 of land in eastern Tokyo had sunk below mean high-tide level by 1969; the lowest ground was about 2.3 m below mean sea level (Shimizu, 1969, Table 3). Two million people live in this area bordering Tokyo Bay. To prevent flooding and loss of life many protective measures have been taken. These have been described in part by Yamamoto in Case History 9.4. Banks of through-flowing rivers have been raised several metres, a wall has been built to surround the entire area that is below

high-tide level, and many water gates have been built to prevent high water from entering the depressed area.

During the early 1960's, restrictions were established on pumping from certain depth zones and drilling of new wells, and extraction of ground water for industry in the Koto district began decreasing. By 1965 pumpage had decreased by one-half (Aihara, et al., 1969, Fig. 1). As a result the artesian head subsequently has recovered 10 to 30 m or more since the 1965 low level, and the land surface has almost completely stopped subsiding. In fact, a few centimetres of land-surface rebound has been observed. However, the rebound never will amount to more than a few per cent of the subsidence. Consequently this area and its resident population of two million people are faced with the fact that all water originating in the area below sea level, or introduced into the area for domestic or industrial supply or by flooding, will have to be pumped out as long as people live there or possibly until the land surface might be raised above sea level by a long-term project of importing a massive landfill. Despite the protective measures taken, the danger of major flooding due to typhoons or to failure of dikes or pumps caused by a violent earthquake is ever present.

Two other subsidence areas in Japan have extensive areas that have sunk below high-tide level. They are Osaka (100 km^2 below high tide) and the Nobi Plain (363 km^2 below high tide). Together with Tokyo they contain about half of the land that has subsided below hightide level in Japan. More than one million people lived in the two areas in 1969. Beginning in the early 1960's the use of ground water in Osaka has been regulated as an alternate supply of surface water became available. As a result a sharp recovery of artesian head occurred in Osaka, beginning in 1962 (see Case History 9.5, Figure 9.5.4); by 1965 the rate of subsidence had decreased markedly. Protective measures taken are similar to those adopted in eastern Tokyo. All areas below sea level are faced with the problem of how to minimize damage from a typhoon.

6.3.2 Ground-water law in Japan

Japan has two laws which regulate and or prohibit ground-water utilization. One is the "Industrial Water Law" and the other is the "Building Water Law." Japan has no law regulating ground-water withdrawal for irrigation (agricultural use).

The Industrial Water Law (law No. 146 CF 1956) is aimed at making contributions to the sound development of industries and the prevention of subsidence of the ground by ensuring a rational supply of industrial water and achieving the conservation of ground-water resources.

The areas where drawing of industrial ground water is controlled are designated by Cabinet Order out of areas where drawing of ground water is causing an abnormal drop in the ground-water level, salinization or contamination of ground water, or subsidence of ground, and water services for industrial use are already installed or the installation work is expected to be commenced within a year.

Prefectural governors issue pumping licenses mentioned if the position of the strainer for the well and the sectional area of the discharge port of the pump fulfill certain technical criteria.

The Building Water Law (law No. 100 CF, 1962) is aimed at protecting the lives and properties of the people by exercising necessary control in order to prevent the subsidence of ground as a result of drawing ground water for buildings at the specified area.

Areas where drawing of ground-water for buildings is controlled are designated by Cabinet Order out of areas where drawing of ground-water for buildings is liable to cause the subsidence of ground and resultant damage due to the high tide and flood.

Prefectural governors or mayors of the designated cities issue licenses upon request from interested individuals provided the position of the strainer for the pumping facilities and the sectional area of the discharge port of the pump fulfill certain technical criteria.

Those who are already drawing ground water for buildings when the area concerned is designated shall be considered to have obtained the license, if their methods of drawing ground water for buildings fulfill the technical criteria, and even in the case of failure to fulfill the technical criteria, they shall be treated as having a license, in principle, for a certain limited term exceeding two years.

The pumping of ground water without a license is punishable with a prison term of less than one year or a fine of less than ¥100,000.

In Case History 9.4 for Tokyo, Yamamoto describes in chronologic order the application of restrictions under the "Industrial Water Law," beginning in 1961, and restrictions under the "Building Water Law," beginning in 1963. The restrictions under the "Industrial Water Law" are designed to reduce ground-water withdrawals by supplying substitute water. The restrictions

under the "Building Water Law" are designed to limit the pumping of ground water for air conditioning and other non-drinking purposes in medium and high-rise buildings (see also Figure 9.4.9).

The local Metropolitan Environmental Pollution Control ordinance restricted the drilling of new wells in areas not covered by the two National laws described above. Also, in 1972 the Tokyo Metropolitan Government bought the mining rights to ground water containing natural gas, thereby stopping the pumping of gas-bearing water from wells 800-2,000 m deep tapping the Kagusa Group of Pliocene age.

The case history of the Nobi Plain (ch. 9.6) contains, two pages of detailed regulations for the withdrawal of ground water. Two small areas (see Figure 9.6.7) designated by the Industrial Water Law are supplied by industrial water from surface sources. Ground-water withdrawal in the remainder of the area is covered through regulation by ordinances of prefectures or of cities (by regulation zone determined by rate of subsidence per year). These ordinances specify depth of well or strainer, inside area of discharge pipe, the power of the pump motor, and the total daily discharge of the well. These complex regulations doubtless are related to the fact that 248 km^2 of the Nobi Plain were below mean sea level in 1976. The regulations have been established in an attempt to minimize the decline of artesian head, the compaction of sediments, and the rate of land subsidence.

6.4 UNITED STATES

6.4.1 Economic and social impacts

Table 1.1 lists 18 areas of land subsidence in United States due to ground-water withdrawal and Figure 1.2 shows the geographic location of 17 (not including the Alabama sinkhole area). Four of these areas border the ocean or bays but two--Savannah and New Orleans--have relatively minor subsidence problems compared to the Houston-Galveston area, Texas, and the Santa Clara Valley at the south end of San Francisco Bay in California. Ranked in terms of the severity of socio-economic problems the three principal subsidence areas in the United States due to ground-water withdrawal are (1) the Houston-Galveston area in Texas, (2) the San Joaquin Valley in California and (3) the Santa Clara Valley in California. Environmental and economic effects of subsidence in these three areas are discussed briefly in following pages. For an expanded analysis of economic effects in these and several other subsiding areas, the reader is referred to a report by Viets, Vaughan, and Harding (1979).

6.4.1.1 Houston-Galveston area, Texas

The principal detrimental effects of land-surface subsidence in the Houston-Galveston area are (1) structural damage, probably due to faulting, that has cracked buildings and disrupted pavements; (2) damage to well casings as a result of compressional stresses; (3) lessened efficiency of storm-drainage facilities and (4) submergence of coastal lowlands. According to Gabrysch (Case History 9.12), most of the damage is related to the lowering of land-surface elevations in the vicinity of Galveston Bay and the subsequent inundation by tidal waters. Several roadways have been rebuilt at higher elevations; ferry landings have been rebuilt; and levees have been constructed to protect some areas. Jones and Larson (1975) estimated the annual cost of subsidence in terms of property value losses during 1969-74 to be about $32 million in 2,450 km^2 of the area most severely affected by subsidence.

The Brownwood subdivision on the west side of Baytown is an outstanding example of both the social and economic impacts of subsidence. The subdivision has subsided about 2.8 m since 1915; some homes are permanently flooded with bay water. After a feasibility study including eight alternative plans, the U.S. Army Corps of Engineers has proposed that the entire subdivision, including 456 homes and 1,550 residents be relocated above the 50-year flood plain, at an estimated cost of about $40 million (using May 1979 price data).

Although no detailed appraisal has been made of overall costs of subsidence in the Houston-Galveston area, partial estimates, including the costs just cited, indicate that total costs to date have been several $100 million.

The most critical socioeconmic hazard to the Houston-Galveston area is the threat of catastrophic flooding by hurricane tides. The severity of the hazard will increase as long as subsidence of the coastal areas continues. Gabrysch reports (Case History 9.12) that hurricanes resulting in tides of 3.0-4.6 metres above sea level strike the Texas coast on the average of once every 10 years. This problem is discussed in more detail by Teutsch (1977).

6.4.1.2 San Joaquin and Santa Clara Valleys, California

San Joaquin Valley.--As discussed in Case History 9.13, the extensive major subsidence in the San Joaquin Valley has caused several problems, primarily economic rather than social. (1) The differential change in elevation of the land surface has created problems in the construction and maintenance of water-transport structures, including canals, irrigation and drainage systems, and stream channels. Three major canals have required remedial work because of subsidence. (2) Many hundreds of irrigation wells 200-900 m deep failed between 1945 and 1970 due to compressive rupture of casings caused by the compaction of the aquifer systems. Costs of well repair or of replacement attributable to subsidence have been many millions of dollars. (3) The need for preconsolidation of deposits susceptible to hydrocompaction increased the construction costs of the California Aqueduct by an estimated $25 million. (4) Increased cost and number of surveys made by governmental agencies and by private engineering firms to determine the elevations of bench marks to establish grades on construction sites, for revision of topographic maps, for construction of subsidence maps, and for land leveling to compensate for effects of subsidence.

No overall estimate has been made of the costs attributable to subsidence in the San Joaquin Valley but if partial estimates are correct, total costs must be in excess of $50 million.

Santa Clara Valley.--As described in Case History 9.14, the subsidence in the Santa Clara Valley has created several major problems, primarily economic. They include: (1) Land adjacent to San Francisco Bay has sunk 2-3 m since 1912, requiring construction and repeated raising of levees to restrain landward movement of bay waters onto lands now below sea level; and also requiring continued maintenance of 60 km of subsiding salt-pond levees. Also, Santa Clara County has built and maintained flood-control levees to correct for subsidence effects at a cost of $9 million. (2) Many hundreds of water-well casings have failed in vertical compression due to compaction of the confined-aquifer system. The estimated cost of repair or replacement is at least $5 million. (3) construction and maintenance of a pump station at the regional sewage treatment plant, needed because of subsidence, at a cost of $10 million (Viets and others, 1979). (4) Costs involved in repair of railroads, roads, and bridges; replacing or increasing the size of storm and sanitary sewers because of change in grade due to subsidence; establishing and resurveying the bench-mark net, and making private engineering surveys; and finally the reduction in value of 44 km^2 of land standing below high-tide level as of 1967 compared to its value if it all still stood above sea level.

No overall estimate has been made of the costs attributable to subsidence in the Santa Clara Valley but the partial relatively firm estimates suggest that total costs must have been at least $35 million.

6.4.2 Legal developments in California and Texas

In California, until the start of the 20th century, the English common law rule of absolute ownership of percolating waters prevailed. According to this doctrine: in the absence of any malice or any contractual or statutory restriction, the owner has the absolute right to intercept the water before it leaves his property and make whatever use of it he pleases, regardless of the effect that such use may have on an adjoining or lower proprietor through whose land the water infiltrates, percolates, or flows (Kooper and Finlayson, 1979).

In 1903, however, the California Supreme Court in Katz v. Walkinshaw (141 Cal. 116) spelled out a set of rules for ground water known as the "correlative rights" doctrine. Owners of land overlying a ground-water basin who used the water on the overlying land were recognized as holding the paramount right. Such owners among themselves were to share the water on a correlative basis, similar to the sharing of surface waters by riparians. Any water surplus to the needs of these overlying owners remained available for appropriation by others (Governor’s Commission to review California water rights law, 1978).

According to Koopman and Finlayson (1979), the rule of law governing liability for subsidence caused by the removal of ground water is not settled in most jurisdictions although the trend appears to be toward greater liability. This change in the law is reflected by a reversal of the position of the American Law Institute in the Restatement of Torts II compared to the Restatement of Torts I.

The Restatement of Torts I stated the rule: "to the extent that a person is not liable for withdrawing subterranean water from the land of another, he is not liable for subsidence of the other’s land which is caused by the withdrawal." Restatement of Torts, Section 318 (1938). The

position stated in the restatement of Torts II is: "One who is privileged to withdraw subterranean water, oil, minerals or other substances from under the land of another is not for that reason privileged to cause the subsidence of the other's land by such withdrawal." Restatement of Torts II, Section 318 (1969).

In 1958, the United States of America sued all the oil and gas producers in the Wilmington oil field in southern California, claiming that their operations had withdrawn undergound support from its Naval Base on Terminal Island and other properties, thereby causing subsidence which seriously damaged the government property. This case was the largest damage suit in United States history for subsidence caused by pumping fluids from the ground. The case was settled out of court. The government was assured of the control of subsidence by passage of the Anti-Subsidence Act of 1958, which compelled the oil producers in the Wilmington field to unitize and undertake to repressurize the depleted reservoir.

Again, according to Koopman and Finlayson (1979), "the statute clearly reflects a desire to retain the economic benefits of the Wilmington oil production, while relying on technology to prevent damage to private property rights. . . The Act shows the intent of the California Legislature to prevent further subsidence, but not to set liability."

As summarized by the Governor's Commission to review California water rights law (1978) "there have been two main approaches in California to instituting successful ground-water management. One has been by formation of a water district with powers to carry out a ground-water management program. The second has been management by a court-appointed watermaster with powers similar to those of a management district, after an adjudication of substantially all rights to extract ground water in the management area.

"The orange County Water District has been the leader in the water district non-adjudication approach to ground-water management. The district has a wide range of management powers, including the power to require pumpers to file periodic 'water production statements' with the district.

"The district's financing powers are extensive. It was the first district to levy a pump tax ('replenishment assessment'). The pump tax applies to all ground-water extraction, so there is no advantage to being an overlying landowner or an early appropriator. The district uses 'basin equity assessments' either to increase or decrease the cost of ground water in order to influence the relative amounts of ground water and surface water that are used, and to regulate pumping patterns.

"A central function of the Orange County Water District is to use imported water to replenish the ground-water supply. The district's replenishment operations include 'spreading' the water in areas chosen because they allow the water to percolate rapidly into the ground-water basin, and 'in-lieu' replenishment. In-lieu replenishment involves substituting a surface water supply for ground-water pumping in a particular area to allow the ground-water level to recover as a result of natural recharge.

"The San Gabriel adjudication watermaster program indicates the direction that the adjudication-watermaster approach to ground-water management is taking. The San Gabriel watermaster has a much more sophisticated range of powers and authority than the California Department of Water Resources has as watermaster for the court in four areas in Southern California. The San Gabriel watermaster, composed of nine members appointed by the court pursuant to an agreement among ground-water users in the adjudicated area, is a policy maker. It can levy a 'replacement water assessment,' which is a charge on pumping in excess of a pumper's adjudicated share of the basin's yield, can conduct a ground-water replenishment program, and has authority to control storage in the basin."

The Santa Clara Valley Water District in Santa Clara County, California, was formed by a special act of the California Legislature that was approved by the voters in 1929. A principal goal of the district in its subsequent management of all available water supplies, to balance supply and demand and hence to stop the land subsidence, has been the reduction in pumpage of ground water. (See Case History 9.14) The annual pumpage of ground water decreased about 20 per cent from 1960-65 to 1970-75. A principal reason for the decrease in pumpage was a use tax levied on a ground-water pumpage since 1964. The enactment of the 1929 legislation providing for the local management of ground-water resources, including the taxing power, represented a major departure from the early rule of absolute ownership.

Historically Texas has followed the English common law rule of absolute ownership to withdraw water from beneath his property with no liability for damage to other lands. In the past five years, however, the trend has clearly been toward holding pumpers of ground water responsible for damage from subsidence. First came the creation of the Harris-Galveston Coastal Subsidence District in 1975, followed by two major legal decisions involving subsidence and liability.

The Harris-Galveston Coastal Subsidence District was created by the Texas Legislature in May 1975 "to provide for the regulation of the withdrawal of ground water within the boundaries of the district for the purpose of ending subsidence which contributes to or precipitates flooding, inundation, or overflow of any area within the district, including without limitation rising waters resulting from storms or hurricanes" (Neighbors, 1979).

The act creating the district provides that water wells located within the district, with casing diameter in excess of five inches, are required to have a permit to withdraw a specified amount of water for a period of not less than one year nor more than five years. The district is supported financially by the permit fees. The current permit fee rate is $4.50 per million gallons (3,785 m^3).

A major court decision in Coastal Industrial Water Authority v. W. B. York (1976) involved the submergence of York's land in the Houston Ship Canal due to the subsidence. The court held that the property owner did not lose title to the land due to the fact that it had become submerged from subsidence as a result of pumping of ground water.

In 1978, according to Neighbors (1979), the Texas Supreme Court reinforced the Legislature's authority to regulate ground-water withdrawal for the purpose of controlling subsidence. In Smith-Southwest Industries, Inc. v. Friendswood Development Co. (1978) the Court referred to the creation of the Subsidence District and other legislative acts in establishing the intent of the Legislature to limit the common-law rule of absolute ownership of ground water. The Court held that ground-water users were not liable for subsidence damages caused by past actions, but could be held responsible for damages due to future pumpage if such were conducted in a negligent or malicious manner. The opinion concludes "Therefore, if the landowner's manner of withdrawing water (in the future) is negligent, willfully wasteful or for the purpose of malicious injury, and such conduct is a proximate cause of the subsidence of the land of others, he will be liable for the consequences of his conduct."

6.5 REFERENCES

AIHARA, SHIGERU, et al. 1969. Problems of groundwater control in Tokyo, in L. J. Tison, ed., Land subsidence, v. 2, IASH/AISH Pub. 89, p. 635-644. Coastal Industrial water Authority v. W. B. York, 532, S.W. 2d 949 (1976). Governor's Commission to Review California Water Rights Law. 1978. Final Report, Sacramento, California, 264 p.

JONES, L. L., and LARSON, JAMES. 1975. Economic effects of land subsidence due to excessive ground-water withdrawal in the Texas Gulf Coast area. Texas Water Resources Institute, Texas A and M Univ., Tech. Report-67, 33 p.

KOOPER,W., and FINLAYSON, D. J. 1979. Legal aspects of subsidence due to well pumping. Am. Soc. Civil Engineers Annual Meeting, Atlanta, Georgia, Oct., preprint no. 3748, 24 p.

NEIGHBORS, R. J. 1979. Subsidence in Harris and Galveston Counties, Texas. Am. Soc. Civil Engineers Annual Meeting, Atlanta, Georgia, Oct., no. 3663, 23 p., also ASCE Jour. Irrig. and Drainage, v. 107, no. IR2, June 1981, p. 161-174.

SHIMIZU, RYOSAKU. 1969. Land subsidence in Japan. Booklet prepared for 1969 Internat. Symposium on Land Subsidence, Tokyo, Japan.

SMITH-SOUTHWEST INDUSTRIES, INC., et al v. FRIENDSWOOD DEVELOPMENT CO., et al. @@ Tex Sup. Ct. J. 105 (Nov. 29, 1978).

TEUTSCH, J. S. 1977. Subsidence in the Houston-Galveston region, A comprehensive analysis. Master's thesis, Rice University, Houston, Texas.

VIETS, V. F., VAUGHAN, C. K. and HARDING, R. C. 1979. Environmental and economic effects of subsidence. Report prepared by EDAW, Inc. and Earth Sciences Associates for Lawrence Berkeley Laboratory, Berkeley, California, under LBL Contract No. 300-3902, 232 p.

YAMAMOTO, SOKI. 1977. Recent trend of land subsidence in Japan. 1AHS/AISH Pub. No. 121, p. 9-15.

7 Review of methods to control or arrest subsidence, by Joseph F. Poland and Working Group

7.1 SUMMARY OF AVAILABLE METHODS

7.1.1 General statement

Methods to control or arrest subsidence include reduction of pumping draft, artificial recharge of aquifers from the land surface, and repressuring of aquifers through wells, or any combination of these methods. The goal is to manage the overall water supply and distribution in such a way that the water levels in wells tapping the compacting aquifer system, or systems, are stabilized or raised to some degree. In other words, at least manage the overall supply in such a way that effective stress in the aquifer system is not increased beyond the stress experienced to date.

The local geologic conditions determine whether artificial recharge can be accomplished by regulated application at the land surface or by repressuring of aquifers by means of injection through wells.

Both the artificial recharge of aquifers from the land surface and the repressuring of aquifers through wells normally require a supply of potable surface water. The question may be asked: "Why not use the supplementary surface supply directly at land surface and thereby reduce ground-water draft, instead of recharging the ground-water supply?" The answer may be that it is impracticable to deliver all the supplementary supply direct to users so part of the supply is recharged to the water table. The ground-water reservoir then acts as the distribution system. Such is the case in the Santa Clara Valley in California (Case History 9.14).

7.1.2 Reduction of pumping draft

Reduction of pumping draft may be accomplished to some degree by one or more of the following methods:

1. Import of substitute surface water.
2. Conservation in application and use of water:
   a. through improvement of irrigation methods, such as change from ditch and furrow or flood irrigation to overhead sprinkler irrigation or to drip irrigation.
   b. through change from crops requiring heavy duty or demand to crops requiring less duty, such as from cotton to orchards.
3. For overdrawn ground-water basins, adjudication (equitable distribution) of available supply.
4. In urban areas, by recirculation and reuse of treated water by industrial plants.
5. By decreasing irrigated area or industrial plants using large quantities of water.
6. By moving the well fields to tap more permeable (less compressible) deposits.
7. By changing the depth range of perforated intervals in well casings or screens to tap less compressible deposits.
8. By legal control.

Whether any one of these remedies is economically justified depends on its cost compared with the costs of continued subsidence. The first requirement for estimating costs is an estimate of the magnitude of subsidence that would occur (1) if the artesian head was maintained at the present level, and (2) in response to an assumed additional decline in head.

7.1.3 Artificial recharge of aquifers from the land surface

Land subsidence usually results from compaction of compressible confined aquifer systems due to intensive withdrawal of ground water and consequent decline of artesian head. Because confining beds restrict the vertical downward movement of water from the land surface, artificial recharge of confined system(s) by application of water at the land surface directly overhead ordinarily

is not practicable. However, the geology of the system may be such that the confined aquifer system may crop out at or near the margins of the ground-water basin; this outcrop area may be near enough to the subsiding area so that artificial recharge on the outcrop area will raise the local water table and also the artesian head in the confined system.

7.1.4 Repressuring of aquifers through wells

Repressuring of confined aquifer systems by artificial recharge directly through wells, although expensive, may prove to be the only practical way to slow down or stop land subsidence in a particular area. The Wilmington oil field in southern California is a classic example of subsidence control by injection of water through wells. Repressuring of the oil zones to increase oil production and to control subsidence began on a major scale in 1958. By 1969, when 175 x $10^3 m^3$ (1.1 x 10^6 barrels) of water per day was being injected into the oil zones, the subsiding area had been reduced from 58 to 8 km^2, and locally the land surface had rebounded as much as 0.3 m (Mayuga and Allen, 1969). In 1975 about 80 x 106 m^3 (500 x 10^6 bbls) of water was injected into the oil zones to (1) control subsidence, (2) produce 10 x 10^6 m^3 of oil and (3) utilize 67 x 10^6 m^3 of water produced with the oil. According to Gates, Caraway, and Lechtenberg (1977), the injection of this great quantity of water from diverse sources created many problems which were controlled by various chemical and physical treatments.

Replenishinq ground-water supplies by artificial recharge through wells and pits has been practiced in many areas, including many sites in California and more than a thousand recharge wells on Long Island, New York. The results of such practices have been summarized to 1967 in two annotated bibliographies on artificial recharge of ground water (Todd, 1959; Signor, Growitz, and Kam, 1970). In general, results were satisfactory when the water was clear; most of the problems of recharge through wells involved clogging of the well and aquifer. In a study of problems in artificial recharge through wells in the Grand Prairie region of Arkansas, Sniegocki (1963) found that the principal causes of clogging were air entrainment, suspended particles in the recharge water, and micro-organisms. He concluded that wells should be recharged with treated water and that water-treatment cost and contemplated use of the recharged water are the principal factors involved in determining the economic feasibility of artificial recharge. The availability of water suitable for injection would be another important factor.

Injection of treated fresh water into a confined aquifer system to create an hydraulic barrier (pressure ridge) to sea-water intrusion has been practiced successfully in southern California for 25 years. The operating agency, the Los Angeles County Flood Control District, had 180 injection wells in operation in 1976. According to Rancilio (1977), during two decades of operating experience the District never has had to cease operation of an injection well permanently because of loss of operating efficiency. Because of the continuing success of this massive injection operation for a quarter century, the reader interested in injection wells is referred to the paper by Rancilio (1977) which describes in detail the typical design of a successful injection well, operating conditions and costs, injection rates and heads, clogging problems, and redevelopment of injection wells. Both the cable-tool and reverse-rotary methods were used in construction of the injection wells but at least two-thirds of the wells are reverse-rotary, with asbestos-cement casing and gravel pack. The operational injection heads ranged from 9 to 61 metres and injection rates ranged from 6 to 28 l/s.

7.2 REVIEW OF METHODS USED

7.2.1 Summary statement

Table 1.1 lists 42 areas of land subsidence due to ground-water withdrawal. Methods used to control or arrest subsidence in these areas may be summarized as follows:

In 15 areas, ground-water draft has been reduced as a result of substituting imported or locally treated surface water.
In 4 areas, ground-water draft has been reduced by regulation but surface water import not reported.
In one area, pumping of gas-bearing water was stopped by legal action (Po Delta, Italy); in another area (Niigata, Japan) reinjection of all gas-bearing water has been required since 1973.
In one area, ground-water pumped from mines has been led outside rock compartments or injected into a leached dolomite aquifer through 10 boreholes since 1973.
In 20 areas no methods for control have been reported.

7.2.2 Shanghai, China

Land subsidence in Shanghai, China, was first reported in 1921. By 1965 the maximum cumulative subsidence in the city was 2.63 m (Case History 9.2). Injection of river water through wells to recharge the principal aquifers began about 1964. By 1966, more than 100 industrial plants operating more than 200 wells had joined in the recharge operation to build up pressure in the confined aquifer system. As shown by the record from typical bench marks in the urban area of Shanghai (Figure 9.2.1), the cessation of subsidence was virtually instantaneous. Within a year or two, bench marks apparently were rising and from 1966 to 1976, as much as 34 mm of rebound occurred.

The injection of river water through production wells is undertaken chiefly in the winter months when many factories are not operating and when the river water is coldest. Because much of the ground water withdrawn is used for cooling purposes in the factories in the summer, any decrease in water temperature in the aquifers is beneficial. As a result of careful monitoring of river-water temperature to obtain water of minimum temperature for injection, the ground-water temperature at one site reportedly has been lowered 6° C.

7.2.3 Venice, Italy

After studying by mathematical model the physical mechanism and the quantitative relationship linking the pumping rate to the resulting subsidence of Venice, the behavior of the aquifer system and ground surface became well understood. (See Case History 9.3.) Because land subsidence was caused by pressure drawdown in the aquifer system, it was apparent that the only remedy consisted of raising the pressure surface beneath Venice.

Injection of water through injection wells was suggested as a possible measure by a number of experts. However this solution would have required water with chemical properties similar to those of the underground water. Moreover the effectiveness of this remedy could not be scientifically proven.

An uplift experiment on a small island near Venice was successfully carried out by pressure grouting using special cement mortars (Marchini and Tomiolo, 1977). Unfortunately, the experiment could not be transferred to uplift such an extensive area as Venice.

Other proposed solutions, including the construction of a deep wall acting as a hydraulic barrier for the city, were soon abandoned on the grounds of impracticability.

The recognition of the physical mechanism underlying the subsidence of Venice and the results provided by theoretical and experimental patterns showed that the most effective and cheapest solution consisted of reducing the withdrawal rate in the Venetian area. The recovery of the flow field was shown to be rather fast and the arrest of the settlement was proven to be almost instantaneous.

Accordingly, the Venice Municipality prompted the completion of the planned aqueduct and the construction of a new one to supply the industrial area with water taken from the Sile and the Brentella Rivers, which flow in the vicinity of the Venetial Lagoon. More that 90 per cent of the water used for industrial purposes now is supplied by surface water from the local rivers. Furthermore, as soon as the aqueducts became operative, the Magistrato alle Acque (Civil Engineers Branch) of Venice issued a prohibition against opening new wells and an injunction to close the existing wells.

To date, more than 70 per cent of the artesian wells that were active in 1969 have been gradually shut down; this trend still continues and a constant improvement of the subsidence situation in Venice has been observed (see Case History 9.3)

7.2.4 Japan

The ten principal subsidence areas in Japan, due to excessive ground-water withdrawal, are listed in Table 1.1. In all of these areas ground-water withdrawal has been reduced by regulation; in parts of Tokyo withdrawal of ground water from wells has been prohibited completely. (See Case History 9.4). In seven areas surface water has been imported as a replacement for ground water. In several areas, industrial waste water is being treated and reused.

In Niigata (Case History 9.7) experiments of water injection into the confined aquifers containing methane gas were carried out from 1960 to 1963 (Ishiwada, 1969). The purpose of the injection was the maintenance of reservoir pressures and reduction of the rate of subsidence. Both degassed formation water and river water were used as the injection fluids. According to

Ishiwada, the permeability of the main reservoirs ranges from 10 to 50 darcys, the injection rate is less than one-quarter of the production rate, and back-washing at adequate time intervals is necessary to continue long-term injection.

Since 1973, all degassed formation water has been reinjected into the gas-bearing reservoirs by law.

7.2.5 United States

Table 1.1 describes 18 areas of land subsidence in the United States. Of these, six have imported surface water to satisfy water demands. This has led to the reduction of pumping draft and the local stabilizing or raising of artesian pressures. They include the Santa Clara Valley and three areas in the San Joaquin Valley in California, as well as Las Vegas Valley in Nevada and the Houston-Galveston area in Texas. A major aqueduct to import Colorado River water to south-central Arizona now (1980) is under construction.

Repressuring through injection wells has not been used in any of these areas and artificial recharge of a substantial part of the imported surface water has been practiced only in the Santa Clara Valley. In the other five areas, imported surface water has been used as a direct replacement or substitute for ground-water pumpage.

7.3 REFERENCES

GATES, G. L., CARAWAY, W. H., and LECHTENBERG, H. J. 1977. Problems in injection of waters in Wilmington oil field, California. IAHS-AISH Pub. 121, p. 319-324.

ISHIWADA, YASUFUMI. 1969. Experiments on water injection in the Niigata gas field. IAHS-AISH Pub. 89, p. 629-634.

MARCHINI, S., and TOMIOLO, A. 1977. The use of mud-jacking for the upheaving of urban zones. Computer control of the works. Experimental application to the problem of Venice. IAHS-AISH Pub. 121, p. 63-94.

MAYUGA, M. N., and ALLEN, D. R. 1969. Subsidence in the Wilmington oil field, Long Beach, Calif., USA. IAHS-AISH Pub. 88, p. 66-79.

RANCILIO, J. A. 1977. Injection well operation and maintenance. IAHS-AISH Pub. 121, p. 325-333.

SIGNOR, D. C., GROWITZ, D. J., and KAM, WILLIAM. 1970. Annotated bibliography on artificial recharge of ground water, 1955-1967. U.S. Geological Survey Water-Supply Paper 1990, 141 p.

SNIEGOCKI, R. T. 1963. Problems in artificial recharge through wells in the Grand Prairie region, Arkansas. U.S. Geological Survey Water-Supply Paper 1615-F, 25 p.

TODD, D. K. 1959. Annotated bibliography on artificial recharge of ground water through 1954. U.S. Geological Survey Water-Supply Paper 1477, 115 p.